

University of Warwick institutional repository: <http://go.warwick.ac.uk/wrap>

**A Thesis Submitted for the Degree of PhD at the University of Warwick**

<http://go.warwick.ac.uk/wrap/71200>

This thesis is made available online and is protected by original copyright.

Please scroll down to view the document itself.

Please refer to the repository record for this item for information to help you to cite it. Our policy information is available from the repository home page.

IN-PROCESS CONTROL OF GRINDING

A thesis submitted to  
the Department of Engineering  
at the University of Warwick for  
the degree of  
DOCTOR OF PHILOSOPHY

by

B. G. FOWELL  
M.Sc.,(Birmingham), B.Sc., (Leeds)

Department of Engineering  
University of Warwick

September, 1983

**BEST COPY**

**AVAILABLE**

Poor quality text in  
the original thesis.

## SUMMARY

The grinding process must achieve the desired component surface finish without producing detrimental workpiece surface layer alterations. These objectives have traditionally been achieved intuitively by skilled operators. Adaptive control, however, offers an opportunity to monitor and control surface integrity during the grinding process.

The cylindrical plunge grinding machine adapted for the purposes of this research monitors normal and tangential grinding forces, wheelpower and the amplitude of chatter vibration. The control system is capable of achieving constant normal force machining by adjusting the plunge infeed rate of the wheel. This research is concerned with the feasibility of controlling surface integrity on this and similar grinding machines.

The research has been carried out by a combination of long duration tests to examine the behaviour of grinding forces, wheelpower and vibration levels with respect to time and shorter duration tests to examine component surface finishes. The results of the tests have enabled models to be developed which relate component surface finishes to metal removal rates, normal grinding forces and chatter vibration levels.

Workpiece burn and its prevention have also been studied. A method of eliminating workpiece burn has been proposed which utilises in-process normal and tangential force monitoring.

## ACKNOWLEDGEMENTS

The author wishes to express his gratitude to Prof S K Bhattacharyya, Lucas Professor of Manufacturing Systems, for his continued guidance and encouragement throughout the research.

Sincerest thanks are also due to Dr K Harrison, Senior Research Fellow and Dr J Wallbank, Lecturer, Department of Engineering, for their valuable contributions.

The support of SERC is duly acknowledged without whom this research could not have been undertaken.

Finally, I would like to thank my wife, Alison, for her patience throughout the last four years.

## CONTENTS

Page No

1.0	INTRODUCTION	1
2.0	LITERATURE SURVEY	5
2.1	General Introduction	5
2.2	Grinding Forces	10
2.3	Grinding Temperature	18
2.4	Grinding Chatter	25
2.5	Surface Integrity	33
2.6	Wheel Dressing	37
2.7	High Speed Grinding	42
2.8	Adaptive Control of the Grinding Process	45
3.0	THE GRINDING MACHINE	52
3.1	Introduction	52
3.2	Grinding Machine Hardware	52
3.2.1	Control Strategy	53
3.2.2	Axis Servo Systems	53
3.2.3	Wheel Spindle and Work Motors	54
3.2.4	Digital Inputs/Outputs	55
3.2.5	Watchdog Timer	55
3.3	CNC Grinding Machine Operation	56
3.3.1	Manual Mode Operations	57
3.3.2	Manual Part Programming	58
3.3.3	Automatic or Machining Model	59
3.4	Adaptive Control	59
3.4.1	Grinding Force Measurement	60

## CONTENTS

Page No

3.4.2	Vibration Measurement	61
3.4.3	Wheelpower Measurement	61
3.5	Adaptive Control Software Structure	62
3.5.1	The Identification Stage	63
3.5.2	Constant Force Machining	65
3.5.3	Vibration & Wheelpower Software	67
3.6	System Monitoring During Non-Adaptive Control Grinding Operations	67
4.0	EXPERIMENTAL APPROACH	81
4.1	Introduction	81
4.2	Test Strategy	82
4.3	Long Duration Constant Metal Removal Rate CNC Tests	83
4.3.1	Test Conditions	84
4.3.1.1	The Grinding Wheel	84
4.3.1.2	Workpieces	85
4.3.1.3	Coolant	85
4.3.1.4	Wheel Dressing Conditions	85
4.3.1.5	Grinding Conditions	86
4.4	Long Run Constant Force Machining Tests	86
4.4.1	Test Conditions	86
4.4.1.1	Grinding Conditions	87
4.5	Short Run Tests for the Investigation of Component Surface Finish	87
4.5.1	Surface Finish Test Conditions	88
4.5.1.1	Grinding Conditions	88

## CONTENTS

Page No

4.6	Wheel Dressing	89
4.6.1	Test Conditions	90
4.6.1.1	Workpiece Material	90
4.6.1.2	Dressing Conditions	90
4.6.1.3	Grinding Conditions	91
4.6.2	Test Procedure	91
4.6.2.1	Short Run Test Procedure	92
4.7	Coding System for Test Identification	92
4.7.1	Coding System Example	93
5.0	RESULTS	94
5.1	Constant Metal Removal Rate Tests	94
5.2	Constant Normal Force Machining Tests	94
5.3	Component Surface Finish Investigation	95
5.4	Wheel Dressing Tests	95
5.4.1	Long Run Test Results	95
5.4.2	Short Run Test Results	96
6.0	ANALYSIS AND DISCUSSION	174
6.1	Long Duration Constant Metal Removal Rate Tests	174
6.1.1	Grinding Forces and Wheelpower	174
6.1.2	Self-Excited Chatter	174
6.2	Constant Normal Force Machining Tests	179
6.2.1	Tangential Force and Wheelpower	179
6.2.2	Self-Excited Chatter Vibration	179
6.2.2.1	Attritious Wear	179
6.2.2.2	Fracture Wear	181

## CONTENTS

	Page No
6.2.3 Component Surface Finish	182
6.3 Investigation of Component Surface Finish	183
6.3.1 Grinding Forces and Wheelpower	183
6.3.2 Self-Excited Chatter Vibration	184
6.3.3 Component Surface Finish	184
6.4 Wheel Dressing Investigation	189
6.4.1 Effect of Dressing on Grinding Forces and Wheelpower	189
6.4.2 Self-Excited Chatter Vibration	193
6.4.3 Influence of Dressing on Component Surface Finish	195
6.4.4 Component Surface Finish Model	196
6.5 Grinding Process Control Considerations	196
6.5.1 Re-Dressing the Grinding Wheel	197
6.5.2 Workpiece Surface Finish Control	197
7.0 PRELIMINARY INVESTIGATION OF WORKPIECE THERMAL DAMAGE	223
7.1 Introduction	223
7.2 The Abrasive Belt Research Machine	225
7.2.1 The Abrasive Belt Head	225
7.2.2 The Surface Grinding Table	225
7.3 Experimental Technique	226
7.3.1 Possible Sources of Error	227
7.4 Results	227
7.5 Discussion	228
7.5.1 Adaptive Control Application	231

CONTENTS

Page No

CONCLUSIONS	241
RECOMMENDATIONS FOR FUTURE WORK	246
REFERENCES	248
APPENDIX 1 - Vibration Transducer Technical Data Sheet	262
APPENDIX 2 - EN3 and EN8 Material Specifications	265
APPENDIX 3 - Metal Removal Rate Calculation	272
APPENDIX 4 - Average Amount of Material Removed per Abrasive Grit	274
APPENDIX 5 - Significance Tests	280
APPENDIX 6 - Regression Analysis Results	298

LIST OF TABLES

Page No

5.1	Grinding Forces and Wheelpower Results from the Constant Metal Removal Rate Tests	97
5.2	Tangential Force and Wheelpower Results from the Constant Normal Force Tests	108
5.3	Workpiece Surface Finishes on Test Calculation	119
5.4	Metal Removal rates	120
5.5	Grinding Data from the Short Duration Interrupted Tests	121
5.6	Grinding Forces and Wheelpower Results from the Dressing Tests	129
5.7	Surface Finish Data from the Short Run Tests	132
6.1	Summary of the Regression Analysis with Component Surface Finish as the Dependent Variable	200
6.2	Self-Excited Chatter Vibration Magnitude for Constant Normal Force Tests	201
6.3	Summary of Surface Finish Chatter Vibration Regression Results	202

LIST OF TABLES

Page No

6.4	Vibration Amplitudes of Short Duration Tests	203
6.5	Coefficient of Determination, $R^2$ , Results of Surface Finish Data	211
6.6	Coefficient of Determination, $R^2$ , for Individual Test Conditions	212
6.7	Coefficient of Determination Values from the Multiple Regression Analysis Calculations Performed on LR-NF-Surface Finish Results	213
6.8	Use of the LR-NF Test Regression Analysis Model to Predict the SR-MRR-1 Surface Finish Results	214
6.9	Use of the LR-NF Test Regression Analysis Model to Predict the SR-MRR-2 Surface Finish Results	215
6.10	Band Pass Rectified Vibration Levels from the Dressing Tests	216
6.11	Investigation of Dressing Influence on Component Surface Finish	219
6.12	Coefficient of Determination, $R^2$ , Results for the Dressing Tests Surface Finish Data	220

LIST OF TABLES

Page No

7.1 Abrasive Belt Grinding Data

234 (i)

7.2 Average Volume Removed/Grain/Belt Revolution

234 (v)

LIST OF FIGURES

Page No

2.1	Equivalent Chip Thickness Grinding Charts	50
2.2	Grinding Force - Time Relationships	50
2.3	Grinding Wheel Composition	51
3.1	Minic Control System	61
3.2	Cylindrical Plunge Grinding Machine	70
3.3	Grinding Machine Schematic	71
3.4	D.C. Axis Servo Motor	72
3.5	C.N.C. Set-Up Routine	73
3.6	Hydrostatic Pad	74
3.7	Hydrostatic Journal Bearing	75
3.8	Wheel Spindle Bearing Differential Pressure Transducers	76
3.9	Grinding Cycle Time Periods	77
3.10	Normal Force Identification Stage	78

LIST OF FIGURES

Page No

3.11 A.C. Set-Up Routine	79
3.12 Normal Force - Feedrate Relationship	80
5.1 Vibration Spectrum Analysis Results from the Constant Metal Removal Rate Tests	135
5.2 Vibration Spectrum Analysis Results from the Constant Normal Force Tests	146
5.3 Vibration Spectrum Analysis Results from the Short Duration Tests	157
5.4 Vibration Spectrum Analysis Results from the Wheel Dressing Tests	165
6.1 Material Relaxation Phenomenon when using a Single Point Cutting Tool	221
6.2 Material Relaxation Phenomenon when Grinding	222
7.1 Abrasive Belt Research Machine Schematic	235
7.2 Abrasive Belt Research Machine	236
7.3 Belt Tensioning Mechanism	237

LIST OF FIGURES

Page No

7.4	Graphs of Normal and Tangential Forces vs Volume Removed per Grit per Belt Revolution	238
7.5	Surface Layer Alteration Caused by Workpiece Burn	239
7.6	Structure of Thermally Unaffected Component	240
A4.1	Abrasive Belt Surface	278
A4.2	Belt Workpiece Contact Length	279

## 1.0 INTRODUCTION

Grinding is a metal removal process which employs bonded abrasives. The process is capable of producing precision components with tolerances of  $\pm 0.005$  mms on final grind dimensions and surface finishes of the order of  $0.025 - 1.6 \mu\text{m}$  [1;1972]. These accurate dimensional and surface finish results are usually obtained by two grinding cycles; a larger metal removal rate operation to remove the bulk material, commonly known as rough grinding, which is followed by an operation to achieve the desired surface integrity of the final component, finish grinding.

It has been reported [2;1981] that grinding could be a replacement metal removal process for up to 25% of work currently carried out by turning and milling. Several developments have made a contribution to this forecast: the reduced stock removal requirements of parts forged or cast to near final dimension, improvements in machines and abrasives, and improvements in machine controls. The workpiece can also be held in one clamping operation if the grinding process is used for the initial or bulk machining operation and for the finishing operation.

Workpiece materials are contributing towards the increasing importance of the grinding process. New alloy developments, particularly in the aerospace industry, are increasingly dictating manufacturing methods. These high strength and heat resisting alloys are difficult to machine by conventional milling or turning applications. The requirements for the grinding process to become more efficient and competitive to the conventional processes is, therefore, gaining greater impetus.

Optimum grinding conditions may be defined as achieving the maximum metal removal rate whilst maintaining the required surface integrity of the finished component. In order to achieve this objective the process has to satisfy certain surface integrity specifications (dimensional control, surface finish, geometrical and metallurgical condition) together with certain high productivity objectives (low scrap, low dressing cost, high reliability and maximum metal removal rates). An operation requires sufficient data so that the selection of the relevant parameters will achieve certain productivity levels and maintain the required component surface integrity. This subjective judgement has been termed the 'art of grinding' [3;1977] and represents an increasingly expensive and scarce skill.

Adaptive control presents a solution to the manual skill problem. Highly developed adaptive control technology has been successfully implemented in the laboratory [4;1977]. It has often proved, however, to be an expensive solution and the merits of the introduction have not necessarily provided an economic benefit.

Computer numerically controlled (CNC) grinding machines are being marketed by a number of manufactures. These machines are potentially dangerous because unlike any other machining process a collision between the tool and the workpiece can have disastrous consequences. Grinding wheels, particularly those operating at high speeds with large centrifugal forces, are susceptible to shock impact loads. Axial shock loads are particularly detrimental and can cause a grinding wheel to shatter. Collision detectors or gap eliminators developed for adaptive control grinding machines are vital if CNC grinding machines are to be accepted by a workforce traditionally suspicious of the grinding process.

CNC grinding machines are also providing a further impetus for adaptive control since a processor, necessary for adaptive control computations, may already be available on the machine. The costs of installing adaptive control will, therefore, be greatly reduced.

The purpose of this study is to examine the feasibility of adaptively controlling the cylindrical plunge grinding process to achieve optimum grinding conditions, i.e. achieving a maximum metal removal rate whilst maintaining the required surface integrity of the final component. Although the investigation is primarily concerned with the indirect on-line identification of the workpiece surface finish, thermal damage and the possibility of its detection is also examined.

Ground components often operate under severe environmental conditions and hence need a high degree of surface integrity. To achieve this, the grinding process should not produce undesirable defects such as micro-cracks, surface layer hardening or softening, or residual tensile stresses. At the point where a grinding wheel is in contact with the workpiece, considerable heat is generated and the majority of this energy enters the workpiece. This heat is responsible for the undesirable surface integrity defects which are termed grinding burn or thermal damage.

Direct on-line monitoring of the surface finish of a component presents many problems (see Section 2.5 Surface Integrity). A method of indirect measurement of the surface finish by monitoring various grinding process output parameters has, therefore, been investigated. The normal force intensity between the wheel and the workpiece has been identified [5;1969] as having a significant influence on the workpiece surface finish. This investigation examines the relationship between normal force and the grinding process input parameters particularly the in-feed rate.

Surface finish is also affected by wheel regenerative chatter vibrations. These vibrations produce a detrimental surface finish on the workpiece and hence the wheel must be redressed before the magnitude of vibration becomes too large. Wheel dressing limits the productivity of the grinding operation since the process needs to be interrupted to perform this function. This study investigates the influence of chatter vibrations on workpiece surface finish. It also includes determining the influence of the grinding process input variables on the rate of increase of the chatter vibration. The latter study is important since redressing frequency has a significant influence on productivity.

## 2.0 LITERATURE SURVEY

### 2.1 General Introduction

Earlier work [6;1914: 7;1915] had been carried out to determine relationships for chip thickness during grinding, but it was not until 1950 that grinding was recognised as a process similar to that of single point cutting [8;1950]. Analysis of the grinding process followed [9;1952: 10;1958: 11;1956: 12;1958: 13;1952] which used single point cutting theory to explain the grinding process. Marshall and Shaw [13;1952] found the specific energy during grinding to be 200 to 300 times higher than that required for single point cutting. Chip thickness was identified [9;1952] as the most important parameter in grinding. When the underformed chip thickness was below a certain critical value, the specific grinding energy was high since the shear strength of the chips approached the theoretical shear strength of the material. For chip thicknesses below this critical value, slip between atomic layers was thought to take place rather than the formation and movement of dislocations normally associated with single point cutting. Research carried out on laboratory grown whiskers [14;1952: 15;1951] have shown that as the specimen size decreases the strength approaches a critical value. Recent research [16;1979], however, found no evidence of high strengths to be expected from a dislocation free lattice. Malkin and Joseph [17;1975] showed that the minimum specific energy in grinding was close to the melting energy per unit volume of workpiece material. This particular value of minimum energy is attributed to the severe constraint imposed by the highly negative rake angles in grinding. When cutting steel with a single diamond grit, Sargarda and Khimach [18;1973] showed that at high grinding speeds, the cutting temperature asymptotically approached the melting point of the workpiece, which further supported the minimum energy hypothesis.

Various workers [9;1952: 11;1956: 19;1955: 20;1960] have all derived equations for the calculation of chip thickness in terms of process variables and grinding wheel characteristics. The variety of equations arising from these studies illustrates the complexity of the grinding process.

The validity of single point cutting models for the grinding process have been questioned [21;1966: 22;1966]. Such theories require assumptions for average rake angles, shape of the chip, shape of the grain and distance between grains etc. The assumption that a single true chip is produced by each grain edge has also been a subject of critical discussion [21;1966: 22;1966]. These researchers indicate that single abrasive grains may have numerous cutting edges of varying rake angles and hence if a chip is produced, then more than one chip might be produced by a single grain.

Three distinct grinding mechanisms have been reported by Hahn [23;1963]:-

- (i) rubbing, where grains remove little or no material and cause elastic/plastic deformation of the work material.
- (ii) ploughing, a mechanism where grains plough through the work material causing it to plastically deform along the direction of the cutting vector, metal particles are 'broken off and thrown up on the edges of the resulting grooves' with little metal removal.
- (iii) cutting, where fracture takes place slightly in front of the grain in the plastically stressed zone, causing chip formation and producing fairly large metal removal rates.

Hahn [23;1963] stated that the formation of wear areas on wheel surface grains reduces the stress concentration at the leading edge of the grain. As a result, higher force intensities are required to exceed the ploughing-cutting transition as the geometry of the chip is dramatically altered. The occurrence of rubbing, ploughing or cutting depends on the number and geometry of active cutting edges on the wheel surface, which in turn depend on the characteristics of both the wheel and work material and the machining parameters. Nakayama and Shaw [24;1967-68] showed that the number of active cutting edges decreases very dramatically for small chip thicknesses. Single point cutting tests using diamonds and abrasive grains were performed to investigate the size effect more accurately [25;1974]. Ploughing rather than cutting was observed as wear lands developed on the cutting edge for small depths of cut and also at the commencement of deep cuts. Specific energy was found to decrease by as much as 50% on the transition for ploughing to cutting. A paradoxical result was found when testing 'hard' ( $R_c 63$ ) and 'soft' ( $R_c 34$ ) bearing steel. Specific energies for both 'states' of the steel were approximately equal. This was attributed to the 'soft' steel being more ductile than the 'hard' steel and hence involving greater strain in the deformation of chips. What the 'soft' steel lacked in strength was compensated for by its greater ductility.

Kannappan and Malkin [26;1972] investigated the effects of grain size and operating parameters on the mechanics of grinding. It was proposed that cutting energy could be partitioned into chip formation energy and ploughing energy. Malkin and Joseph [17;1975] used the partition concept to explain the increase in specific energy with decreasing chip thickness.

It was proposed [17;1975] that, at large stock removal rates (at 0.05 to 0.08mm depth of cut), the ploughing and the sliding energy components became negligible and the minimum grinding energy is equal to the specific chip formation energy. It was assured that the ploughing and sliding components make an increasing contribution to the overall specific energy as the depth of cut is reduced. A number of parameters influence the grinding operation. Determination and verification of an equation to include all these parameters would require a considerable quantity of grinding data. The number of grinding tests to acquire this data could be drastically reduced if some relevant basic quantity, combining a number of grinding parameters, could be obtained. Shaw [28;1971] proposed an equation which included a term known as the undeformed chip thickness. This volume continuity equation was defined as:

Stock removal rate = mean chip volume x number of cutting edges/  
unit time

$$(V_w \cdot a \cdot b) = (l_c \cdot h \cdot b) \cdot (V_s \cdot c \cdot b)$$

where  $V_w$  = workpiece speed

a = depth of cut

b = wheel width

$l_c$  = mean undeformed chip length

h = mean undeformed chip thickness

b = mean undeformed chip width

$V_s$  = Wheel speed

c = number of active cutting edges per unit wheel surface

Several attempts have been made to define the undeformed chip thickness mathematically [29;1971]. The disadvantage with this parameter, however, is that it cannot easily be measured because knowledge of the cutting edges of the wheel cannot be eliminated from the equation. For this reason the Grinding (G) Group of CIRP [29;1971] used an equation of the form

$$h = A.a.\frac{V_w}{V_s}$$

where A was a non-dimensional factor influenced by the wheel and dressing characteristics.

Despite problems in its determination, the undeformed chip thickness was found to be an important parameter [30;1973]. A semi-empirical equation was presented for the average chip thickness during grinding. It was found that surface finish had a better correlation with average chip thickness than with the metal removal rate.

Snoeys, Peters and Decneut [31;1974] demonstrated that a large amount of data referring to cylindrical grinding could be correlated in terms of a parameter denoted as the equivalent chip thickness, which was defined as the product of the wheel depth of cut and the ratio of the work speed to the wheel speed. It should be emphasised, however, that such relationships apply only to particular wheel-workpiece and dressing combinations. Nevertheless grinding charts were produced [32;1975] containing information on how to vary grinding parameters (wheel and workpiece velocity and infeed rate) which would achieve particular requirements with regard to surface finishes, work accuracy, minimum cut and required surface integrity.

These charts (Figure 2.1) have equivalent chip thickness as abscissa and represent relationships between force, surface roughness, grinding ratio, tool life and the equivalent chip thickness.

## 2.2 Grinding Forces

The grinding force, or more correctly, the grinding force intensity (force per unit width of wheel - workpiece contact) is a very important parameter in the grinding process. Hahn et al [33;1966] stated that the stock removal, the wheel wear and the surface finish are primarily determined by the normal force intensity between the wheel and the workpiece. Plunge grinding infeed rate, G-ratio, rate of wheel wear and surface finish were shown to be related to normal force intensity for a number of wheel-workpiece combinations. Charts produced from these relationships were used to define a grinding cycle which comprised of two distinct portions; a roughing section and a finishing section. Expanding this work, Hahn and Lindsay [5;1969] also considered the thermal damage phenomenon relative to the normal force intensity. It was experimentally established that the most influential factors in determining surface finish in precision grinding were the interface force intensity between the wheel and workpiece and the manner in which the wheel was dressed.

Marshall and Shaw [13;1952] developed a surface grinding dynamometer which was capable of measuring normal and tangential forces separately. This work was the earliest attempt to examine the influence of grinding parameters on the individual grinding force components.

The forces were observed to be proportional to the width of the workpiece, the depth of cut and the table speed, and inversely proportional to wheel speed. A parameter, specific energy, defined as the product of tangential force and wheel peripheral speed, divided by the amount of metal removed per minute, was proposed as a means of interpreting grinding data.

An analytical force expression for the different types of grinding grit shapes was developed by Kobayashi [34;1961]. It was found that wheel glazing and loading both increase grinding forces whilst grit fracture decreased the grinding forces. Hahn [35;1956] analysed the grinding forces and proposed a rubbing end grain hypothesis. Previous research [9;1952: 11;1956: 13;1952] using single point cutting theory, considered forces to be generated by chips acting against the rake face of the grit and neglected any frictional forces on the clearance face of the grit. Hahn [35;1956], however, suggested that the cutting forces on the rake of the grains were negligible: rubbing forces on the clearance face of the grains were of much greater significance. Grisbrook [36;1960] confirmed these findings. Armarego and Brown [37;1962] showed that the rubbing forces were the major cause of the high specific energies encountered during the grinding process.

Grisbrook et al [38;1962] examined the relationship between specific energy and metal removal. This work illustrated that the specific energy decreased almost linearly with an increasing metal removal rate, once a certain level of metal removal rate was achieved. These researchers also proposed a parameter, the coefficient of grinding, which was defined as the ratio between the tangential and the normal grinding forces. Cebalo [39;1977] proposed an efficient range of grinding coefficient values.

A coefficient below 0.4 results in the production of grinding surface burn and surface cracks because in such conditions frictional forces rather than cutting forces predominate. When values of the coefficient greater than 0.6 occurred, excessive wheel wear was experienced. Optimum grinding conditions were thus proposed to lie in the region  $0.4 < \mu < 0.6$ . Lichun and Jizai [40;1980] experienced similar results. The ratio between normal and tangential forces were analysed with respect to chip formation forces and frictional forces. The value of the grinding coefficient was generally found to lie in the range 0.2 - 0.59.

Numerous studies [36;1960: 41;1970: 42;1971: 43;1972: 44;1974: 45;1978: 46;1981] have observed the relationship between grinding forces and time. Grisbrook [36;1960] concluded that forces usually increased as grinding proceeded from a freshly dressed wheel. Constant grinding force also occurred in a minority of the tests. Bhattacharyya [41;1970] explained these findings by examining the predominant wear mechanism. It was concluded that forces increase when the wear mechanism was attritious whereas they remained constant for the fracture type of wear mechanism. Malkin and Cook [42;1971] also observed grinding forces to increase when the wear mechanism was attritious. Both the horizontal and the vertical force components increased linearly with wear flat area until workpiece burn occurred. The linear increase in the vertical force component (normal force on the surface grinding machine) was attributed to a constant contact pressure between the wear flats and the workpiece. The horizontal force component increased linearly because the grinding coefficient remained constant until surface burning was observed. In their investigation of dressing depth of cut on the performance of an alumina grinding wheel, Pacitti and Rubenstein [43;1972] observed four different grinding force-time relationships (Figure 2.2)

- STAGE A: Characterised by high wheel wear rate and a reduction of grinding force as grinding proceeds.
- STAGE B: Characterised by low rate of wheel wear along with a slow increase in grinding force.
- STAGE C: Characterised by an increase in wheel wear rate and a rapid increase in grinding force.
- STAGE D: Characterised by a decrease in grinding force while the wheel wear rate may be higher/lower than than of Stage C

Makino [44;1974] also observed a decrease in the normal grinding force as chatter became severe. In the case of the attritious wear mechanism, the normal force was found to rise gradually until saturation was reached, and then the magnitude of the force began to decrease. This decrease was used to signify the end of useful wheel life since it coincided with severe chatter. Makino [44;1974] confirmed the findings of Bhattacharyya [41;1970] when examining forces during the fracture wear mechanism. The force was observed to remain constant between dressings. More recently Fletcher [45;1978] discovered forces to rise immediately after redressing a wheel, remain constant and then finally decrease. It was stated that the most efficient metal removal occurred during the period when the grinding forces remained constant.

All the findings [36;1960: 41;1970: 42;1971: 43;1972: 44;1974: 45;1978] essentially follow one of two trends. Forces remain constant for fracture wear whereas for attritious wear, forces increase, saturate and finally decrease. No attempt has been made to explain this decrease. The author proposes that a reduction in forces could arise from two sources. As the wear flat area of individual grits increases the workpiece surface is thermally damaged [42;1971].

Thermal damage of the work piece could result in a reduction in the material flow stress and hence a reduction in the grinding forces. An alternative explanation could arise from the wear mechanism. As the grinding force increases with an increasing wear flat area, a transient point might be reached which could cause the wear mechanism to change from attritious to fracture wear. A reduction in grinding force would follow as new sharp cutting edges were generated. This new grinding force level may not be sufficiently large to sustain fracture wear and hence attritious wear would again predominate. A similar cyclic pattern of increasing, peaking and decreasing forces was observed by Makino [44;1974]. The thermal damage hypothesis is an equally relevant explanation for this cyclic force pattern. A reduction in flow stress would result in lower forces and thus lead to a lower grinding temperature. As grinding progressed, non-thermally damaged material would eventually contact the grits. This thermally unaffected material would have a higher flow strength than the thermally damaged material and hence the forces would once again rise, wear flats develop and workpiece burn eventually occur.

The normal component of the grinding force is responsible for local wheel-workpiece deflections. These deflections can have a considerable affect upon precision grinding results. Hahn [47;1955] first postulated the elastic deflection on individual grains in a vitrified wheel. Nakayama, Breckner and Shaw [48;1971] conducted static loading tests on grinding wheels and estimated the magnitude of elastic deflections of grains to be of the same order of magnitude as the undeformed chip thickness. These significantly large deflections (50 to 100 $\mu$ m) not only influence the size accuracy of the ground surface, but also increase the energy required when grinding by increasing the number of active cutting edges at the wheel-workpiece interface [49;1980].

Many of these cutting edges slide on the workpiece without removing material. Kumar and Shaw [50;1981] discovered that the influence of local wheel-work deflections on contact length was relatively minor and that the predominant effect was due to wheel deflection and not work deflection. More work, however, is necessary to explain the behaviour and mechanisms of the contact deflections in dynamic grinding conditions [49;1980].

Hahn [51;1981] examined the role of normal grinding force on geometric accuracy and surface integrity of the workpiece. The force between the wheel and the workpiece at which cutting ceases is defined as the threshold force. This threshold force often results in dimensional errors, out of roundness of the workpiece, changes in surface finish etc., and is a function of the wheel speed, the difference in curvature between the wheel and workpiece, the work material, the wheel and the coolant. Production grinding cycles often consist of a rough grinding portion followed by a spark out portion to obtain size and surface finish. When such a cycle is instigated no stock removal will commence until the wheel head and work head 'springs' have been compressed sufficiently to cause the induced normal force to exceed the threshold force. During the spark out process, the interface normal force intensity decreases exponentially to the threshold force. Variations in the threshold force from one component to another will cause a sizing error at the end of the spark out period. Hahn [51;1981] reported that variations in the threshold force occur frequently during internal grinding operations. This variation is especially significant at wheel change time when a new large wheel replaces the used, smaller wheel. The corresponding change in equivalent diameter is the predominant reason for this variation.

Recent research into grinding forces has concentrated on developing mathematical models which link the forces experienced during grinding with various process parameters. Werner [52;1978] derived a grinding force model in which wheel speed, work speed, depth of cut, equivalent wheel diameter and the static edge density were the independent variables. This model was then used to assess the applicability of advanced grinding techniques such as high speed grinding and creep feed grinding on different work materials. High speed grinding was only recommended for a special group of work materials which are unproblematic when grinding at conventionally low speeds, e.g. bearing steels. It was suggested that austenitic steels, stainless steels, nickel based alloys, brittle-hard materials, e.g. tungsten carbide and soft-ductile materials, e.g. copper should not be ground at high speeds. When grinding these materials the forces remain virtually constant as the cutting speed is increased and hence the increased rate of energy input will cause the work surface temperature to increase proportionally to the speed. Materials which tend to load the surface of the grinding wheel, such as low carbon steel, aluminium alloys, copper and copper alloys, also show increased surface temperatures. When using creep feed grinding, conventionally low wheel speeds were recommended for all materials. Creep feed grinding also requires the use of softer wheels than conventional grinding because the average load per individual cutting edge is lower.

The relationship between grinding forces and process parameters for varying workpiece materials were determined experimentally by changing the wheel speed, work speed and the depth of cut, and measuring the normal and tangential grinding forces [40;1980].

Chip formation force constitutes the major force component when easy-to-grind materials such as medium carbon steel or bearing steel are ground. When grinding materials which are known to be difficult-to-grind such as high speed steel, frictional force was observed to be larger than chip formation force. The value of the total grinding force is thus much greater for difficult-to-grind materials and hence is one of the reasons for classifying these materials 'difficult -to-grind'. Lichun and Jizai [40;1980] also examined the role of equivalent chip thickness. Contrary to the findings of the CIRP Grinding (G)-Group [31;1974: 32;1975], equivalent chip thickness was found to be unable to determine the value of the grinding force in all grinding conditions. Equivalent chip thickness was only capable of predicting grinding force for a given material and condition when a 'sharp' wheel is grinding an 'easy-to-grind' material. In such conditions, the chip formation force influences the total force to a greater extent than frictional force.

Dynamometers have been developed or have been commercially available for monitoring normal and tangential force components in the surface grinding operation [13;1952: 38;1962: 41;1970: 42;1971: 43;1972: 45;1978: 46;1981]. The author is not aware of any commercially available dynamometer for a similar study of the force components in cylindrical grinding. Vertical and horizontal forces generated at the wheel/workpiece interface during cylindrical grinding have been measured [39;1977: 44;1974] by the use of strain gauges mounted on the work holding centres. During grinding the centres are deflected, which causes a change in the resistance of the strain gauges, resulting in a voltage difference across the Wheatstone bridge strain gauge network. This change of voltage is proportional to the workpiece deflection and hence proportional to the deflecting force.

There are a number of disadvantages with this method of force measurement which make it unsuitable for use in a production environment. The output of the strain gauge Wheatstone bridge network is proportional to the deflection of the centres. This deflection is dependent on the stiffness of the centres, the load applied and the stiffness of the workpiece. For a given load and given centre stiffness, the output will be dependent on the workpiece stiffness. The system must, therefore, be calibrated for a particular workpiece and re-calibrated every time a different shape or size workpiece is to be machined. A further requirement of strain gauges is that for maximum accuracy of measurement, the output of the strain gauge circuits needs to be as high as possible, i.e. the deflection of the centres must be as large as possible. This is in conflict with the basic requirement of grinding; that for good dimensional accuracy the method of work holding must be as rigid as possible.

### 2.3 Grinding Temperature

The temperature of the wheel/workpiece interface during grinding is a very important parameter in the grinding process. Moran [54;1967] observed that the grinding process specific energy was expended mainly in the form of heat and hence heat generation is significant because of the high specific energies associated with the process [13;1952]. Heat generation arises from a number of sources [55;1972]:-

- (i) Plastic deformation of the work material
- (ii) Friction between the chip and the grit
- (iii) Friction between the grit and the workpiece.

These sources combine to influence the work surface integrity and the cutting characteristics of the wheel. Surface and sub-surface material properties can be altered during the grinding process. If the temperature is sufficiently high, workpiece burn will occur. Grinding temperature has also been linked to the workpiece/wheel adhesion problem [55;1972]. Three distinct mechanisms were found to occur when grinding workpieces exhibiting high adhesion.

- TYPE I     Grits become worn by attritious wear and the temperature in the grinding zone was relatively high.
- TYPE II    Occurring at increased metal removal rates. Lower grinding temperatures were experienced and isolated, tiny areas of workpiece material adhered to the grits.
- TYPE III   Occurring at still higher metal removal rates. Areas of the wheel, large in comparison to the size of the grit, were covered by adherent work material.

During the TYPE III mechanism the grinding temperature was relatively low. Yossifon and Rubenstein [56;1981] explained these mechanisms by considering the oxide layer on the surface of the work material. The high grinding temperatures of the TYPE I mechanism, caused the oxide layer to form at a sufficiently high rate to prevent the welding of work material to grinding grits. Reducing the grinding zone temperature (TYPE II and III) reduces the rate of oxidation and hence lowers the degree of protection.

Thermal damage of the workpiece surface has received attention from a number of researchers [5;1969: 57;1974: 58;1975: 59;1974: 60;1978: 61;1978: 62;1976]. Hahn and Lindsay [5;1969] proposed a correlation between thermal damage and normal force intensity. The authors concluded that thermal damage of workpieces can be controlled or avoided by grinding at relatively high work speeds under controlled force intensities with wheels whose sharpness is maintained above certain levels. Forces were observed to rise rapidly when the initial workpiece burn was observed [42;1971]. This was confirmed by Kirk [57;1974] who defined three regions of grinding activity:

- (i) preburn - the region of low forces
- (ii) transition - in this region, forces rapidly increased, and the workpiece showed a visible 'burn' area developing.
- (iii) Afterburn - the region beyond uniform workpiece burn in which the forces are large and no longer change

The end of period 1 was designated the end of useful wheel life.

Workpiece burn can be difficult to visually detect and hence research has concentrated on methods of preventing this phenomenon. Lur'e [58;1975] proposed an algorithm for maximum stock removal without thermally damaging the workpiece. The algorithm considers thermal damage to be a function of surface layer temperature and the heating time of the ground surface and proposes a table of maximum feed rate values to achieve burn free conditions. The algorithm is, however, limited because it considered only one material type and assumes that workpiece burn is a steady state problem independent of the grinding wheel condition.

This is unlikely to be the case. Hahn and Lindsay [5;1969] recognised the sharpness of the wheel as being an important parameter when considering workpiece thermal damage. Expanding on grinding energy research [59;1974], Malkin [60;1978: 63;1974] also proposed an algorithm to prevent thermally damaged workpieces by limiting the grinding power or energy. The burning threshold was found to correspond to reaching a critical zone temperature. On the basis of this hypothesis and a thermal analysis of the grinding process, Malkin obtained an expression for the critical grinding energy input at the onset of burning in terms of grinding parameters and the workpiece material characteristics. It was stated that this limiting energy equation could be used to control metal removal rate in an adaptive control constraint system to achieve burn-free workpieces.

It has been reported that abrasive grinding may damage a workpiece [5;1969: 57;1974: 58;1975: 59;1974: 60;1978] but the physical phenomenon and the metallurgical factors influencing its occurrence have received considerably less attention. Torrance [61;1978] reported that the surface of a workpiece is always altered metallurgically to some extent by the passage of a grinding wheel. Plastic flow produced by the stress ahead of the grit, which cause chips to form when the grit is favourably placed, leave the workpiece surface in a state of plastic strain. Redundant work is done in removing metal in this way, requiring considerable energy at the contact between a grinding wheel and the workpiece. Powell and Howes [64;1978] stated that if the rise in power at the contact zone is sufficiently high, it cannot be dissipated without an excessive rise in workpiece temperature, which may cause grinding burn or cracks. Malkin [62;1976] reported that workpiece burn was associated with wear flat area on the grinding wheel surface.

Workpiece burn commences when the wear flat area reaches a critical value. As the wear flat area increases, there is a proportional increase in the sliding energy input during grinding, thereby causing the grinding temperature to rise. The burning condition occurs when the wear flat area becomes sufficiently large such that a critical grinding zone temperature is reached.

Thermally damaged workpieces often exhibit cracks in addition to workpiece burn. Torrance [61;1978] observed cracks only in burnt workpieces and never in unburnt specimens. The tendency of the workpiece to crack could be reduced by modifying the method of heat treatment prior to grinding. This would reduce boundary quenching strains. Thermal cracks are the result of residual tensile stresses present in the surface layer of the component. These stresses may develop due to the rapid cycle of heating and cooling during the grinding process [59;1974]. As the grinding zone is heated a reduction in the yield strength of the component will cause it to plastically distort. Cooling will result in plastic strain and hence residual tensile stresses will result. These tensile stresses may produce surface as well as sub-surface cracking which could lead to a catastrophic failure when subjected to cyclic loading. Torrance [61;1978] recommended that ductile workpieces, designed to support a low stress, may be usable even in a state of high tensile stress, since the stress may be relieved by plastic flow in service; but hard, highly stressed components, such as bearing surfaces, should never be used in service when damaged in anyway. To avoid tensile residual stresses a "gentle" grinding process is necessary [5;1969: 61;1978]; favourable residual compressive stress are present after such a process. Despite previous research [5;1969: 57;1974: 58;1975: 59;1974: 60;1978; 61;1978: 62;1976] more work is necessary since the potential of thermally damaged components cannot yet be predicted satisfactorily [65;1981].

Creep feed grinding is less likely to experience workpiece thermal damage. Some researchers [52;1978: 66;1980: 67;1978] have explained this phenomenon. With the increased depth of cut in creep feed grinding, the surface temperature first reaches a maximum and then declines. The generated heat to an increasing amount is removed with the chips and the remainder of the heat is dissipated deeper into the workpiece.

Thermocouples have been employed [68;1952: 69;1954: 70;1972] in the measurement of grinding process temperatures. Outwater and Shaw [68;1952] used the wheel/workpiece interface as the hot junction of a thermocouple circuit. The results indicated that surface temperatures were far in excess of the transformation temperatures in steel. To measure sub-surface temperatures embedded thermocouples were used [69;1954]. Sauer [70;1972] used thermocouples inserted into the workpiece to develop a temperature predicting model. Thermocouples, however, cannot be used in a production environment: it is not practical to set thermocouples into workpieces to measure the interface temperature. Malkin and Anderson [59;1974] questioned the validity of thermocouple measurements. It was claimed that results from such measurements are limited by the fact that the temperature probes are always much larger than the cutting area of the individual abrasive grains. Difficulties associated with such temperature measurement are due to the small area of grinding energy input and the existence of very steep temperature gradients with respect to both time and space. Unless the temperature probe is very much smaller than the cutting area of the individual abrasive grain, any measured temperature distributed represents only a distribution of some average temperature. Because of such difficulties, many attempts have been made [23;1963: 71;1961: 72;1972] to predict grinding interface temperatures analytically by using Jaeger's moving heat source theory [73;1942].

The temperature of the grinding zone is affected by grinding fluids. These fluids affect the grinding temperature by providing both lubrication and cooling functions. The majority of the energy input into the grinding process is transformed into thermal energy at the cutting zone [59;1974]. This energy must be dissipated by the grinding fluid if grinding burn is to be avoided [64;1978]. Mayer and Shaw [74;1957] compared the relative merits of oil- and water- based fluids. Oil-based fluids gave lower interface temperatures because of their superior lubrication properties whereas water-based fluids gave better overall cooling properties. This work confirmed the research of Hahn [35;1956] which concluded that the main advantage of grinding fluids is the lubrication function which reduces the friction component and hence the grit/workpiece interface temperature.

For grinding fluids to perform efficiently, they must penetrate into the grinding zone. The conventional nozzle technique of applying coolant is relatively ineffective [75;1962]. Careful selection of the direction of the grinding fluid application, however, does yield improvements. Such improvements are possible by directing the grinding fluid along the periphery of the wheel for 2-3 inches before it reaches the grinding zone. Several researches [75;1962: 76;1963] accomplished this by using a shield placed over the grinding fluid delivery nozzle.

The problem of grinding fluid penetration into the grinding zone is more acute for high speed grinding. Konig et al [77;1971] explained the problem of an air layer which accompanies the wheel at its circumference, particularly at high wheelspeeds. To penetrate the grinding zone under these conditions it is necessary to deflect the air layer and employ a high pressure coolant delivery system [77;1971]. This combination was found to be very successful.

## 2.4 Grinding Chatter

In precision production grinding operations, chatter can cause poor workpiece quality and may also limit the production rate because frequent wheel re-dressing would be required [78;1979]. Three distinct types of vibration are associated with the grinding process [79;1974: 80;1966]:-

- (i) forced vibration
- (ii) transient vibration
- (iii) self excited vibrations

Forced vibrations are due to wheel unbalance and are always present because a wheel can never be perfectly balanced. Transient vibrations are experienced in reciprocating table surface grinding because of the impact loading of this interrupted type of grinding process. It is with the third type of grinding vibration, self excited vibration, that this study is primarily concerned.

Self-excited vibration or chatter can be divided into two categories:

- (i) wheel regenerative chatter
- (ii) workpiece regenerative chatter.

Wheel regenerative chatter arises from local wheel wear fluctuations. A small vibrating disturbance of the grinding wheel will cause a fluctuation in the force between the wheel and the workpiece. This causes a local fluctuation of the instantaneous amount of wheel wear producing a transient force variation on subsequent whole revolutions of the wheel and further local wheel wear fluctuations.

If the system is stable these disturbances disappear. If, on the other hand, the system is unstable, these minor disturbances increase. Many researchers [81;1969: 82;1975: 83;1977] have concluded that in the majority of cases grinding is performed in the unstable region. There are indications that wheel regenerative vibrations are present during all stages of the grinding operation [84;1954], but fortunately this level of instability is low for much of the grinding time, and hence satisfactory results can be achieved before this level of unstable activity can cause unsatisfactory work conditions.

In workpiece regenerative chatter the waviness occurs on the workpiece as in other machining operations. A small disturbance in the system causes a small transient wave to be ground onto the workpiece. One revolution of the workpiece later, this wavy surface acts as a driving force to cause the system to again vibrate. Under unstable conditions a small wavelet can develop and extend around the workpiece circumference. Workpiece regenerative chatter occurs at the start of the grinding operation [85;1977] whereas wheel regenerative chatter occurs gradually. It is very important, therefore, to obtain stability with regard to workpiece regenerative chatter particularly in finish grinding operations. High grinding forces, large wheels, low workspeeds and soft wheels all tend to prevent workpiece regenerative chatter [78;1979].

Many researchers [79;1974: 82;1975: 86;1959: 87;1976] have investigated wheel regenerative chatter. Peklenik [86;1959] stated that worn grains were responsible for force fluctuations and hence for wheel regenerative chatter. Ranatunga [79;1974] concluded that the combination of attritious and fracture wear on a wheel caused wheel lobing: the greater wear rate associated with fracture causes parts of the wheel to be worn away faster and hence the wheel loses concentricity.

The product of the number of these waves and the wheel rotational speed, was found to be equal to the frequency of the self-excited vibration [82;1975]. This was confirmed by Fukuda [87;1976]. This work suggested that the frequency components observed in chatter are integral multiples of the wheelspeed frequency. These phenomena are not associated with all wheels. No waves were generated when using extremely soft wheels [88;1968]. The possibility also exists for a reduction in the amplitude of wheel lobing [89;1972]. In both of these cases fracture would be the dominant wear mechanism.

Kaliszer [90;1970] applied various degrees of unbalance to wheels to analyse wheel regenerative chatter. The increased metal removal rate from the unbalanced section of the wheel was found to cause local wheel wear fluctuations, which in turn, promote the formation of waves around the wheel circumference. Increased amounts of unbalance were found to cause an increased rate of lobing. In this work, tests were also carried out on a wheel divided into different hardness sections. Waves were found to initiate at the hard spots and spread around the wheel. It was, therefore, concluded that "hard spots" in a wheel can be considered as a potential source of self-excited vibrations.

Increasing levels of self-excited vibrations have been associated with deteriorating surface finish of the workpiece [78;1979: 91;1974: 92;1971]. Hahn [78;1979: 93;1969] classified grinding vibrations by examining the workpiece surface. Chatter patterns were classified as:

- (i) spiral, caused by vibration during dressing or transverse feed.
- (ii) mottled, a random pattern caused by variations in the local wheel hardness
- (iii) straight line.

An observation of the characteristic of the straight line chatter pattern, i.e. the wavelength, enabled the frequency of the vibration to be determined. If the frequency corresponded to the wheelspeed the vibration was classified into one of two types:

- (i) wheel or spindle unbalance
- (ii) geometric run-out of the wheel surface at the point of grinding.

If the frequency did not correspond to the wheelspeed a further three categories were classified:

- (iii) general forced vibrations due to pulleys etc.
- (iv) wheel regenerative type in which the straight line chatter frequency is independent of the wheel speed but corresponds approximately to the natural frequency of the wheelhead/workpiece system
- (v) work regenerative type where the straight line frequency corresponds to the natural frequency but where the workpiece develops a wavy surface.

Theoretical evaluations of regenerative vibrations have been performed by a number of researchers [81;1969: 90;1970: 94;1969: 95;1970]. The application of feedback techniques in the analysis of machine tool stability and the prediction of the onset of chatter vibrations is an invaluable tool for testing and comparing machine tool structures. However, several complications exist in applying these feedback techniques for grinding operations [81;1969]. The wear pattern of the grinding wheel causes fluctuations in the depth of cut. This should be incorporated into any analysis as a second feedback loop.

A second complication arises from the wheel/workpiece interface zone: the relationship between grinding force and the contact area deformation will have an influence on the stability and must, therefore, be considered. A third complication concerns the interpretation of the theoretical analysis. The issue is not 'how to stabilize grinding' but 'how to delay the instability problem'. Several researchers [90;1970: 94;1969: 95;1970] also used closed loop representations of the grinding process to determine stability conditions for cylindrical grinding. Peters and Aerens [96;1977] used the theoretical model for determining grinding chatter developed by Snoeys and Brown [81;1969]. This work established that an increase in the wheel/workpiece contact stiffness or wheelspeed increases grinding wheel life whilst an increase in grinding wheel width or wheel diameter decrease wheel life.

Although the previous studies [81;1969: 90;1970: 94;1969: 95;1970: 96;1977] have considered the effect of fluctuating depths of cut associated with the wear pattern of grinding wheels, these studies did not consider the effects of differing depths of cut for various sections of the grinding cycle. Takayanagi et al [97;1978] investigated the stability of a practical grinding cycle in which the depth of cut increased gradually at the beginning of the grinding, from zero to the infeed rate, and decreased during the period of spark out. The source of the varying depth of cut in a practical grinding cycle is the combination of the elastic deformation of the grinding wheel and the mechanical structure of the grinding system. This work concluded that the occurrence of workpiece regenerative chatter can be expected to occur during periods of small depths of cut (at the beginning of the cycle and during spark out) even if the system is stable during the steady state phase with respect to the depth of cut.

This confirmed the work of Inasaki et al [83;1977] who stated that the grinding process becomes unstable during spark out.

All the theoretical and experimental research into the stability of the grinding process [81;1969: 82;1975: 83;1977: 90;1970: 94;1969: 95;1970: 96;1977: 97;1978: 98;1982] agrees that most cylindrical grinding is performed under unstable conditions. There are indications that regenerative vibrations are present at all stages of the grinding operation [84;1954] but fortunately this level of instability is ineffectual for much of the actual grinding time, enabling satisfactory results to be achieved before the level of unstable activity can cause poor working conditions

Hahn [78;1979] gives the following rules for eliminating wheel regenerative chatter.

1. dress the wheel more frequently
2. reduce the feedrate or force intensity
3. increase the equivalent wheel diameter
4. increase the stiffness of the wheel and/or workpiece supports.
5. reduce the width of cut or wheelface
6. reduce the wear rate of the wheel by using grinding fluid
7. reduce the workspeed.

Several of these, however, may not be acceptable in a production environment. Assuming, therefore, that production grinding cycles will have an unstable nature and that as grinding proceeds, the amplitude of vibration will increase, the emphasis of research should be placed on delaying the build up of self-excited vibrations rather than trying to prevent their occurrence [81;1969].

Bartalucci et al [99;1973] proposed a method of delaying the onset of chatter vibrations. During the grinding operation the wheel speed was altered by forcing the d.c. wheel spindle motor to follow a sinusoidal or square wave input. This research showed that provided action is taken immediately after re-dressing a wheel, before the build up of chatter amplitude takes place, changes in the wheel speed can substantially delay the occurrence of severe chatter. Cegrell [100;1973] also varied the wheel speed in a study of the grinding process metal removal rates. A 50-60% improvement in the metal removal rate was possible, without violating a vibration constraint, when variable wheelspeed tests were compared to constant wheelspeed tests. It can be concluded from this that varying the wheelspeeds prevents the level of vibration from increasing. Takayanagi et al [97;1978] showed that periodically varying the workspeed was effective in delaying or even preventing the onset workpiece regenerative chatter. This was even found to be successful during the periods of the cycle when the system is most susceptible to workpiece regenerative chatter: during the periods of small depths of cut, at the beginning of the cycle and during spark out.

Chatter in a grinding operation, manifests itself as an increasing vibration amplitude at a particular chatter frequency. Hahn [101;1953] and Doi [102;1958] suggested that this frequency should coincide with one of the natural frequencies of the system. Ranatunga [79;1974] agreed with these findings. The frequency of the chatter vibration was found to be the natural frequency of the wheel/workpiece configuration. Kaliszer [90;1970] reported that the chatter frequency was close to but higher than this natural frequency.

A reduction in the chatter frequency has been reported by a number of researchers [87;1976: 90;1970: 103;1969]. Kaliszzer [90;1970] explained this phenomenon by relating it to the wheel contact stiffness. As the amplitude of vibration increases, the magnitude of the wheel contact stiffness will decrease, causing a reduction in the natural frequency of the wheel/workpiece system. The chatter frequency will, therefore, decrease as its magnitude increases.

The previous studies [81;1969: 83;1977: 90;1970] concluded that the grinding process is generally an unstable one. Regenerative vibrations increase from a relatively low level after re-dressing the wheel [84;1954] and saturate [104;1969]. Banek [82;1975] observed a stage beyond the saturation of chatter vibrations. Chatter amplitude was found to increase in proportion to the grinding time and then if the conditions were favourable, a fall in the level of vibration was experienced. Banek stated that this indicated self-sharpening of the grinding wheel. This phenomenon was not reported by previous researches [81;1969: 83;1977: 84;1954: 92;1971] since research into precision grinding is unlikely to experience the phenomenon: the small depths of cut associated with precision grinding operations are likely to produce unstable conditions [83;1977: 97;1978]. A second explanation could arise from the wear mechanism. The small depths of cut in precision grinding are unlikely to produce a sufficiently high force for self-sharpening to occur.

The magnitude of the chatter vibration has been proposed as a criterion for wheel life [92;1971: 105;1959]. Lurie [105;1959] proposed that the magnitude of the chatter vibration could be monitored and compared against a limiting value. Once the monitored level exceeded the constraint an automatic dressing cycle could be initiated.

The magnitude of chatter vibration to initiate such a cycle, could be determined by some unacceptable level of surface finish since increasing levels of self-excited vibrations have been associated with a deterioration in surface finish [78;1979: 91;1974: 92;1971]. To use self-excited vibrations to indicate the end of useful wheel life, the frequency at which the chatter occurs must be identified and the magnitude at this frequency monitored. Vibrations associated with the cylindrical grinding process have been monitored by accelerometers situated on the machine centres [44;1974: 100;1973: 104;1969]. This system is easily calibrated and is reliable enough to be used in a production environment.

## 2.5 Surface Integrity

The grinding process can have a detrimental effect on the performance of a component by causing workpiece surface damage. Field and Koster [106;1972] identified this damage as microhardness changes, phase changes, plastic deformation, microcracks, and residual stresses. Residual stresses can, in turn, affect the distortion of components. These surface integrity alterations primarily result from a high temperature and the large temperature gradients generated by the grinding process. Nee and Tay [107;1981] established a relationship between the peak grinding temperature and the surface integrity deterioration.

Generally ground components operate under severe environmental conditions. Surface integrity must, therefore, be guaranteed to avoid premature failure of the component in service. Detrimental temperature related workpiece surface alterations must be avoided and residual compressive stresses should be present in the workpiece on completion of the grinding operation [61;1978].

Hahn and Lindsay [108;1973] observed that favourable residual compressive stresses resulted from finish grinding operations. When grinding with sharp wheels at low infeed rates to achieve a good surface finish, the residual stresses were compressive rather than tensile. Three qualitative grinding operations have been identified [106;1972]: gentle, conventional and abusive. Gentle grinding conditions (low infeed rates etc.) produce good surface finishes, almost no evidence of surface layer alterations and residual compressive stresses, whereas abusive grinding (high infeed rates etc) produce poorer surface finishes, workpiece burning and residual tensile stresses which can lead to surface and sub-surface cracking on the workpiece [59;1974]. It is possible to select grinding parameters to ensure good surface integrity (good surface finish, no workpiece burn and favourable residual compressive stresses) but these conditions dictate a low rate of productivity (gentle grind) [109;1978].

A ground surface consists of a large number of scratches created by the cutting action of individual edges on the surface of a grinding wheel [110;1978]. Analytical formulae have been presented for workpiece surface roughness values produced when grinding. These relationships expressed mean peak to valley heights that should be obtained from a ground surface in terms of grinding process parameters. The studies neglected grain wear and assumed the shape of the groove or scratch to be equal to the shape of the chip produced. Practical values for surface finish are frequently found to be greater than the theoretical values [111;1980]. Analytical studies did not take into account phenomenon such as vibrational effects, variations in grinding wheel geometry or the effects of workpiece material adhering to the wheel surface and being redeposited onto the workpiece surface on subsequent wheel revolutions.

The latter effect was found to be significant [111;1980], but the use of lubricants which effectively prevent metal to metal contact was found to cause the work surface roughness to approach the theoretical value for low vibrational conditions.

Hahn and Lindsay [5;1969: 112;1966] reported that the workpiece surface finish is affected primarily by the normal force intensity between the wheel and workpiece and the wheel dressing conditions. The surface finish on the ground workpiece decreased with a reduction in the force intensity. A proportional relationship, with a certain amount of variance, was also found between the surface finish and the metal removal rate. Expanding on the earlier work, Lindsay [30;1973] found that this variance was greatly reduced when considering the relationship between the surface finish data and the average chip thickness. Average chip thickness, however, is a difficult parameter to measure and hence the Grinding Research Group of CIRP [31;1974] proposed the equivalent chip thickness, which can be readily calculated from the wheel and workspeed and the infeed rate, as a means of evaluating output parameters of the grinding process. A good correlation was observed between the surface finish data and the equivalent chip thickness parameter.

In-process detection of surface finish during the grinding process has obvious advantages. Closing the loop on a model to predict surface finish could be used to optimise grinding parameters from a surface finish viewpoint. A method of optical reflection for detecting workpiece surface roughness during machining was proposed by Takeyama et al [113;1976]. Coolant flow, however, restricts the application of such a system. Verkerk and Pekelharing [114;1978] proposed the use of a steel blade to measure the work surface roughness. The steel blade records the axial profile of the wheel.

The surface finish of this profile represents a limiting value of surface finish that can be achieved after the spark out process with the wheel in its current condition. The obvious disadvantage with this proposal, however, arises from the need to measure the surface roughness of the blade.

The previous methods of in-process surface roughness measurements have distinct disadvantages. A method is required, either contacting or non-contacting, direct or indirect, which is not inhibited by such drawbacks. Conventional stylus instruments cannot be used for such measurements because they are limited by a maximum relative velocity of 0.5 mm/sec [115;1980]. Salje et al [115;1980] overcame this restriction by developing a damped spring-mass sensing element. The method used a contacting transducer which was capable of in-process measurement of the work surface roughness. A piezoelectric transformer converts the mechanical vibration into an electrical signal which after calibration, is proportional to the workpiece centre-line average (CLA) measurement.

Workpiece surface finish is influenced by the amplitude of chatter vibration present during the grinding operation. This relationship is of particular importance because in the majority of cases grinding is performed under unstable conditions [81;1969: 82;1975: 83;1977] and hence the amplitude of vibration increases as grinding proceeds from a freshly dressed wheel. Increasing levels of self excited vibrations have been associated with deteriorating surface finish of the workpiece by many researchers [78;1979: 83;1977: 91;1974: 92;1971]. If an upper limit on the amplitude of chatter vibration is introduced and hence a surface finish constraint, a method could be developed for indirectly monitoring the surface finish of the workpiece and controlling the redress life of the wheel [92;1971: 105;1959].

An automatic dressing cycle could be initiated once this upper vibration level was exceeded [105;1959].

Malkin [60;1978: 63;1974] proposed an algorithm to prevent thermally damaged workpieces by limiting the grinding energy or power. The use of such an algorithm, which utilises an expression linking the threshold energy with the onset of burning, could be used to control the metal removal rate to achieve burn free workpieces. A combination of a vibration and an energy constraint would yield burn-free workpieces of an acceptable surface finish.

## 2.6 Wheel Dressing

A grinding wheel consists of a random distribution of abrasive grains, bonding material and voids (Figure 2.3). All are important for removing material efficiently during the grinding process. As grinding proceeds with a new wheel, the wheel acts too 'hard': particularly in precision grinding. The sharp cutting edges may dull because the grinding interface force may not be sufficient to cause grit- or bond- fracture and the voids which accommodate grinding chips may become loaded with grinding debris. Thus, workpiece thermal damage could result. In order to enable the wheel to remove material efficiently again, the bond material and the grinding debris between the grits must be removed so that space is available for grinding chips to be accommodated, and new sharp cutting edges must be created by either grit- or bond- fracture [43;1972]. The process of restoring the efficient cutting action of the wheel is termed 'wheel dressing'.

The most influential factors in determining the surface finish of a workpiece in precision grinding are the interface force intensity between the wheel and workpiece, and the manner in which a wheel is dressed [5;1969]. Plunge form grinding relies upon the use of a shaped wheel and hence the dressing method used to produce the required shape is one of the most important considerations in the process. The wheel must be formed to the reverse of the part shape, under the same conditions as the actual grinding operation [2;1981].

The dressing process influences:-

- (i) the geometry of the wheel surface
- (ii) the wheel wear characteristics
- (iii) the active grit density [116;1971].

Different dressing treatments can also be used to make wheels behave either harder or softer [117;1980].

Diamond is the most common material used in the dressing process. The properties of diamond which make it particularly suitable for dressing are:-

- (i) its hardness
- (ii) low coefficient of sliding friction
- (iii) the ability to dissipate heat rapidly

Three dressing methods are commonly used [2;1981]:-

- single point diamond
- crush roll
- diamond roll

The choice of the process is generally made on the basis of the production volume requirement. For low volume applications, the single point diamond dressing tool is used. The diamond is traversed across the wheel to produce new cutting edges. If a profile wheel is required a template follower may be used. This method of dressing is, however, slow and the useful life of the wheel is the shortest of the three dressing methods. Single point dressing, however, can produce excellent surface finishes on the workpiece.

Crush roll dressing utilises a carbide, high-speed steel or cast iron roll shaped to the profile of the component. The roll is applied against the face and is fed into the wheel gradually until the complete profile is transferred onto the wheel. This dressing procedure is used in medium volume production and is the best method for producing a wheel which is free cutting. Crush dressing breaks down the bond of the material and removes whole abrasive grains, leaving sharp new grains for efficient cutting. It is the best method where fine detail, radii and chamfers are required, and provides the longest life between dressings.

The third method of dressing, the rotating diamond roll, has the wear resistance and durability required for high production runs. The profile of the workpiece is ground onto a metal roll, which is then studded with diamonds using a matrix type diamond composition or single set diamonds. To transfer the profile to the wheel, diamond rolls are rotated at high speed and fed into the wheel. This operation can be completed in 5-10 seconds compared to several minutes for crush dressing. Surface finishes produced by this method are, however, poorest of the three dressing mechanisms because of the wavy pattern transferred to the wheel by the action of individual diamond tips.

Hahn and Lindsay [5;1969] identified the dressing ratio, twice the depth of dress divided by the dressing lead, as an important parameter of single point diamond dressing. A dressing ratio of unity was shown to yield a 'sharp' wheel whereas values approaching zero caused the dressed wheel to be 'dull'. When performing tests with 'sharp' and 'dull' wheels, 'sharp' wheels were found to have superior metal removal rates but produced inferior surface finishes.

Research has been performed [42;1971: 43;1972: 45;1978: 116;1971: 118;1972] to examine the effects of single point diamond dressing on some of the grinding process output parameters (i.e. grinding force, surface integrity and wheel wear). In each case grinding is qualitatively defined as coarse or fine. The researchers, however, had different preferences in distinguishing between the two grinding conditions. Malkin and Cook [42;1971] used the same basic dressing treatment for both conditions and added an extra two spark out passes with no extra diamond depth of cut as the 'fine' condition. Other studies [43;1972: 45;1978] increased the diamond depth of cut for the 'coarse' condition whilst keeping the diamond traverse rate constant. Bhateja et al [116;1971: 118;1972] varied the traverse rate whilst keeping the depth of cut constant. The aim of all the studies was to create greater grit damage during dressing in the case of the coarse condition.

Reviewing the studies [42;1971: 43;1972: 45;1978: 116;1971: 118;1972] yield a number of common conclusions:- coarser dressing causes inferior surface finishes, lower grinding forces, higher wheel wear rate but increased useful wheel life, and a reduced tendency to produce thermally damaged workpieces than a 'fine' dressing treatment.

The longer useful working life of a wheel associated with coarse dressing should not be neglected since dressing costs are as important as machine and operator costs for the grinding operation but wheel wear costs are negligible [119;1972]. Malkin and Cook [42;1971] concluded that coarse dressing should be used for rough grinding and fine dressing for finishing.

Fletcher [45;1978] examined the effects on the grinding process of cross-feedrate and diamond depth of cut. Cross-feedrate and diamond geometry were found to have the greatest influence, with the diamond depth of cut of secondary importance. This study also revealed that the dressing process only effects the workpiece surface finish during the primary wear stage. During the other wear stages the surface finish was dependent only on the grinding conditions.

Research has been performed [43;1972: 45;1978: 120;1979] to ascertain optimum dressing conditions which combine the advantages of coarse and fine dressing. Pacitti and Rubenstein [43;1972] observed that too fine a dressing greatly reduced the useful life of a wheel and resulted in thermally damaged workpieces. Too severe dressing conditions, however, also, shortened the useful working life of a wheel, by causing the premature on-set of bond fracture, since coarse dressing removed more bond material and reduced the 'grit pull out' force. Fletcher [45;1978] also proposed 'ideal' dressing conditions. Practical grinding tests revealed this condition to be one of minimum diamond overlap on the diamond traverse rate: excessive overlap caused higher forces and too high a traverse rate caused the early onset of chatter vibration. Pande and Lal [120;1979] stated that this traverse rate lay in the region of 0.75 - 1.5m/min.

## 2.7 High Speed Grinding

The abrasive machining operation is increasingly performing machining operations traditionally done by turning or milling [2;1981]. Several developments are contributing to this trend: the reduced stock removal requirements of parts forged or cast to near shape; improvements in machines and abrasive; and improved machine controls. High speed grinding has been frequently proposed as a means of improving surface finish, wheel wear and productivity [77;1971]. These improvements arise from the decreasing depths of cut and grinding chip cross-sections resulting from higher wheelspeeds. Konig et al [77;1971] stated that the first useful and systematic investigations using high speed wheels in precision grinding were performed by Ernst [121;1964] who ground with wheelspeeds up to 60m/sec and Guhring [122;1967] who combined high wheelspeeds of 90m/sec with metal removal rates comparable with turning and milling ( $100\text{mm}^3/\text{mm}\cdot\text{sec}$ )

Opitz and Guhring [123;1968] achieved metal removal rates of  $110\text{mm}^3/\text{mm}\cdot\text{sec}$  with wheelspeeds of 90m/sec. This greatly improved metal removal rate over conventional wheelspeeds was not achieved at the expense of a deteriorating workpiece surface finish. Wheel wear, so critical in plunge profile grinding, was also improved by increasing the wheelspeed from 20 to 90m/sec. In the most unfavourable case (grinding a hardened high speed steel) a ten-fold improvement in wheel life was achieved, whilst a thousand-fold improvement was achieved for C45 machining steel, (a mild steel having the following constituents, 0.42-0.5% carbon, 0.15-0.35% silicon, 0.5-0.8% manganese and 0.045% max sulphur). This research demonstrated that high speed grinding can be successfully used as a high efficiency metal removal process offering similar workpiece surface characteristics to conventional grinding.

Brown et al [124;1979] conducted tests at six wheelspeeds over the range 30–180m/sec using a special grinding wheel consisting of 24 segments retained by an epoxy bond on the periphery of a steel hub. By doubling the wheelspeed, the metal removal rate was found to double without any increase in grinding force, workpiece surface finish, energy required/volume of material removed or residual stress level in the final component.

Thompson [125;1977] reported that improved stability accompanies high speed grinding. Hahn in the discussion of this work, however, stated, that since most grinding operations are performed in the unstable regime the question of improved stability was only partially significant. The amount of material that can be removed before the amplitude of chatter vibration tends towards an unsatisfactory level is a more important consideration.

High speed grinding can only be recommended for a special group of materials which are unproblematic when grinding at conventionally low speeds, e.g. bearing steels [52;1978]. Materials which tend to load the surface of the grinding wheel (e.g. low carbon steel, aluminium alloys etc.) characteristically show increased surface temperatures and constant grinding forces at constant metal removal rates as wheelspeeds are increased. The reason for this anomaly (high speed grinding has been reported [77;1971: 123;1968] to reduce forces whilst removing metal at a constant rate) is that a loaded wheel can no longer remove material by normal chip formation. The loaded areas of the wheel will instead force the material out of the contact zone.

One of the most serious drawbacks with high speed grinding is thermal damage imparted to the workpieces [55;1972]. Increased metal removal rates at higher wheelspeeds cause the grinding temperature to be above the critical temperature at which workpiece burn is experienced [123;1968]. Attempts [121;1964: 123;1968] have been made to overcome this problem. Ernst [121;1964], as cited by Konig [77;1971], observed an air layer at the circumference of the wheel which acts as a barrier restricting coolant access to the grinding zone. By deflecting this air layer, better contact was provided between the coolant and the grinding zone. This reduced the heating in the contact zone and helped to reduce the extent of thermal damage. Opitz and Guhring [123;1968] employed a high pressure coolant system (oil pressure of 10kp/mm<sup>2</sup> and a flowrate of 150l/min) to penetrate the air layer. The use of an oil- instead of a water- based coolant was also shown to be beneficial [123;1968]. The permissible metal removal rate before burning occurred was almost doubled when changing from a water- to an oil- based coolant.

High speed grinding machines require additional features and facilities not demanded by conventional grinding machines [55;1972]. Machines must be developed which are more rigid and more powerful than existing surface and cylindrical grinding machines. Improved guarding and screening are required to both protect the operator against possible wheel burst and contain high pressure coolant delivery systems. Grinding wheel manufacture must be improved to allow wheels to be used at high speeds without centrifugal rupture [126;1972] and wheels need to be balanced dynamically rather than statically since any force due to unbalance is proportional to the square of the wheel velocity.

## 2.8 Adaptive Control of the Grinding Process

Optimum grinding conditions, whereby a workpiece is machined in the shortest possible time without violating constraints imposed on the dimensional accuracy or surface integrity of the final component, are seldomly achieved. The complex cutting action and the variable compliance and structure of the wheel, combine to make a prediction of this optimum condition very complex. If, however, the grinding conditions are monitored during the process, the input variables, namely feedrates and/or cutting speeds, can be adjusted towards optimum grinding conditions. This form of in-process monitoring of the output parameters and controlling the input variables to achieve optimum grinding conditions is known as adaptive control.

In the past few years, adaptive control has progressed to become a viable concept with the development of new sensors and controllers. By definition [4;1977], adaptive control is achieved by automatically and continuously regulating each parameter in the machining process against an external disturbance or change in internal conditions, and maintaining the process in the desired condition.

A classification system for adaptive control distinguishes between geometrical adaptive control and technological adaptive control [127;1975]. The former is concerned with monitoring the shape and dimension of a machined component. This relies upon some in-process gauging instrument with a very short time response to record information concerning the geometry of the component. The index of performance of such a system is the shape and dimension of the final component.

Technological adaptive control encompasses two sub-classifications; adaptive control optimisation (ACO) and adaptive control constraint (ACC). As the name suggests the former relies on some form of optimisation technique which has to have a well defined index of performance (e.g. optimise component production costs). The latter, on the other hand, describes a system where one or more constraints are specified for the output parameters and the input variables are adjusted to keep the outputs within these constraints.

Compared to other machining processes, the application of adaptive control to the grinding process has been rather slow. Hahn [128;1964] developed a method of reducing errors when internal grinding by using the concept of controlled force machining. This method eliminates random size and taper fluctuations caused by the variations in the machine tool deflection. It was considered [4;1977] to be the earliest example of A.C.C. aimed at geometrical adaptive control. By monitoring the deflection of the grinding spindle and adjusting the feedrate to maintain this deflection (and hence the grinding force) constant, an improved component accuracy was accomplished.

Controlled force grinding was incorporated in a Japanese system, developed at the Toyoda Machine Works [129;1971]. The difference in pressure between the front and rear fluid pockets of the hydrostatic wheel bearing were used to calculate the force acting at the wheel/workpiece interface. Wada recognised the importance of grinding force for controlling surface finish of the final component. By relying upon the skill of the operator or tables produced after exhaustive tests the normal force constraint could be used to produce a component with a specified surface finish from a particular work material.

The proposed system was able to predict the redress life of a wheel by examining the expected metal removal rate at a particular grinding force and comparing this with some pre-determined value.

The Bendix Research Laboratories implemented adaptive control on a surface grinding machine [130;1972]. The system's aim was for maximising machine tool utilisation without violating a surface finish constraint. In order to achieve this, chatter vibration and the torque on the wheel spindle were monitored and the feedrate was used to maintain the necessary constraints on these values.

Inoue et al [131;1974] proposed an adaptive control cylindrical plunge grinding machine comprising of two grinding cycles; a body or roughing cycle where various limitations would be imposed on torque, wheel power and force to avoid constraint violations, and a sizing feed where the diameter of the workpiece was monitored by means of a feedback loop. A mathematical model relating the wheel life to the amplitude of chatter vibration was also proposed.

The previously mentioned systems [128;1964: 130;1972: 131;1974] are examples of adaptive control constraint (ACC) systems. Although research has been carried out into adaptive control optimisation (ACO) systems, few, if any, of these systems are used in industry [132;1981]. The main difficulties with such systems have been associated with the need to specify an index of performance together with an appropriate control policy. Sensors also require further development which can reliably measure the process parameters in the production environment. Adaptive control optimisation strategies have, however, been developed for the abrasive cut-off operation by Gall [133;1969] and the University of Delft, Netherlands (cited by Wada and Kodama [4;1977]). Both systems monitor wheel wear and control the infeed rate of the wheel to achieve a minimum cost operation.

Adaptive control optimisation systems have not found widespread use in surface or cylindrical grinding operations [132;1981]. Such systems rely on in-process detection of wheel wear to enable decisions to be made to achieve minimum cost or maximum production rate operations. This has proved to be a complex task. Tipton [134;1979] stated that optimum economic machining conditions are constrained by the available power of a machine tool and that optimum conditions are often found at, or near, the intersection of two constraints, e.g. force and power. Optimum conditions can, therefore, often be obtained with a simple constraint type controller.

Various researchers [5;1969: 42;1971: 57;1974: 60;1968: 63;1974] have proposed a link between grinding forces (or energy) and thermal damage to the workpiece. Malkin [60;1978: 63;1974] obtained an expression for the critical grinding energy input at the onset of burning in terms of the grinding parameters. It was also stated that this limiting energy equation could be used to control the metal removal rate in an adaptive control constraint system to achieve a component free from burn. A number of ACC systems [3;1977: 132;1981: 135;1974: 136;1977] have been proposed or developed which use the prevention of thermal damage as an objective and constrain wheel power to achieve this. These systems monitored wheel power to indirectly control grinding temperature since no reliable direct means of temperature measurement was available for use in a production environment.

In recent years, research has been performed in the field of geometric adaptive control for the grinding process. Kaliszer et al [137;1979] are developing an in-process closed loop system for monitoring the diameter, error of form and surface roughness of a ground component.

The monitored parameters are to be used as feedback signals to control the geometrical and surface finish requirements of the workpiece during the infeed and spark-out stages of a cylindrical grinding machine.

Monitoring the surface finish of a ground component, whilst having obvious advantages for controlling the process, does have practical difficulties. The optical [113;1976] and blade techniques [114;1978] discussed previously have fundamental limitations: coolant presents a problem for the optical technique and the surface finish of the blade needs to be measured in the steel blade technique. Conventional stylus instruments cannot be used for in-process workpiece surface roughness measurements because they are limited to a maximum relative velocity of 0.5 mm/sec [115;1980]. Salje et al [115;1980] proposed a stylus type technique which overcame this problem. A damped spring-mass system was used to contact the workpiece surface during the grinding operation. The mechanical vibration of the transducer, produced by the work surface, is converted by a piezo-electric transformer into an electrical signal which after calibration was proportional to the workpiece CLA measurement.

Despite the research performed, adaptive control grinding machines are still not being used in industry [4;1977: 132;1981]. However, with the tendency towards CNC and DNC machine tools new impetus should arise for adaptive control since the control hardware may already be present on the shop floor.

100Cr6 (IC-143 Cr) HR 62-63		EK60L7VX E 52 2 N/mm <sup>2</sup>	
d <sub>1</sub> (mm) 630	v <sub>s</sub> (m/s) 30-60	CPS 12 100%	Q <sub>1</sub> (l/min, mm) 2
d <sub>2</sub> (mm) 80-150	a (v <sub>s</sub> /v <sub>w</sub> ) 50	v <sub>w</sub> (mm/min) 1000	α <sub>g</sub> (μm) 50-30
d <sub>3</sub> (mm) 75	v <sub>w</sub> (mm/min) 1000	α <sub>g</sub> (μm) 2	α <sub>g</sub> (μm) 50-30
b (mm) 30	h <sub>eq</sub> (μm) 49	A (B/F) 0008	C (B/F) 38

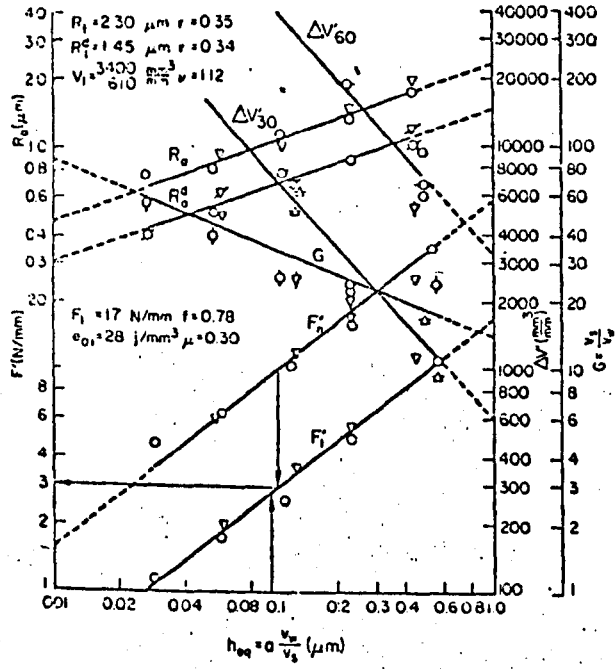


Figure 3. Grinding chart for 100Cr6, EK60L7VX with oil lubricant (EPSI 2100%).

100Cr6 (IC-143 Cr) HR 62-63		EK60L7VX E 52 2 N/mm <sup>2</sup>	
d <sub>1</sub> (mm) 630	v <sub>s</sub> (m/s) 30-60	SB-C 3%	Q <sub>1</sub> (l/min, mm) 2
d <sub>2</sub> (mm) 82	a (v <sub>s</sub> /v <sub>w</sub> ) 60	v <sub>w</sub> (mm/min) 200	α <sub>g</sub> (μm) 10-2
d <sub>3</sub> (mm) 73	v <sub>w</sub> (mm/min) 200	α <sub>g</sub> (μm) 15	α <sub>g</sub> (μm) 50-30
b (mm) 30	h <sub>eq</sub> (μm) 49	A (B/F) 0004 0005	C (B/F) 367-37

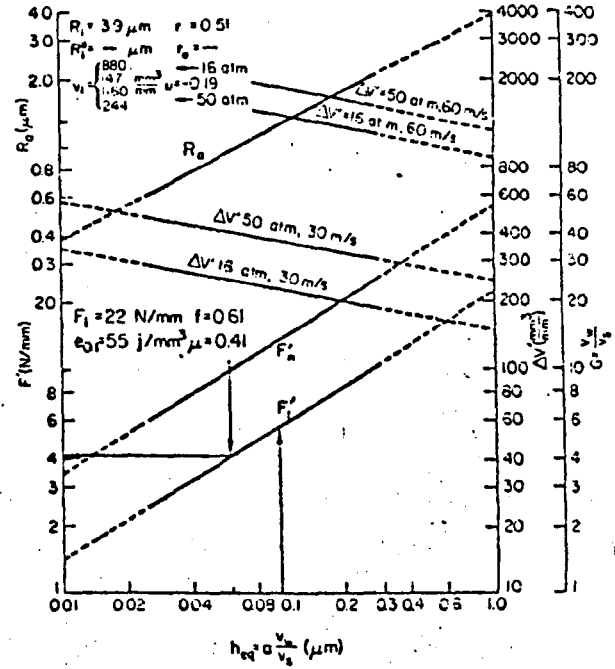


Figure 4. Grinding charts for 100Cr6, EK60L7VX with emulsion SB-C 3%.

FIGURE 2.1 EQUIVALENT CHIP THICKNESS GRINDING CHARTS (32)

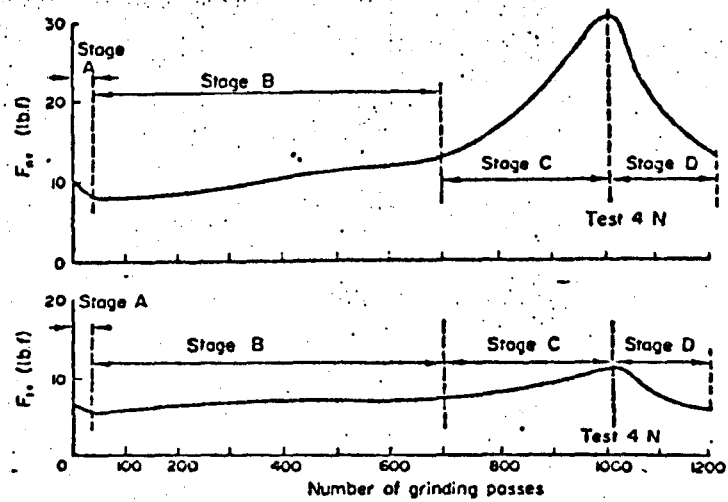


Fig. 3. The variation in grinding force components with grinding time showing stages A-D—Test 4N.

FIGURE 2.2 GRINDING FORCE-TIME RELATIONSHIPS (43)

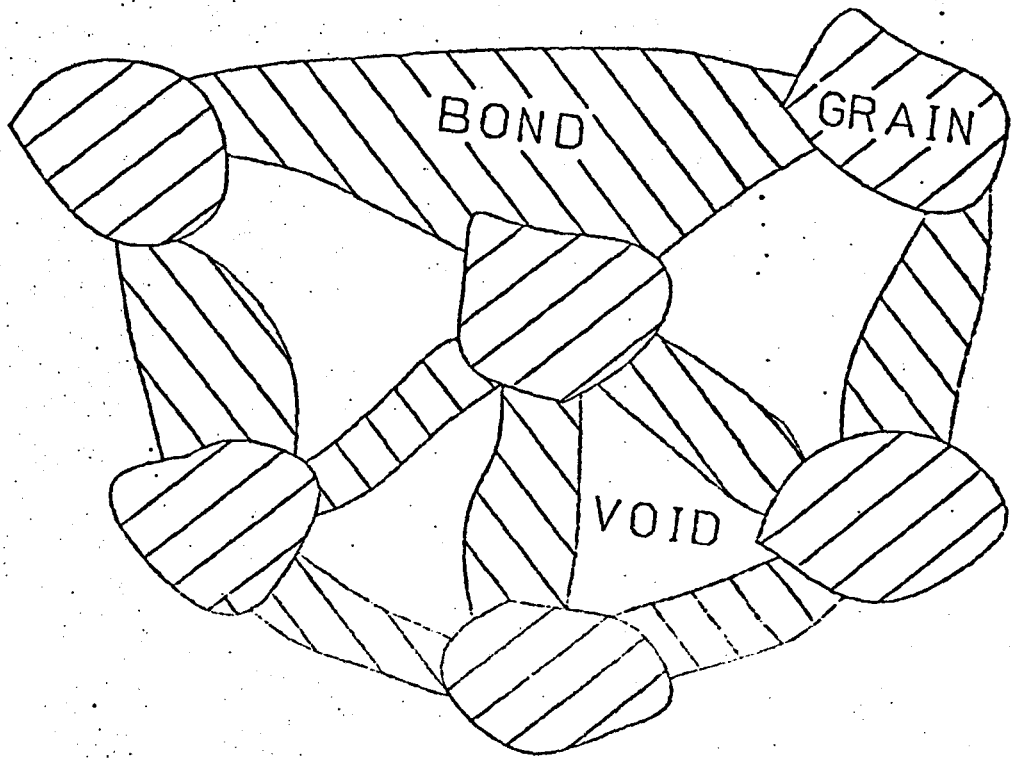


FIGURE 2.3 GRINDING WHEEL COMPOSITION

### 3.0 THE GRINDING MACHINE

#### 3.1 Introduction

The grinding machine used in this experimental work is a T.I. Matrix GP 33 external cylindrical plunge grinding machine. This machine is manufactured as a hydraulically controlled manual machine and a significant amount of modification was necessary to enable it to be used in adaptive control grinding research. A control system was required which was capable of monitoring the grinding process and effecting the changes in infeed rate necessary to achieve adaptive control. A MINIC CNC 500 computer (Figure 3.1) was retrofitted to the machine tool to provide this control. It is not the intention of this thesis to describe the controller since Wallis [138;1981] provided a full computer specification. This chapter will, however, describe the CNC grinding machine development, the adaptive control monitoring hardware [138;1981: 139;1978] and the software written to control the process [140;1982].

#### 3.2 Grinding Machine Hardware

The overall grinding machine and control system is shown in Figure 3.2 and represented schematically in Figure 3.3. The MINIC-M minicomputer is interfaced to the machine tool via a bi-directional bus system. CNC executive software written for the MINIC-M controls and monitors

- (i) the servo systems for positioning the wheelhead and table.
- (ii) the wheel spindle and work motors.
- (iii) digital inputs and outputs for machine tool logic
- (iv) the watchdog timer.
- (v) the operator visual display unit (VDU) and keyboard.

### 3.2.1 Control Strategy

The computer control operates as a real time system. The executive CNC software is scheduled to run every 15 m sec. A real time clock connected to the interface bus (Figure 3.3) interrupts the processor every 15 m sec and acts as an enable signal to cycle through the CNC executive program. This program instructs the axis servo with the distance to be moved in the next 15 m sec; controls the wheel- and workspeeds and any necessary digital output signals; and monitors the watchdog timer, digital input lines and the operator keyboard. A further clock interrupt 15 m sec later re-initialises the CNC executive software.

### 3.2.2 Axis Servo Systems

Machine tool axis motion is provided by recirculating ball screws which are connected to d.c. motors via a worm and wheel gearbox (Figure 3.4). Control of the d.c. motor servo systems is provided every 15 m sec by the CNC executive software. The computer outputs a 16-bit digital signal to each axis control circuit board. This signal comprises a 12-bit data word containing the traverse distance of each axis in the next 15 m sec and a 1-bit directional flag. The axis servo controllers, however, operate by converting a pulse train into an electrical excitation of the d.c. motor. Each axis control circuit board, therefore, has to generate a pulse train of the correct frequency from the digital output of the computer. This process is repeated every 15 m sec when the clock interrupt re-initialises the CNC executive software.

A servo control system requires feedback to monitor its performance. Position and velocity feedback are integral parts of the axis servo controllers. Slide position feedback is achieved by means of a brushless resolver mounted on the end of the motor shaft whilst a tachometer provides velocity feedback. The pulse and directional signals are read into buffer register counters. These counters, therefore, contain the distance to be traversed by the respective slides in the next 15 m sec time period. By comparing the actual position of the slide, provided by the brushless resolvers, with the demanded position stored in the buffer counters, a positional error is obtained. The magnitude of error supplies the closed loop positioning feedback signal which in turn provides a motor velocity demand. The larger the positional error the higher the velocity demand. Once the move for a particular 15 m sec time period has been completed a signal is generated to inform the computer that the required movement has been completed. The next clock interrupt will generate further traverse information.

### 3.2.3 Wheel Spindle and Work Motors

Alternating current motors are used to rotate the grinding wheel and the workpiece. The cost of these systems is higher than that of any equivalently rated d.c. motor and drive but a.c. motors have the advantage of having no wound rotors [140;1982]. This enables the motor unit to be precision dynamically balanced which is essential for the production of good surface finishes and geometric accuracies associated with the grinding process.

The motors are controlled by DANFOSS static frequency controllers which convert an analogue voltage input into an analogue current. The DANFOSS controller is interfaced to the computer by means of a propriety DANFOSS interface. Once the operator specifies the wheelspeed and workspeed, the computer converts these parameters into an 8-bit word and an analogue output board in the interface rack provides the required analogue voltage signal to the DANFOSS static frequency controller. The resulting analogue current is then used to thyrstically control the wheel- and workspeed respectively.

#### 3.2.4 Digital Inputs/Outputs

Digital inputs and outputs are used in the CNC system for establishing and controlling the status of various machine features. These digital signals include maximum travel limit switches, hydraulic pressure sensing transducers, on-off switches etc. They are used for monitoring the status of the machine and preventing various non-desirable situations, e.g. wheel spindle rotating without hydrostatic bearing lubrication, or travel beyond a limit switch. The execution of the executive CNC software every 15 m secs causes the inputs to be read and any necessary output states to be modified.

#### 3.2.5 Watchdog Timer

A watchdog timer is interfaced to the computer. The activation of this device, by an input pulse, causes a timer to operate. At the end of a preset timed length an output pulse is generated. Retriggering the watchdog timer before it completes the timed interval causes the system to begin timing again and suppresses the output pulse.

The watchdog timer is used for sensing manually inputted, or computer instigated, emergency stops by connecting the output of the device to an emergency switch circuit. The retriggering of the timer is performed by the executive CNC software every 15 m sec. If retriggering is not inhibited, the output of the timer will not switch the emergency circuit, since the timer will reset and suppress any output. If, however, this retriggering is prevented by manual or computer intervention, the emergency switch circuit is activated and the wheel is retracted from the workpiece and the power removed from the machine. The following situations will cause the emergency switch circuit to operate.

- Manual emergency stop procedure (available on all machine tools)
- Computer instigated emergency procedure from normal force overload (refer to Section 3.4.1.)

### 3.3 CNC Grinding Machine Operation

The grinding machine has two modes of operation.

- (1) Manual mode
- (2) Automatic or machining mode

The manual mode is used to enable an operator to position the grinding wheel. Various continuous and incremental jogs are available for this purpose. These jogs operate on both axis servo systems.

The machining mode is controlled by a CNC part program. Component geometry is input into the CNC system and the axes are controlled during the automatic cycle to machine this geometry.

### 3.3.1 Manual Mode Operations

The following manual features are available on the machine:

- Rapid Advance : moves the wheelhead 32 mms towards the workpiece at rapid traverse rate.
- Rapid Retract : moves the wheelhead 32 mms away from the workpiece at rapid traverse rate.
- Incremental Jog: jog sizes of 1 micron, 10 microns, 100 microns, 1 millimetre and 10 millimetres are available for both axes.
- Continuous Jog

The use of the rapid advance and retract features provide a simple means of keeping the wheel clear of the workpiece. This is especially useful when removing and inspecting components, which can be achieved without inputting new co-ordinates into the CNC system.

Each grinding cycle commences with a 32 mm rapid wheelhead advance and when the component has been ground the cycle is terminated with an identical length wheelhead retraction. It is not possible, however, to request two advances of the wheelhead.

When the wheel has been advanced, the wheel must be retracted prior to a further advance. This is a safety factor to prevent the wheel/ component collision which could occur should the operator accidentally advance the wheelhead.

### 3.3.2 Manual Part Programming

Before any automatic cycle can be initiated the operator must input a CNC part program to define the grinding wheel toolpath. This is input via a questionnaire displayed on the computer VDU as shown in Figure 3.5. The operator is prompted for the following information.

1. **BLOCK NUMBER:-** CNC terminology for the program line. The information is used in program execution since the lowest block number remaining in the program is always executed first.
2. **TRAVERSE DISTANCE:-** Table axis movement
3. **INITIAL GRINDING POSITION:-** Diameter at which the rapid wheel infeed rate terminates and the grinding infeed rate commences.
4. **FINAL GRINDING POSITION:-** Required component diameter
5. **GRINDING FEEDRATE:-** Programmed wheel infeed rate
6. **DWELL TIME:-** Spark-out time
7. **RETRACT POSITION:-** Position to which wheel will retract.
8. **WHEELSPEED**
9. **WORKSPEED**

### 3.3.3 Automatic or Machining Mode

When the part program has been input the machining cycle can be initiated by the operator. This will cause the part program to be executed in the following sequence:

1. The table will traverse by the amount specified in the part program.
2. The wheel advances 32 mms at rapid traverse.
3. The wheel advances to the initial grinding position at rapid traverse.
4. The component is ground to the final dimension at the specified grinding feedrate.
5. The wheel dwells at this position for the specified dwell time.
6. The wheel retracts to the retract position.
7. Operations 1-6 are repeated for all programmed blocks
8. The wheel retracts 32 mms.

### 3.4 Adaptive Control

Adaptive control differs from the CNC philosophy outlined in the previous section because it requires the feedback of process output parameters. This feedback is utilised to modify the input parameters of the system to achieve some pre-defined optimum process control.

The adaptive control strategy developed by this research requires the normal force and vibration level at the wheel/ workpiece interface and the power of the grinding - wheel spindle motor to be monitored. Transducers have been developed [138;1982: 139;1978] for monitoring these parameters.

Grinding Force Measurement

The grinding machine used for this research work utilises a hydrostatically supported wheel spindle. Hydrostatic bearings consist of a load supporting pad as illustrated schematically in Figure 3.6. Lands surround a recessed pocket which is fed, via a restrictor, with fluid at constant pressure. As the pressure increases in the pocket, the load is lifted and fluid escapes from the pocket. Equilibrium is reached once the clearance,  $h$ , is sufficiently high to allow the correct flowrate. The correct flowrate is one which creates the required pocket pressure to balance the load. A hydrostatic journal bearing consists of a ring of these hydrostatic pads encircling a shaft (see Figure 3.7).

The hydrostatic journal bearing on the grinding machine provides an alternative method of monitoring the grinding forces. Any applied force on the grinding wheel spindle causes a proportional deflection of that spindle. This deflection will produce a difference in pressure between opposite pairs of bearing pockets and these pressures can be monitored. The area over which they act is known, and therefore it is possible to calculate the force acting in each direction.

Edwards [139;1978] installed differential pressure transducers to the hydrostatic bearing pockets of the research machine (Figure 3.8). Each pressure transducer provides a pressure difference between diametrically opposite pockets. By combining the outputs of the pressure transducers electronically using the following two empirical relationships, the normal and tangential grinding forces are monitored by the system.

$$F_n = 1793.5V_2 + 1690.5V_3 + 1005.5V_4 + 1026.2V_5$$

$$F_t = 1950V_1 - 981V_2 + 901.5V_3 - 1762.5V_4 + 1792.5V_5$$

where  $F_n$  = normal force

$F_t$  = tangential force

$V_1-V_5$  = outputs of the 5 differential pressure  
transducers

#### 3.4.2 Vibration Measurement

A vibration sensor (refer to Appendix 1 for specification) situated on the tailstock of the machine is used to monitor the amplitude of grinding chatter vibration. Several other locations were investigated on the wheelhead and tailstock but at alternative locations, other frequency vibrations predominated and the chatter vibrations were found to be severely damped.

#### 3.4.3 Wheel Power Measurement

An electronic power meter was designed [138;1981] for the measurement of three-phase electrical power input to the wheelhead spindle motor. The power meter multiples, electronically, the outputs of the voltage and current transformers which respectively monitor the line voltages and currents of the DANFOSS controller. The wheel power is calculated from the three-phase supply relationship.

$$P = 3VI \cos \phi$$

where

P = Power

V = Line Voltage

I = Current

$\phi$  = Phase angle between current and voltage

The output of the electronic multiplication is subject to a mains frequency of 50 Hz and hence is fed through a low pass filter to eliminate the 50 Hz effects. The signal is finally amplified and sampled by the analogue input section of the computer. This provided the computer with a signal proportional to the wheelpower.

### 3.5 Adaptive Control Software Structure [140;1982]

Algorithms have been developed for monitoring normal force, vibration and wheelpower. These algorithms operate in a time sharing mode on the computer control system to enable the same software to be used for each monitored grinding parameter. The overall time cycles for the adaptive control monitoring phases are shown in Figure 3.9.

The adaptive control strategy utilises the monitored normal force to control the infeed rate of the cylindrical plunge grinding machine. The success of the control strategy depends on a relationship between normal force and infeed rate. Any relationship will be unique for a particular grinding wheel/grinding wheel condition/ workpiece combination and will, therefore, be difficult to predict.

Identification of the relationship is possible, however, if the normal force and feedrates are monitored during grinding. Once the relationship is established, it can be used to control the infeed rate to achieve constant force machining.

Two grinding cycles have been developed for adaptively controlling the process:

1. A model identification cycle
- and 2. A constant force machining cycle.

On entering an adaptive control grinding operation the computer begins to develop the normal force - feedrate relationship in the model identification cycle. This is achieved by increasing the feedrate in steps of 0.01 mms/min and measuring the corresponding normal force for each feedrate. When the model is established, the second grinding cycle utilises an operator programmed normal force level and the calculated normal force - feedrate relationship to achieve constant force machining through infeed rate control.

The following sections are more detailed descriptions of the two grinding cycles.

### 3.5.1 The Identification Stage

The identification stage flow diagram is shown in Figure 3.10. This flow diagram has been extracted from the overall adaptive control monitoring flow diagram ACFEX [140;1982]. In the following description three assumptions will be made:

1. The wheel is grinding
2. The normal force monitoring stage is active (refer to Figure 3.9).
3. No readings of normal force have been taken.

At the commencement of the grinding cycle the computer calculates twenty feedrates for use in the identification of normal force - feedrate model. These feedrates are calculated by interactively adding 0.01 mm/min to the operator programmed feedrate,  $f$ , to yield  $f+0.01$ ,  $f+0.02$  etc.

The cycle time of the identification stage is 6 seconds (Figure 3.9). This was found to be the time necessary for satisfactory completion of the algorithms. Normal force monitoring is performed for 1.5 seconds every cycle.

The adaptive control program is initiated every 15 m sec by the real time clock interrupt. One hundred readings of normal force are therefore taken and the mean of these readings is calculated. The first results of the normal - force feedrate model, feedrate  $f$  and the associated normal force, are stored in memory. The feedrate is then incremented to  $f+0.01$ .

After a lapse of 4.5 seconds, the time used for monitoring the additional grinding parameters and performing calculations, 100 normal force readings are again taken, a mean value is produced and stored. This procedure is repeated for a feedrate of  $f+0.02$ . Three normal force - feedrate values are now stored. A regression analysis to calculate the gradient of the normal force - feedrate relationship is performed. The gradient is calculated from the expression:

$$\text{GRAD} = \frac{\sum (\text{NF} \cdot \text{FR}) - N \cdot \bar{\text{NF}} \cdot \bar{\text{FR}}}{\sum (\text{FR}^2) - N(\bar{\text{FR}})^2}$$

where NF = Average normal force readings

FR = Feedrate readings

N = Number of average readings

NF = Mean of all average normal force values

FR = Mean of all feedrates

To give confidence to this regression analysis a further one hundred normal force readings are taken for the feedrate  $f \pm 0.03$  and a further regression analysis is performed on the four stored readings. An approach of this type makes it possible to progressively compare gradients and if the results do not differ by more than 5% an accurate prediction of the normal force - feedrate relationship is assumed and the identification cycle is terminated in favour of constant force machining.

### 3.5.2. Constant Force Machining

During constant force machining the feedrate is adjusted to maintain the normal force within an acceptable tolerance zone about the required normal force level. Both the normal force level and its associated tolerance zone are specified by the operator during component part programming (refer to Figure 3.11).

The constant force machining cycle time is only 1.5 seconds instead of the 6 seconds for the identification stage. Few feedrate changes and computations are needed and hence a time reduction was possible. Normal force monitoring accounts for 0.3 seconds of the grinding cycle and hence twenty normal force readings are taken and their mean computed.

The mean value is compared with the lower and upper limits of the normal force tolerance zone specified initially by the operator. If the monitored normal force is within the two levels of force constraint then grinding will proceed without parameter alteration. If, however, the force is lower than the lower constraint the feedrate is increased by an amount calculated from

$$\text{Feedrate increase} = \frac{(\text{Required Force}) - (\text{Monitored Force})}{\text{Force - feedrate gradient}}$$

Similarly, a feedrate decrease would be calculated by

$$\frac{(\text{Monitored Force}) - (\text{Required Force})}{\text{Force - feedrate gradient}}$$

The normal force feedrate relationship for both the identification stage and constant force machining is shown in Figure 3.12. The identification stage is represented by the portion of the graph az and the constant force machining occurs from z onwards. Timescales represented on the graph for the two stages, however, are not linear.

The identification stage may last only 30 seconds whereas constant force machining may continue for as long as 50 minutes with only minor feedrate changes. This schematic representation is intended purely to illustrate the principles of the identification and normal grinding stages.

The identification stage commences with the initial CNC programmed feedrate represented by 'a' in Figure 3.12. After taking 100 normal force readings, an average value of the normal force (the value at 'a') is calculated for this feedrate. The feedrate is then incremented to the value at 'b' and the corresponding normal force at 'b' is monitored. This procedure is repeated until the gradient,  $\theta$ , can be accurately predicted which in practice occurs after 5 - 8 results. The identification stage is followed by constant force machining where the gradient is utilised to adjust the feedrate to maintain the normal force within the tolerance zone.

### 3.5.3 Vibration Level and Wheel Power Software

Although the hardware for monitoring vibration and wheel Power was used in this research, the software algorithms for wheel power and vibration were not utilised. For this reason these algorithms will not be described.

### 3.6 System Monitoring During Non-Adaptive Control Grinding Operations

With the existing system, a CNC part program can be input into the controller and the component ground without the adaptive control strategy being active. Incorrect part program data could cause a collision between the wheel and wheelpiece and so a safety feature has been written into the CNC executive software. This feature is operational at all times and is independent of the adaptive control software.

The grinding force is monitored by the executive CNC software every 15 m sec. If this force exceeds a preset maximum value, the wheel is retracted and the grinding cycle is aborted. Spurious results, however, could cause the cycle to be aborted unnecessarily and hence ten consecutive readings above the preset maximum are needed to abort any cycle. This inevitably incorporates a delay into aborting a cycle. Tests performed [140;1982] by programming the wheel to collide with the workpiece at the full axis speed of 1 m/min, however, caused the wheel to retract before any serious damage occurred. If a higher rapid feedrate is subsequently specified for the machine it may be necessary to reduce the number of spurious readings which will cause the cycle to be aborted.

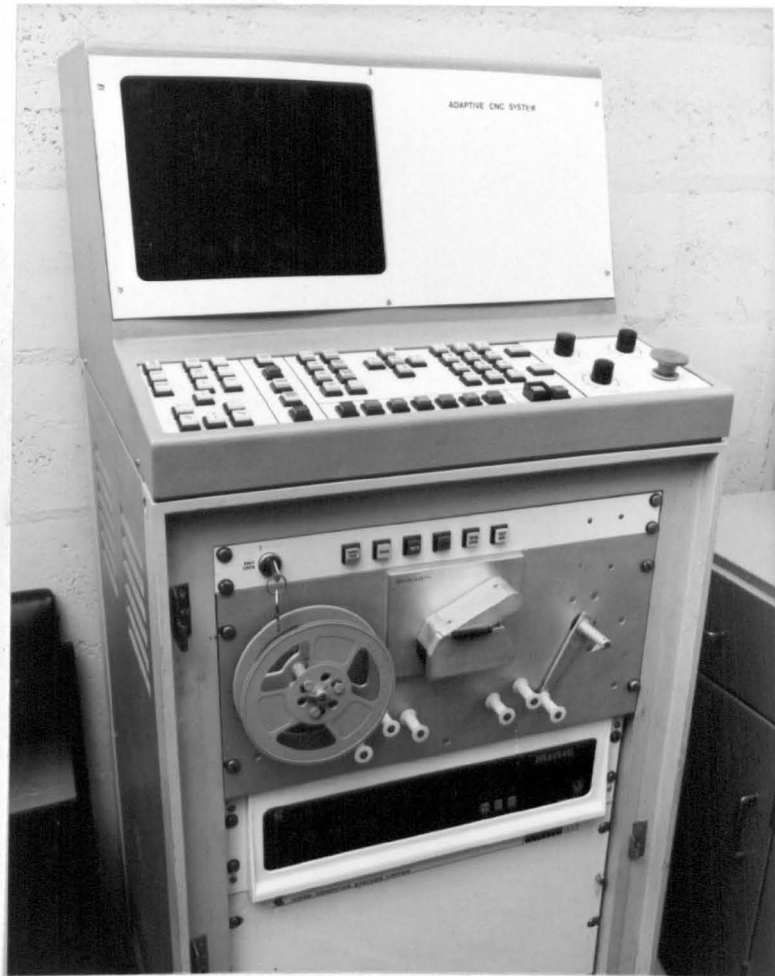


FIGURE 3.1 MINIC CONTROL SYSTEM

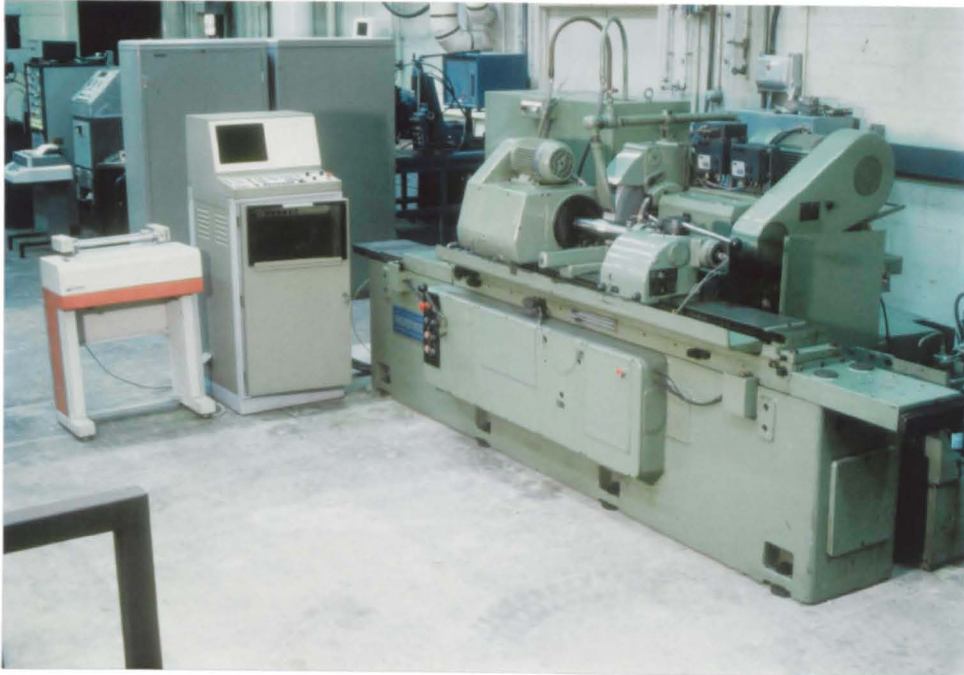


FIGURE 3.2 CYLINDRICAL PLUNGE GRINDING MACHINE

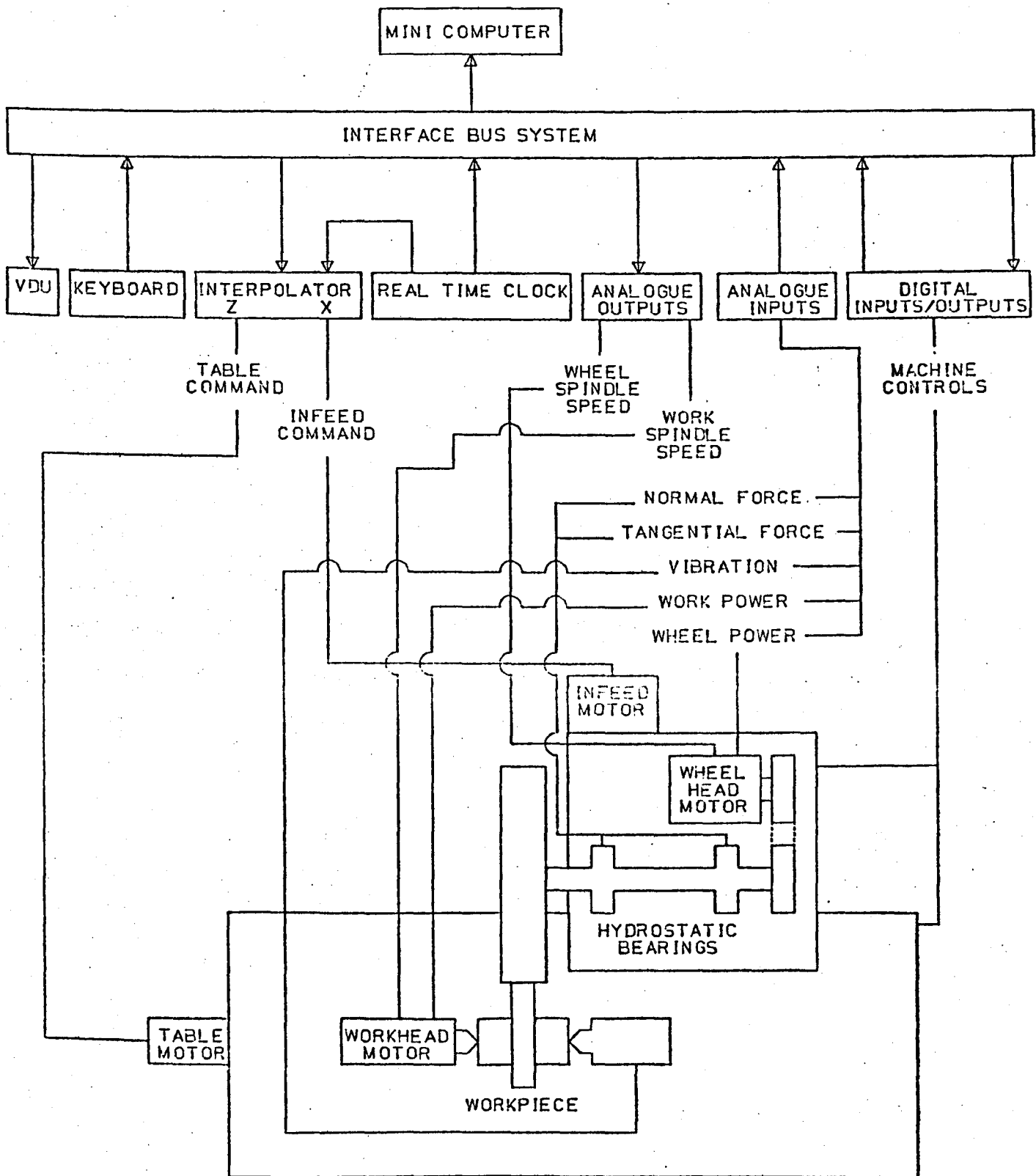


FIGURE 3.3 GRINDING MACHINE SCHEMATIC



FIGURE 3.4 D.C. AXIS SERVO MOTOR

CNC PROGRAM  
\*\*\*\*\*  
SETUP

PARAMETER	CURRENT	NEW
BLOCK NO		3
TRAVERSE DIST	UM	0
RETRACT POSN	UM	18000
INIT GRIND POSN	UM	17000
FINISH GRIND POSN		16000
FEDRATE	UM/MIN/10	50
DWELL TIME	S	5
WHEELSPEED	RPM	■

FIGURE 3.5 CNC SET-UP ROUTINE

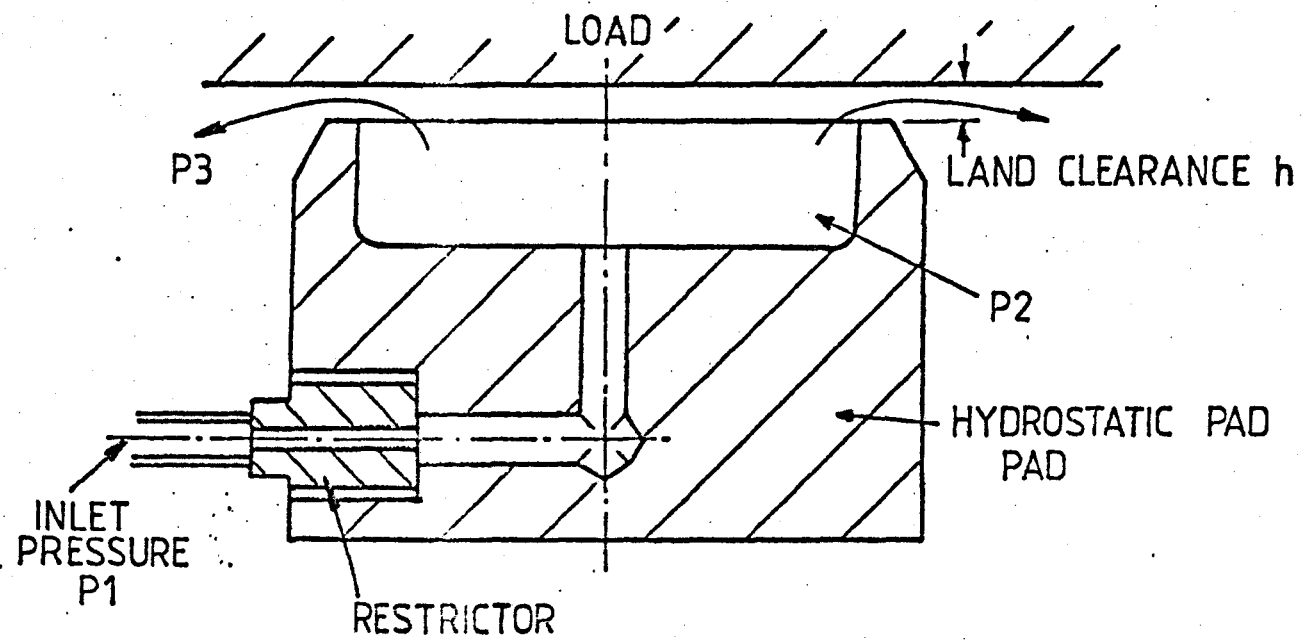


FIGURE 3.6 HYDROSTATIC PAD

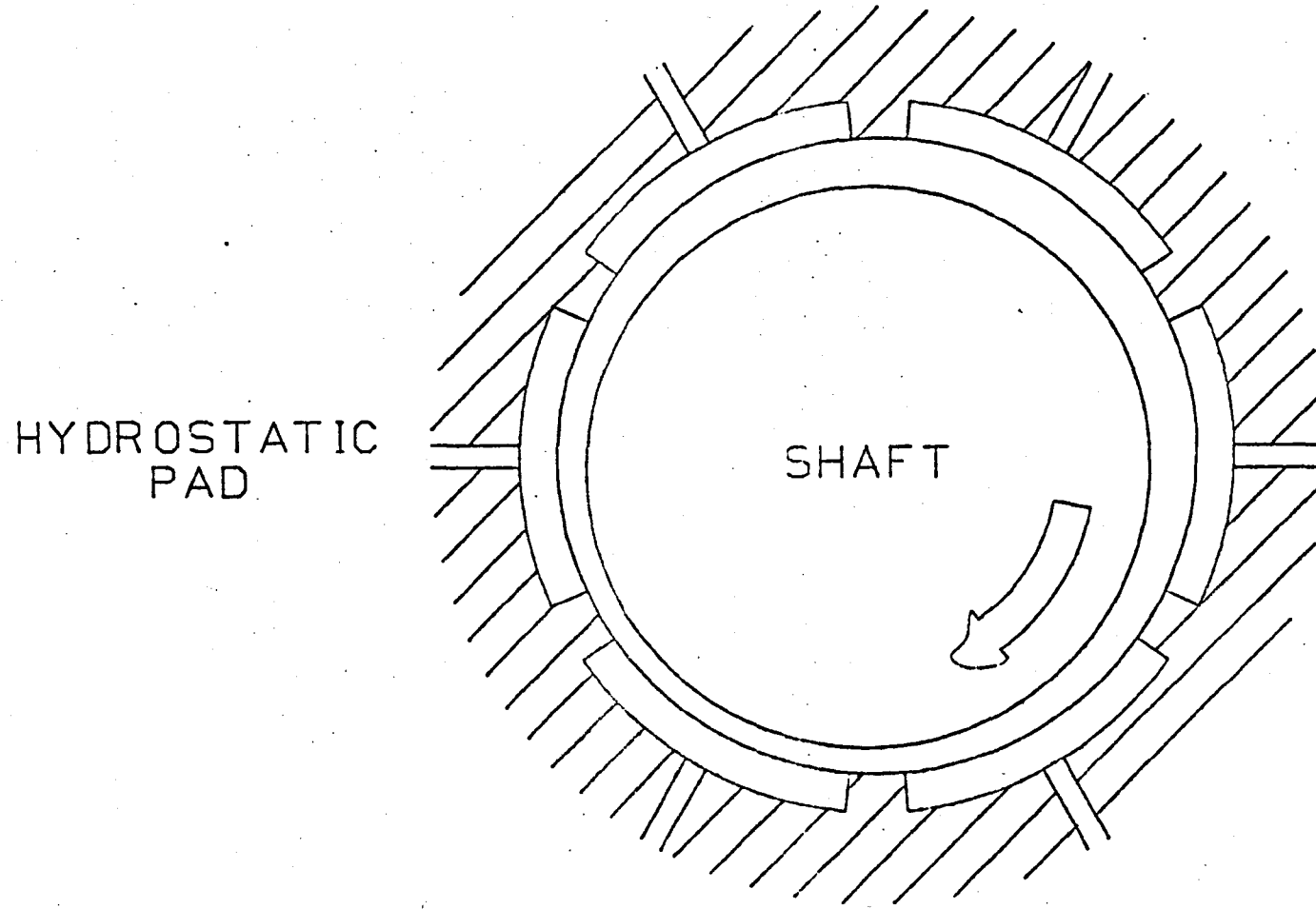


FIGURE 3.7 HYDROSTATIC JOURNAL BEARING

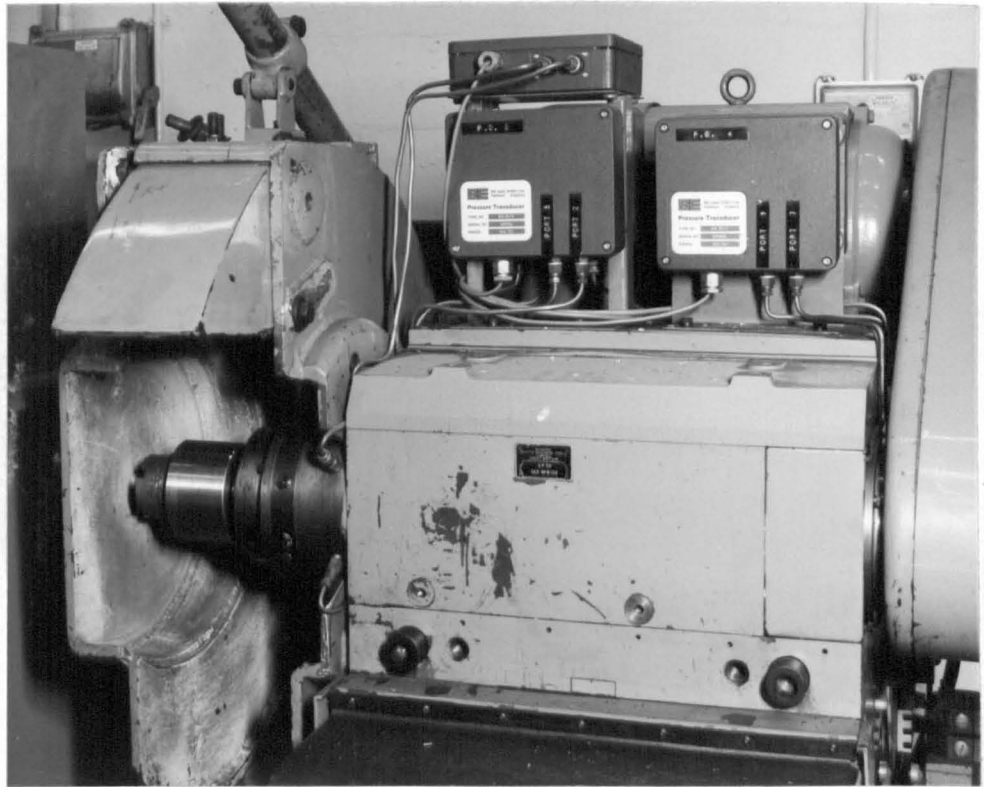
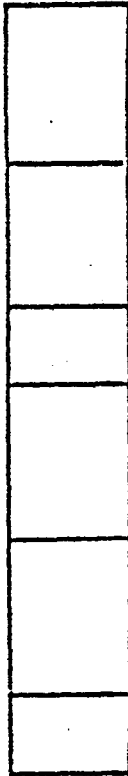


FIGURE 3.8 WHEEL SPINDLE BEARING DIFFERENTIAL PRESSURE TRANSDUCERS

FIGURE 3.9 GRINDING CYCLE TIME PERIODS

REGULAR GRINDING CYCLE (FOREGROUND MODE)

- MONITOR WHEELPOWER
- MONITOR NORMAL FORCE
- CHANGE INFEEED RATE IF NECESSARY
- MONITOR WHEELPOWER
- MONITOR VIBRATION
- COMPARE VIBRATION



0.75Secs

1.5Secs

IDENTIFICATION CYCLE (FOREGROUND MODE)

- STORE NORMAL FORCE VALUES FOR 1.5 SECS. COMPUTE AVERAGE & STORE IN REGRESSION
- ALTER FEEDRATE
- MONITOR WHEELPOWER
- STORE VIBRATION VALUES FOR 1.5 SECONDS
- CHECK VIBRATION AGAINST CONSTRAINT
- MONITOR WHEELPOWER



3 Secs

6 Secs

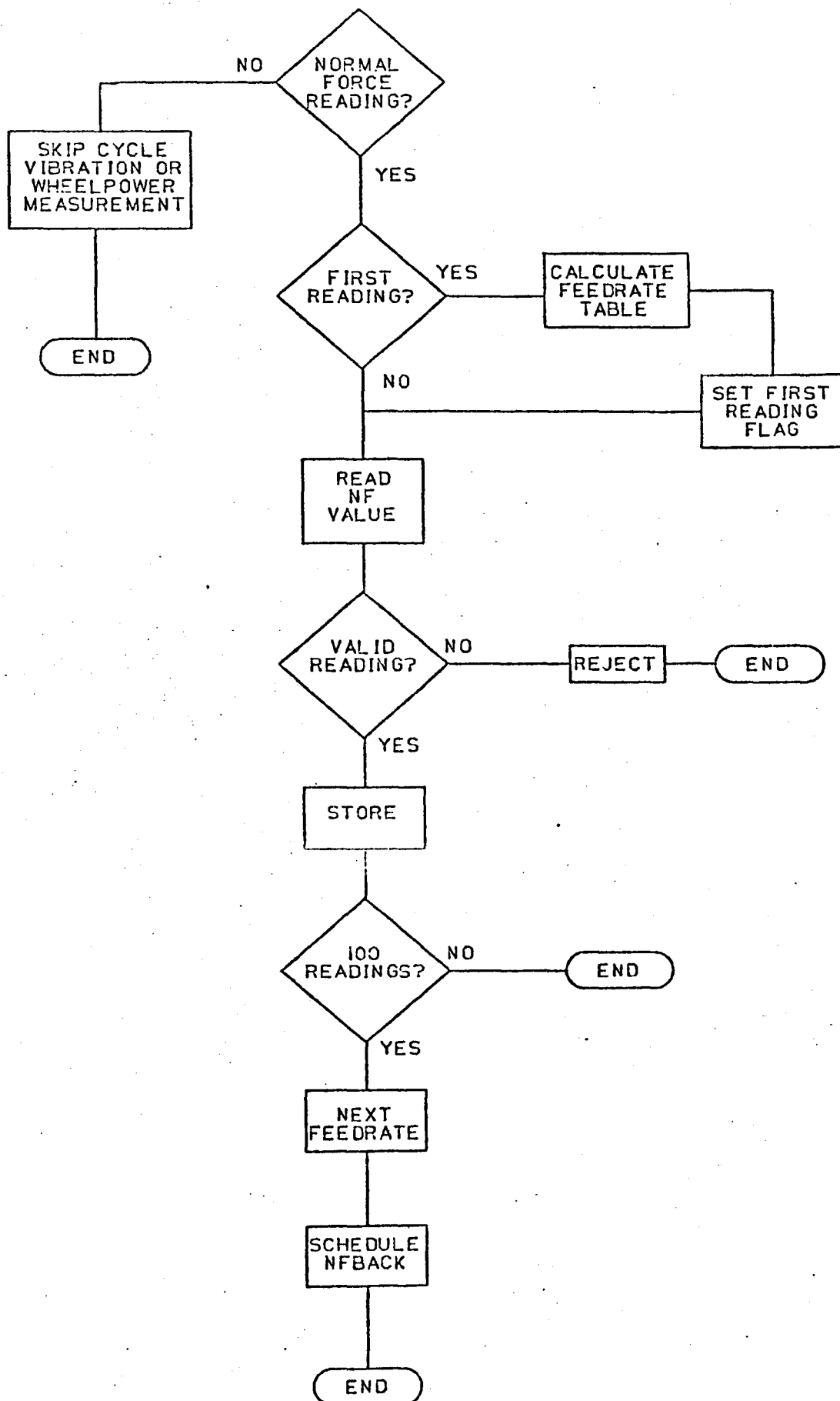


FIGURE 3.10 NORMAL FORCE IDENTIFICATION STAGE

**ADAPTIVE CONTROL INITIALISATION**  
**PARAMETER SETUP**

PARAMETER	CURRENT	NEW
MAXIMUM NORMAL FORCE	350	250
TOLERANCE ON NORMAL FORCE	10	
MAXIMUM VIBN LEVEL	60	90
MAXIMUM WHEEL POWER	50	90

FIGURE 3.11 A.C. SET-UP ROUTINE

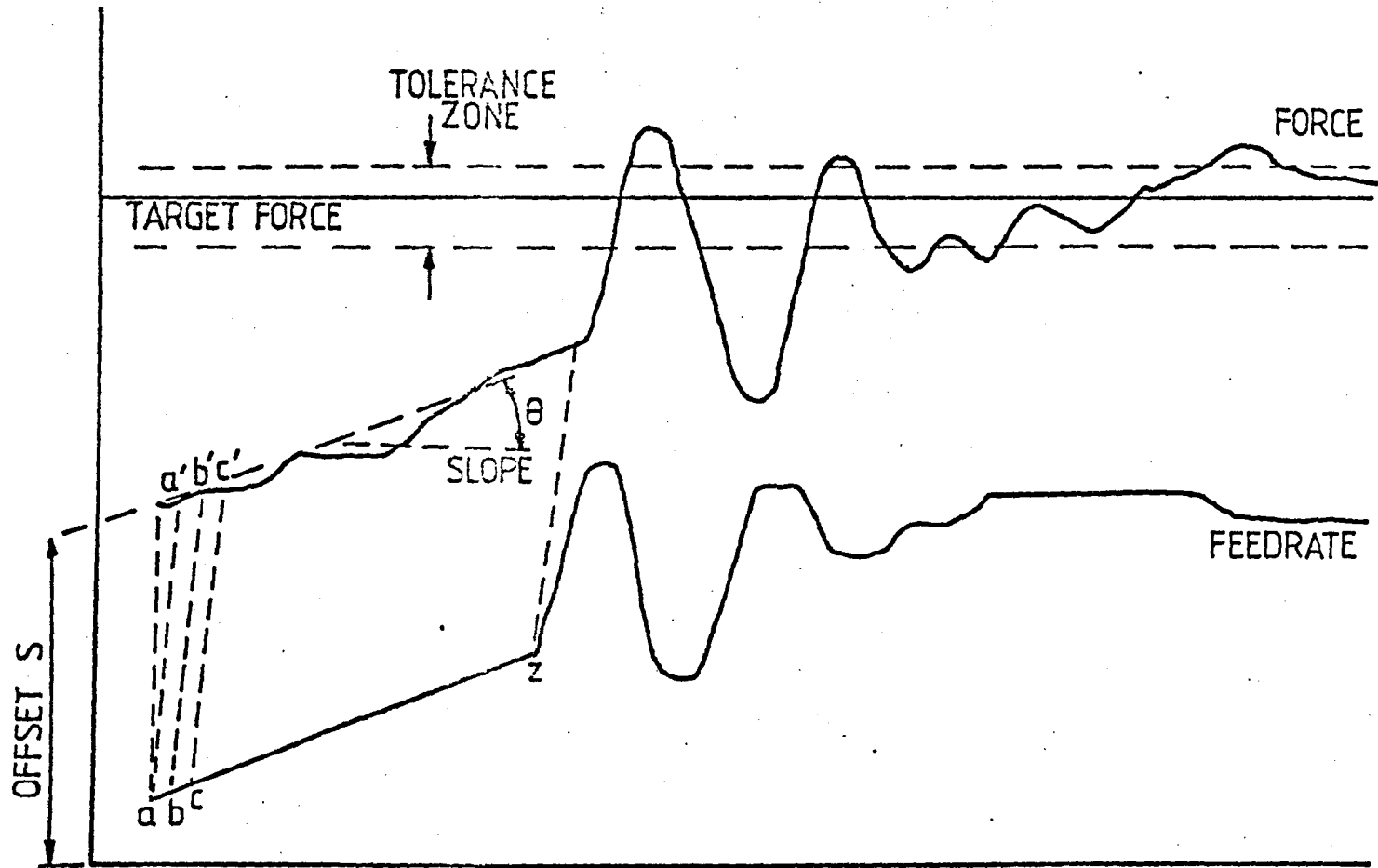


FIGURE 3.12 NORMAL FORCE FEEDRATE RELATIONSHIP

## 4.0 EXPERIMENTAL APPROACH

### 4.1 Introduction

This investigation examines the feasibility of adaptive control during production grinding to achieve the maximum metal removal rate while maintaining surface integrity. Low metal removal rates ensure good surface finishes, the absence of workpiece burn and the presence of favourable residual compressive stresses (see Section 2.5). This relationship, however, is at present subjective, with grinding conditions being described as gentle, conventional or abusive by many authors and the metal rates required to attain these conditions varying from one publication to another. An understanding of the metal removal rate-surface finish relationship, however, is necessary to develop algorithms to control component surface finish. These algorithms can then be utilised to achieve the maximum metal removal rate during grinding whilst maintaining the desired surface finish.

An adaptive control philosophy based on component surface integrity requires the surface finish of the component to be monitored during the grinding process. Direct on-line monitoring of component surface finish during grinding, however, has many inherent problems (Section 2.5) and, hence this approach was rejected. An alternative method is to indirectly monitor surface finish through the measurement of grinding parameters which are

- (a) more easily monitored
- and (b) have a direct correlation to the component surface finish

Both the normal force intensity and the amplitude of self-excited chatter vibrations between the wheel and the workpiece have been found to be related to the surface finish obtained on a ground component (Section 2.5). This influence, however, requires quantifying and developing into a model before it can be used in an adaptive control strategy. A model relating normal force and chatter levels to component surfaces finish could then be used to predict component surface finish during grinding.

Achieving the desired surface finish is an important objective of the grinding operation. An equally important consideration, however, is preventing thermal damage. Workpiece burn has been shown to be a function of wheelpower and, the normal and tangential grinding forces (see Section 2.3) and these parameters are thus also monitored.

Normal and tangential forces, wheelpower and vibration levels have therefore been shown to influence the attainable metal removal rates and workpiece surface integrity. Any developed algorithm will have to reflect the respective influences. It was therefore, proposed that the correlation between surface integrity and normal and tangential forces, wheelpower and vibration levels should be investigated and the feasibility of surface finish control examined.

#### 4.2 Test Strategy

Two types of testing techniques were adopted in the investigation. These tests can be divided into:

1. Long run tests
2. Test of short duration

The long run tests, in excess of 30 minutes duration, were designed to examine the behaviour of the monitored grinding parameters with respect to time. They did not, however, monitor the component surface finish because of the difficulties of in-process surface finish monitoring. A second series of tests were, therefore, carried out which, in addition to monitoring the same parameters as the tests of longer duration, were interrupted periodically to measure the component surface finish. The readings of the various monitored grinding parameters were then compared with the resulting surface finish data and the test was resumed to collect further data. To examine the authenticity of the interrupted test results, a comparison between the results of the long run tests and the short run tests was made to determine whether an interruption of the test significantly affected the grinding parameters. In the absence of any significant variation, a model could be developed to correlate the surface finishes with normal and tangential forces, wheelpower and vibration levels.

In the following sections the individual tests will be described in more detail.

#### 4.3 Long Duration Constant Metal Removal Rate CNC Tests

Two grinding process variables, metal removal rate and the ratio of wheelspeed to workpiece speed (Q-ratio), were investigated during these tests. These variables were chosen because of their significance in the underformed chip thickness equation and the success of this parameter to correlate grinding data (see Section 2.1).

Metal removal rate and Q-ratio are interrelated as shown in Appendix 3. To investigate the individual parameters and their cross-correlations, a factorial experimental technique has to be used. This technique incorporates nine tests to investigate three metal removal rates and three Q-ratios.

The combination of the highest metal removal rate and the highest wheel/workspeed ratio in the factorial experimental will, require the highest wheelpower (see Appendix 3). Limitations of the power available at the spindle have led to only a small range of Q-ratios within the factorial design being investigated and therefore two additional tests at higher Q-ratios have been carried out at the lowest metal removal rate.

#### 4.3.1 Test Conditions

##### 4.3.1.1 The Grinding Wheel

Type:- WA60KV.A vitrified aluminium oxide, general purpose wheel  
with a grit size of 60 and a medium hardness grade K.

Maximum recommended speed:- 1050 rpm

Diameter:- 24"

Width:- 3"

#### 4.3.1.2 Workpieces

Material: EN3 (full specification given in Appendix 2) was used in this initial test because it was classified as easy-to-grind (refer to Section 2.2)

Diameter: 225mms

Width: 70mms

#### 4.3.1.3 Coolant

Type: A water based grinding fluid, Houghtogrind, was used in a dilution of 1 part Houghtogrind to 80 parts water.

Coolant delivery rate: 160 litres/minute

#### 4.3.1.4 Wheel Dressing Conditions

Type: The research machine is fitted with a single point dressing tool which is mounted at a positive drag angle of 15° to impart greater grit damage.

Dressing procedure: The wheel was dressed in the following manner before each factorial test

Diamond depth of cut = 50µm

Diamond traverse rate = 100 mms/min

Number of passes = 4

This provided a dressing ratio of unity which has been proposed as the optimum dressing condition (see Section 2.6)

At the end of each dressing cycle the diamond was rotated through 90 degrees to prevent it from being excessively worn on one face. This helped the diamond retain its ability to produce a keen, sharp wheel.

#### 4.3.1.5 Grinding Conditions

Wheelspeed = 32 m/sec (maximum recommended wheelspeed)

#### Factorial Test Conditions

Metal removal rates: 1, 2 and 3 mm<sup>3</sup>/mm/sec

Q-Ratios:- 30, 40 and 50

Two additional wheel/workspeed ratios of 70 and 90 were added for a metal removal rate of 1 mm<sup>3</sup>/mm/sec.

#### 4.4 Long Run Constant Force Machining Tests

The results from the previously described constant metal removal rate tests provided information concerning the behaviour of the grinding forces, vibration and wheelpower levels with respect to time. These test results formed the basis for the development of grinding process control algorithms which included levels of grinding forces, wheelpower and vibration in a feedback loop. The research machine, however, is adaptively controlled to provide constant force machining and hence algorithms developed from constant metal removal rate tests may not be consistent with this philosophy. A series of constant normal force machining tests were, therefore, proposed to examine the behaviour of the tangential forces, wheelpower and vibration levels under the proposed adaptive control strategy.

##### 4.4.1 Test Conditions

The grinding wheel, workpieces, coolant and dressing conditions are unchanged from the previous tests.

#### 4.4.1.1 Grinding Conditions

A factorial experimental design of three normal force values, 100, 200 and 300N and three wheel/workspeed ratios, 30, 40 and 50 were adopted for this series of tests. The inclusion of two additional test conditions for wheel/workspeed ratios of 70 and 90 at the normal force value of 100N enabled the test to be expanded in a similar manner to the constant metal removal rate tests.

#### 4.5 Short Run Tests for the Investigation of Component Surface Finish

These tests, in addition to monitoring normal and tangential grinding forces, wheelpower and chatter vibration levels, were also periodically interrupted to measure the surface finish of the workpiece. The magnitudes of the forces, wheelpower and vibration levels prior to test interruption can then be assumed to be those responsible for producing the measured component surface finish. Testing was then continued without dressing the wheel to obtain further results.

The criteria for the duration of a test was based on the level of self-excited vibration. This parameter has been associated with deteriorating workpiece surface finish (Section 2.5) and consequently is a better indicator of significant change in surface finish than would be time or metal removed.

The spectrum analysis results for the long run tests described in Sections 4.3 and 4.4 showed that vibration levels peaked and saturated at a signal level of 20 dBs which corresponds to an accelerometer reading of 10 m/sec<sup>2</sup>. Test interruption was, therefore, carried out at a number of equispaced vibration levels in the 20 dB range.

The choice of the dBs scale rather than a linear scale allowed more data points to be acquired at the small vibration levels associated with precision grinding and also allowed more equispaced time results since the magnitude of chatter vibrations increase gradually during the early stages of grinding but increase rapidly during the latter stages; a phenomenon attributed to the unstable nature of the process (Section 2.4). The vibration levels chosen for the test interruption were therefore, 4, 8, 12, 16 and 20 dBs which corresponded to accelerometer readings of 1.5, 2.5, 4, 6.3 and 10 m/sec<sup>2</sup>.

#### 4.5.1 Surface Finish Test Conditions

The grinding wheel, workpieces, coolant and dressing conditions were unchanged from the previous tests.

##### 4.5.1.1 Grinding Conditions

A factorial experimental design of two metal removal rates, 1 and 2 mm<sup>3</sup>/mm/sec and three wheel/workspeed ratios, 30, 40 and 50 were adopted for these tests. Two additional wheel/workspeed ratios of 70 and 90 were again included at the lowest metal removal rate.

This test programme differed from previous test programmes in that a metal removal rate of 3 mm<sup>3</sup>/mm/sec was not investigated. Results obtained from the previous test programmes described in Sections 4.3 and 4.4 showed increasing levels of chatter vibration with respect to time for metal removal rates of 1 and 2 mm<sup>3</sup>/mm/sec. This was not the case for the test results at a metal removal rate of 3 mm<sup>3</sup>/mm/sec where vibration levels were observed to decrease.

The philosophy of these tests cannot therefore be applied in the case of grinding this particular work material at a metal removal rate of  $3\text{mm}^3/\text{mm}/\text{sec}$ .

This restriction is not a severe one. British Standards [1;1972] have referred to an expected range of surface finish values produced by the grinding process ( $0.025\text{--}1.6\mu\text{m}$ ). The surface finish results obtained for the  $3\text{mm}^3/\text{mm}/\text{sec}$  condition are in the upper region, and in some cases above these values, and hence it is not unreasonable to classify this metal removal rate as "rough grinding". This programme is concerned with obtaining a surface finish correlation which is appropriate to precision grinding. Any rough grinding cycles will only be utilised for removing the bulk of the material and not for producing the final component geometry.

#### 4.6 Wheel Dressing

Dressing conditions have a significant influence on grinding forces and workpiece surface finishes (Section 2.6). The previous test programmes, however, have not utilised wheel dressing as a variable: the same dressing treatment has been used in each programme. This investigation, therefore, proposes to examine the influence of the wheel dressing treatment on the workpiece surface finish, normal and tangential grinding forces, wheelpower and chatter vibration levels. Results obtained from this investigation will be used in automatic dressing cycles which will be developed to become an integral part of the grinding process adaptive control strategy.

Dressing conditions have been described as "fine", "medium" and "coarse" (Section 2.6). These differing dressing treatments have been achieved in a number of ways but the diamond cross-feed rate has been reported to have the most significant influence on the grinding process. The present investigation, therefore, proposed to vary the traverse rate of the single point diamond dressing tool and examine the resulting effect on the grinding process.

#### 4.6.1 Test Conditions

The grinding wheel, coolant and workpiece dimensions were the same as the previous three test programmes.

##### 4.6.1.1. Workpiece Material

To enable the effect of wheel dressing and a different work material, EN8 (Appendix 2) was selected for these tests.

##### 4.6.1.2 Dressing Conditions

Three dressing conditions "fine", "medium" and "coarse" were investigated. The "medium" dressing condition was chosen to be the same as that of previous tests (see Section 2.6 and 4.3.1.4). The diamond traverse rate was then halved and doubled for the "fine" and "coarse" dressing treatments respectively. The dressing treatments were, therefore, as follows:

Fine dressing	Diamond depth of cut = 50 $\mu\text{m}$
	Diamond traverse rate = 50 mms/min
	Number of passes = 4

Medium dressing Diamond depth of cut = 50  $\mu\text{m}$   
Diamond traverse rate = 100 mms/min  
Number of passes = 4

Coarse dressing Diamond depth of cut = 50  $\mu\text{m}$   
Diamond traverse rate = 200 mms/min  
Number of passes = 4

The terms fine, medium and coarse used here are relative and not intended to indicate correlation with other workers' [42;1971: 43;1972: 45;1978: 116;1971: 118;1972] designations.

#### 4.6.1.3. Grinding Conditions

A 3 x 3 factorial experimental design was utilised to investigate three metal removal rates, 0.75, 1.5 and 2.5 mm<sup>3</sup>/mm/sec, at each of the three dressing treatments.

The largest metal removal rate used during the test programme was reduced from 3 to 2.5 mm<sup>3</sup>/mm/sec because the former value required a wheelpower in excess of the grinding machine wheel spindle motor (rated at 11.4 KW) and hence stalled the wheel.

#### 4.6.2 Test Procedure

Each of the 27 test conditions were investigated by a long run test to provide normal and tangential grinding force, wheelpower and vibration information and an interrupted test to provide surface finish data.

#### 4.6.2.1 Short Run Test Procedure

Dressing has been reported to influence the process during the primary wear stage of the wheel, but to have no influence in subsequent wear stages (Section 2.6).

Interruption of the dressing tests once the vibration level reached a pre-determined magnitude could have yielded secondary wear rather than primary wear results and hence a periodical test interruption of two minutes was used.

#### 4.7 Coding System for Test Investigation

A coding system will be used for identifying individual grinding test conditions. This will comprise a four-level code of the form SR-MRR-2-30. An explanation of the code follows:

Level 1 Identifies the type of the test. Tests to examine the behaviour of normal and tangential forces, wheelpower and chatter vibration levels with respect to time will be coded LR for long run tests. Alternatively, tests conducted to examine surface finish data are coded SR for short run tests.

Level 2 Identifies the grinding conditions. Three independent grinding conditions were examined, constant metal removal rate, constant normal force, and the programme of tests to examine wheel dressing conditions.

The coding system distinguishes between these as follows:

MRR	Constant Metal Removal Rate
NF	Constant Normal Force
CD	Coarse Wheel Dressing Programme
MD	Medium Wheel Dressing Programme
FD	Fine Wheel Dressing Programme

Level 3 Identifies the metal removal rate or the normal force value used in the constant normal force tests.

Level 4 Identifies the wheel/workspeed ratio of the test

#### 4.7.1 Coding System Example

SR-MRR-2-50 = Interrupted short run test conducted at a constant metal removal rate of 2 mm<sup>3</sup>/mm/sec and a wheel/workspeed ratio of 50

## 5.0 RESULTS

### 5.1 Constant Metal Removal Rate Tests

The wheelpower and the normal and tangential grinding forces for each of the eleven factorial test conditions are given in Tables 5.1a - 5.1k.

Grinding chatter manifests itself as an increasing amplitude of vibration at a particular chatter frequency (see Section 2.4). The chatter vibration results for this test programme have, therefore, been presented as spectrum analysis plots shown in Figures 5.1a-5.1k. This form of representation enables a study to be undertaken of the behaviour of grinding chatter with respect to time.

Eight vibration levels were recorded during the tests; one every 4 minutes. All eight plots are not shown, however, because this would unnecessarily complicate the figures. Instead three or four plots have been reproduced to illustrate the chatter behaviour.

Although the long run tests were designed to be of 30 minutes duration, four tests were terminated early because of severe chatter.

### 5.2 Constant Normal Force Machining Tests

The magnitudes of the wheelpower and tangential force for each test condition are given in Tables 5.2a - 5.2k and the corresponding chatter vibration spectrum analysis plots are presented in Figures 5.2a - 5.2k.

The surface finish of the component at the end of each test is presented in Table 5.3.

This series of constant normal forces tests were designed to complement the constant metal removal rate tests. To enable a comparison to be made between the two test philosophies, the initial and final metal removal rates for each of the constant normal force tests are given in Table 5.4

### 5.3 Component Surface Finish Investigation

This programme of test was halted to measure the component surface finish as the magnitude of chatter vibration exceeded the following levels: 1.5, 2.5, 4, 6.3 and 10 m/sec<sup>2</sup>. The time taken to reach each vibration level; the normal and tangential grinding force and the wheelpower prior to test interruption; and the surface finish of the workpiece are given in Tables 5.5a-5.5h. Figures 5.3a-5.3h are spectrum analysis plots which show the behaviour of the chatter vibration with respect to time.

Each test was to be terminated if the level of chatter vibration exceeded the upper limit of 10 m/sec<sup>2</sup>. Not all tests, however, reached this value (refer to the previous spectrum analysis results in Figures 5.1 and 5.2) and hence tests were terminated after 60 minutes of grinding even if the upper vibration level had not been exceeded.

### 5.4 Wheel Dressing Tests

#### 5.4.1 Long Run Test Results

The magnitudes of the wheelpower and the normal and tangential grinding forces for each of the three metal removal rates are given in Tables 5.6a-5.6c. The spectrum analysis chatter vibration results are given in Figures 5.4a-5.4i.

#### 5.4.2 Short Run Test Results

Tables 5.7a-5.7c present the surface finish data obtained from each of the three metal removal rate tests.

TEST LR-MRR-1-30

TIME MINS	NORMAL FORCE NEWTONS	TANGENTIAL FORCE NEWTONS	GRINDING COEFFICIENT $\mu$	WHEELPOWER KWS
2	110	60	0.55	5.4
6	110	65	0.59	5.4
10	140	70	0.5	5.8
14	150	80	0.53	6.0
18	150	90	0.6	6.8
22	160	90	0.56	7.0

TABLE 5.1a

Note:- Grinding Coefficient = the ratio of tangential to normal grinding force

GRINDING FORCES & WHEELPOWER RESULTS  
FROM CONSTANT METAL REMOVAL RATE TESTS

TEST LR-MRR-1-40

TIME MINS	NORMAL FORCE NEWTONS	TANGENTIAL FORCE NEWTONS	GRINDING COEFFICIENT $\mu$	WHEELPOWER KWS
2	125	70	0.56	5.6
6	140	75	0.54	5.6
10	140	80	0.57	5.8
14	150	90	0.6	6.6
18	150	95	0.63	6.6
22	175	90	0.51	6.6
26	175	100	0.57	6.8
30	175	100	0.57	6.6

TABLE 5.1b

TEST LR-MRR-1-50

TIME MINS	NORMAL FORCE NEWTONS	TANGENTIAL FORCE NEWTONS	GRINDING COEFFICIENT $\mu$	WHEELPOWER KWS
2	125	60	0.48	5.0
6	110	70	0.64	5.4
10	125	80	0.64	6.4
14	125	85	0.68	6.2
18	140	85	0.61	6.4

TABLE 5.1c

TEST LR-MRR-1-70

TIME MINS	NORMAL FORCE NEWTONS	TANGENTIAL FORCE NEWTONS	GRINDING COEFFICIENT $\mu$	WHEELPOWER KWS
2	100	55	0.55	4.8
6	110	65	0.59	5.2
10	125	70	0.56	5.6
14	140	85	0.6	6.0
18	140	90	0.64	6.2
22	150	90	0.6	6.2
26	150	90	0.6	6.4
30	150	95	0.6	6.4

TABLE 5.1d

TEST LR-MRR-1-90

TIME MINS	NORMAL FORCE NEWTONS	TANGENTIAL FORCE NEWTONS	GRINDING COEFFICIENT $\mu$	WHEELPOWER KWS
2	110	60	0.55	4.4
6	130	70	0.54	5.0
10	140	80	0.57	5.6
14	140	80	0.57	5.4
18	160	90	0.56	6.0
22	160	95	0.59	6.0
26	170	95	0.56	6.0
30	180	100	0.56	6.4

TABLE 5.1e

TEST LR-MRR-2-30

TIME MINS	NORMAL FORCE NEWTONS	TANGENTIAL FORCE NEWTONS	GRINDING COEFFICIENT $\mu$	WHEELPOWER KWS
2	250	130	0.52	10.0
6	225	120	0.53	9.0
10	225	125	0.56	9.6
14	240	130	0.54	9.6
18	240	130	0.54	9.4

TABLE 5.1f

TEST LR-MRR-2-40

TIME MINS	NORMAL FORCE NEWTONS	TANGENTIAL FORCE NEWTONS	GRINDING COEFFICIENT $\mu$	WHEELPOWER KWS
2	210	120	0.57	9.2
6	200	115	0.58	8.4
10	210	130	0.62	9.2
14	225	135	0.6	9.8
18	240	130	0.54	9.4

TABLE 5.1g

TEST LR-MRR-2-50

TIME MINS	NORMAL FORCE NEWTONS	TANGENTIAL FORCE NEWTONS	GRINDING COEFFICIENT $\mu$	WHEELPOWER KWS
2	175	105	0.6	7.4
6	190	115	0.61	8.0
10	190	120	0.63	8.4
14	190	115	0.61	8.4
18	200	120	0.6	8.6
22	200	120	0.6	8.4
26	200	120	0.6	8.4
30	210	120	0.57	8.0

TABLE 5.1h

TEST LR-MRR-3-30

TIME MINS	NORMAL FORCE NEWTONS	TANGENTIAL FORCE NEWTONS	GRINDING COEFFICIENT $\mu$	WHEELPOWER KWS
2	310	160	0.52	11.0
6	300	160	0.53	10.6
10	300	170	0.57	10.4
14	300	170	0.57	10.6
18	290	150	0.52	10.2
22	290	150	0.52	10.4
26	300	160	0.53	9.8
30	300	160	0.53	9.8

TABLE 5.1i

TEST LR-MRR-3-40

TIME MINS	NORMAL FORCE NEWTONS	TANGENTIAL FORCE NEWTONS	GRINDING COEFFICIENT $\mu$	WHEELPOWER KWS
2	310	150	0.48	11.2
6	310	140	0.45	10.8
10	310	140	0.45	10.0
14	310	150	0.48	9.4
18	310	150	0.48	8.8
22	310	160	0.52	8.8
26	300	150	0.5	8.6
30	310	150	0.48	8.4

TABLE 5.1j

TEST LR-MRR-3-50

TIME MINS	NORMAL FORCE NEWTONS	TANGENTIAL FORCE NEWTONS	GRINDING COEFFICIENT $\mu$	WHEELPOWER KWS
2	300	165	0.55	11.4
6	300	160	0.53	11.2
10	300	155	0.52	10.6
14	300	155	0.52	10.4
18	290	145	0.5	10.2
22	300	150	0.5	10.2
26	300	155	0.52	10.0
30	290	150	0.52	10.0

TABLE 5.1k

TEST LR-NF-100-30

TIME MINUTES	TANGENTIAL FORCE NEWTONS	GRINDING COEFFICIENT $\mu$	WHEELPOWER KWS
2	70	0.7	4.2
6	75	0.75	4.6
10	75	0.75	4.6
14	70	0.7	4.0
18	70	0.7	4.4
22	70	0.7	3.8
26	70	0.7	4.0
30	75	0.75	4.4

TABLE 5.2a

TANGENTIAL FORCE & WHEELPOWER RESULTS  
FOR CONSTANT NORMAL FORCE TESTS

TEST LR-NF-100-40

TIME MINUTES	TANGENTIAL FORCE NEWTONS	GRINDING COEFFICIENT $\mu$	WHEELPOWER KWS
2	65	0.65	4.2
6	75	0.75	4.6
10	70	0.7	4.6
14	75	0.75	4.6
18	75	0.75	4.8
22	80	0.8	4.6
26	80	0.8	4.8

TABLE 5.2b

TEST LR-NF-100-50

TIME MINUTES	TANGENTIAL FORCE NEWTONS	GRINDING COEFFICIENT $\mu$	WHEELPOWER KWS
2	75	0.75	4.0
6	70	0.7	3.8
10	75	0.75	4.0
14	70	0.7	3.6
18	70	0.7	3.6
22	70	0.7	3.4
26	75	0.75	3.6
30	70	0.7	3.4

TABLE 5.2c

TEST LR-NF-100-70

TIME MINUTES	TANGENTIAL FORCE NEWTONS	GRINDING COEFFICIENT $\mu$	WHEELPOWER KWS
2	70	0.7	4.2
6	80	0.8	4.2
10	80	0.8	4.4
14	75	0.75	4.2
18	80	0.8	4.4
22	70	0.7	4.2
26	75	0.75	4.2
30	80	0.8	4.4

TABLE 5.2d

TEST LR-NF-100-90

TIME MINUTES	TANGENTIAL FORCE NEWTONS	GRINDING COEFFICIENT $\mu$	WHEELPOWER KWS
2	70	0.7	4.6
6	70	0.7	4.4
10	70	0.7	4.4
14	80	0.8	4.4
18	75	0.75	4.2
22	70	0.7	3.8
26	75	0.75	4.0
30	70	0.7	3.8

TABLE 5.2e

TEST LR-NF-200-30

TIME MINUTES	TANGENTIAL FORCE NEWTONS	GRINDING COEFFICIENT $\mu$	WHEELPOWER KWS
2	110	0.55	7.4
6	120	0.6	7.4
10	120	0.6	7.6
14	120	0.6	7.6
18	125	0.63	7.6
22	125	0.63	7.8
26	125	0.63	7.4
30	120	0.6	7.6

TABLE 5.2f

TEST LR-NF-200-40

TIME MINUTES	TANGENTIAL FORCE NEWTONS	GRINDING COEFFICIENT $\mu$	WHEELPOWER KWS
2	120	0.6	9.6
6	130	0.65	9.2
10	130	0.65	9.2
14	125	0.63	8.8
18	120	0.6	8.4
22	120	0.6	8.2

TABLE 5.2g

TEST LR-NF-200-50

TIME MINUTES	TANGENTIAL FORCE NEWTONS	GRINDING COEFFICIENT $\mu$	WHEELPOWER KWS
2	120	0.6	7.8
6	125	0.63	8.4
10	130	0.65	8.4
14	130	0.65	8.4
18	130	0.65	8.2
22	130	0.65	8.0

TABLE 5.2h

TEST LR-NF-300-30

TIME MINUTES	TANGENTIAL FORCE NEWTONS	GRINDING COEFFICIENT $\mu$	WHEELPOWER KWS
2	170	0.57	11.4
6	170	0.57	11.4
10	160	0.53	11.0
14	160	0.53	10.6
18	155	0.52	10.4
22	160	0.53	10.2
26	160	0.53	10.2
30	155	0.52	10.0

TABLE 5.2i

TEST LR-NF-300-40

TIME MINUTES	TANGENTIAL FORCE NEWTONS	GRINDING COEFFICIENT $\mu$	WHEELPOWER KWS
2	175	0.58	11.0
6	185	0.62	10.8
10	190	0.63	11.2
14	185	0.62	10.2
18	175	0.58	9.6
22	165	0.55	9.2

TABLE 5.2j

TEST LR-NF-300-50

TIME MINUTES	TANGENTIAL FORCE NEWTONS	GRINDING COEFFICIENT $\mu$	WHEELPOWER KWS
2	150	0.5	10.4
6	150	0.5	10.0
10	155	0.52	9.8
14	155	0.52	9.8
18	160	0.55	10.0
22	155	0.52	9.8
26	150	0.5	9.8
30	155	0.52	10.0

TABLE 5.2k

TEST LR-NF-	SURFACE FINISH $\mu\text{m Ra}$
100-30	0.44
100-40	0.65
100-50	0.63
100-70	0.67
100-90	0.72
200-30	1.07
200-40	1.19
200-50	1.27
300-30	3.2
300-40	2.2
300-50	1.91

TABLE 5.3

WORKPIECE SURFACE FINISH ON  
TEST CONCLUSIONS

TEST LR-NF-	METAL REMOVAL RATE mm <sup>3</sup> /mm/sec	
	Test Commencement	Test Conclusion
100-30	0.67	0.36
100-40	0.94	0.56
100-50	0.85	0.37
100-70	0.98	0.62
100-90	0.95	0.52
200-30	1.86	1.09
200-40	2.03	1.58
200-50	2.21	1.66
300-30	2.81	3.03
300-40	2.67	2.53
300-50	2.66	2.48

TABLE 5.4

METAL REMOVAL RATES

TEST SR-MRR-1-30

The vibration amplitude failed to exceed 4 dBs for the 60 minutes of test duration

Final results:-	Normal Force	= 160 Newtons
	Tangential Force	= 110 Newtons
	Grinding Coefficient	= 0.69
	Wheelpower	= 5.8 KWs
	Surface finish	= 1.09 $\mu$ m Ra

TABLE 5.5a

GRINDING DATA FROM SHORT DURATION INTERRUPTED TESTS

TEST SR-MRR-1-40

VIBRATION LEVEL dBs	TIME TO EXCEED LEVEL mins	NORMAL FORCE NEWTONS	TANGENTIAL FORCE NEWTONS	GRINDING COEFFICIENT $\mu$	WHEELPOWER KWS	COMPONENT SURFACE FINISH $\mu\text{m Ra}$
4	0.5	150	95	0.63	5.4	0.56
*	-	150	90	0.6	4.8	0.98

\* Vibration level never exceeded 8dBs. Readings taken after 60 minutes

TABLE 5.5b

TEST SR-MRR-1-50

VIBRATION LEVEL dBs	TIME TO EXCEED LEVEL mins	NORMAL FORCE NEWTONS	TANGENTIAL FORCE NEWTONS	GRINDING COEFFICIENT $\mu$	WHEELPOWER KWS	COMPONENT SURFACE FINISH $\mu\text{m Ra}$
4	38.0	150	95	0.63	5.4	0.94
8	39.5	160	100	0.62	6.2	0.92
*	-	160	100	0.62	5.8	0.9

\* Vibration level never exceeded 12dBs. Readings taken after 60 minutes

TABLE 5.5c

TEST SR-MRR-1-70

VIBRATION LEVEL dBs	TIME TO EXCEED LEVEL mins	NORMAL FORCE NEWTONS	TANGENTIAL FORCE NEWTONS	GRINDING COEFFICIENT $\mu$	WHEELPOWER KWS	COMPONENT SURFACE FINISH $\mu\text{m Ra}$
4	26.0	160	95	0.59	5.4	0.8
8	27.5	160	100	0.62	6.0	0.74
12	29.0	150	95	0.63	5.8	0.82
16	31.5	160	105	0.66	6.2	0.79
20	32.5	170	110	0.65	6.4	0.84

TABLE 5.5d

TEST SR-MRR-1-90

VIBRATION LEVEL dBS	TIME TO EXCEED LEVEL mins	NORMAL FORCE NEWTONS	TANGENTIAL FORCE NEWTONS	GRINDING COEFFICIENT $\mu$	WHEELPOWER KWS	COMPONENT SURFACE FINISH um Ra
4	0.5	140	85	0.61	7.8	0.49
8	1.5	130	80	0.62	7.6	0.58
12	16.5	100	75	0.75	5.6	0.94
16	20.5	120	80	0.67	5.8	0.9
20	32.5	140	90	0.64	6.0	1.02

TABLE 5.5e

TEST SR-MRR-2-30

VIBRATION LEVEL dBs	TIME TO EXCEED LEVEL mins	NORMAL FORCE NEWTONS	TANGENTIAL FORCE NEWTONS	GRINDING COEFFICIENT $\mu$	WHEELPOWER KWS	COMPONENT SURFACE FINISH $\mu\text{m Ra}$
4	3.5	140	100	0.71	7.6	1.14
8	6.5	160	110	0.69	8.0	1.13
12	9.5	190	120	0.63	8.4	1.25
16	12	200	130	0.65	8.4	1.33
12*	48	230	135	0.57	8.0	2.32

\*Vibration level decreased and hence never reached 20 dBs. Reading taken once vibration fell below 12 dBs again

TABLE 5.5f

TEST SR-MRR-2-40

VIBRATION LEVEL dBs	TIME TO EXCEED LEVEL mins	NORMAL FORCE NEWTONS	TANGENTIAL FORCE NEWTONS	GRINDING COEFFICIENT $\mu$	WHEELPOWER KWS	COMPONENT SURFACE FINISH um Ra
4	7.0	150	90	0.6	8.0	1.11
8	9.0	160	100	0.62	8.4	1.18
12	18.0	190	125	0.66	8.6	1.34
16	24.5	210	130	0.62	8.8	1.36
20	29.5	230	135	0.59	9.0	1.41

TABLE 5.5g

TEST SR-MRR-2-50

VIBRATION LEVEL dBs	TIME TO EXCEED LEVEL mins	NORMAL FORCE NEWTONS	TANGENTIAL FORCE NEWTONS	GRINDING COEFFICIENT $\mu$	WHEELPOWER KWS	COMPONENT SURFACE FINISH $\mu\text{m Ra}$
4	2.5	150	80	0.53	7.8	1.04
8	18.0	180	110	0.61	8.0	1.36
12	25.0	210	125	0.6	8.6	1.49
16	40.0	230	130	0.57	8.6	1.61
20	41.0	225	130	0.58	8.6	1.62

TABLE 5.5h

METAL REMOVAL RATE = 2.5 mm<sup>3</sup>/mm/sec

MATERIAL = EN8

VARIABLE	NORMAL FORCE NEWTONS			TANGENTIAL FORCE NEWTONS			WHEELPOWER KWS		
	Fine	Medium	Coarse	Fine	Medium	Coarse	Fine	Medium	Coarse
Dressing Treatment									
Time Mins									
2	250	320	200	140	155	105	10.4	10.4	7.4
6	300	280	240	160	155	125	10.8	10.2	8.2
10	320	380	230	165	170	130	11.0	11.0	8.2
14	330	360	240	170	175	135	10.8	11.4	8.6
18	320	360	260	160	175	140	10.4	11.4	9.0
22	340	-	290	170	-	150	10.4	-	9.2
26	330	-	340	170	-	180	10.4	-	9.6
30	310	-	360	160	-	190	10.2	-	10.0

TABLE 5.6a

GRINDING FORCES & WHEELPOWER RESULTS FROM  
DRESSING TESTS

METAL REMOVAL RATE = 1.5 mm<sup>3</sup>/mm/sec

MATERIAL = EN8

VARIABLE	NORMAL FORCE NEWTONS			TANGENTIAL FORCE NEWTONS			WHEELPOWER KWS		
	Fine	Medium	Coarse	Fine	Medium	Coarse	Fine	Medium	Coarse
Dressing Treatment Time Mins									
2	200	210	190	120	110	100	7.2	6.8	6.0
6	210	190	210	130	115	110	7.6	7.2	6.2
10	210	190	210	135	115	115	7.6	7.2	6.8
14	220	210	230	130	120	120	7.6	7.2	6.8
18	220	200	220	135	120	120	7.6	7.2	6.8
22	220	250	260	135	130	135	7.6	7.4	7.0
26	230	210	250	140	130	130	7.8	8.0	7.2
30	250	220	250	140	135	130	7.8	8.0	7.2

TABLE 5.6b

METAL REMOVAL RATE = 0.75 mm<sup>3</sup>/mm/sec

MATERIAL = EN8

VARIABLE	NORMAL FORCE NEWTONS			TANGENTIAL FORCE NEWTONS			WHEELPOWER KWS		
	Fine	Medium	Coarse	Fine	Medium	Coarse	Fine	Medium	Coarse
Dressing Treatment Time Mins									
2	150	125	125	80	70	70	4.8	4.8	3.6
6	155	140	140	90	75	75	5.0	4.8	4.0
10	190	135	140	95	80	80	5.2	4.8	4.2
14	180	130	150	95	80	85	5.2	4.8	4.4
18	160	125	150	95	80	85	5.0	4.8	4.4
22	170	165	145	95	85	85	5.0	5.0	4.4
26	170	150	150	95	85	85	4.8	5.2	4.4
30	160	160	170	95	90	95	4.8	5.2	4.8

TABLE 5.6c

METAL REMOVAL RATE = 2.5 mm<sup>3</sup>/mm/sec

TIME MINS	DRESSING CONDITIONS		
	FINE	MEDIUM	COARSE
2	0.75	0.76	1.23
4	0.90	0.89	1.33
6	1.06	0.99	1.28
8	1.06	1.08	1.29
10	1.07	1.13	1.37
12	1.09	1.20	1.38
14	1.18	1.15	1.37
16	1.16	1.23	1.36
18	1.17	1.18	1.36
20	1.29	1.16	1.32

TABLE 5.7a

SURFACE FINISH DATA,  $\mu$ mRa FROM SHORT  
RUN TESTS

METAL REMOVAL RATE = 1.5 mm<sup>3</sup>/mm/sec

TIME MINS	DRESSING CONDITIONS		
	FINE	MEDIUM	COARSE
2	0.67	0.62	0.96
4	0.67	0.69	1.01
6	0.78	0.71	1.02
8	0.81	0.77	1.03
10	0.82	0.84	1.10
12	0.87	0.84	1.10
14	0.89	0.79	1.10
16	0.88	0.79	1.11
18	0.90	0.79	1.11
20	0.88	0.82	1.12

TABLE 5.7b

METAL REMOVAL RATE = 0.75 mm<sup>3</sup>/mm/sec

TIME MINS	DRESSING CONDITIONS		
	FINE	MEDIUM	COARSE
2	0.50	0.53	0.82
4	0.52	0.55	0.82
6	0.53	0.56	0.69
8	0.58	0.57	0.77
10	0.58	0.61	0.74
12	0.57	0.60	0.70
14	0.61	0.62	0.76
16	0.61	0.58	0.82
18	0.65	0.65	0.75
20	0.66	0.62	0.70

TABLE 5.7c

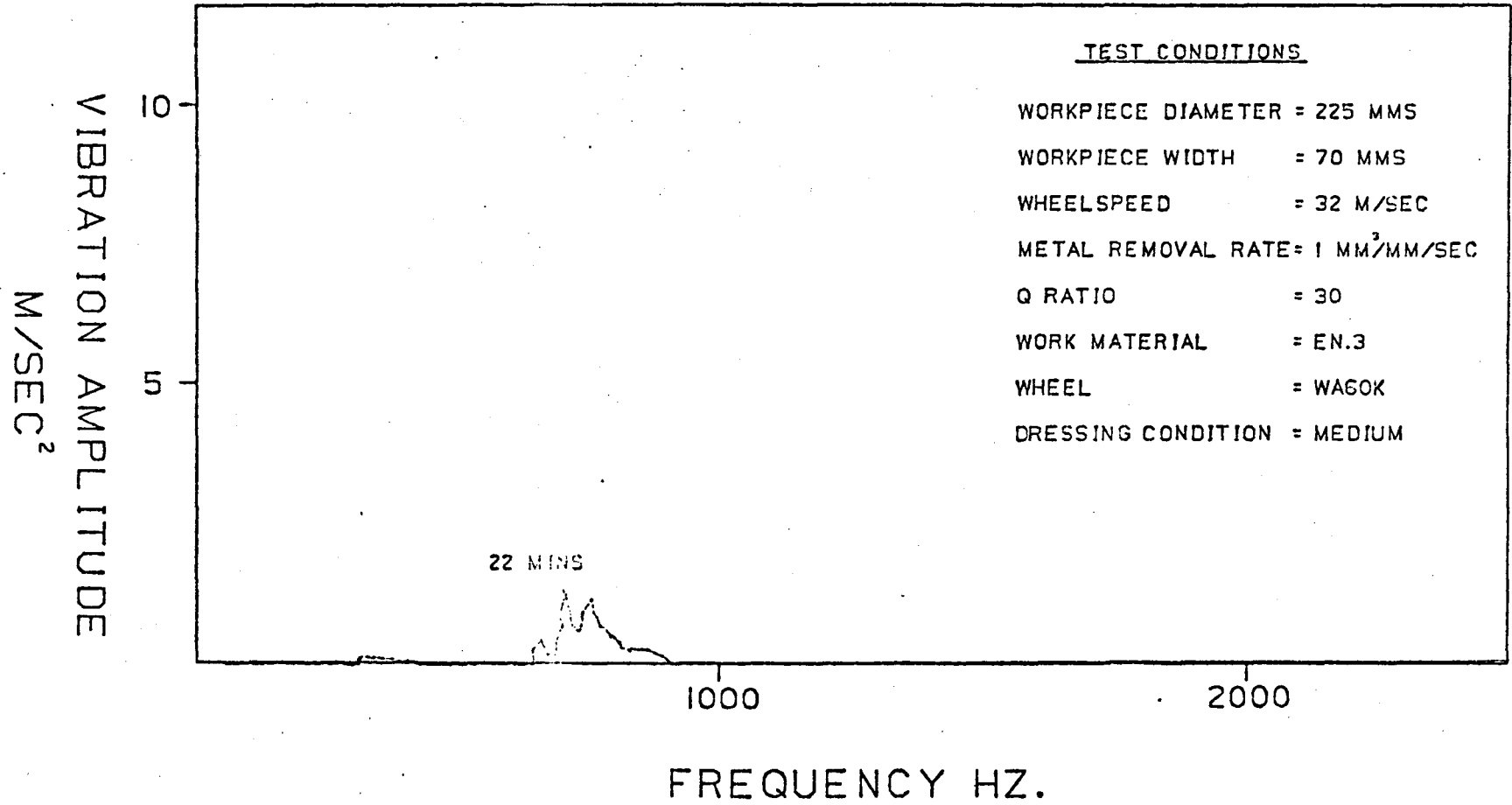


FIGURE 5.1a

FIGURE 5.1 VIBRATION SPECTRUM ANALYSIS RESULTS FROM THE CONSTANT METAL REMOVAL RATE TESTS

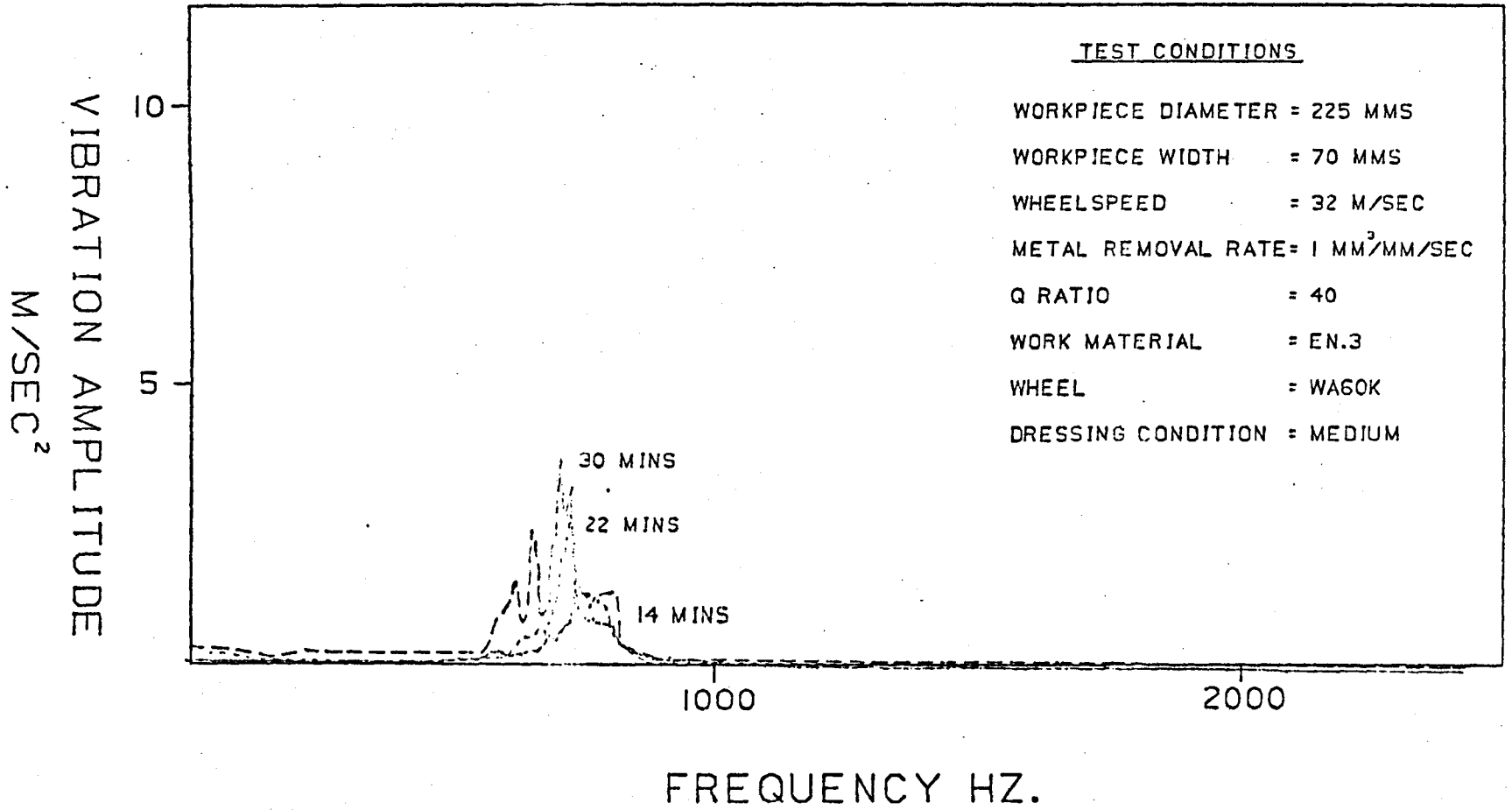


FIGURE 5.1b

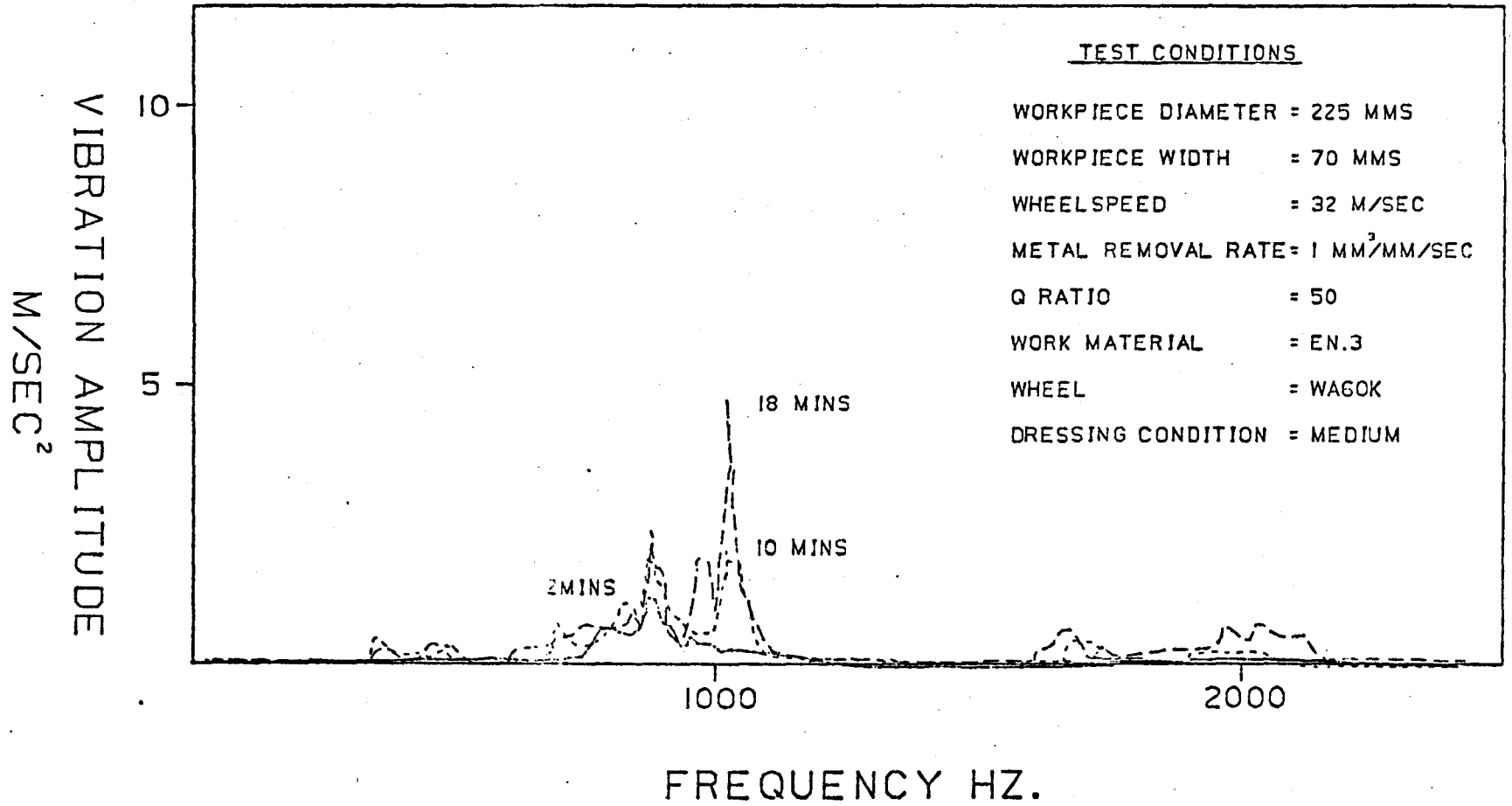


FIGURE 5.1c

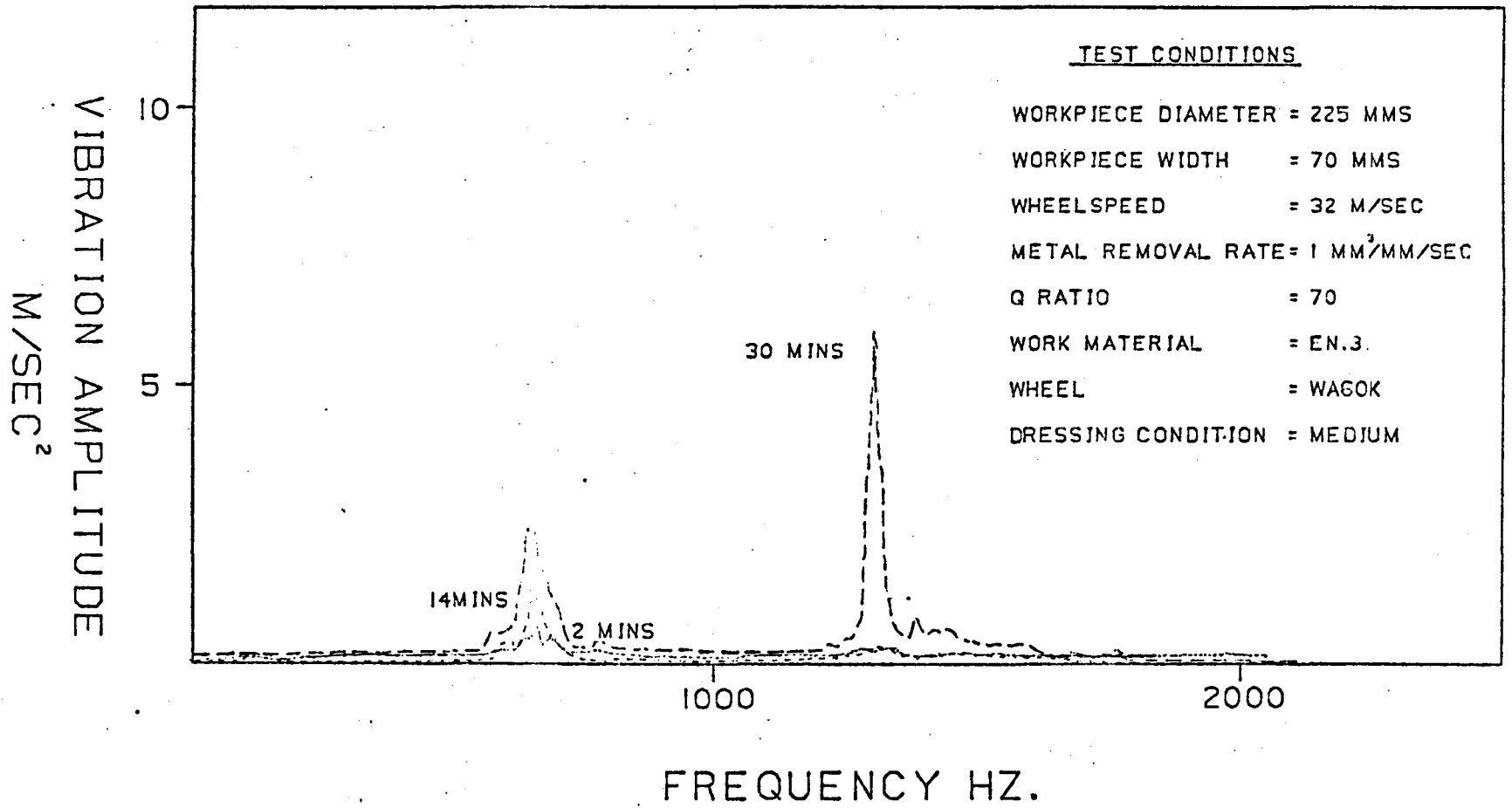


FIGURE 5.1d

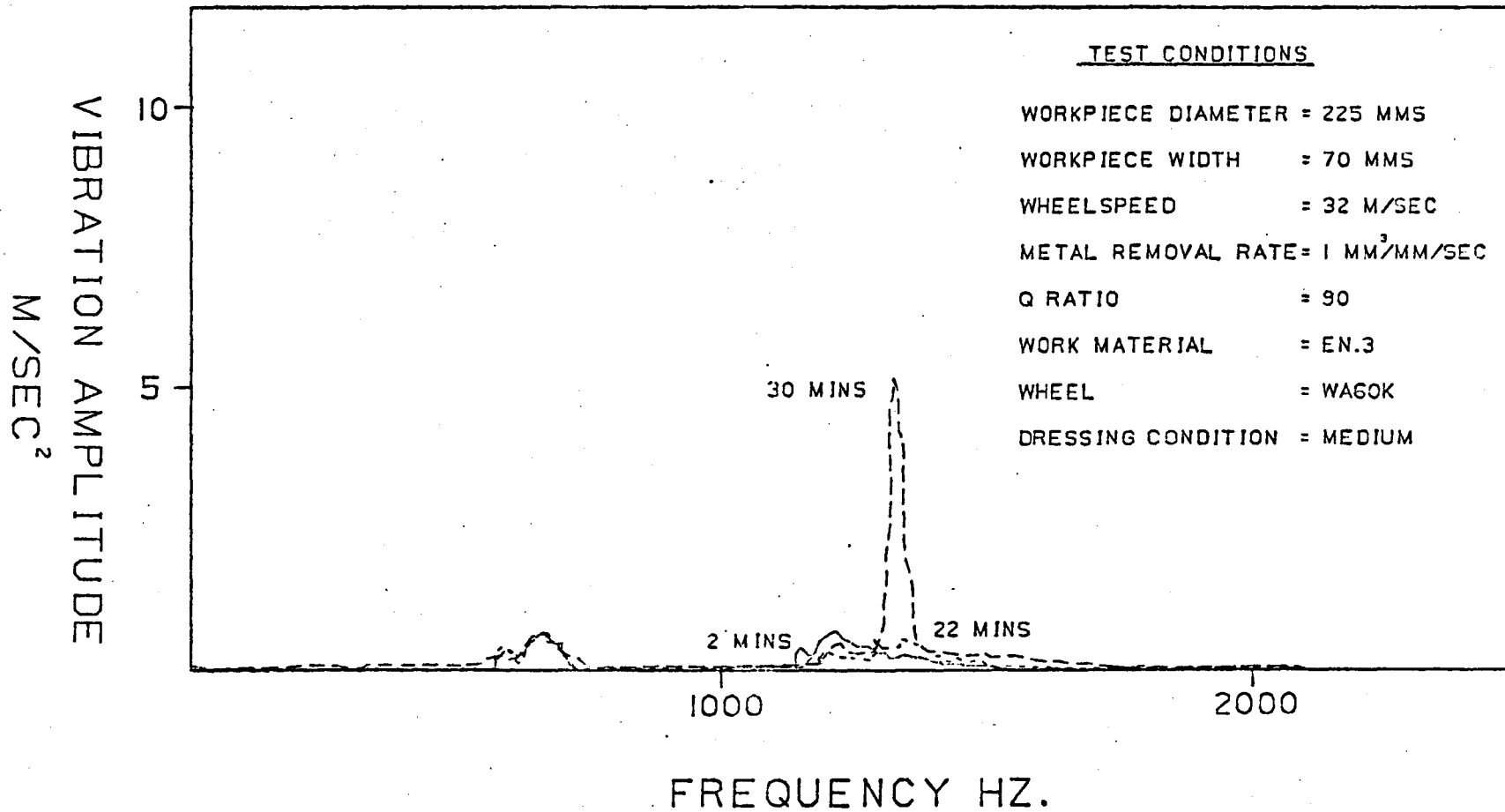
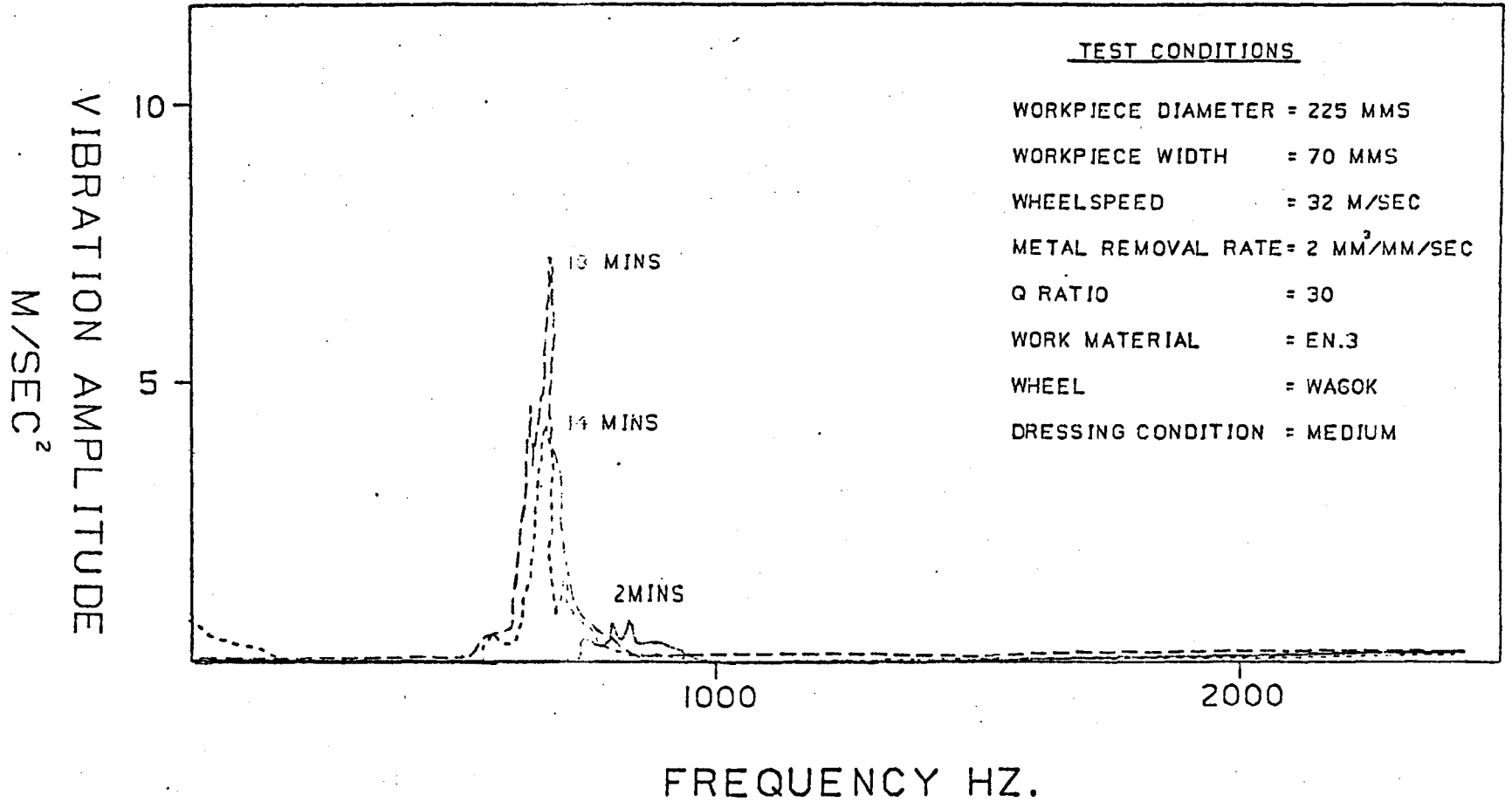


FIGURE 5.1e



FREQUENCY HZ.

FIGURE 5.1f

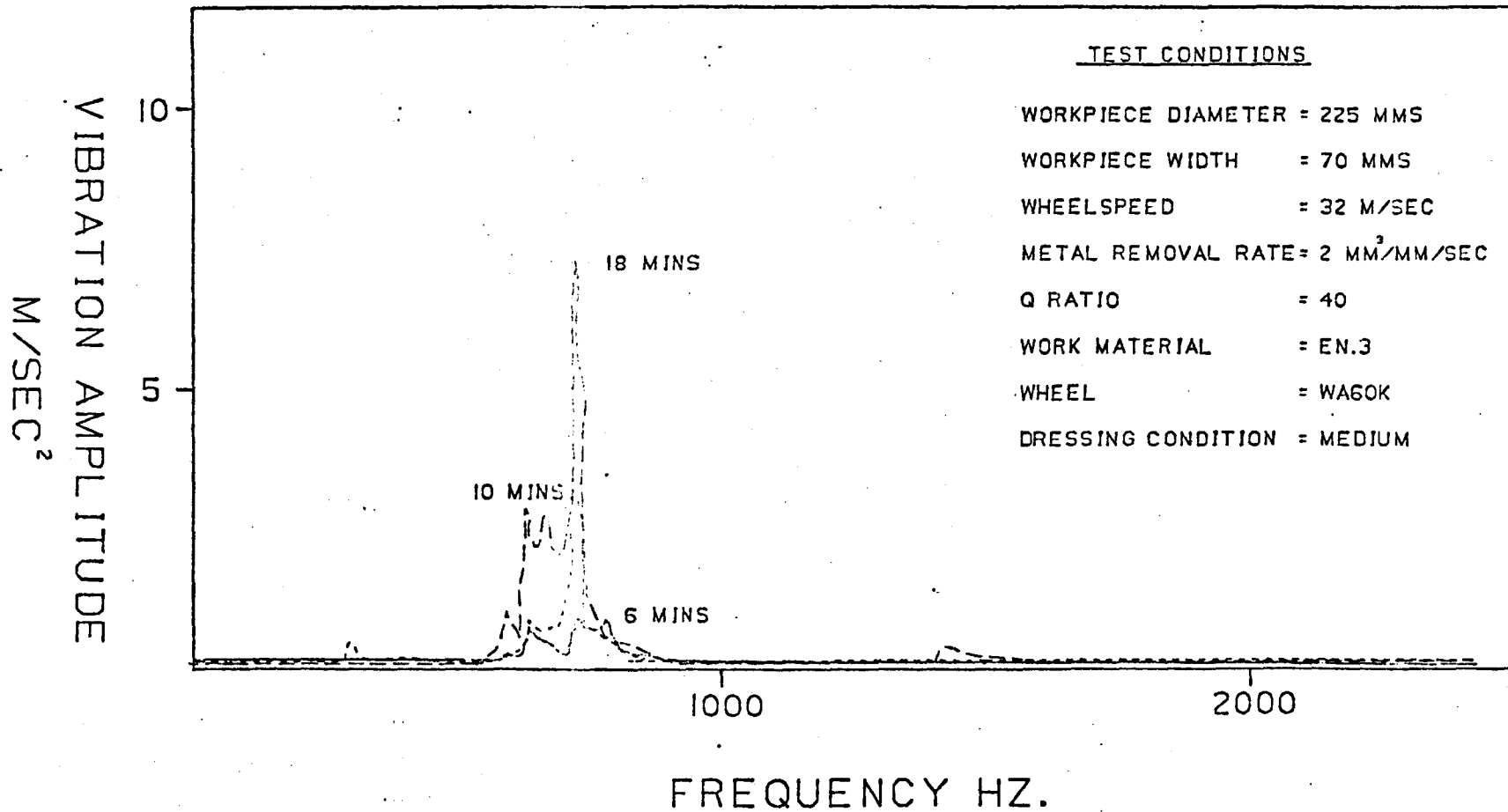


FIGURE 5.1g

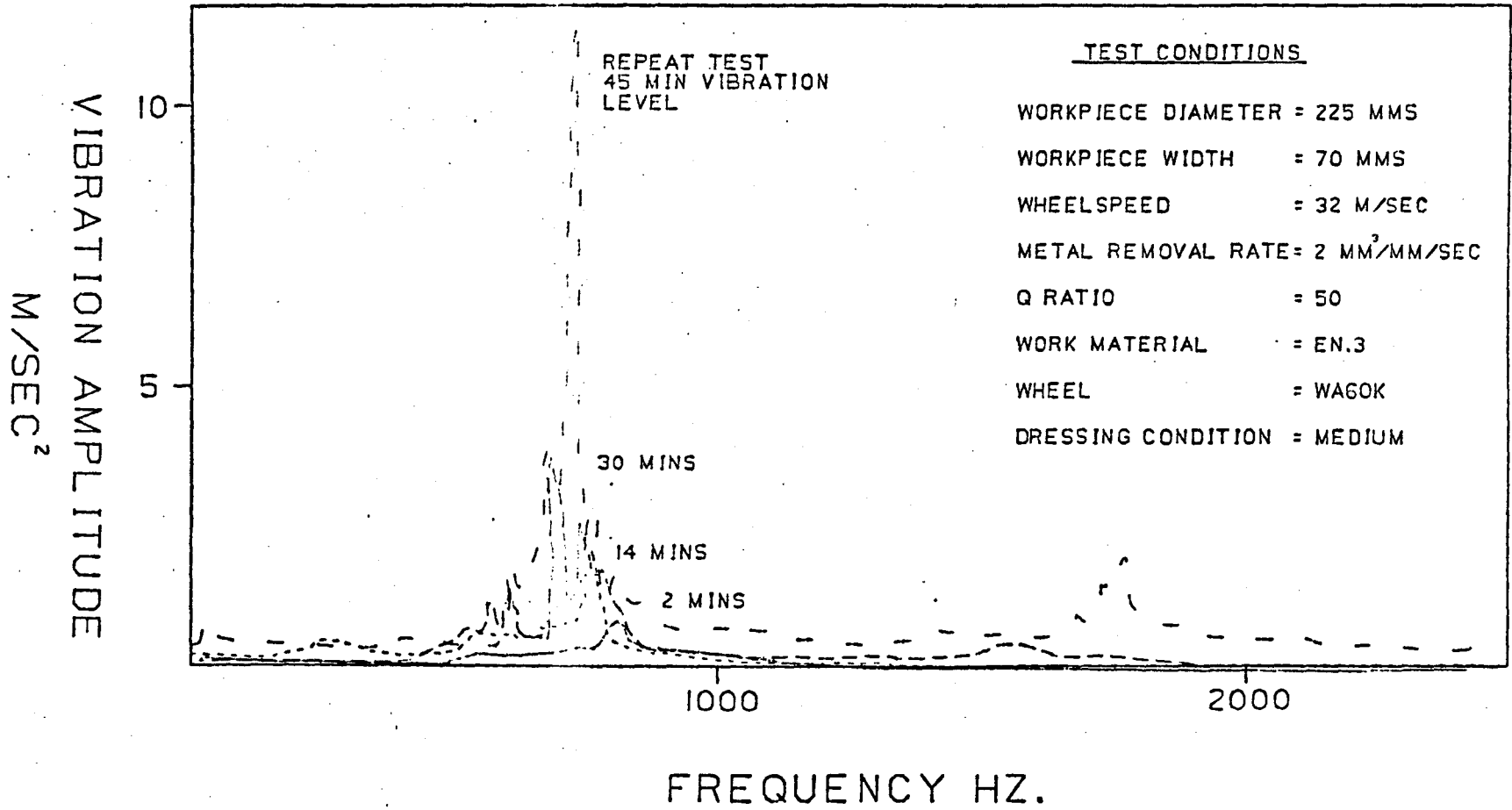


FIGURE 5.1h

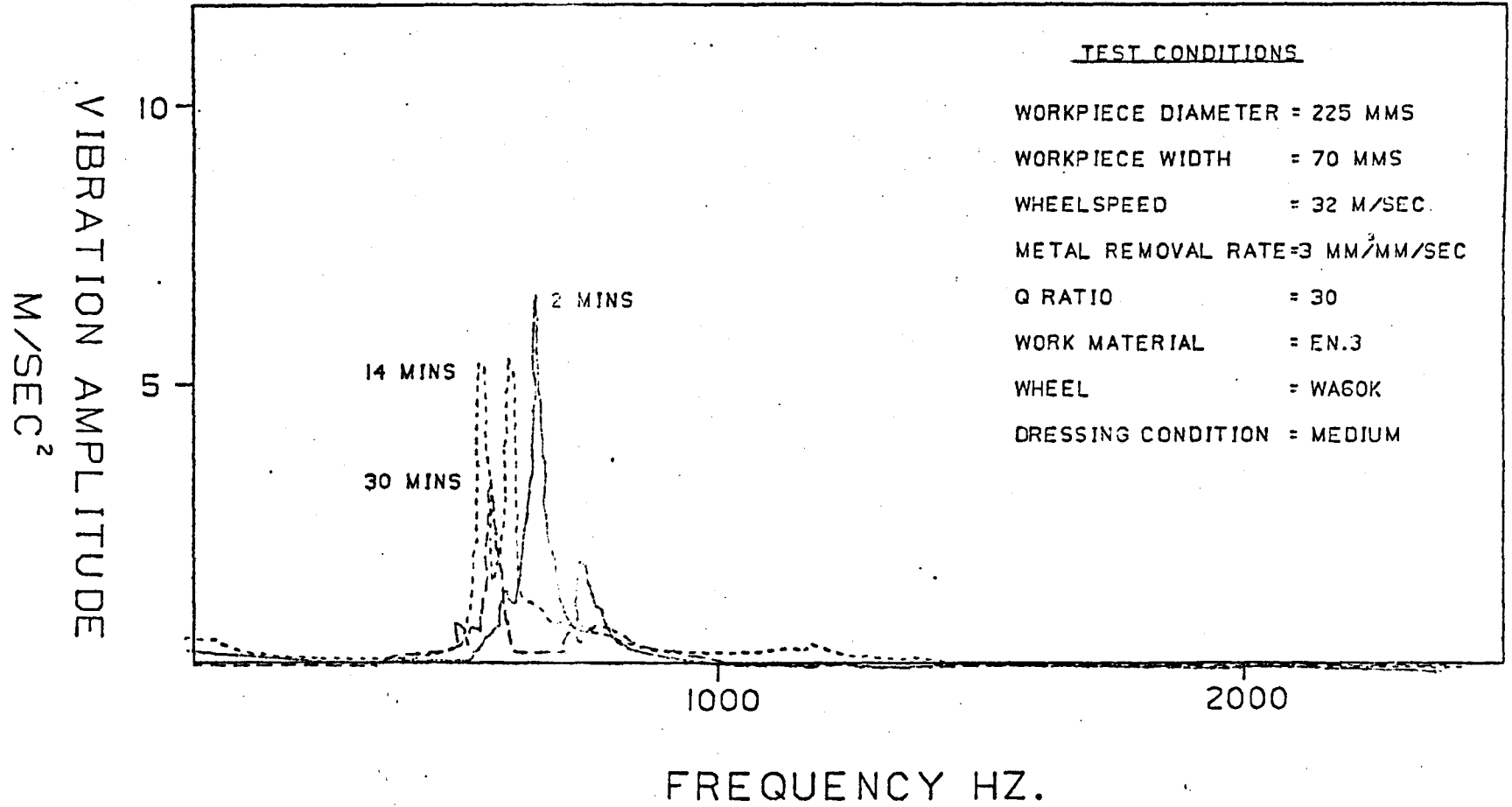


FIGURE 5.11

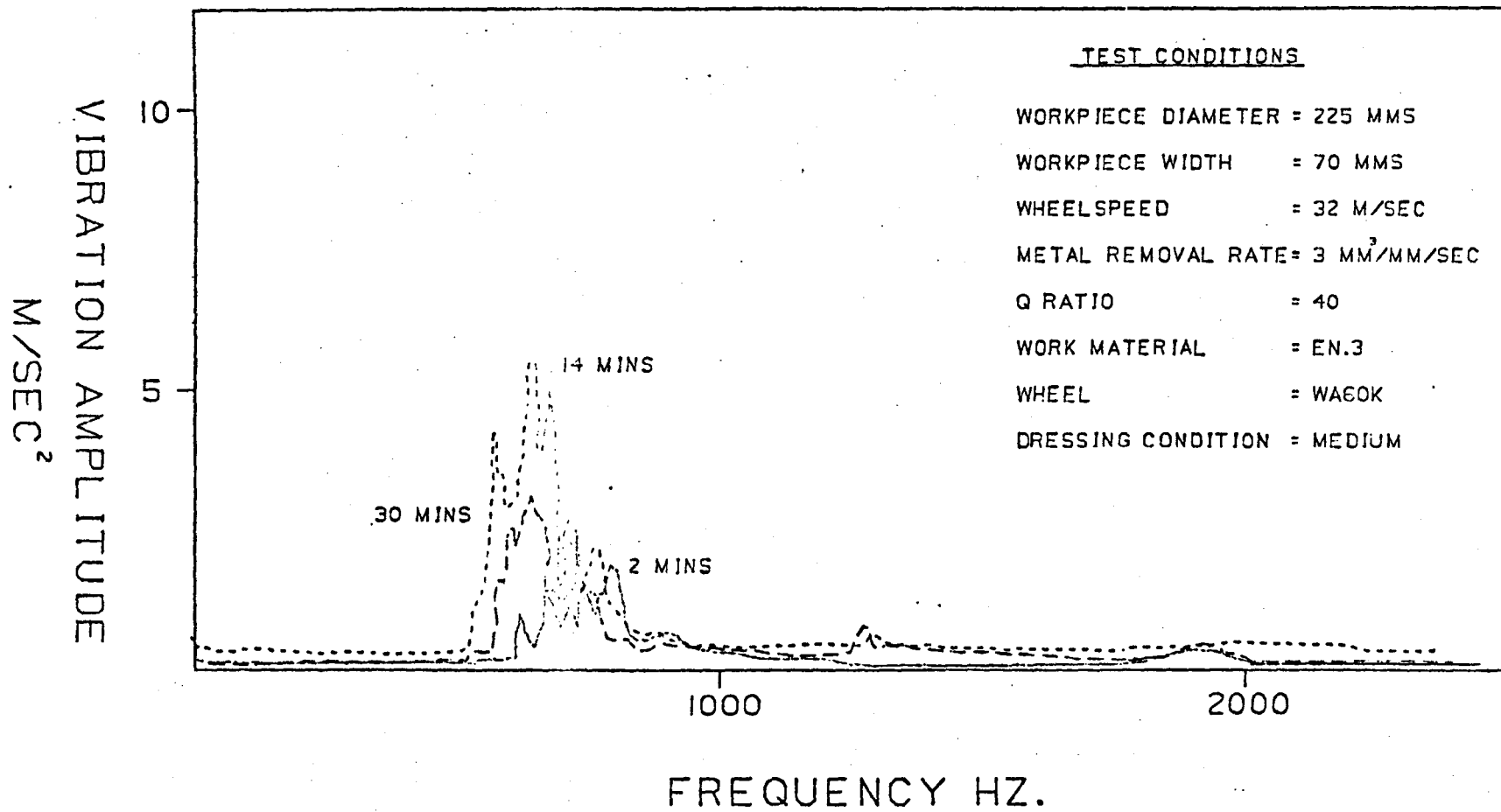


FIGURE 5.1j

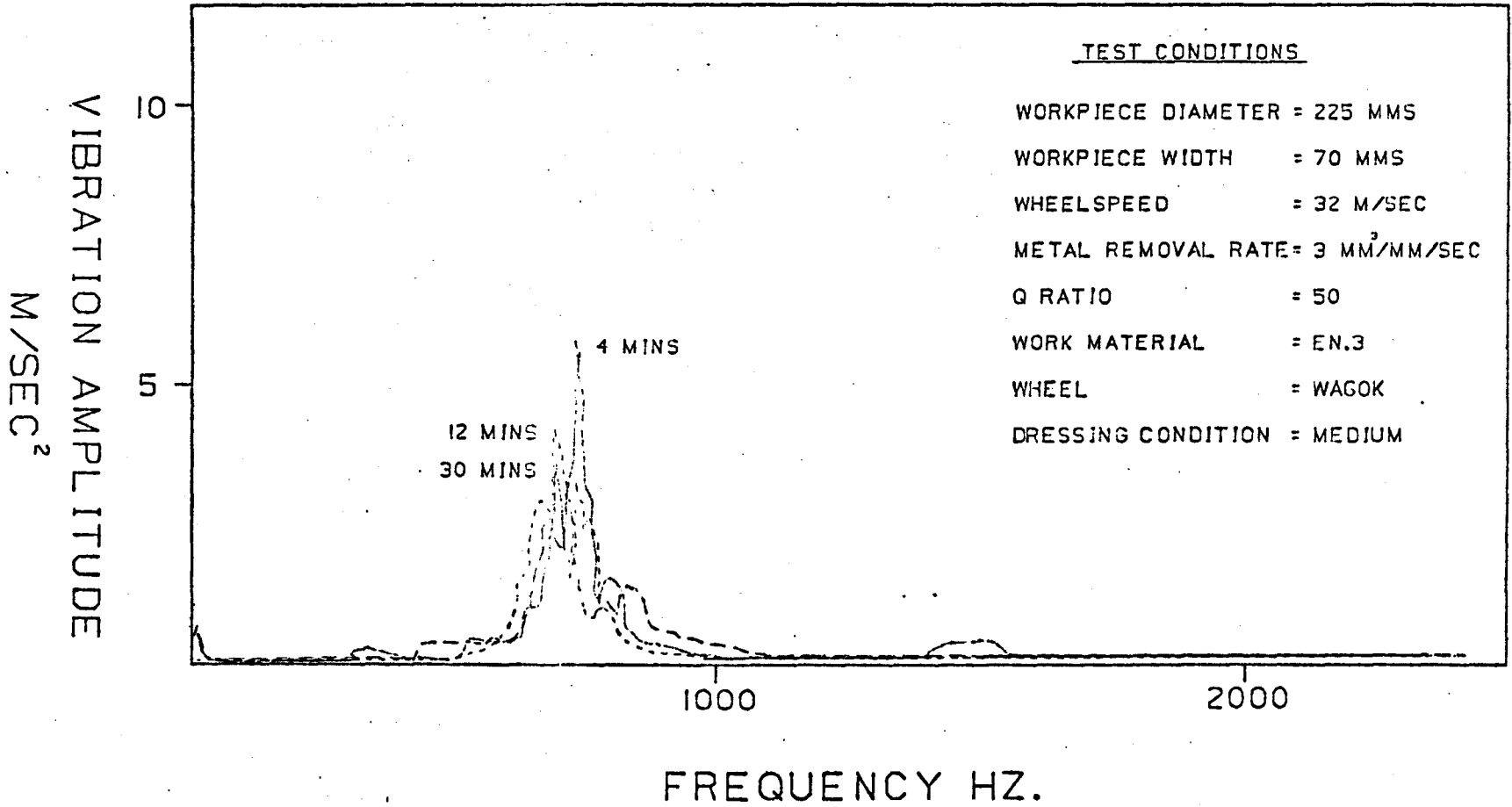


FIGURE 5.1k

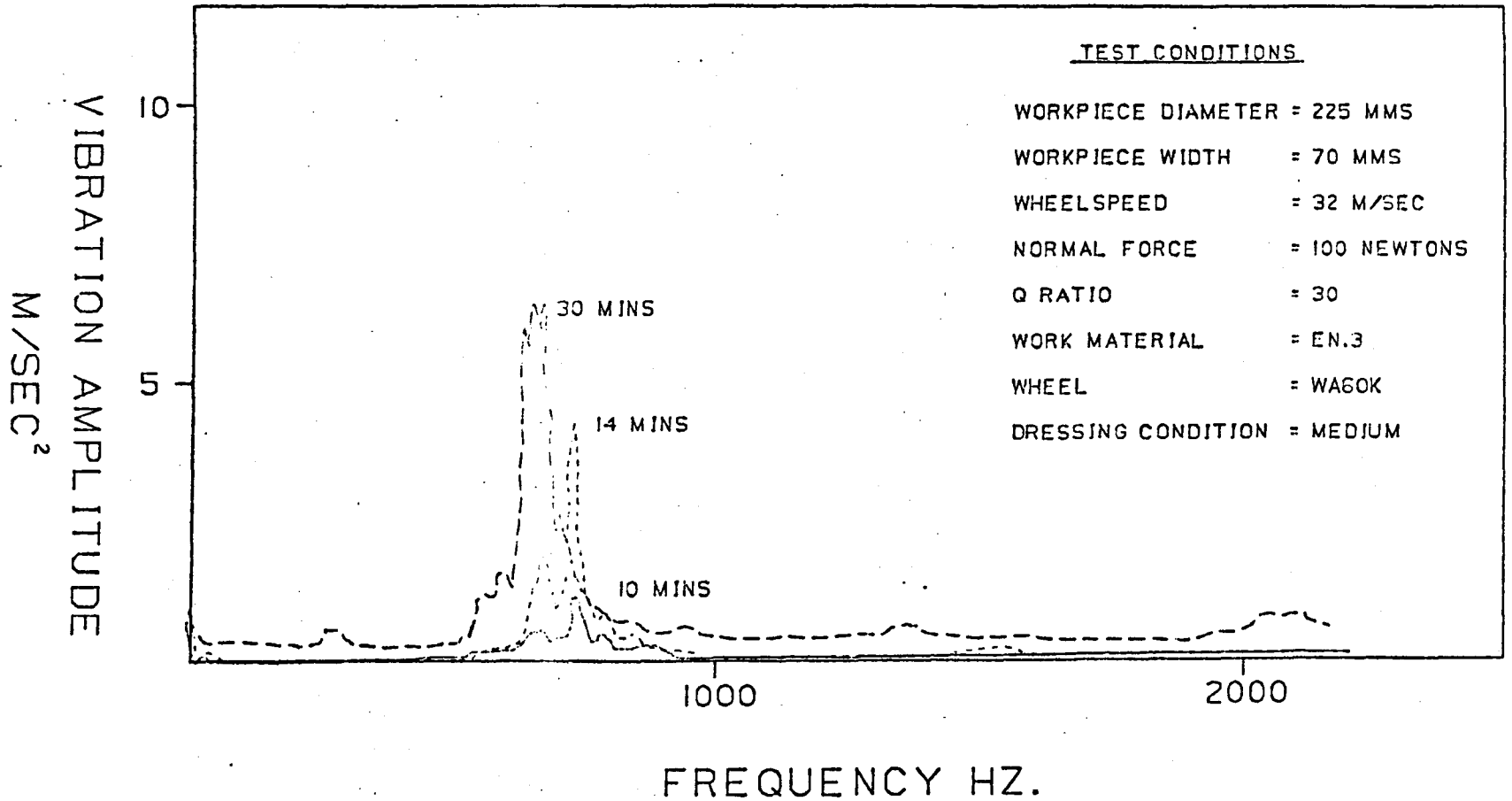


FIGURE 5.2a

FIGURE 5.2 VIBRATION SPECTRUM ANALYSIS RESULTS FROM THE CONSTANT NORMAL FORCE TESTS

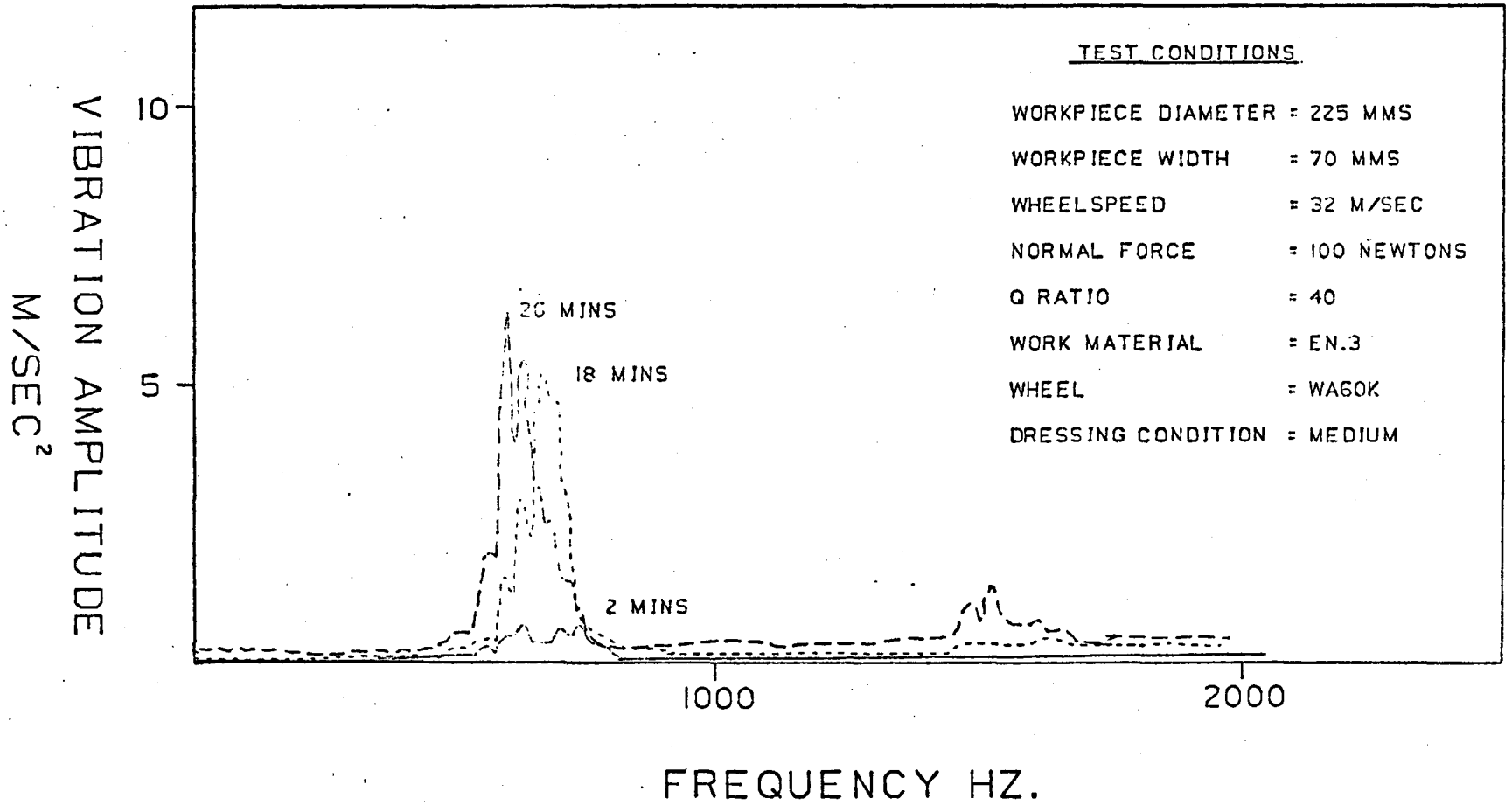


FIGURE 5.2b

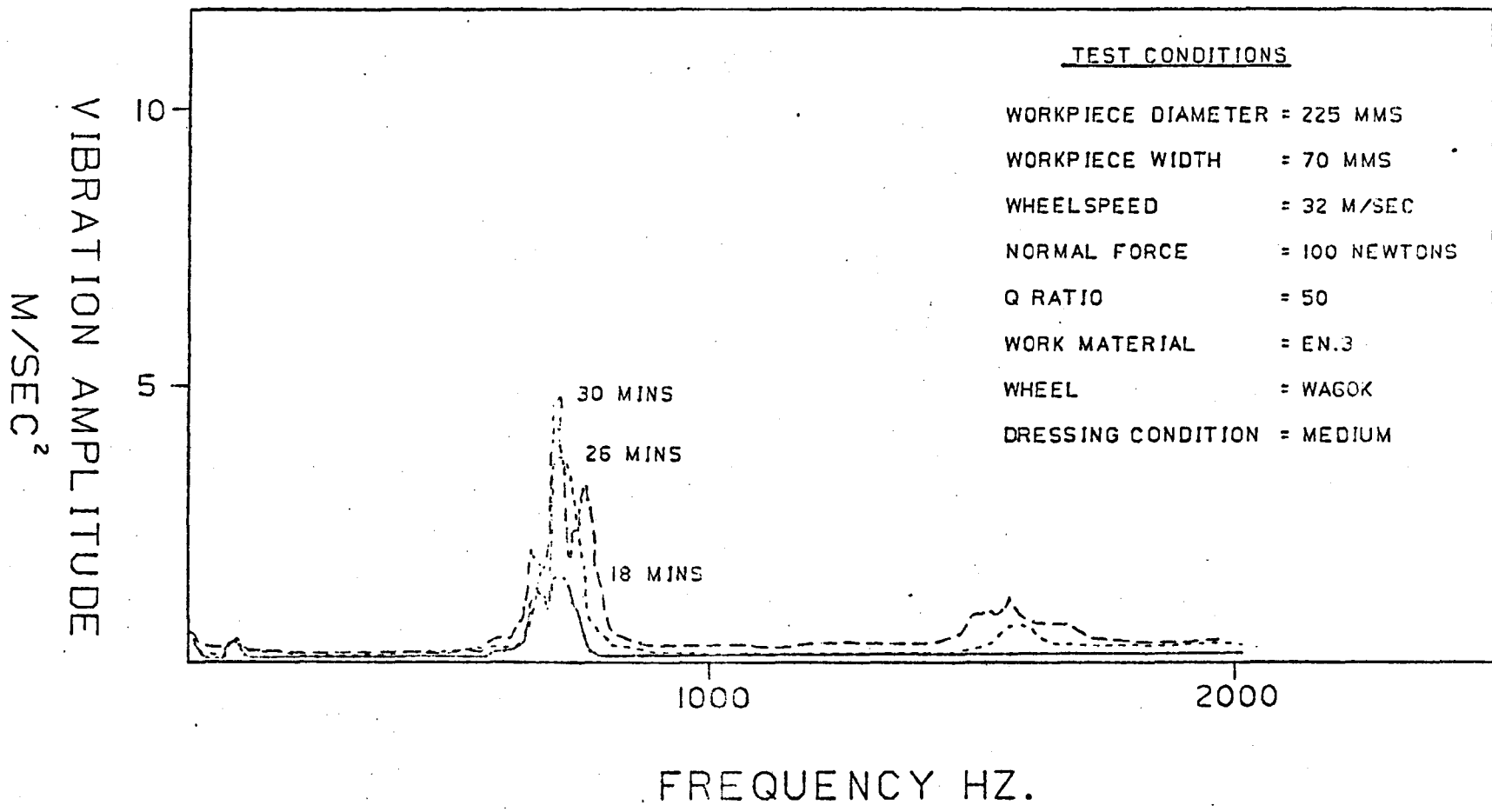


FIGURE 5.2c

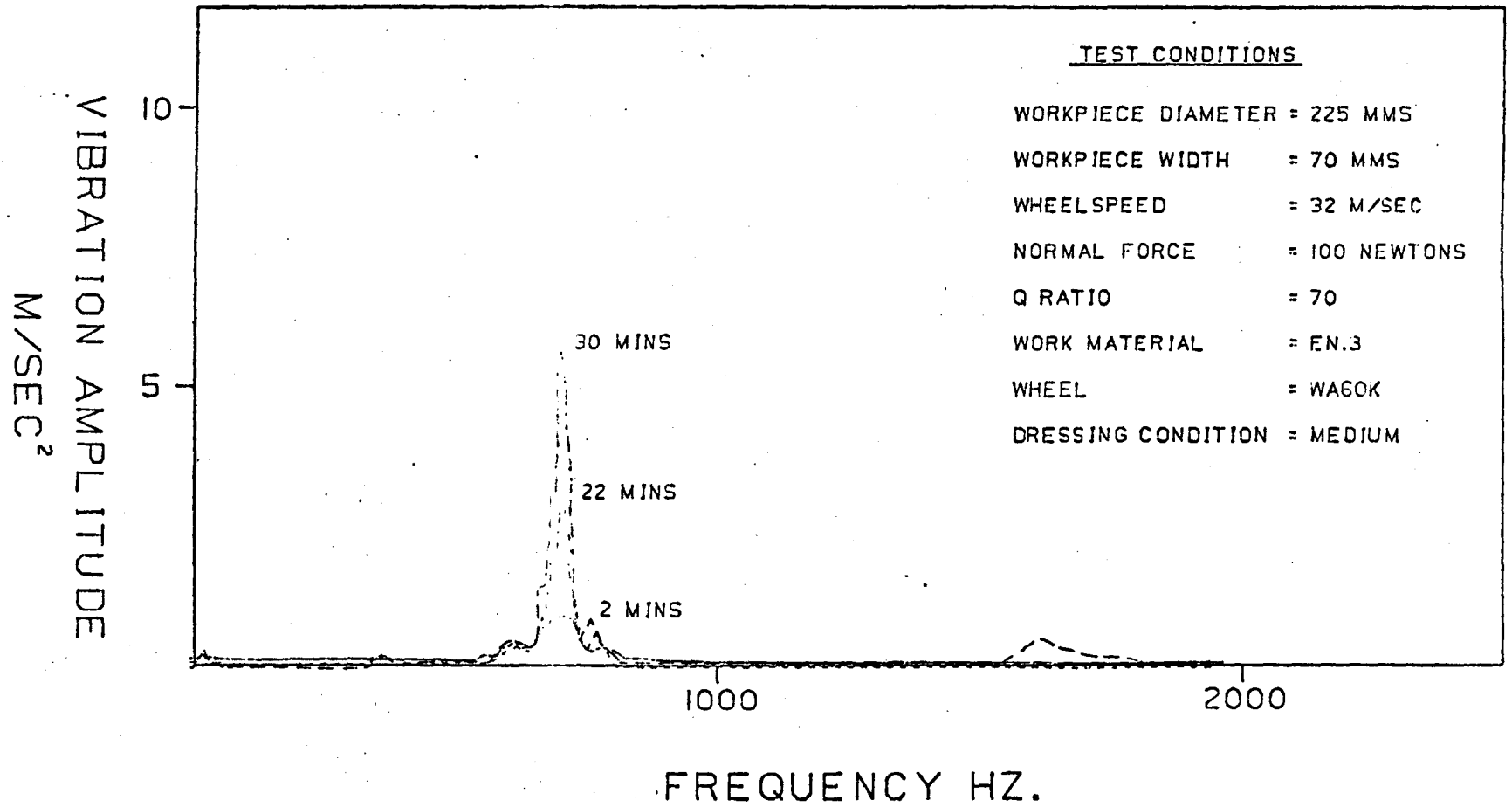


FIGURE 5.2d

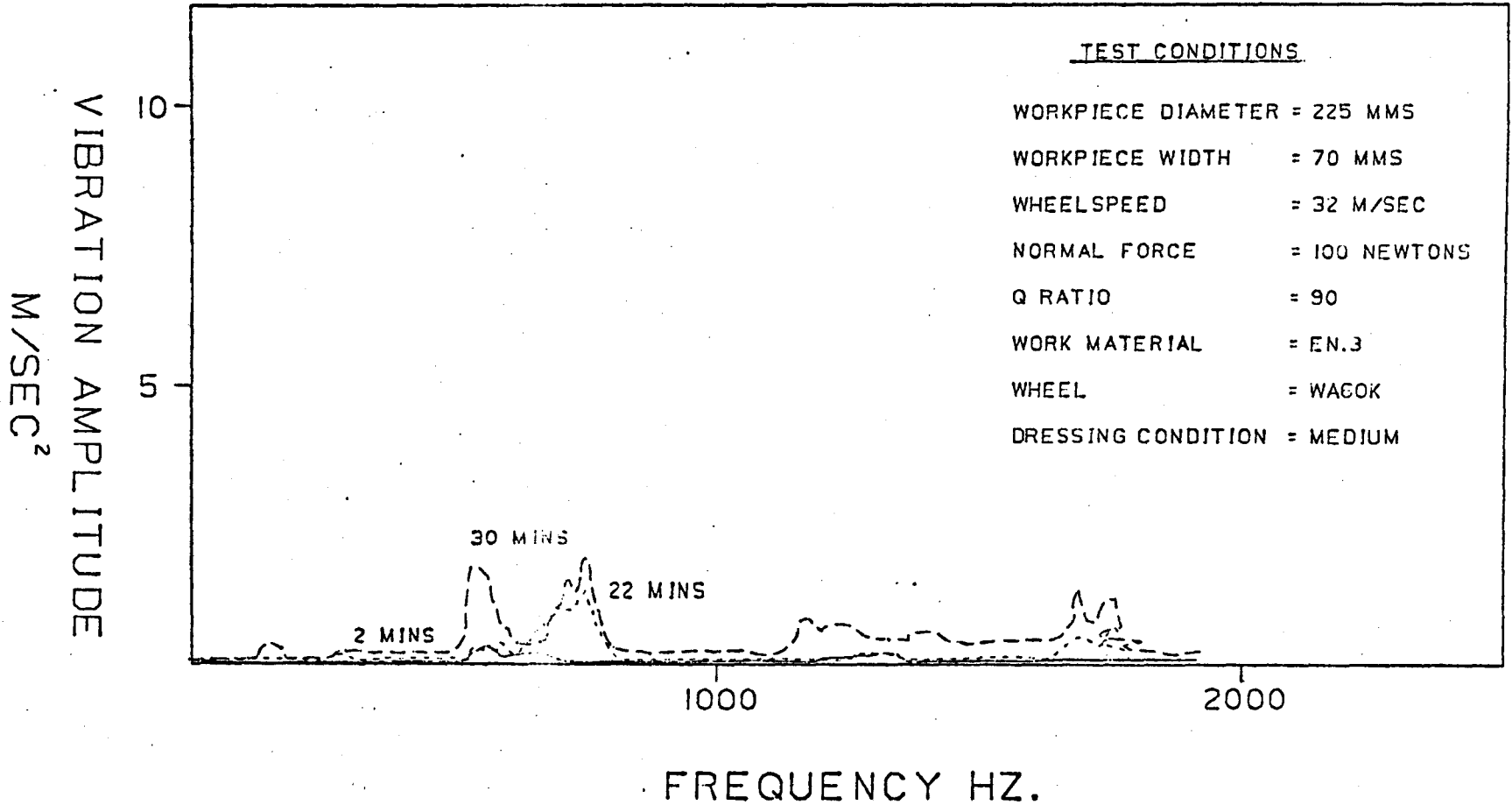


FIGURE 5.2e

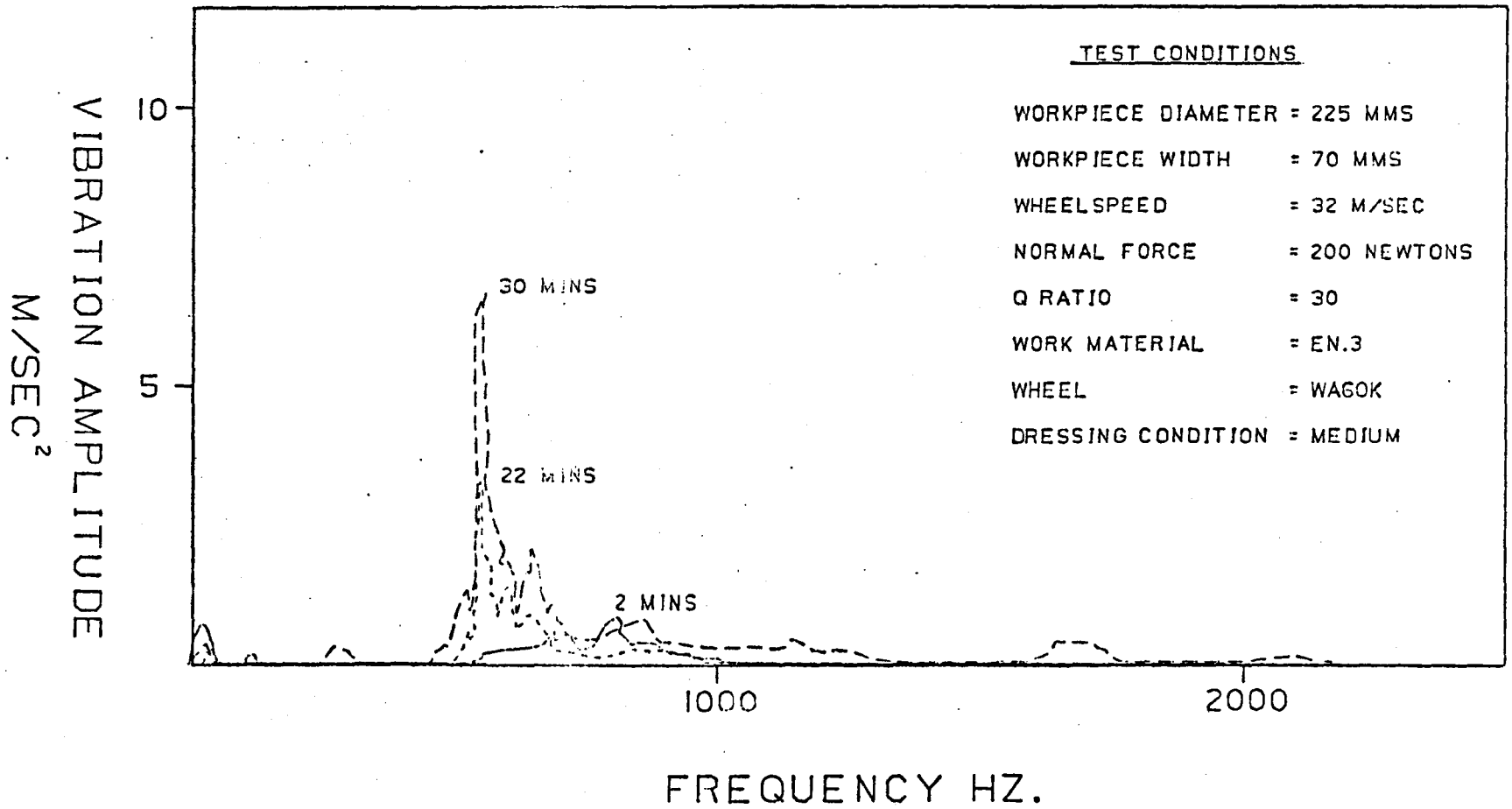


FIGURE 5.2f

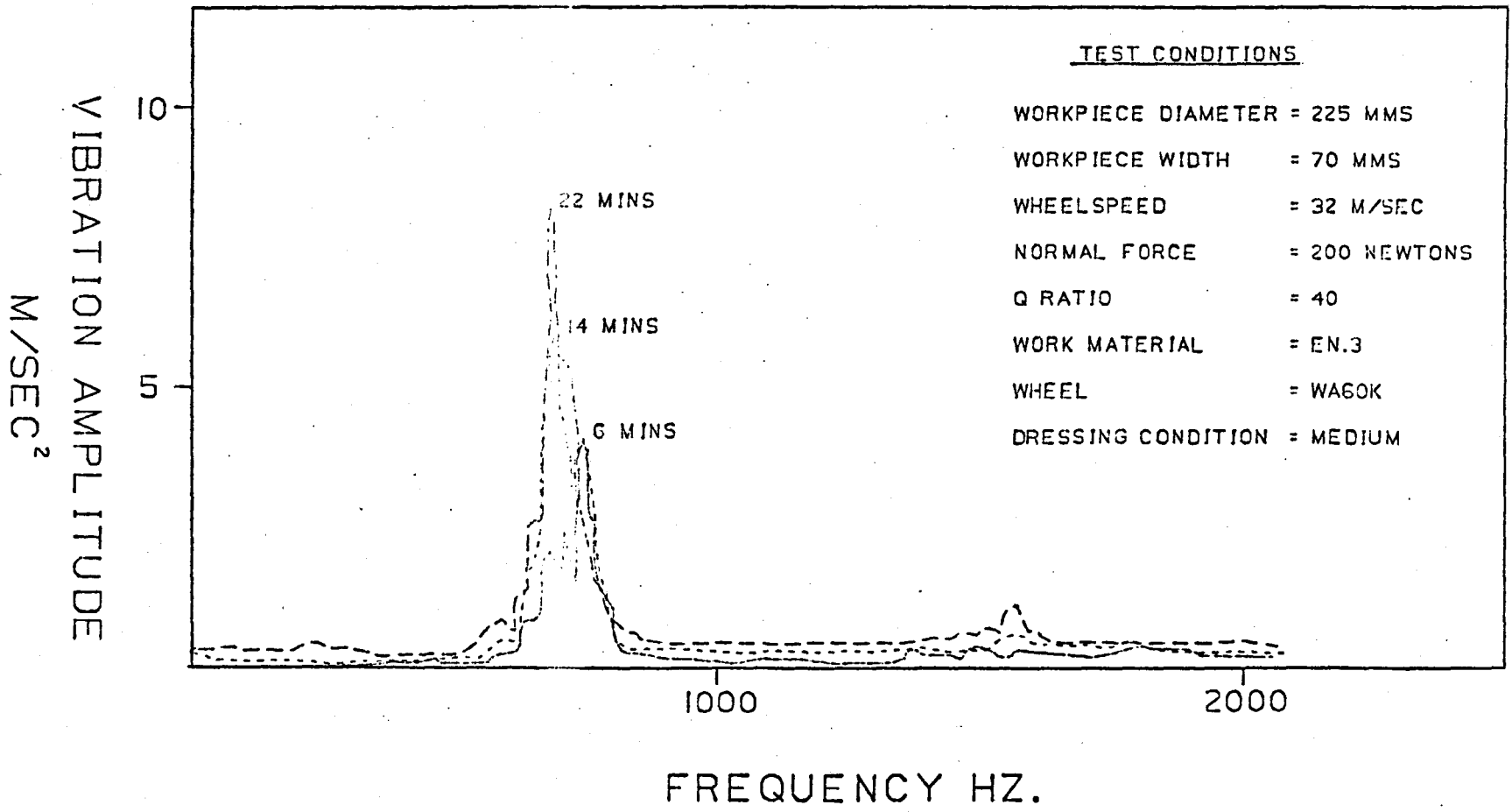


FIGURE 5.2g

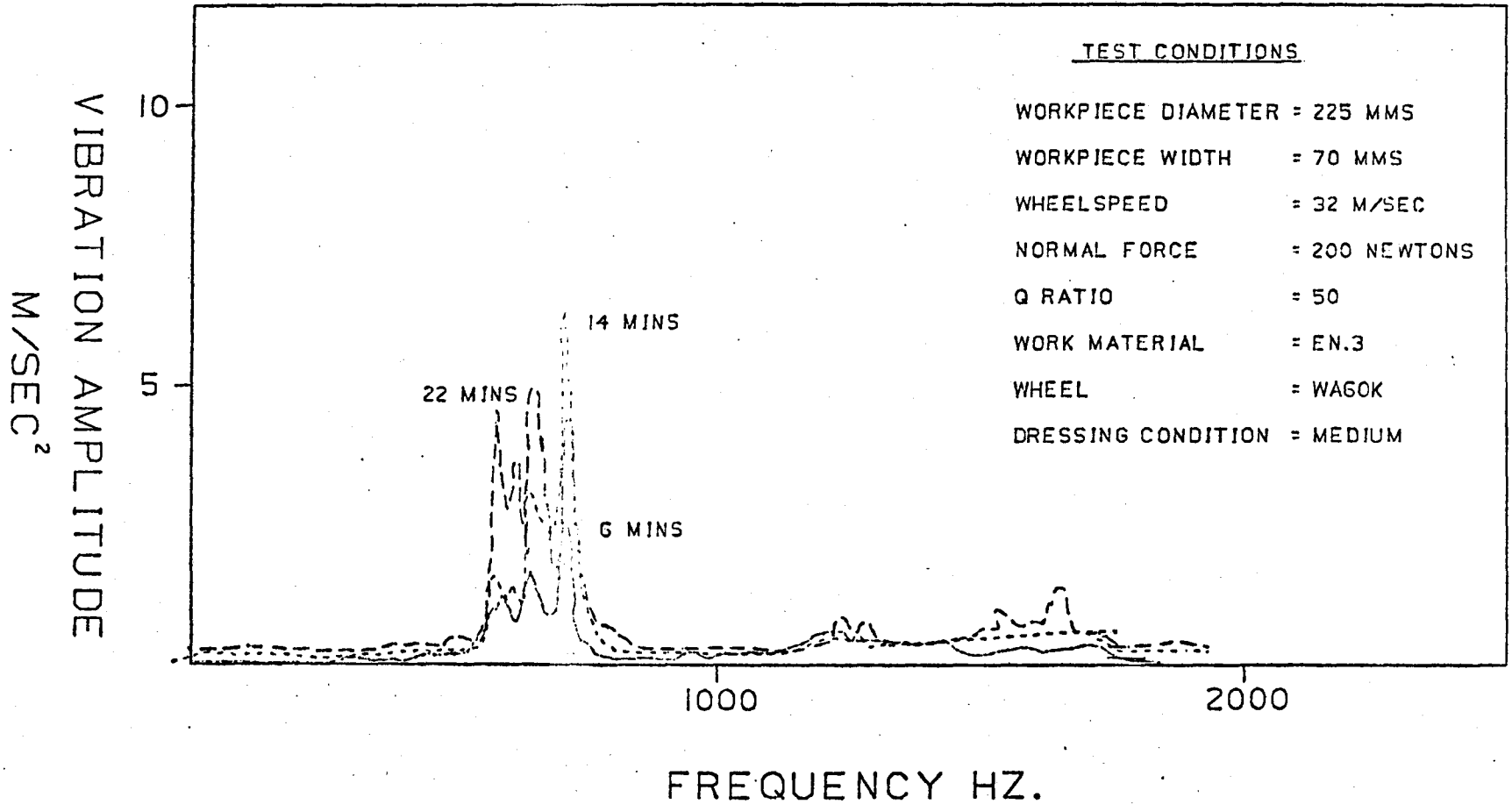


FIGURE 5.2h

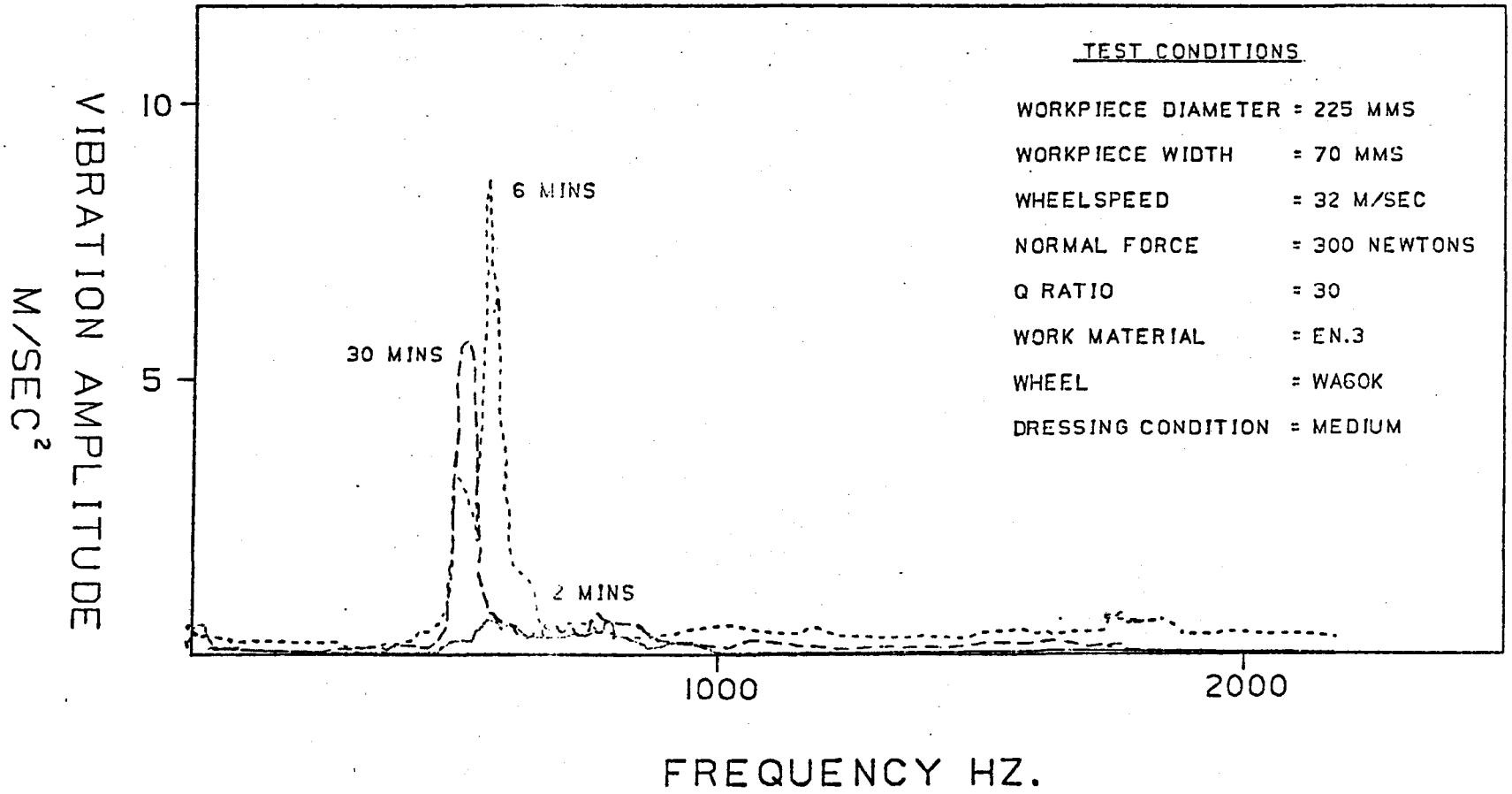


FIGURE 5.21

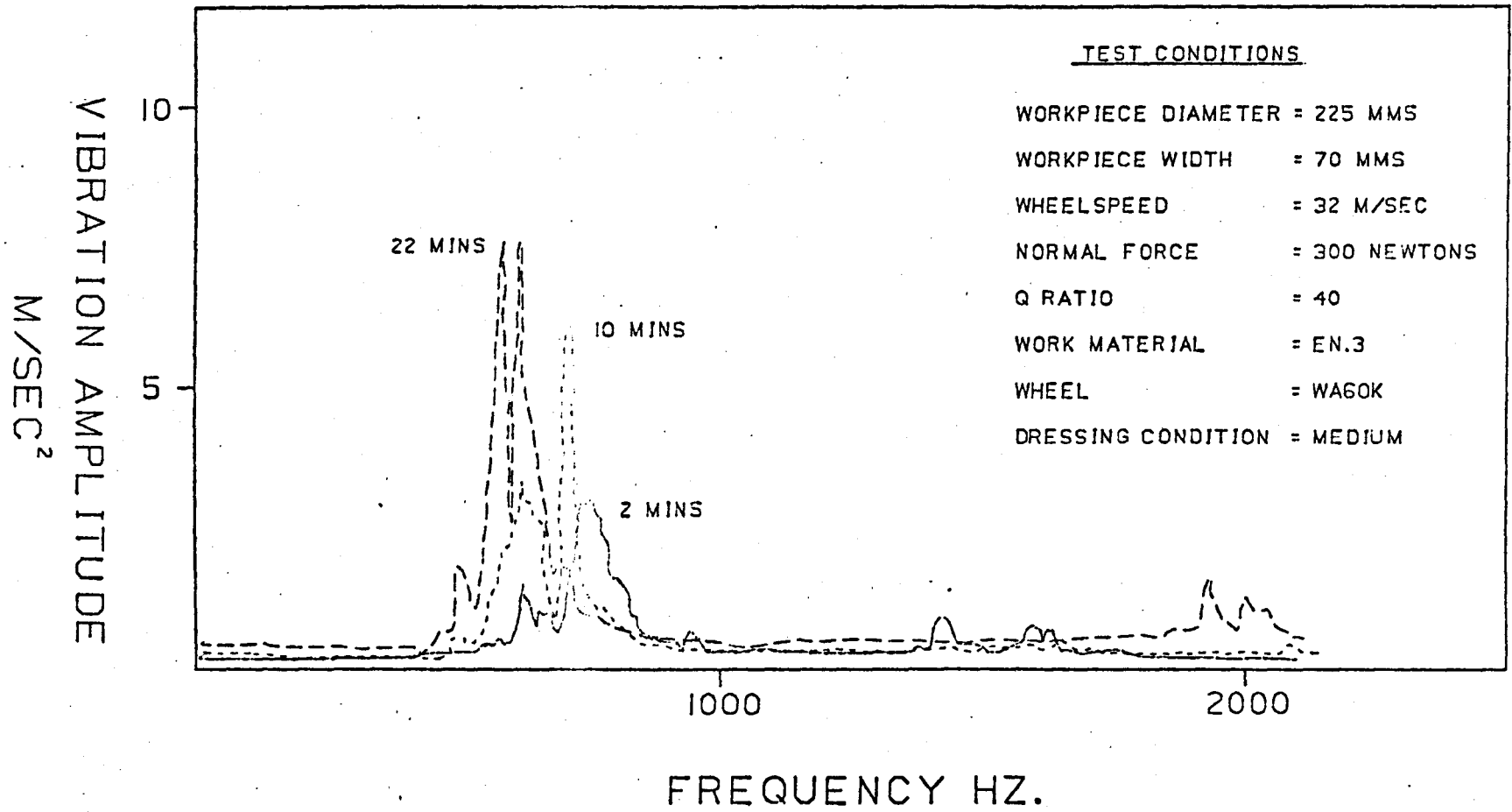


FIGURE 5.2j

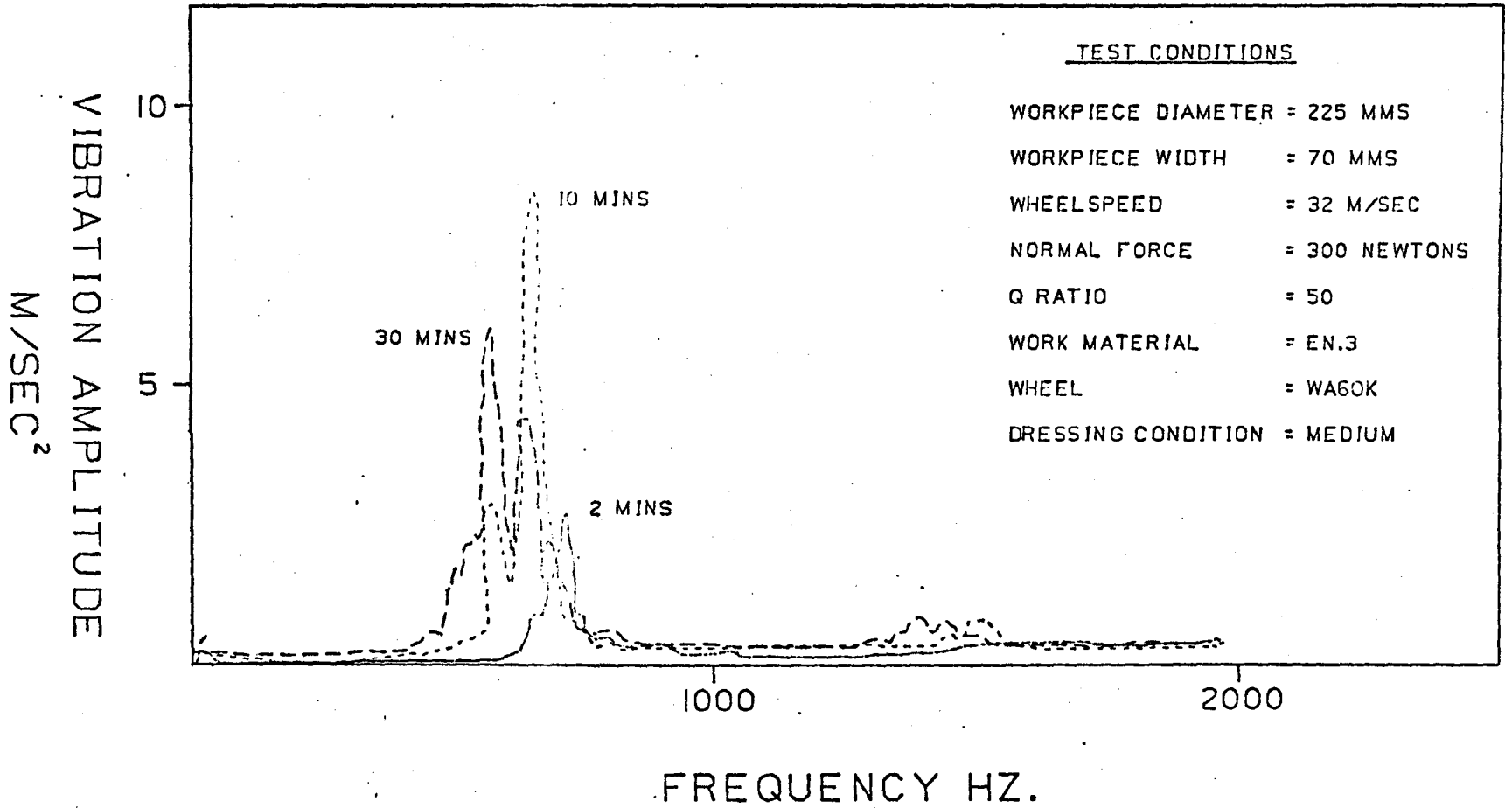


FIGURE 5.2k

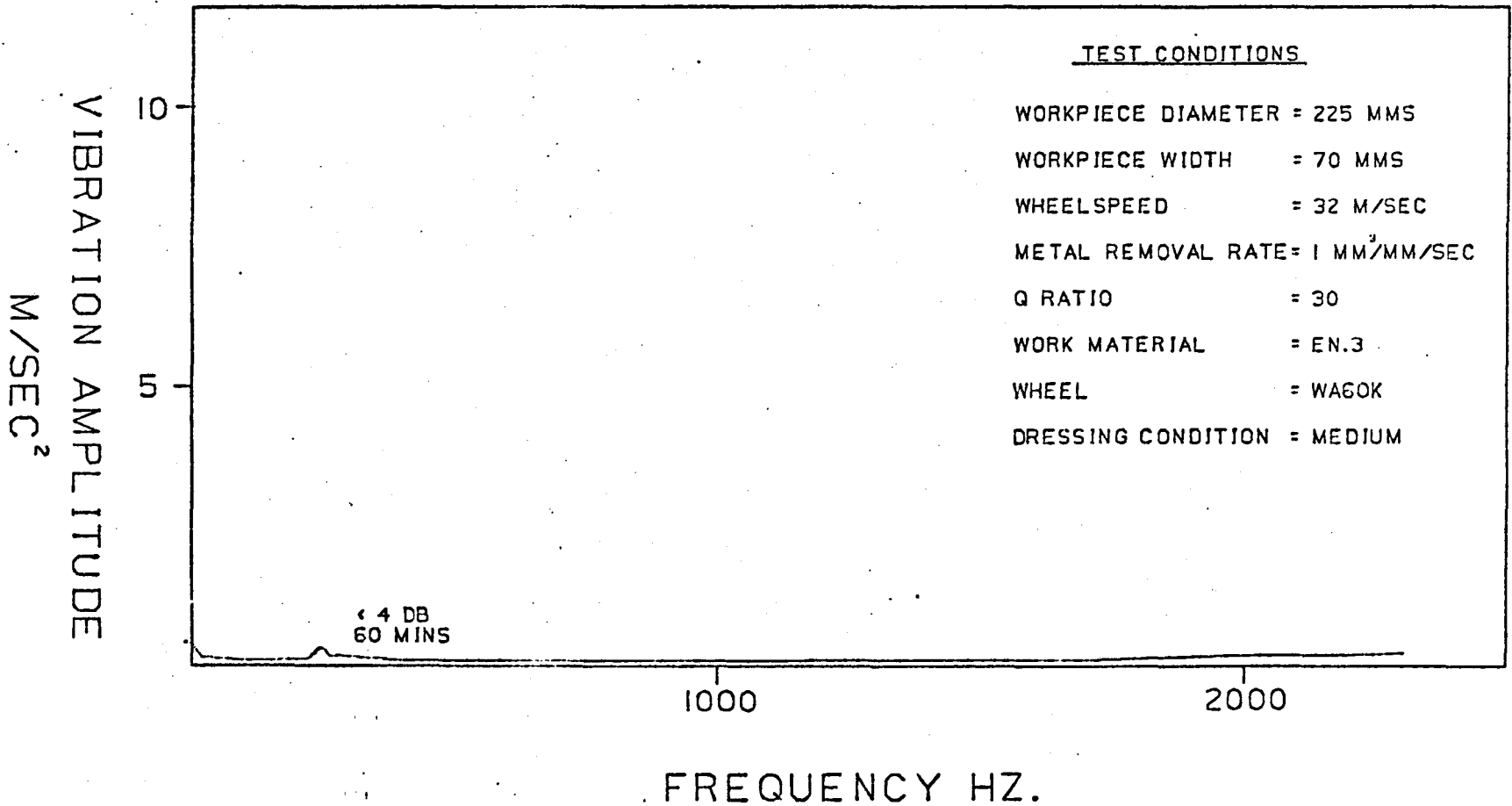


FIGURE 5.3a

FIGURE 5.3 VIBRATION SPECTRUM ANALYSIS RESULTS FROM THE SHORT DURATION TESTS

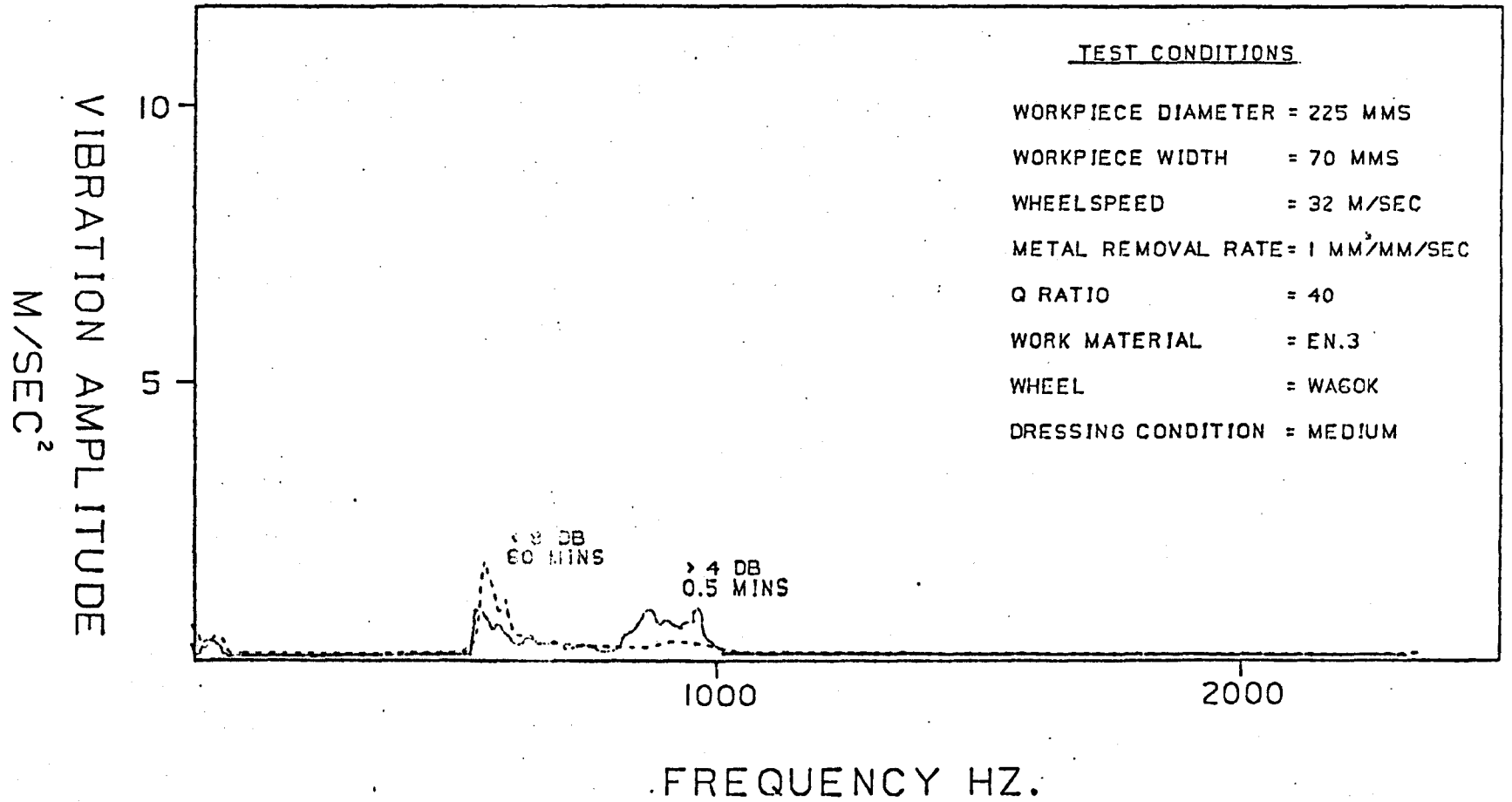


FIGURE 5.3b

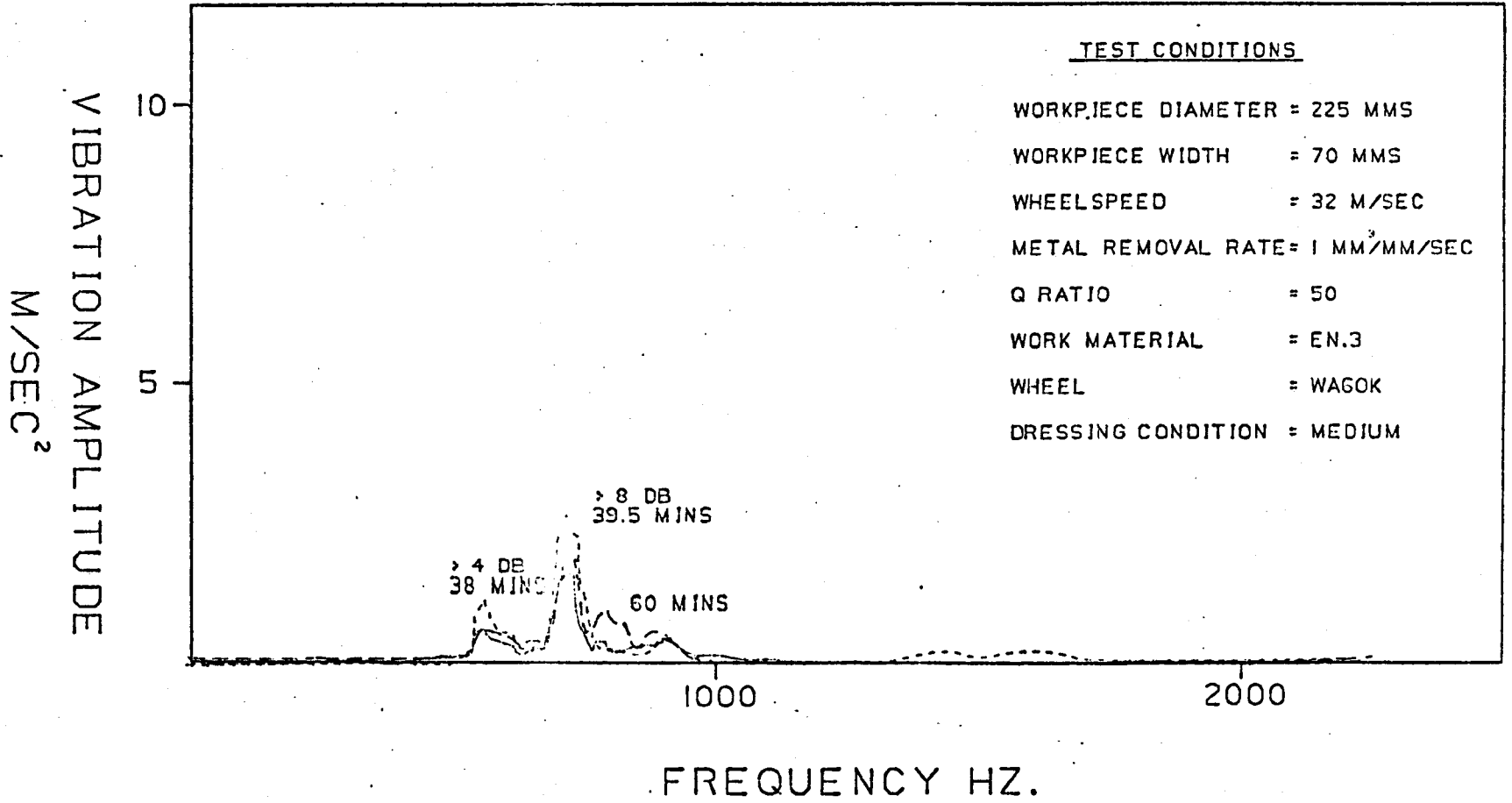


FIGURE 5.3c

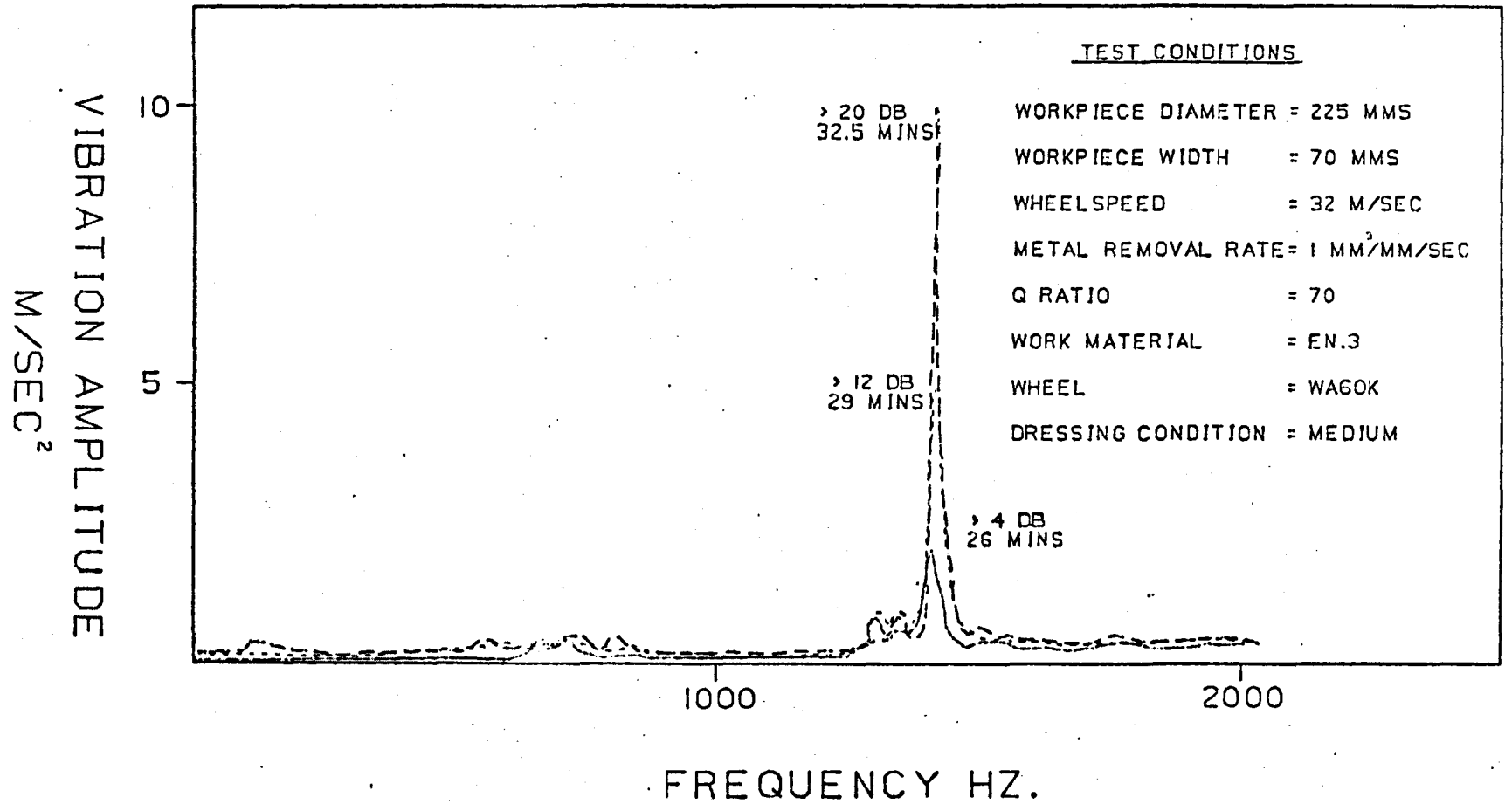


FIGURE 5.3d

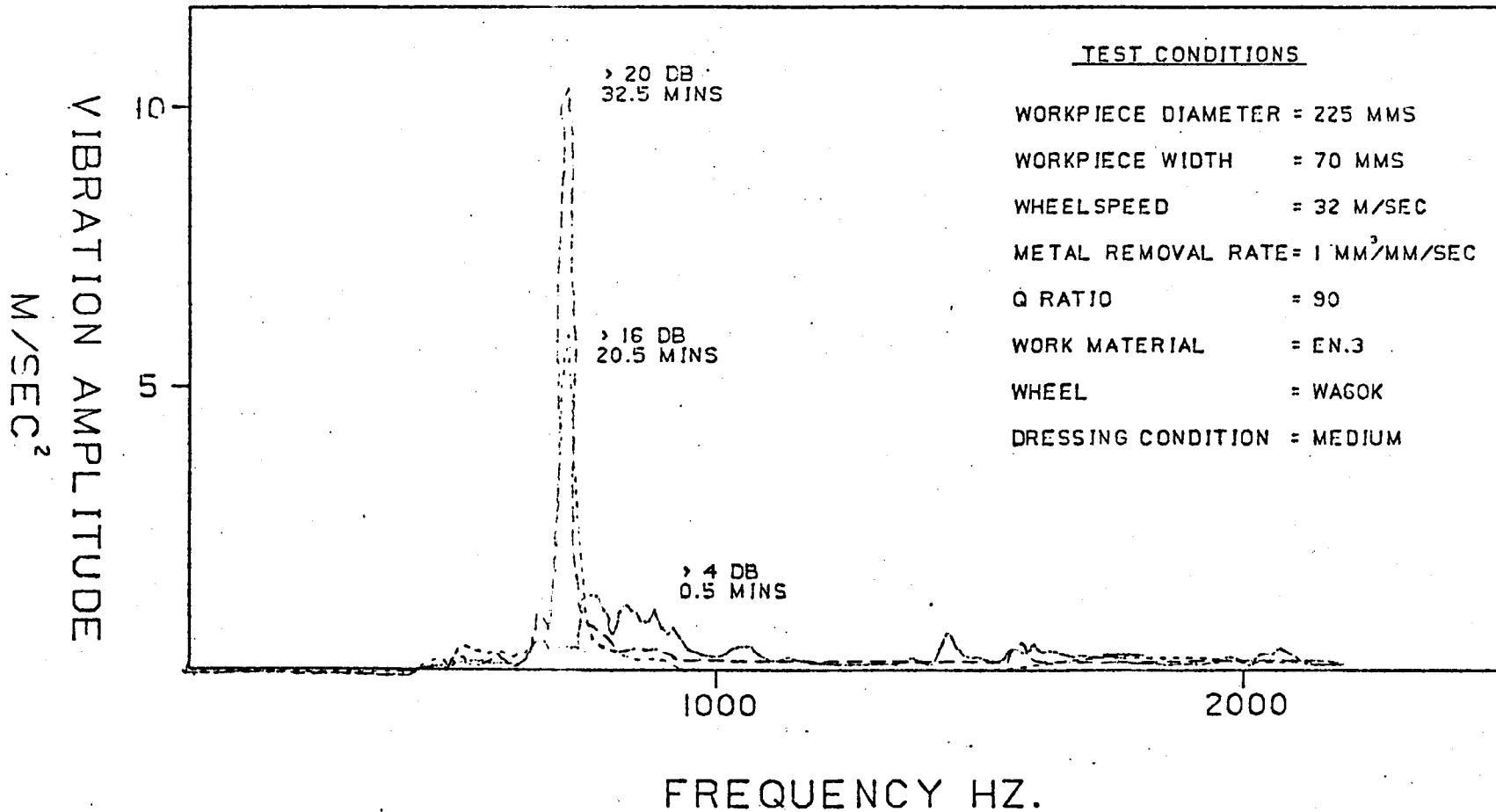


FIGURE 5.3e

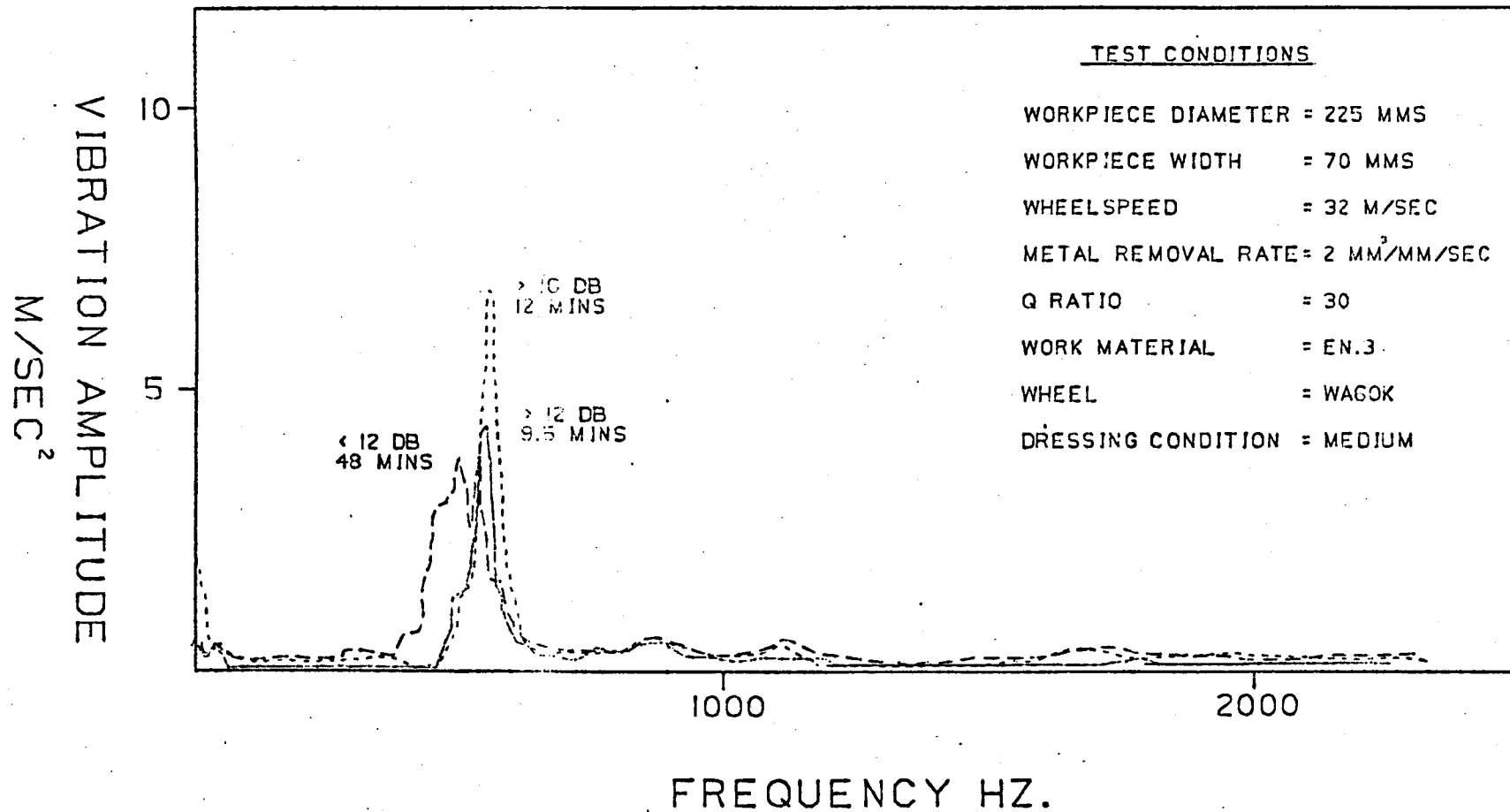


FIGURE 5.3f

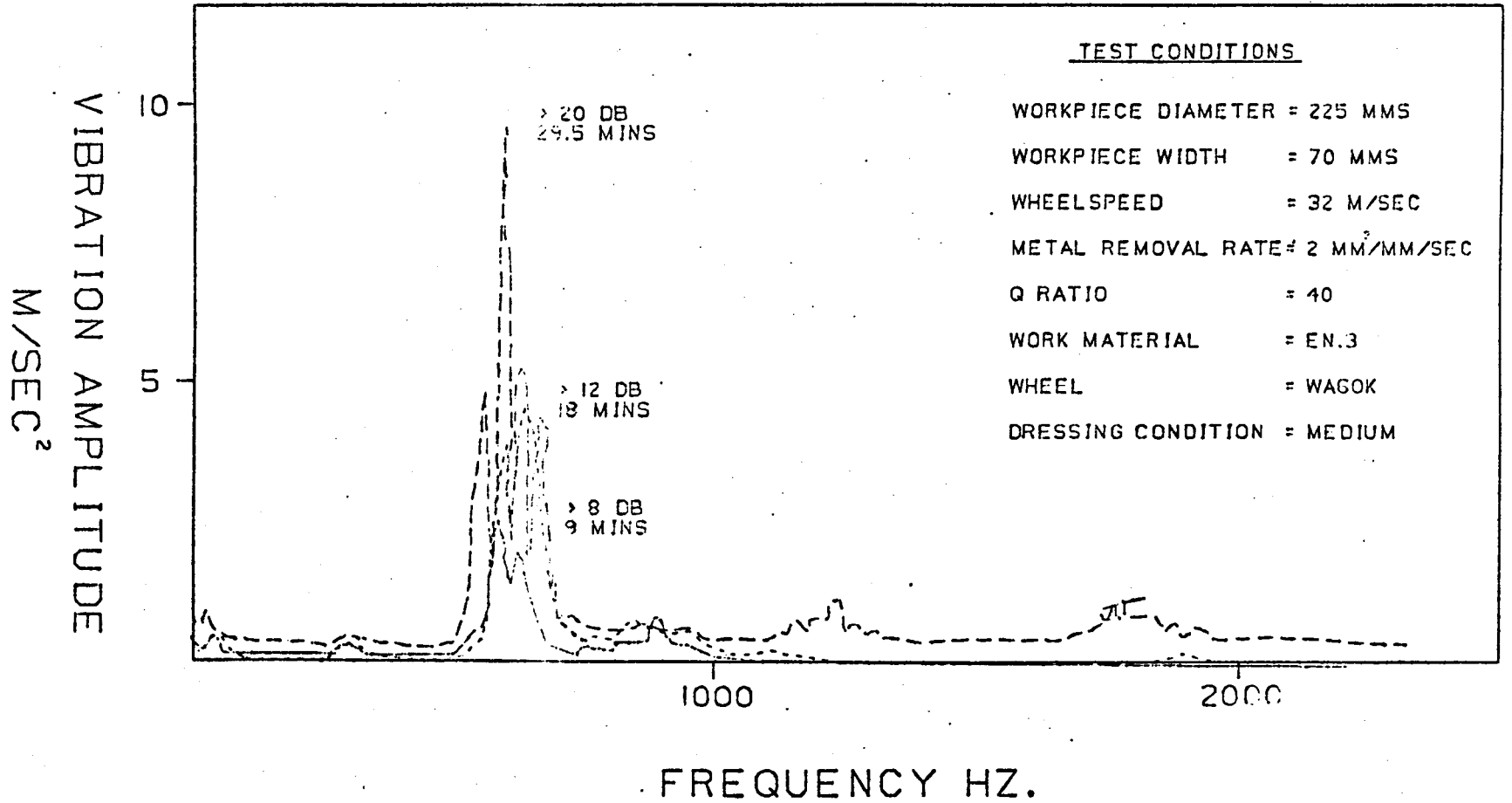


FIGURE 5.3g

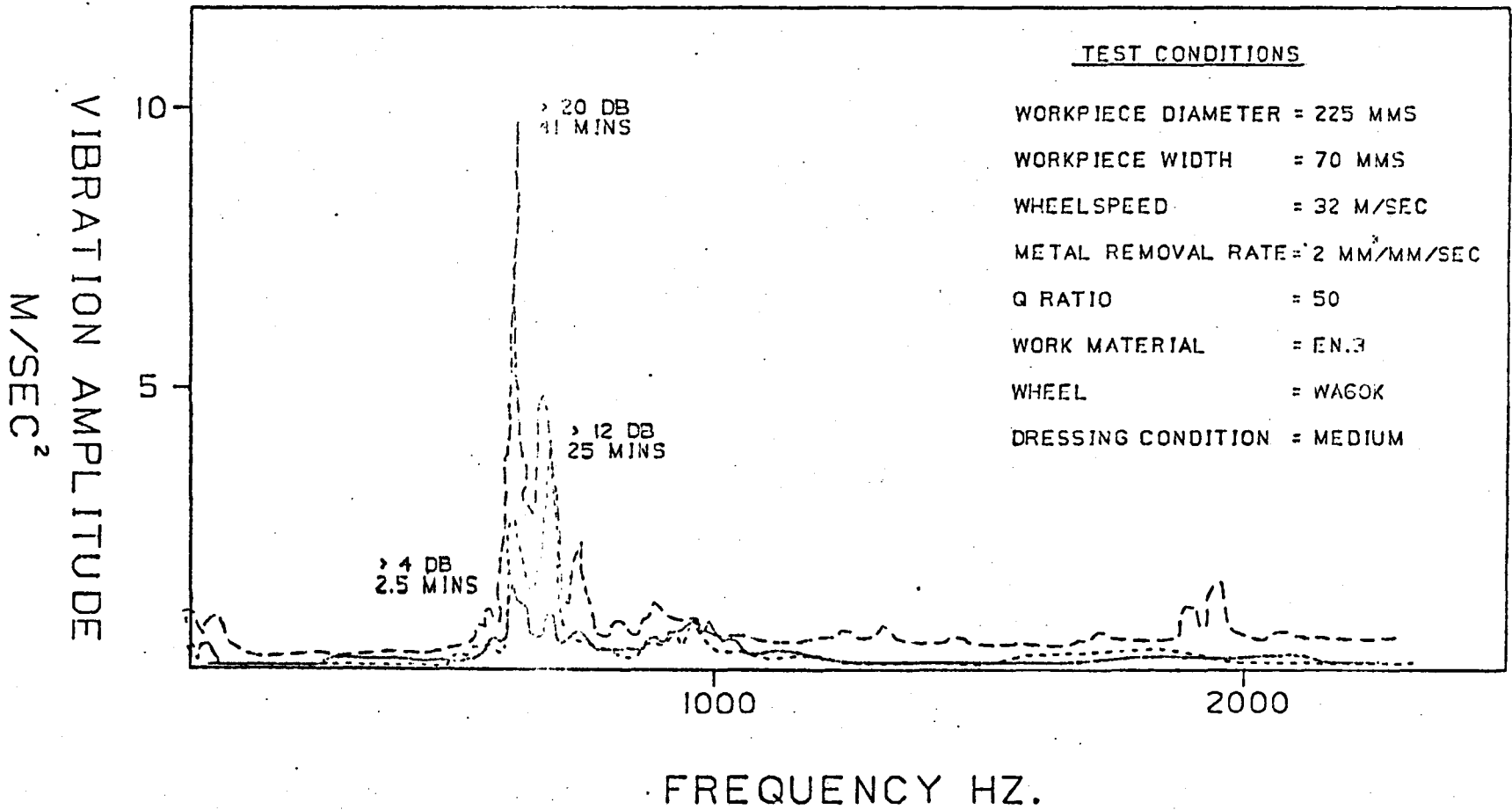


FIGURE 5.3h

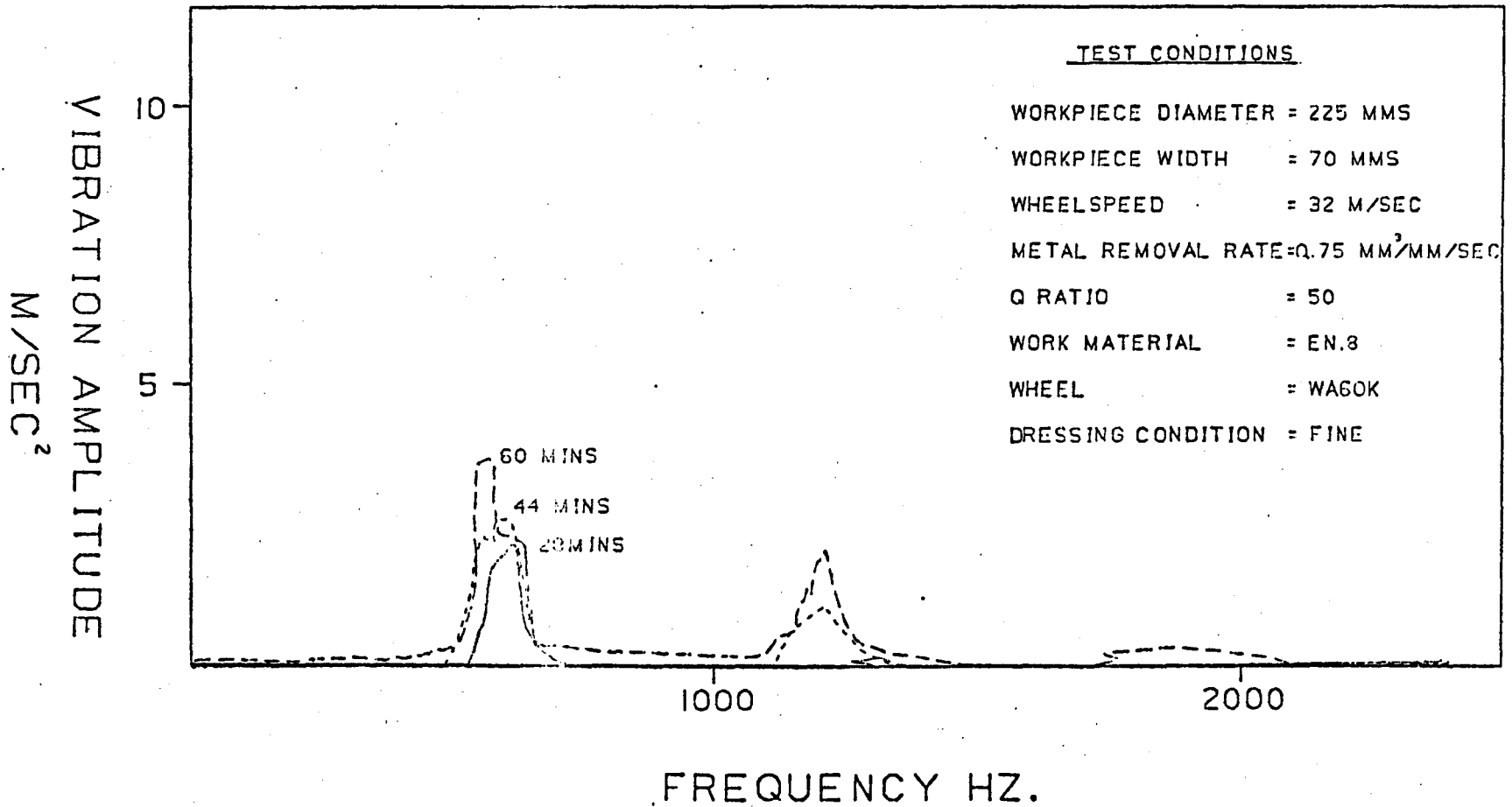


FIGURE 5.4a

FIGURE 5.4 VIBRATION SPECTRUM ANALYSIS RESULTS FROM THE WHEEL DRESSING TESTS

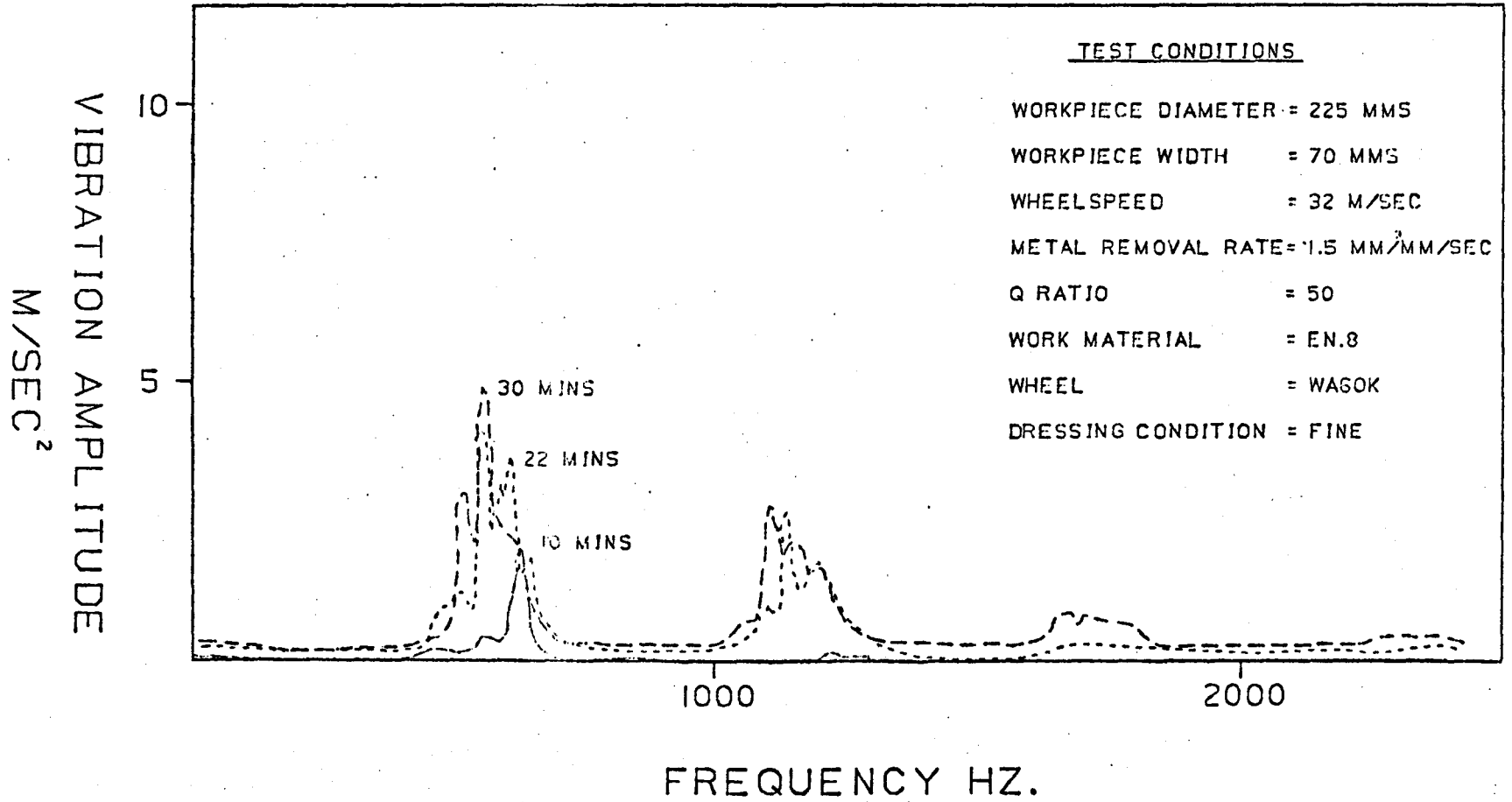


FIGURE 5.4b

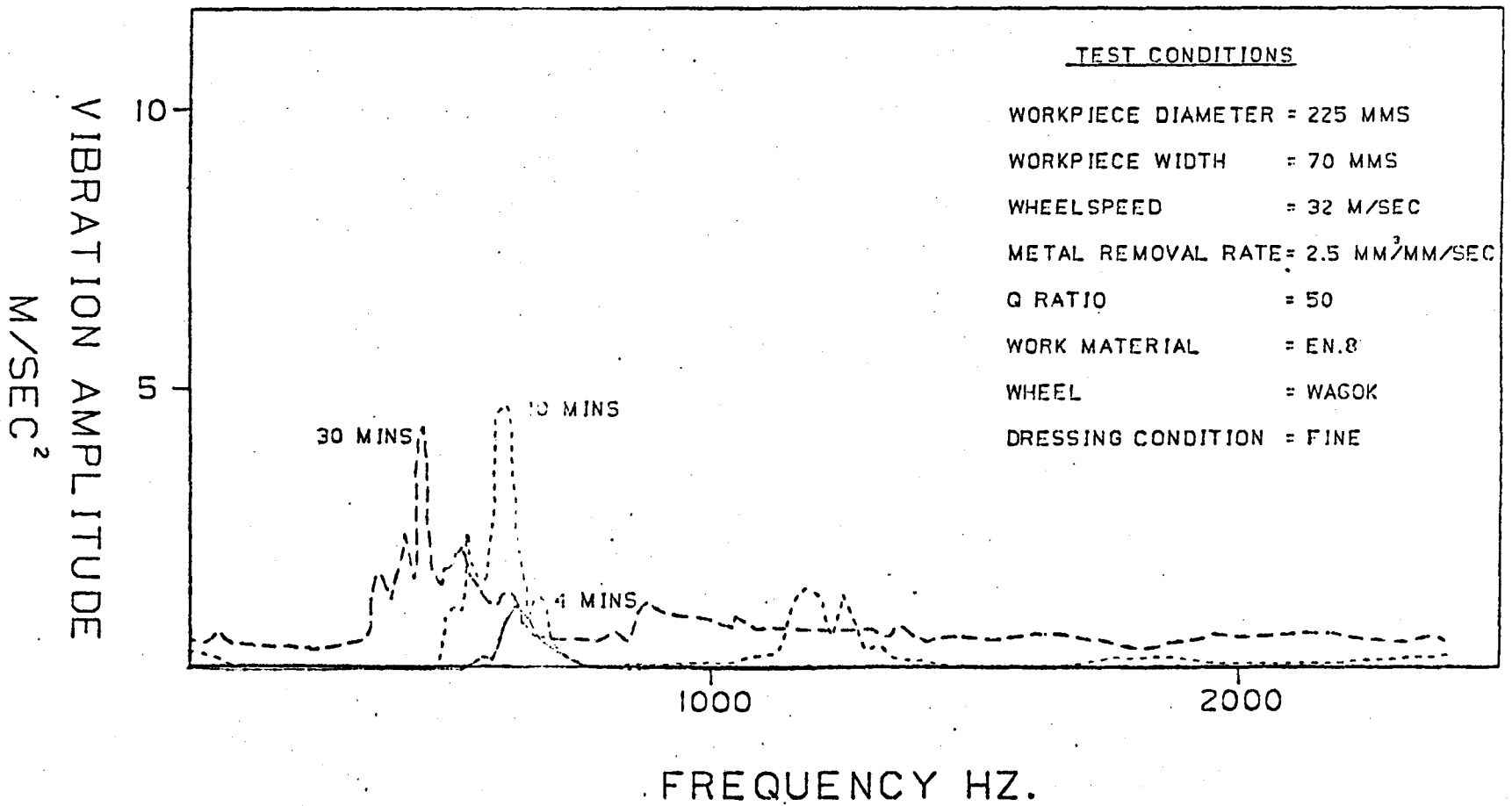


FIGURE 5.4c

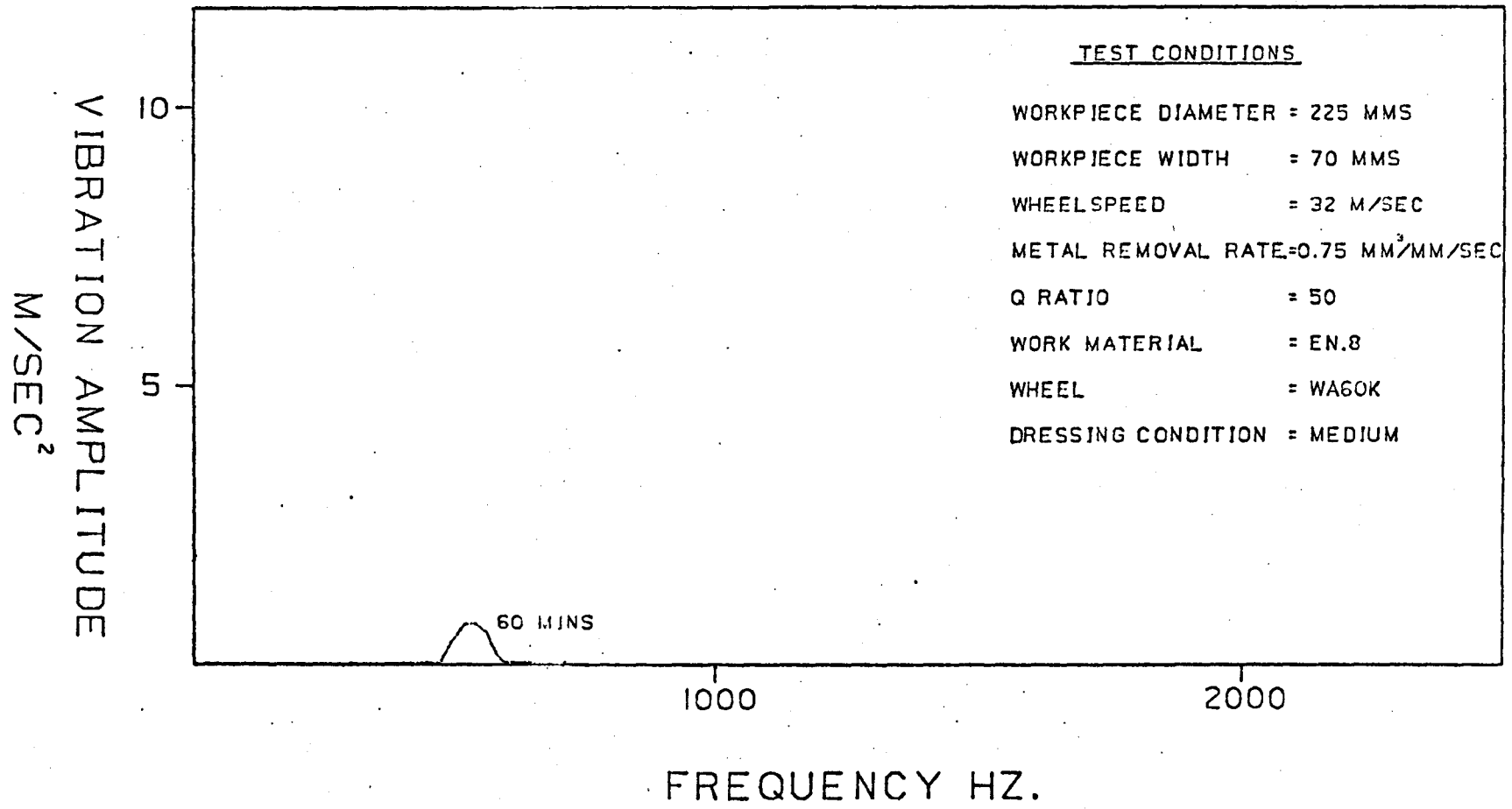


FIGURE 5.4d

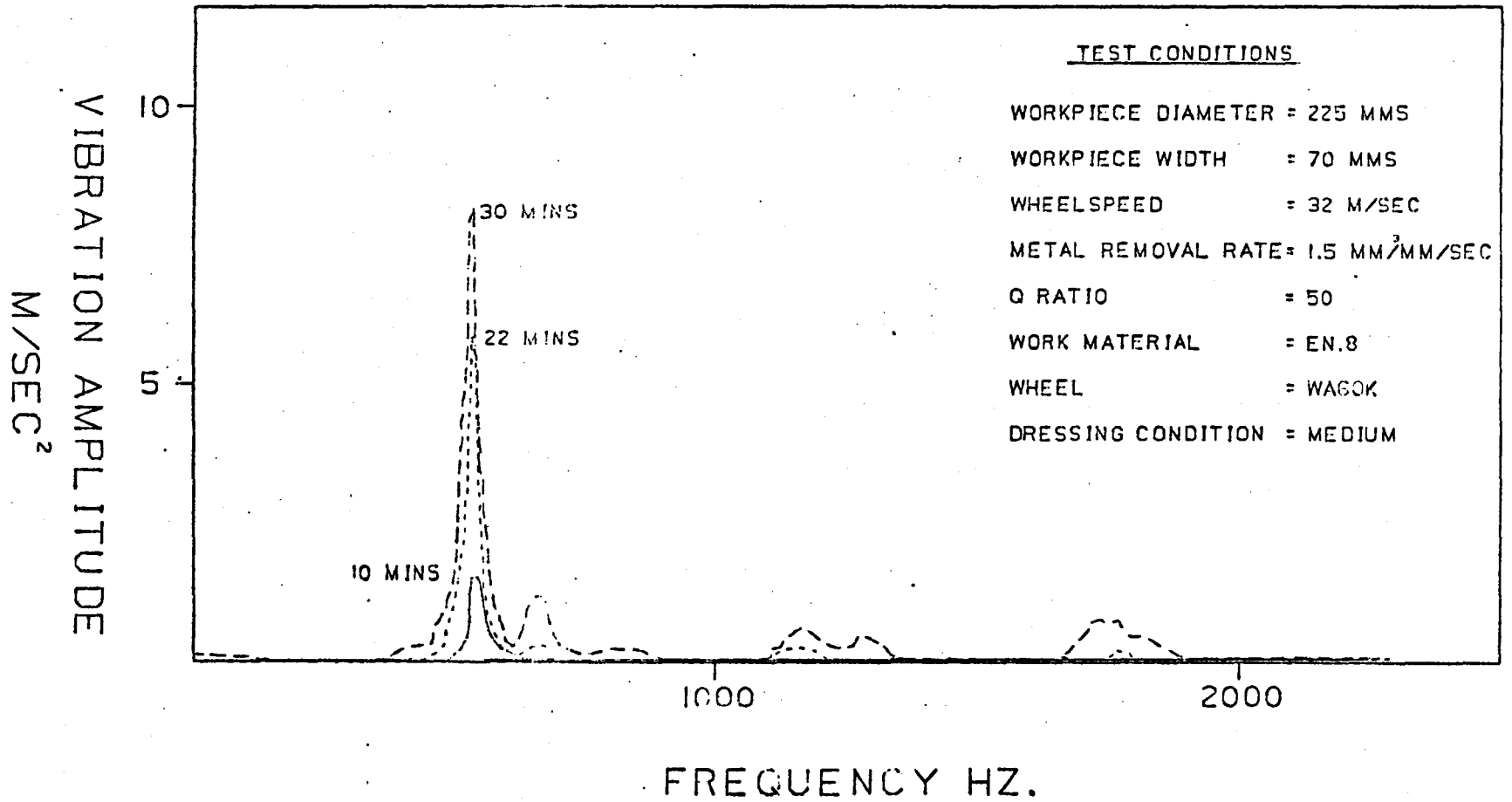


FIGURE 5.4e

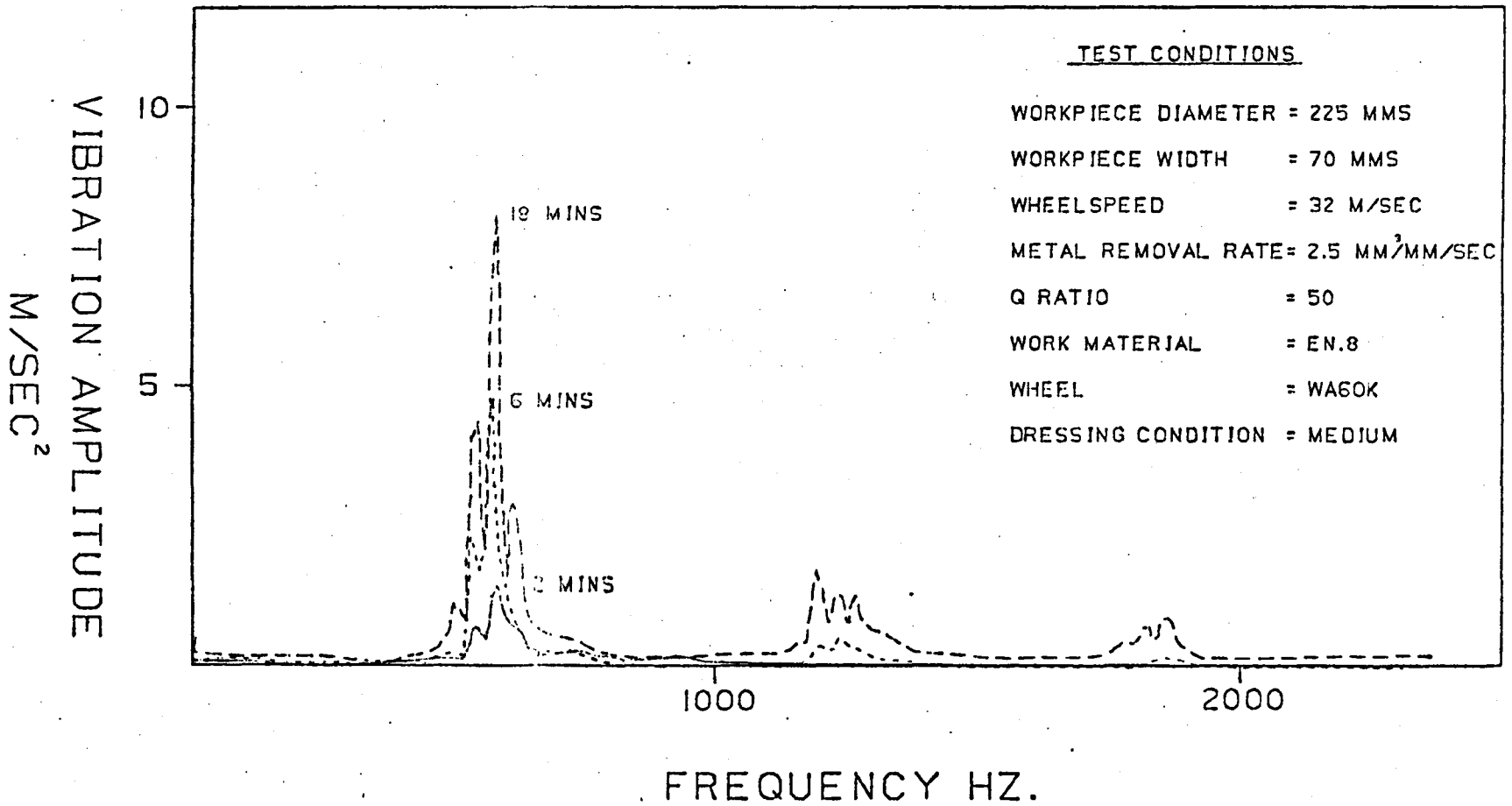


FIGURE 5.4f

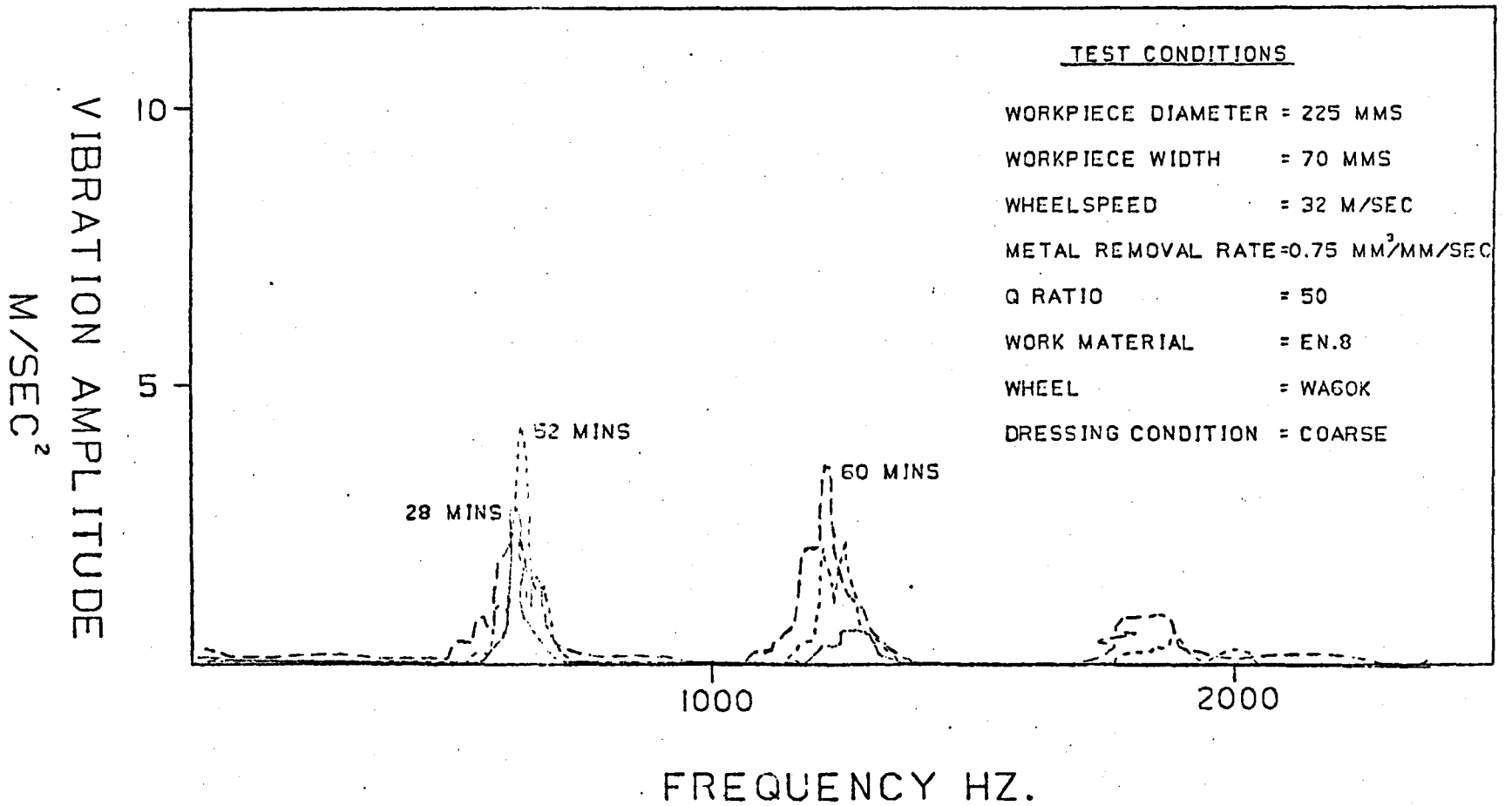


FIGURE 5.4g

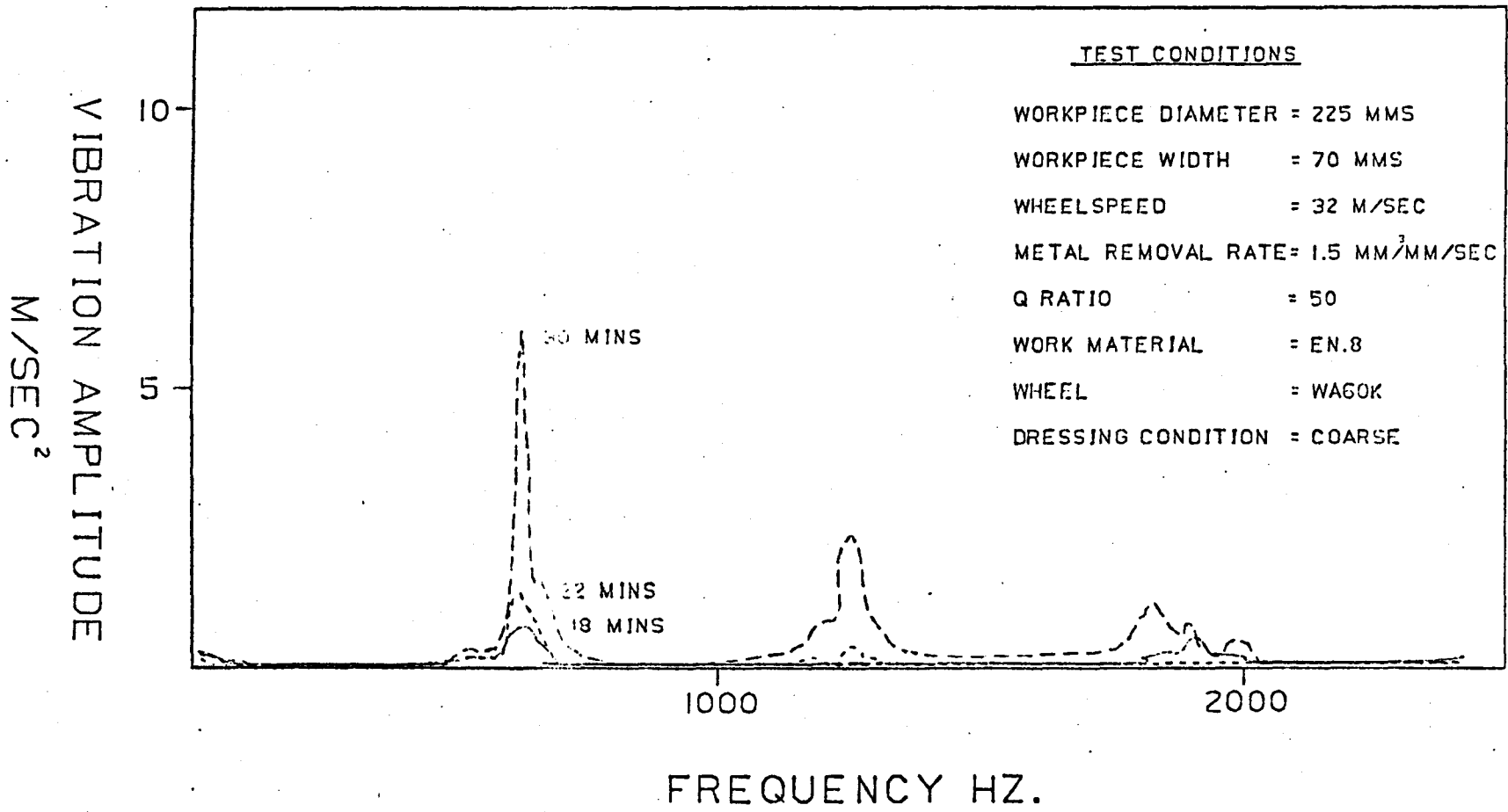


FIGURE 5.4h

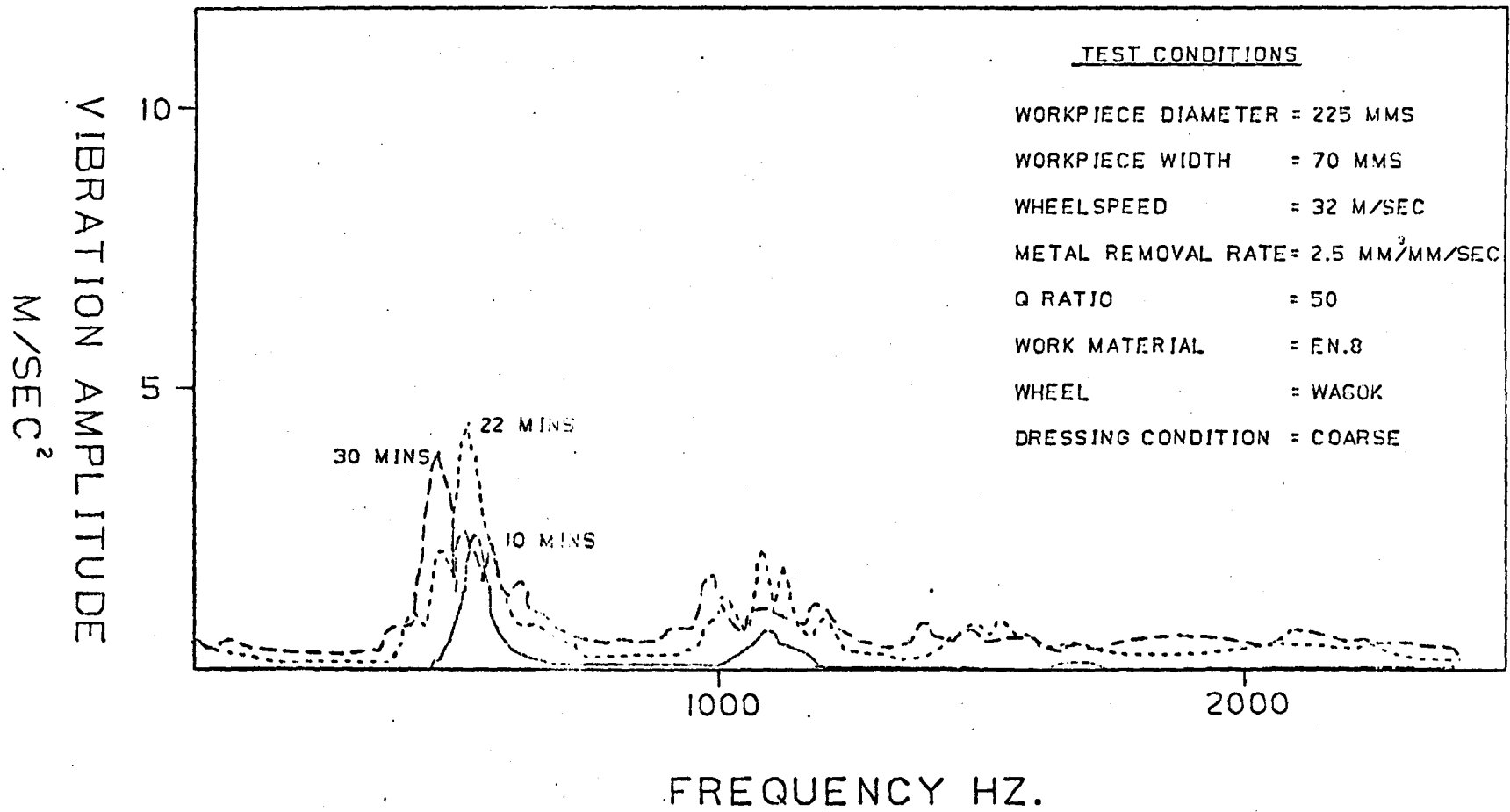


FIGURE 5.41

## 6.0 ANALYSIS AND DISCUSSION

### 6.1 Long Duration Constant Metal Removal Rate Tests

#### 6.1.1 Grinding Forces and Wheelpower

Normal and tangential grinding forces increased from the initial value observed after re-dressing the wheel in all the tests at metal removal rates of 1 and 2 mm<sup>3</sup>/mm/sec. This phenomenon has been reported by a number of researchers [36;1960: 41;1970: 42;1971: 43;1972] and the occurrence has been attributed to the attritious wear of the abrasive grains [41;1970] (Section 2.2). Grinding forces, however, remained constant during the tests at a metal removal rate of 3 mm<sup>3</sup>/mm/sec which indicated that fracture wear was the predominant abrasive wear mechanism [41;1970].

The monitored wheelpower during grinding varied in a manner similar to that of the forces. Wheelpower was found to increase with respect to time during the 1 mm<sup>3</sup>/mm/sec metal removal rate tests, remain constant throughout the 2 mm<sup>3</sup>/mm/sec tests and decrease during the 3 mm<sup>3</sup>/mm/sec tests.

#### 6.1.2 Self-Excited Chatter Vibration

The spectrum analysis results shown in Figures 5.1a-5.1k indicate the time history of the wheel/workpiece vibration levels. Tests performed at metal removal rates of 1 and 2 mm<sup>3</sup>/mm/sec exhibited increasing levels of chatter vibration at a particular chatter frequency. This vibration was identified by Taiyrod examination of the work surface and, was wheel rather than workpiece regenerative chatter because of the absence of a surface wave pattern on the workpiece.

The history of the vibration level also confirms the existence of wheel regenerative chatter because workpiece regenerative chatter occurs at the commencement of the grinding operation whereas wheel regenerative chatter has been found to increase with grinding time from low initial values [85;1977].

Normal and tangential force readings indicated that attritious wear was the predominant wear mechanism for metal removal rates of 1 and 2 mm<sup>3</sup>/mm/sec. Attritious wear of the abrasive grains produce transient force variations on subsequent whole revolutions of the grinding wheel and hence further local wheel wear fluctuations (Section 2.4). If the grinding process was stable, these disturbances would disappear. The evidence from the spectrum analysis results (Figures 5.1a-5.1h) is that the process is unstable and hence these disturbances are amplified. The level of unstable activity is, however, low for much of the actual grinding time (15-20 mins) and hence satisfactory results, free from severe chatter influence, can be expected before the level of the unstable activity is unacceptable.

The tests carried out at metal removal rate of 3 mm<sup>3</sup>/mm/sec did not exhibit increasing levels of self-excited chatter vibration. The magnitude of vibration peaked and decreased as grinding proceeded from a freshly dressed wheel. These peaks occurred early in the LR-MRR-3-30 and the LR-MRR-3-50 tests (2 and 4 minutes respectively).

Reductions in vibration levels have been attributed [82;1975: 89;1972] to fracture wear of the abrasive grains, a condition frequently termed 'self dressing'. The normal and tangential force, and wheelpower results obtained when grinding with a metal removal rate of 3 mm<sup>3</sup>/mm/sec supported this theory. The vibration level, however, initially increased from a freshly dressed wheel in all of the LR-MRR-3 tests. This suggests that fracture wear may only have occurred after a certain time. An alternative explanation may be that grits, fractured or dislodged during the dressing operation, often remain lodged in the voids of the wheel. This might account for the initial rise in vibration levels with the peak vibration being reached when the grinding process has dislodged the majority of the free grits. It has been proposed [53;1972] that a wheel should be 'conditioned' by grinding prior to testing. Conditioning was not undertaken in this study, however, because conditioning still cannot guarantee to remove all the grinding debris from the wheel and for this reason it is proposed that a filtering technique to eliminate any statistically unacceptable results occurring at the start of the test would be a more logical approach.

The presence of decreasing vibration amplitudes during the 3 mm<sup>3</sup>/mm/sec tests suggested that a reduction in vibration amplitude may eventually occur in the tests which had shown an increase (LR-MRR-1 and LR-MRR-2) if a longer duration test was used. LR-MRR-2-50 was, therefore, repeated and the test was continued until the vibration amplitude was approximately twice that of the original test (see Figure 5.1h).

No reduction in vibration was experienced before safety considerations dictated that the test should be terminated. It must be concluded, therefore, that the tests conducted at metal removal rates of 1 and 2 mm<sup>3</sup>/mm/sec were carried out with unstable grinding conditions.

The frequency of the chatter vibration remained constant in all the tests which exhibited increasing levels of self-excited vibration (LR-MRR-1 and LR-MRR-2). This was contrary to the findings of previous research workers [87;1976: 90;1970: 103;1969] where it was reported that a reduction in the chatter frequency accompanied an increase in the vibration amplitude. Kaliszer [90;1970] explained this reduction in terms of the wheel/workpiece contact stiffness. As the amplitude of vibration increases, the magnitude of the wheel contact stiffness will decrease, causing a reduction in the natural frequency of the wheel/workpiece system. This phenomenon will be present in the grinding conditions used in the present research. The chatter frequency, however, did not decrease and hence some factor(s) must be present, which when acting in isolation would tend to increase the natural frequency. A combination of all these factors could then be deemed responsible for no significant change in natural frequency. An increase in the natural frequency will result from an increase in the stiffness of the wheel/workpiece system. Two factors contribute to increase the system stiffness.

1. increasing grinding forces
2. increasing wheel/workpiece contact

Both of these factors are present in the LR-MRR-1 and LR-MRR-2 tests. Thus a combination of high vibration levels reducing the stiffness, and increasing forces and contact area increasing the stiffness, appears to have created a minimal variation in the natural frequency of the system.

The vibration spectrums of the tests conducted at metal removal rates of 3 mm<sup>3</sup>/mm/sec show two variations from those conducted at lower metal removal rates (see Figures 5.1i-5.1k)

1. The amplitude of vibration decreased rather than increased
2. The frequency of vibration decreased rather than remained constant

The former phenomenon has previously been explained as being caused by fracture wear. The latter phenomenon results from a reduction in the stiffness of the wheel/workpiece system. This reduction does not originate from an increase in chatter vibration amplitude since the magnitude of the self-excited vibrations decreased. No significant reduction of forces was experienced (Table 5.1i-5.1k) to effect a stiffness reduction and hence an alternative explanation is required. Fracture wear, the predominant wear mechanism during the 3 mm<sup>3</sup>/mm/sec tests, produces grinding grits which have a reduced wheel/workpiece contact area. This reduction in the contact area causes a reduction in the wheel/workpiece stiffness and hence a reduction in the frequency of the self-excited vibration.

## 6.2 Constant Normal Force Machining Tests

### 6.2.1 Tangential Force and Wheelpower

Maintaining a constant normal force magnitude by varying the metal removal rate also appears to impose constraints on the tangential force and wheelpower. Both parameters remained constant throughout the majority of the tests. The only exceptions were two tests at the highest normal force value, LR-NF-300-30 and LR-NF-300-40 during which the wheelpower decreased. This reduction is similar to the one experienced during the long duration constant metal removal rate tests and can again be explained by a reducing workpiece diameter.

### 6.2.2 Self-Excited Chatter Vibration

#### 6.2.2.1 Attritious Wear

Attritious wear is the predominant wear mechanism in all of the 100 Newton constant force tests and in the following tests at normal force values of 200 Newtons:- LR-NF-200-30 and LR-NF-200-40. In all of these tests the amplitude of the chatter vibration increased and the frequency decreased (see Figures 5.2a-5.2g). This frequency decrease was not observed in the corresponding constant metal removal rate tests where the chatter frequency remained constant (Figures 5.1a-5.1h). This constant frequency phenomenon has been attributed (Section 6.1.2) to a reduction in the wheel/workpiece contact stiffness as the vibration amplitude increased and increases in the wheel/workpiece contact area and grinding forces.

If this hypothesis is applied to the normal force spectrum analysis results, the increase in the amplitude of vibration will have a tendency to reduce the system stiffness and hence the natural frequency; and the the increase in wheel/workpiece contact area produced by attritious wear will have a tendency to increase the stiffness. The increasing grinding forces which contributed to an increase the system stiffness during the constant metal removal rate tests, are constrained when grinding with constant normal forces. The net effect of this constraint will be an imbalance in the direction of reducing system stiffness, and hence a reduction in the chatter frequency will accompany an increase in the amplitude of vibration during the constant normal force tests.

The LR-NF-200-50 test did not exhibit an increasing peak vibration amplitude as the test proceeded (see Figure 5.2h). This result differed from all the other results obtained at or below this metal removal rate (LR-MRR-1, LR-MRR-2, LR-NF-100, LR-NF-200-30 and LR-NF-200-40) which all displayed increasing levels of vibration as testing proceeded. Examination of the LR-NF-200-50 vibration spectrum (Figure 5.2h) reveals that although the peak amplitude of vibration is decreasing, the average magnitude in a frequency band centred on the natural frequency, is actually increasing. This was confirmed by an overall increase in the peak-to-peak vibration level observed on an oscilloscope. It appears that average vibration amplitudes obtained from band pass filters are a better representation of vibration magnitude than are peak values. Peak values would not have caused the LR-NF-200-50 test to be terminated.

#### 6.2.2.2 Fracture Wear

Fracture wear was the predominant wear mechanism in two of the tests performed under the largest normal forces (LR-NF-300-30 and LR-NF-300-50). Vibration spectrum analysis of these tests (Figures 5.2i and 5.2k) revealed similar results to those obtained from the largest constant metal removal rate tests (Figure 5.1i-5.1k). The decreasing levels of vibration experienced in these tests illustrate the advantage of using normal force values to remove the bulk of the material before finish grinding. Wheels operating under high normal forces will be self-dressing and hence productivity will be improved. Profile grinding, an operation performed by dressing a profile onto the grinding wheel, will, however, require a dressing operation between the roughing and finishing cycles since the high wheel wear rates associated with self-dressing are likely to degrade the wheel profile. Sharp corners and small radii are particularly vulnerable to profile variation.

The five tests (LR-MRR-3-30, LR-MRR-3-40, LR-MRR-3-50, LR-NF-300-30 and LR-NF-300-50) all have decreasing levels of vibration. The level of vibration during the LR-NF-300-40 tests, however, actually increased (Figure 5.2j). This illustrates a possible disadvantage with constant force machining. If the initial grinding force is slightly below the attritious-to-fracture wear transition force it will remain so throughout the whole of the grinding operation. The compensation for attritious wear will be a decreasing metal removal rate. If, however, the initial grinding force is slightly below the transition force in constant metal removal rate grinding, attritious wear will result in higher forces and hence fracture wear.

This phenomenon may account for the cyclic pattern of increasing and decreasing forces experienced by Makino [44;1974].

### 6.2.3 Component Surface Finish

Linear regression analysis of component surface finish and the various grinding parameters monitored during the constant normal force tests are presented in Appendices 6.1 and 6.2 and summarised in the Table 6.1. Two correlations were obtained with the final metal removal rate as the independent variable and the surface finish as the dependant variable. The first relates to all the data and the second to the results of the tests considered to be 'precision' grinding [1;1972]. Both analyses produced good correlations between metal removal rate and component surface finish ( $R^2$  of 0.9 and 0.94 respectively). These straight line relationships result because larger metal removal rates necessitate larger individual grit depths of cut and hence will produce deeper troughs on the work surface. Excellent correlations were also obtained using normal forces ( $R^2=0.9$ ) and tangential forces ( $R^2=0.89$ ) individually as the independent variable. These correlations, however, were obtained from 'clusters' of results (e.g. 5 values of 100 and 3 values of 200 for normal force) and hence these results may produce a model which is unrepresentative of intermediate points.

The chatter vibration levels existing at the end of all the constant force grinding tests are given in Table 6.2. This table presents the peak vibration levels and the average vibration values based on band pass filters of 100, 200, 300 and 400 Hz (i.e. the natural frequency  $\pm 50\text{Hz}$ ,  $\pm 100\text{Hz}$ ,  $\pm 150\text{Hz}$  and  $\pm 200\text{Hz}$ ). The band pass values were calculated from the spectrum analysis results (Figures 5.2a-5.2k).

Workpiece surface finish is influenced by the amplitude of chatter vibration present during the grinding operation [78;1979: 83;1977: 91;1974: 92;1971]. Increasing levels of self-excited chatter vibration produce a deteriorating component surface finish. This relationship was investigated in the present study by using linear regression analysis. The results are presented in Appendix 6.3 and summarised in Table 6.3.

The results indicate no correlation at a 5% significance level between component surface finish and chatter vibration amplitude. The analysis was carried out on a wide range of grinding conditions and illustrates that vibration has an insignificant effect on surface finish when compared to other grinding parameters. If the other grinding parameters are eliminated from the computation, however, by maintaining constant values throughout a test, a direct study of component surface finish and vibration amplitude could be undertaken. Such a study is discussed in the next section.

### 6.3 Investigation of Component Surface Finish

#### 6.3.1 Grinding Forces and Wheelpower

Interrupting the test to measure the component surface finish had little effect on the normal and tangential forces or the wheelpower levels. The time-history magnitudes of these parameters were similar to those of the long duration tests (see Tables 5.1a-5.1h and 5.5a-.5.h).

### 6.3.2 Self-Excited Chatter Vibration

The vibration spectrum analysis results for the short duration tests are shown in Figures 5.3a-5.3h. These results were also similar to those obtained from the long duration tests (Figures 5.1a-5.1h) since chatter was observed to increase in amplitude at a particular frequency as grinding proceeded from a freshly dressed wheel. The stiffness hypothesis used to describe this phenomenon in the long duration tests (Section 6.1.2) is therefore applicable to the interrupted tests.

### 6.3.3 Component Surface Finish

Regression analysis on all the data from the constant normal force tests suggests a poor correlation between component surface finish and chatter vibration amplitudes (Table 6.3). Other parameters, particularly normal force and metal removal rate, have a controlling influence on surface finish (Section 6.2.3). Restricting these parameters, however, does enable the effects of vibrational levels on component surface finish to be studied. This section proposes to investigate these effects. The vibration levels for this analysis are presented in Table 6.4a-6.4h. Appendices 6.4-6.10 and Tables 6.5 and 6.6 contain the regression analysis and summaries of the results respectively.

At least 65% of the results could be explained by the regression model relating surface finish and average vibration levels when all the results at a metal removal rate of  $2\text{mm}^3/\text{mm}/\text{sec}$  were considered. The coefficient of determination was improved in many cases to values in excess of 90% when the wheel/workspeed ratio was also constrained, with logarithmic values of vibration providing a marginally better least squares fit to the data than linear vibration levels (see Table 6.6).

There was little or no correlation, however, between all of the surface finish and vibration results taken from the 1 mm<sup>3</sup>/mm/sec metal removal rate tests. Even the results of the individual tests (e.g. SR-MRR-1-70) which provided a constraint on the wheel/workspeed ratio, failed to achieve consistently high values of the correlation coefficient. This anomaly between the 1 and 2 mm<sup>3</sup>/mm/sec results may be explained by considering an analogy of a constant amplitude signal with a random superimposed noise level. If the signal/noise ratio is high a good representation of the signal amplitude can be obtained by measuring the resultant output. If, however, the signal level is reduced without reducing the noise level, measuring the resultant output may result in significant errors in the determination of the constant amplitude level. Vibration can be considered to be a noise superimposed on a constant amplitude wheel infeed rate. If the in-feed is high, the vibration level will not significantly affect the resultant wheel infeed rate but as the wheel infeed rate is reduced without a corresponding reduction in the vibration level, the signal/noise ratio will decrease and the instantaneous wheel infeed ratio will become increasingly dependant on the magnitude of the vibration level. This accounts for the absence of a correlation between surface finish and vibration levels at low metal removal rates since surface finish is highly dependant on metal removal rate (Section 6.2.3). The correlation between surface finish and vibration, however, will improve as the metal removal rate is increased.

The limiting factor on the improvement will probably be the attritious-fracture wear transition point since the model was developed for conditions of attritious wear and hence is unlikely to predict conditions outside the range of the model.

Time was also included as an independent variable in the surface finish regression analysis (Appendices 6.4 and 6.5). A first order linear model with surface finish as the dependant variable and time as the independent variable accounted for 92% of the surface finish readings at a metal removal rate of 2 mm<sup>3</sup>/mm/sec and 69% of the surface finish readings at a metal removal rate of 1 mm<sup>3</sup>/mm/sec.

Surface finish measured in terms of the arithmetic mean deviation ( $R_a$ ) increased linearly with grinding time. This feature cannot be explained by the increase in the level of vibration alone since the correlation coefficient between surface finish and time is higher than that between surface finish and vibration. Another variable must be contributing to the deteriorating component surface finish. Wheel wear has been shown to influence component surface finish. The predominant wear mechanism in each of these short duration tests was attritious. Flats on the surface of a grit produced by this wear mechanism, however, should tend to reduce the arithmetic mean deviation ( $R_a$ ) value because flats on the grits will not produce the same deep troughs on the work-surface as a sharp grit. This is the main reason why 'dull' wheels, produced by fine dressing conditions, are used to produce excellent component surface finishes. These excellent surface finishes, however, are only achievable for short periods after dressing before component surface finish deterioration is experienced (Section 2.6).

Attritious wear is, therefore, responsible for producing increasing rather than decreasing component arithmetic mean deviation values.

Changes in the work surface profile may be explained by considering the compressive stresses present in the workpiece during the machining operation. Pekelharing [141;1966] and Wallbank [142] propose that the large compressive stresses present in the material shear plane when using a single point cutting tool are relaxed once the material encounters the clearance and rake faces of the tool (see Figure 6.1). A tool with a wear flat will prevent the material from relaxing until it is clear of this wear flat. If this theory is applied to the case of wear flats on an abrasive grit, relaxation of the compressive stresses will occur in the direction of the least resistance. This direction will depend on the grit geometry. As the area of the wear lands increase the direction of least resistance is likely to be at  $90^\circ$  to the direction of grit motion. No relaxation of the material in this direction will be possible until redundant work is done and material is forced along the sides of the grits. This will create the peaks shown in Figure 6.2. It is recognised that this must occur before the grit loses contact with the workpiece. This phenomenon, however, may account for the increase in arithmetic mean deviation with time since increasing wear lands will cause increasing amounts of material to be displaced.

Although vibration levels and grinding time have been considered as independent variables in models to predict component surface finish, successful models have only been developed for the individual short duration tests where other grinding parameters are constrained.

Vibration and time, therefore, cannot be used to predict surface finish when considered in isolation, but may be of use in a model where other parameters are used to account for differences in grinding conditions. This possibility was investigated by multiple regression analysis on the long duration test data. The results of the analysis (Appendix 6.11) are summarised in Table 6.7.

Excellent correlations between surface finish and the independent variables of metal removal rate, normal force and vibration levels were obtained from the multiple regression analysis. All the results, however, include a negative coefficient value for the vibration level (see Appendix 6.11). This will mean that the surface finish should improve as the vibration levels increase: a phenomenon that is unlikely to occur (Sections 2.5 and 5.3). Previous regression analyses (Appendices 6.3-6.10) provided a positive coefficient for vibration levels. The multiple regression analysis for the long duration testing, however, does not consider vibration as an increasing or decreasing phenomenon since all the results were taken at the end of the tests when the vibration levels were high.

The long duration test models illustrate a problem when developing mathematical relationships in this way. The model is only capable of predicting the value of the dependent variable accurately for the range of independent variables values used in the original model development. Any attempts to expand this model to predict parameter ranges not considered during the initial testing can produce inaccurate results.

Tables 6.8 and 6.9 show the use of one of the long duration test models to predict the surface finish results during the short run tests. The model is capable of explaining 93% of the long duration surface finish results. The predicted results from the short turn tests, however, vary by as much as 100% from the monitored value. Predictions of the component surface finish are more accurate at the end of the test since these conditions were similar to those used to develop the model. Predictions of the component surface finish were also more accurate for the 2 mm<sup>3</sup>/mm/sec results than for the 1 mm<sup>3</sup>/mm/sec.

Despite the inaccuracies of the predicted surface finish results, normal force and vibration monitoring offers a potential for developing models to control the workpiece surface finish. This technique, however, will be dependant on developing in-process surface finish monitoring facilities because the wide range of grinding parameters used during the grinding operation will prohibit the use of previously defined models.

#### 6.4 Wheel Dressing Investigation

##### 6.4.1 Effect of Dressing on Grinding Forces and Wheelpower

The 3 x 3 factorial experiment, comprising three metal removal rates and three dressing conditions, enabled the effect of dressing on grinding forces and wheelpower to be studied. A third variable time mean that 24 significance tests were strictly needed to fully investigate the dressing influence; eight tests of normal force, tangential force and wheelpower.

Normal and tangential grinding forces and wheelpower, however are related and hence if dressing significantly affects one it is likely to affect all three. It was, therefore, decided to complete a significance test on one of the three variables.

Normal or tangential grinding force or wheelpower had to be selected for the dressing significance testing. The choice was made on the basis of a regression analysis performed on the grinding data after 2 minutes of testing (see Appendix 6.12). Two minutes was considered to be a sufficiently long grinding time to enable any grits dislodged during the dressing process to be cleared from the wheel, but was also considered to be sufficiently close to the start of the test to benefit from the period of greatest dressing influence (Section 2.6).

The results from the regression analysis indicated the following correlations:

Normal vs tangential force,  $R^2 = 0.95$

Normal force vs wheelpower,  $R^2 = 0.81$

Tangential force vs wheelpower,  $R^2 = 0.93$

Tangential force was, therefore, selected as the parameter most likely to adequately represent all three grinding parameters.

The tests to examine the significance of dressing on tangential grinding forces are presented in Appendices 5.1-5.3. These results show that there is no evidence at a 5% significance level to show that dressing influenced the magnitude of grinding forces after 2, 6 or 10 minutes of grinding.

No further tests were carried out since if there was no statistical evidence to indicate any influence in the initial part of the test where dressing is reported to have the greatest effect (Section 2.6), there is unlikely to be any influence at the end of the test.

This result contradicts the previous work carried out on the influence of dressing on grinding forces (Section 2.6). Dressing conditions have been found to influence forces. The present investigation used a 1000 rpm wheelspeed during dressing and hence the dressing rates of 50, 100 and 200 mms/min (See Section 4.6.1.2) produced dressing leads of 0.05, 0.1 and 0.2 mms/revolution of the grinding wheel. Size-60 grinding grits have a diameter of 0.25 mms. This will mean that in fine dressing, the diamond will 'machine' the grit an average of five times, in medium dressing an average of two and a half times and in coarse dressing will 'machine' 80% of the grits once only. These calculations assume that the diamond tip has a zero thickness, an assumption which will only be valid for no dressing depth of cut. The depths of cut used, however, are small enough not to seriously affect this argument.

The first impact with a hard diamond will probably fracture a grinding grit and subsequent contacts are likely to 'smooth' the fractured surface to produce grits which are ideal for producing excellent surface finishes during the initial stages of grinding. Coarse dressing is likely, therefore, to produce sharp grits whereas fine and medium dressing will produce smooth grits.

It may not be unreasonable to assume then that the diamond traverse rates chosen for this investigation will yield different wheel conditions for coarse dressing but similar wheel conditions for fine and medium dressing. This may explain the lack of statistical evidence of the influence of dressing on grinding forces. A more significant analysis could possibly be one which only considers the fine and coarse dressing conditions.

Statistical significance tests used to compare the tangential force results obtained after fine and coarse dressing (Appendices 5.4-5.6), showed that fine dressing produced higher tangential force readings than coarse dressings in the tests conducted at metal removal rates of 0.75 and 1.5 mm<sup>3</sup>/mm/sec. There was no evidence, however, to support this hypothesis even at a 5% significance level in the case of the 2.5 mm<sup>3</sup>/mm/sec tangential force readings. The absence of the statistical evidence in the 2.5 mm<sup>3</sup>/mm/sec metal removal rate test is due to the final two coarse dressing results, i.e. those after 26 and 30 minutes of grinding (see Appendix 5.4). If these results are omitted from the analysis by considering only the first 22 minutes of the test, then there is evidence at a 2.5% significance level to support the hypothesis that fine dressing produced higher tangential forces than coarse dressing during the 2.5 mm<sup>3</sup>/mm/sec test. It is quite legitimate to consider the first six readings of the test in this way because dressing will only be significant at the beginning of the test when primary wear occurs (Section 2.6). The final two readings of the 2.5 mm<sup>3</sup>/mm/sec coarse dressing test were probably from the secondary wear stage where dressing has no influence.

#### 6.4.2 Self-Excited Chatter Vibration

The chatter vibration spectrum analysis results (Figures 5.4a-5.4i) were similar to the one observed from previous tests (Figures 5.1a-5.1k, 5.2a-5.2k and 5.3a-5.3h). Five of the tests exhibited increasing levels of vibration without a change in chatter frequency (LR-MD-0.75-50, LR-MD-1.5-50, LR-MD-2.5-50, LR-CD-0.75-50, LR-CD-1.5-50) (Figures 5.4d, 5.4e, 5.4f, 5.4g and 5.4h respectively), two tests exhibited increasing levels of chatter vibration with a decreasing chatter frequency (LR-FD-0.75-50 and LR-FD-1.5-50) (Figures 5.4a and 5.4b); and two tests exhibited a decreasing vibration amplitude with a decreasing chatter frequency (LR-FD-2.5-50 and LR-CD-2.5-50).

The vibration spectrum analysis results which illustrated an increasing magnitude of vibration at a particular chatter frequency and those which showed a decreasing magnitude of vibration, can be explained by the wheel/workpiece stiffness hypothesis proposed in Section 6.1.2. The vibration spectrum anomalies in this series of tests were the fine dressing tests at metal removal rates of 0.75 and 1.5 mm<sup>3</sup>/mm/sec which show an increasing level of chatter at a reducing chatter frequency. The stiffness hypothesis proposed that a reduction in the chatter frequency arises from an increase in the vibration level; and an increase in the chatter frequency arises from increasing grit wear flat areas and/or an increasing grinding force.

The reducing chatter frequency of the LR-FD-0.75-50 and LR-FD-1.5-50 tests can be explained by this hypothesis if:

1. The vibration amplitude is larger in the LR-FD-0.75-50 and LR-FD-1.5-50 tests than in the tests which exhibited an increasing chatter amplitude at a particular chatter frequency.
2. Wear area increase is smaller for the LR-FD-0.75-50 and LR-FD-1.5-50 tests.
- or 3. Forces decrease, or increase at a slower rate in the case of the LR-FD-0.75-50 and LR-FD-1.5-50 tests.

The vibration levels for the dressing test are presented in Table 6.10a-6.10c. Vibration levels were no higher for the fine dressing conditions than for the other dressing conditions (Table 6.10b and 6.10c). The force increases in the case of the LR-FD-0.75-50 and LR-FD-1.5-50 were also similar to those of other comparable tests (Tables 5.6b and 5.6c) and thus the reduction in natural frequency must be attributed to the wear rates being smaller in the case of the LR-FD-0.75-50 and LR-FD-1.5-50 tests (Condition 2).

The wheels of the two tests which exhibited an increasing amplitude of chatter at a reducing chatter frequency were dressed using the fine treatment. The diamond dressing tool, therefore, 'machined' each grit five times and produced a smooth flat on the grits. Subsequent attritious wear during grinding would then not substantially increase this wear area. The effect of the increase in wheel/workpiece stiffness due to increasing wear lands, which is especially pronounced in a coarse dressing/attritious wear combination, will not be as significant for fine dressing conditions.

Attritious wear occurring on grits treated by fine dressing will, therefore, not increase the natural frequency of the wheel/workpiece system and hence the increasing levels of vibration experienced in the LR-FD-0.75-50 and LR-FD-1.5-50 will cause the frequency of chatter to decrease.

Seven of the long duration tests undertaken to examine the influence of dressing on the grinding process were performed under unstable grinding conditions since vibration levels increased (Section 2.4). It is important that the level of unstable activity is low for much of the actual grinding time so that satisfactory component surface finish results can be achieved. Dressing has been reported to influence the build up of chatter (Section 2.6). Significance testing (Appendix 5.7) showed, however, that metal removal rate and not dressing conditions have the greater influence on the build-up of chatter vibration.

#### 6.4.3 Influence of Dressing on Component Surface Finish

The influence of wheel dressing on component surface finish was investigated by a 3 x 3 factorial experiment using the three qualitative dressing treatments and three metal removal rates (0.75, 1.5 and 2.5mm<sup>3</sup>/mm/sec). Each test was periodically interrupted to measure the component surface finish. Statistical significance tests were then performed on the results (Appendices 5.8-5.17). Table 6.11 contains a summary of the analyses.

The results indicate that finer dressing conditions will produce better surface finishes than coarse dressing but this influence will only occur during the early stages of grinding.

#### 6.4.4 Component Surface Finish Model

Successful models have been developed for predicting surface finish results when grinding EN.3 by constraining as many grinding parameters as possible to simplify the model (Section 6.3.3). The dressing tests used EN8 as the work material and hence it was possible to see if similar models could be developed for surface finish prediction when using an alternative work material. The surface finish and chatter vibration levels were, therefore, taken for each of the grinding tests in the 3 x 3 factorial investigation of dressing and metal removal rate. The tests with significant data points were then subjected to regression analysis. This enabled models to be developed with metal removal rate and dressing variables constrained in a similar manner to the ones developed in Section 6.3.3. The subsequent analyses are given in Appendices 6.13-6.17 and are summarised in Table 6.12.

Very few of the regression results were significant at the 5% level because each analysis was undertaken with few data points. The results, however, do support the findings of the earlier SR-MRR tests since it appears that component surface finishes can be predicted by using chatter amplitude levels provided that the other grinding parameters are constrained.

#### 6.5 Grinding Process Control Consideration

This investigation examined the control of two grinding process output parameters:

1. The re-dress life of the wheel
2. Workpiece surface finish

### 6.5.1 Re-Dressing the Grinding Wheel

The potential of using chatter vibration to signify the end of the useful wheel life has already been reported [92;1971: 105;1959]. The long duration tests (Section 6.1 and 6.2) confirmed this potential.

The predominant wheel wear mechanism was found to have the greatest influence on chatter vibration levels. During the high metal removal rate tests, when fracture was the predominant wear mechanism, the level of vibration remained acceptably low. Rough grinding operations with high metal removal rates will thus not require frequent wheel dressing. The lower metal removal rate operations associated with finish grinding, however, experienced increasing levels of vibration and hence will require frequent wheel redressing.

The amplitude of vibration can be used to control the frequency of dressing when finish grinding. Chatter vibration signals, monitored by the accelerometer on the tailstock of the machine, can be examined by a series of overlapping band pass filters each of which is capable of examining a frequency band of 100Hz (Section 6.2.3). Any amplitude increase in any of these frequency widths could then be compared to a pre-determined maximum value, which if exceeded instigates an automatic dressing cycle or instructs the operator to re-dress the wheel.

### 6.5.2 Workpiece Surface Finish Control

The surface finish results obtained from the constant normal force tests (Section 6.2) illustrate the difficulty of developing a model to predict component surface finishes for all grinding conditions.

Successful models ( $R^2 = 0.9 - 0.97$ ) were developed for these tests (Section 6.3.3) but when these models were used to predict the surface finish values of the short duration tests, the predicted values of surface finish were only accurate to within  $\pm 10\%$  for the  $2\text{mm}^3/\text{mm}/\text{sec}$  results and were considerably less accurate for the  $1\text{mm}^3/\text{mm}/\text{sec}$  results (Table 6.8 and 6.9). These predictions were also carried out without varying the dressing conditions, workpiece material, grinding machine, wheel type etc., which when included will necessitate addition terms in a model to predict surface finish. The development of a model for all grinding conditions is, therefore, impractical since a data base for all grinding process combinations would be very large.

Models which use vibration results to predict workpiece surface finish have been developed by constraining other grinding parameters (Section 6.3.3. and 6.4.4). These models have been expanded to include terms for normal force or metal removal rate. The use of similar models in practical grinding cycles will necessitate the use of in-process surface finish measuring facilities to overcome the large grinding data base requirement. Surface finish could be measured in an identification style similar to the one described for normal forces (Section 3.5.1). When a model which correlates normal force/metal removal rate and vibration levels with component surface finish is developed, the control system will use this model to effect surface finish control by varying the infeed rate of the wheel.

This control will be applicable for the particular dressing/grinding wheel/workpiece - material combination used in the identification stage and will be an extension of the current adaptive control strategy which uses infeed rate control to achieve constant force machining (Section 3.5.2). The identification stage could then be re-initiated to produce a new model once the old model was invalidated by a change in dressing conditions, wheel, component profile or material.

This strategy does not require, but will be more successful with the development of, in-process surface finish measurement. The difficulties, however, of achieving in-process surface finish measurement have already been discussed (Section 2.5). An alternative method of developing a model is to measure the component surface finish when the grinding cycle is completed. This value could then be manually input into the computer. If a significant number of surface finish readings prior to wheel redressing are taken, a model can be developed which correlates the normal force/metal removal rate and vibration levels at the end of the grinding cycle with the resulting component surface finish. This model could subsequently be used to control workpiece surface finishes.

Independent Variable	Test Conditions	Coefficient of Determination R <sup>2</sup>
Metal Removal Rate	LR-NR-300, LR-NF-200 and LR-NF-100	0.9
Metal Removal Rate	LR-NF-200 and LR-NF-100	0.94
Normal Force	LR-NF-200 and LR-NF-100	0.9
Tangential Force	LR-NF-200 and LR-NF-100	0.89
Wheelpower	LR-NF-200 and LR-NF-100	0.85

TABLE 6.1 SUMMARY OF THE REGRESSION ANALYSIS RESULTS WITH COMPONENT SURFACE FINISH AS THE DEPENDANT VARIABLE

Test	Peak Vibration Level m/sec <sup>2</sup>	Band-Pass Average Vibration Level m/sec <sup>2</sup>			
		100Hz	200Hz	300Hz	400Hz
LR-NF-100-30	6.5	3.8	2.6	2.0	1.6
LR-NF-100-40	6.4	3.5	2.5	2.0	1.6
LR-NF-100-50	4.8	2.3	1.9	1.5	1.2
LR-NF-100-70	5.7	1.9	1.2	0.9	0.6
LR-NF-100-90	1.9	1.1	0.8	0.6	0.6
LR-NF-200-30	7.0	2.3	1.6	1.3	1.1
LR-NF-200-40	8.3	3.7	2.6	2.0	1.6
LR-NF-200-50	5.1	2.9	2.7	2.2	1.8
LR-NF-300-30	6.0	2.4	1.6	1.2	1.0
LR-NF-300-40	7.7	4.3	3.0	2.4	2.0
LR-NF-300-50	6.1	2.0	1.4	1.0	0.9

TABLE 6.2 SELF EXCITED CAHTTER VIBRATION MAGNITUDES FOR  
CONSTANT NORMAL FORCE TESTS

Independent Variable	Coefficient of Determination, R <sup>2</sup>
Peak Vibration	0.08
100Hz Vibration	0.01
200Hz Vibration	0.06
300Hz Vibration	0.08
400Hz Vibration	0.10

TABLE 6.3 SUMMARY OF SURFACE FINISH  
CHATTER VIBRATION REGRESSION  
RESULTS

TEST SR-MRR-1-30

The level of vibration failed to reach the first interruption level and hence the readings at the end of the test are given:

Peak Vibration:	0.3 m/sec <sup>2</sup>
Average vibrations, 100Hz	0.2 m/sec <sup>2</sup>
200Hz	0.1 m/sec <sup>2</sup>
300Hz	0.1 m/sec <sup>2</sup>
400Hz	0.1 m/sec <sup>2</sup>

TABLE 6.4a VIBRATION AMPLITUDES OF SHORT DURATION TESTS

TEST SR-MRR-1-40

Test Interruption Point	Peak Vibration m/sec <sup>2</sup>	Average Vibration m/sec <sup>2</sup>			
		100Hz	200Hz	300Hz	400Hz
4dBs	1.8	0.6	0.3	0.3	0.2
*	1.4	0.8	0.5	0.3	0.2

\*Vibration level never exceeded 8dBs. Readings taken after 60 minutes.

TABLE 6.4b

TEST SR-MRR-1-50

Test Interruption Point	Peak Vibration m/sec <sup>2</sup>	Average Vibration m/sec <sup>2</sup>			
		100Hz	200Hz	300Hz	400Hz
4dBs	1.5	0.9	0.5	0.5	0.4
8dBs	2.5	1.3	0.8	0.6	0.6
*	1.6	1.0	0.8	0.6	0.6

\*Vibration level never exceeded 12dBs. Readings taken after 60 minutes.

TABLE 6.4c

TEST SR-MRR-1-70

Test Interruption Point	Peak Vibration m/sec <sup>2</sup>	Average Vibration m/sec <sup>2</sup>			
		100Hz	200Hz	300Hz	400Hz
4dBs	1.7	0.8	0.6	0.5	0.4
8dBs	2.5	1.3	0.9	0.7	0.6
12dBs	4.1	1.5	0.9	0.7	0.6
16dBs	6.3	2.2	1.3	1.0	0.8
20dBs	10.0	2.3	1.3	1.0	0.8

TABLE 6.4d

TEST SR-MRR-1-90

Test Interruption Point	Peak Vibration m/sec <sup>2</sup>	Average Vibration m/sec <sup>2</sup>			
		100Hz	200Hz	300Hz	400Hz
4dBs	1.5	0.8	0.8	0.7	0.6
8dBs	3.3	1.6	1.3	1.1	0.9
12dBs	4.0	2.0	1.1	0.8	0.7
16dBs	6.3	2.7	1.5	1.1	0.8
20dBs	10.7	3.0	1.7	1.2	1.0

TABLE 6.4e

TEST SR-MRR-2-30

Test Interruption Point	Peak Vibration m/sec <sup>2</sup>	Average Vibration m/sec <sup>2</sup>			
		100Hz	200Hz	300Hz	400Hz
4dBs	1.5	1.0	0.6	0.4	0.4
8dBs	2.5	1.4	0.8	0.6	0.4
12dBs	4.5	1.9	1.3	0.9	0.7
16dBs	6.6	2.9	1.8	1.3	1.0
*	3.2	2.7	2.0	1.5	1.2

\*Vibration level decreased and hence never reached 20dBs.  
Readings taken once vibration fell below 12dBs

TABLE 6.4f

TEST SR-MRR-2-40

Test Interruption Point	Peak Vibration m/sec <sup>2</sup>	Average Vibration m/sec <sup>2</sup>			
		100Hz	200Hz	300Hz	400Hz
4dBs	1.5	1.0	0.7	0.5	0.4
8dBs	2.5	1.4	1.0	0.7	0.6
12dBs	4.0	2.4	1.7	1.2	1.0
16dBs	6.3	3.5	2.5	1.9	1.5
20dBs	10.1	3.3	2.8	2.1	1.7

TABLE 6.4g

TEST SR-MRR-2-50

Test Interruption Point	Peak Vibration m/sec <sup>2</sup>	Average Vibration m/sec <sup>2</sup>			
		100Hz	200Hz	300Hz	400Hz
4dBs	1.5	0.6	0.5	0.5	0.4
8dBs	2.5	1.1	1.0	0.7	0.6
12dBs	4.4	2.0	1.1	1.2	0.9
16dBs	6.3	3.2	2.6	1.9	1.6
20dBs	10.3	3.8	2.8	2.2	1.8

TABLE 6.4h

Test Conditions	Independent Variables				
	Peak Vibration	100Hz Level	200Hz Level	300Hz Level	400Hz Level
All SR-MRR-1	0.03 (NS)	0.03 (NS)	Zero (NS)	0.02 (NS)	0.01 (NS)
All SR-MRR-2	0.60 (0.001)	0.65 (0.001)	0.65 (0.001)	0.71 (0.001)	0.73 (0.001)

Significance level in brackets

(NS) = Not significant

TABLE 6.5 COEFFICIENT OF DETERMINATION, R<sup>2</sup>, RESULTS OF SURFACE FINISH DATA

Test Conditions	Independent Variables									
	Peak	Linear Value				Peak	Logarithmic Values			
		100Hz	200Hz	300Hz	400Hz		100Hz	200Hz	300Hz	400Hz
SR-MRR-1-70	0.40 (NS)	0.16 (NS)	0.08 (NS)	0.09 (NS)	0.06 (NS)	-	-	-	-	-
SR-MRR-1-90	0.66 (0.10)	0.83 (0.02)	0.5 (NS)	0.22 (NS)	0.22 (NS)	0.78 (0.02)	0.81 (0.02)	0.51 (NS)	0.23 (NS)	0.24 (NS)
SR-MRR-2-30	0.95 (0.05)	0.91 (0.05)	0.96 (0.05)	0.93 (0.05)	0.99 (0.02)	0.86 (0.10)	0.88 (0.10)	-	-	-
SR-MRR-2-40	0.78 (0.05)	0.91 (0.02)	0.91 (0.02)	0.89 (0.02)	0.9 (0.02)	0.93 (0.01)	0.96 (0.01)	0.97 (0.01)	0.96 (0.01)	0.96 (0.01)
SR-MRR-2-50	0.68 (0.10)	0.82 (0.05)	0.74 (0.10)	0.79 (0.05)	0.77 (0.10)	0.89 (0.02)	0.96 (0.01)	0.89 (0.02)	0.9 (0.02)	0.9 (0.02)

TABLE 6.6 COEFFICIENT OF DETERMINATION, R<sup>2</sup>, FOR INDIVIDUAL TEST CONDITIONS

First Independent Variable	Second Independent Variables									
	Peak	Linear Value				Peak	Logarithmic Values			
		100Hz	200Hz	300Hz	400Hz		100Hz	200Hz	300Hz	400Hz
Metal Removal Rate	0.97	0.97	0.97	0.96	0.96	0.95	0.97	0.96	0.96	0.95
Normal Force	0.93	0.92	0.91	0.9	0.9	0.92	0.92	0.91	0.91	0.91

All values are significant on a 0.1% level

TABLE 6.7 COEFFICIENT OF DETERMINATION VALUES FROM THE MULTIPLE REGRESSION ANALYSIS CALCULATIONS PERFORMED ON THE LR-NF SURFACE FINISH RESULTS

$$\text{MODEL: SURFACE FINISH, } \mu\text{m } R_A = 0.164 + 0.00628 \text{ NF (Newtons)} - 0.0336 V_{\text{PEAK}} (\text{m/sec}^2)$$

Test	Monitored Surface Finish $\mu\text{m}R_A$	Model Prediction $\mu\text{m}R_A$
SR-MRR-1-30	1.09	1.16
SR-MRR-1-40	0.56 0.98	1.04 1.10
SR-MRR-1-50	0.94 0.92 0.9	1.06 1.08 1.12
SR-MRR-1-70	0.8 0.74 0.82 0.79 0.84	1.11 1.08 0.97 0.96 0.9
SR-MRR-1-90	0.49 0.58 0.94 0.9 1.02	0.99 0.87 0.66 0.71 0.68

TABLE 6.8 USE OF THE LR-NR TEST REGRESSION ANALYSIS MODEL TO PREDICT THE SR-MRR-1 SURFACE FINISH RESULTS

MODEL: SURFACE FINISH,  $\mu\text{m RA}$

=

$$0.164 + 0.00628 \text{ NF (Newtons)} - 0.0336 V_{\text{PEAK}} (\text{m/sec}^2)$$

Test	Monitored Surface Finish $\mu\text{mR}_A$	Model Prediction $\mu\text{m R}_A$
SR-MRR-2-30	1.14 1.13 1.25 1.33	0.99 1.08 1.21 1.20
SR-MRR-2-40	1.11 1.18 1.34 1.36 1.41	1.06 1.08 1.22 1.27 1.27
SR-MRR-2-50	1.04 1.36 1.49 1.61 1.62	1.06 1.21 1.33 1.40 1.23

TABLE 6.9 USE OF THE LR-NR TEST REGRESSION ANALYSIS MODEL TO PREDICT THE SR-MRR-2 SURFACE FINISH RESULTS

METAL REMOVAL RATE = 2.5mm<sup>3</sup>/mm/sec

MATERIAL EN8

Time Mins	Fine Dressing Vibration Level m/sec <sup>2</sup>			Medium Dressing Vibration Level m/sec <sup>2</sup>			Coarse Dressing Vibration Level m/sec <sup>2</sup>		
	100Hz	200Hz	300Hz	100Hz	200Hz	300Hz	100Hz	200Hz	300Hz
2	1.66	-	-	1.67	-	-	-	-	-
6	2.27	1.88	-	2.07	-	-	-	-	-
10	2.40	2.09	-	2.62	2.10	1.88	1.87	-	-
14	2.56	2.16	1.96	2.48	2.16	1.96	2.32 1.83	1.96 1.79	1.31 1.7
18	2.56	2.25	1.99	2.71	2.29	2.01	2.56 1.91	2.15 1.82	1.93 1.73
22	2.34	2.26	2.10	Test terminated after 18 minutes			2.34 1.81	2.01 1.75	1.88 1.7
26	2.24	2.16	2.06				2.26	2.10	1.95
30	2.29	2.16	2.05				2.12	2.18	2.05

NOTE: 1 (-) signifies absence of vibration magnitude at particular band-pass value.

2 Where two results appear in the same position in the table, results given are for the chatter frequency and its first harmonic.

TABLE 6.10a

BAND-PASS RECTIFIED VIBRATION LEVELS FROM THE DRESSING TESTS

METAL REMOVAL RATE =  $1.5 \text{ mm}^3/\text{mm}/\text{sec}$

MATERIAL EN8

Time Mins	Fine Dressing Vibration Level $\text{m}/\text{sec}^2$			Medium Dressing Vibration Level $\text{m}/\text{sec}^2$			Coarse Dressing Vibration Level $\text{m}/\text{sec}^2$		
	100Hz	200Hz	300Hz	100Hz	200Hz	300Hz	100Hz	200Hz	300Hz
2	-	-	-	-	-	-	-	-	-
6	-	-	-	-	-	-	-	-	-
10	1.67	-	-	1.58	-	-	-	-	-
14	1.91	1.71	-	1.71	-	-	-	-	-
18	2.24	1.98	1.80	1.85	-	-	-	-	-
22	2.45	2.03	1.86	2.09	-	-	1.63	-	-
26	2.43 2.05	2.10 1.87	1.88 1.75	2.26	-	-	1.83	-	-
30	2.45 2.07	2.10 1.91	1.93 1.80	2.62	2.03	-	2.19 1.87	1.83 1.7	-

TABLE 6.10b

BAND-PASS RECTIFIED VIBRATION LEVELS FROM THE DRESSING TESTS

METAL REMOVAL RATE = 0.75mm<sup>3</sup>/mm/sec

MATERIAL EN8

Time Mins	Fine Dressing Vibration Level m/sec <sup>2</sup>			Medium Dressing Vibration Level m/sec <sup>2</sup>			Coarse Dressing Vibration Level m/sec <sup>2</sup>		
	100Hz	200Hz	300Hz	100Hz	200Hz	300Hz	100Hz	200Hz	300Hz
4	-	-	-	-	-	-	-	-	-
12	-	-	-	-	-	-	-	-	-
20	1.53	-	-	-	-	-	-	-	-
28	1.81	-	-	-	-	-	1.69	-	-
36	1.96	1.72	-	-	-	-	1.89	-	-
44	2.09	1.77	-	-	-	-	1.87	-	-
52	2.14	1.79	-	-	-	-	1.93 1.83	1.70 1.65	-
60	2.14 1.79	1.78 1.63	-	1.54	-	-	2.00 2.00	1.73 1.73	-

TABLE 6.10c

BAND-PASS RECTIFIED VIBRATION LEVELS FROM THE DRESSING TESTS

Time Mins	Calculated F-Statistic	Significance Level $\alpha$
2	38.62	0.005
4	59.12	0.005
6	21.08	0.01
8	12.65	0.025
10	28.73	0.005
12	13.22	0.025
14	22.66	0.01
16	18.6	0.01
18	10.2	0.05
20	5.06	Not signifcant at 0.05

TABLE 6.11 INVESTIGATION OF DRESSING  
INFLUENCE ON COMPONENT  
SURFACE FINISH

Test Conditions	Independent Variables		
	Vibration Level		
	100Hz	200Hz	300Hz
SR-FD-1.5-50	0.77 (NS)	-	-
SR-MD-1.5-50	0.73 (NS)	-	-
SR-CD-1.5-50	-	-	-
SR-FD-2.5-50	0.99 (0.001)	0.68 (NS)	-
SR-MD-2.5-50	0.95 (0.01)	0.99 (NS)	0.94 (NS)
SR-CD-2.5-50	0.59 (NS)	-	-

Significance Level in Brackets

(-) = No result because of insufficient data points

TABLE 6.12 COEFFICIENT OF DETERMINATION,  $R^2$ , RESULTS FOR THE DRESSING TEST SURFACE FINISH DATA

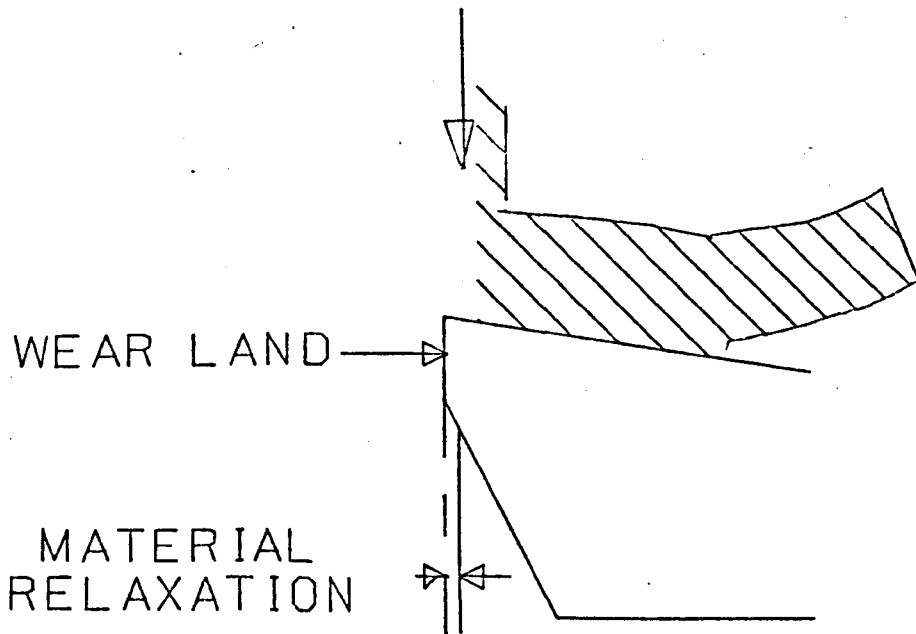
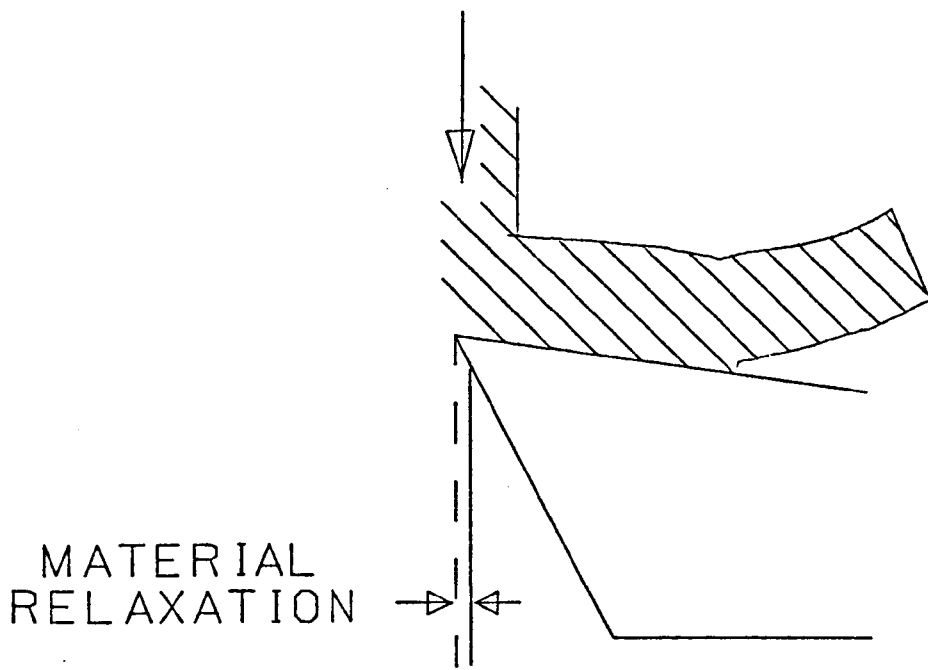
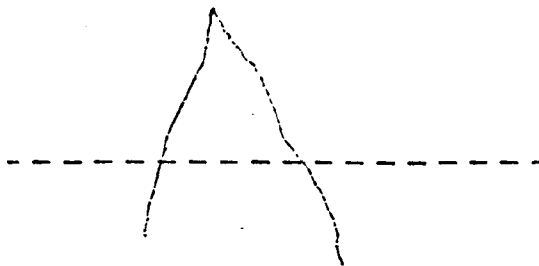
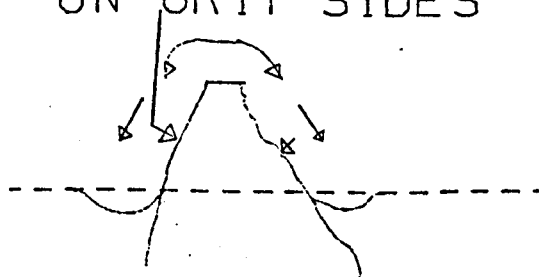


FIGURE 6.1 MATERIAL RELAXATION PHENOMENON WHEN USING A SINGLE POINT CUTTING TOOL (141,142)



NO MATERIAL  
DISPLACEMENT

NO RELAXATION  
POSSIBLE  
ON GRIT SIDES



MATERIAL FORCED  
ALONG GRIT FACE

FIGURE 6.2 MATERIAL RELAXATION PHENOMENON WHEN GRINDING

## 7.0 PRELIMINARY INVESTIGATION OF WORKPIECE THERMAL DAMAGE

### 7.1 Introduction

The majority of ground components operate under severe mechanical conditions. To avoid premature failure of a ground component, surface integrity must be guaranteed by avoiding detrimental temperature related surface alterations. Residual compressive stresses should also be present in the workpiece on the completion of the grinding operation to avoid surface and sub-surface cracks. This can only be achieved by the prevention of workpiece thermal damage [61;1978].

Burn free workpieces can be obtained by using sharp grinding wheels and low metal removal rates. This, however, is contrary to the trend to increase productivity by employing the grinding operation as a rapid metal removal process. If thermal damage does occur, it can be detected and the component rejected by a metallurgical examination on the completion of machining. This solution, however, is unacceptable for the following reasons:

- (i) scrapping a thermally damaged component could be expensive
- (ii) metallurgical examination is usually destructive since the samples need to be taken from the work surface.

Workpiece burn must therefore, be predicted and prevented during the grinding cycle.

Direct on-line monitoring of workpiece surface integrity is inhibited by many problems. Indirect methods do, however, offer an alternative. Correlations have been proposed between normal force intensity or wheelpower and thermal damage (Section 2.5).

These relationships can be developed prior to machining by specifying the grinding material and the grinding conditions. Unfortunately a considerable amount of grinding data is required to undertake such computations particularly if a number of grinding materials are to be considered.

Cebalo [39;1977] proposed that grinding burn was related to the grinding coefficient which was defined as the ratio of the tangential grinding force to the normal grinding force. A coefficient of less than 0.4 results in the production of thermally damaged components. This phenomenon can be utilised to predict and hence prevent workpiece burn during the grinding cycle. It has an advantage over the regression techniques because it requires less grinding data and computation to predict workpiece thermal damage.

The tests to investigate workpiece surface finish (Chapters 5 and 6) did not thermally damage the workpiece because the grinding wheel spindle motor has insufficient power (11.4KWs) to achieve the metal removal rates required to produce surface damage. An alternative machine was therefore needed to examine the influence of workpiece burn on the normal and tangential grinding forces. The use of a second cylindrical plunge grinding machine with a more powerful wheel spindle motor could have been used but such a machine would have had the same restrictions as the initial machine; namely the grinding wheel. If a grinding wheel is operated at the threshold of its capability to investigate workpiece burn the wheel might 'burst' with dangerous consequences. An abrasive belt machine, however, does not have this restriction since the breaking of a belt during the abrasive belt operation is safer than the 'bursting' of a grinding wheel during its operation.

An abrasive belt grinding rig was, therefore, used to examine the thermal damage phenomenon. The results obtained could then be utilised in an adaptive control strategy designed to prevent the occurrence of thermally damaged components.

## 7.2 The Abrasive Belt Research Machine

An abrasive belt test rig has been designed and developed to perform surface and cylindrical grinding [143;1978]. The components of the rig relevant to this particular investigation will be described.

The test rig is illustrated schematically in Figure 7.1 and Figure 7.2 is a photograph of the machine.

### 7.2.1 The Abrasive Belt Head

The belt tracks on two wheels, a contact wheel which transmits the torque to the belt and acts as a rigid support for the belt during grinding, and an idler wheel. An 18 KW three-phase induction motor and a Kopp variator are used to power the contact wheel spindle at speeds in the range of 700-5000rpm. By using a number of different contact wheels this can be converted into a belt surface speed range of 10-80 m/sec.

Adequate belt tension is essential to transmit the torque from the contact wheel to the abrasive belt. This is achieved by the idler wheel which is yoke mounted onto a pneumatic cylinder (see Figure 7.3). The stroke of the pneumatic cylinder can accommodate belt stretch of the order of 2-3%

### 7.2.2 The Surface Grinding Table

A pneumatic cylinder provides the surface grinding table with its reciprocating motion. Incremental depths of cut are supplied to the table at either end of the stroke through a stepping motor/leadscrew arrangement.

The work holding fixture of the table contains a piezo-electric dynamometer. Workpieces are clamped onto the dynamometer which itself is secured onto the surface table. This arrangement permits the normal and tangential grinding force to be monitored during the abrasive belt machining operation.

### 7.3 Experimental Technique

The objective of the investigation was to study the effect of the metal removal rate and the belt speed on workpiece thermal damage; and to observe the corresponding normal and tangential grinding forces both before and after workpiece burn. The time taken to remove the material will be a critical factor in determining the amount of heat conducted into the workpiece [73;1942] and hence the workspeed was kept constant (50 mms/sec) throughout the tests to prevent workpiece heating time being included as an additional variable. Single pass dry surface grinding was used in this study as this technique prevented thermal damaged from occurring via an accumulation of heat in the workpiece from successive grinding strokes.

The abrasive belt used in this investigation was a polyester fibre, X-weight belt using 60 grain aluminium oxide ( $Al_2O_3$ ). Four belt speeds were used; 30, 40, 50 and 60 m/sec. Each belt speed comprised an individual test. An initial metal removal rate of  $5 \text{ mm}^3/\text{mm}/\text{sec}$  was used in a single stroke cutting operation. The workpiece was then visually inspected for workpiece burn and allowed to cool below  $30^\circ\text{C}$  before further grinding was commenced.

The cooling period prevented any heat accumulation in the workpiece. The metal removal rate was then progressively increased by increments of 5 mm<sup>3</sup>/mm/sec and the test procedure was repeated. Once a blue oxide layer was observed on the workpiece surface the depth of this oxide layer was recorded. Testing was carried out until belt breakage. On test conclusion the micro heat effected zone was observed using optical metallography.

#### 7.3.1 Possible Sources of Error

The grinding conditions (belt speed, workspeed and metal removal rate) were accurate to within  $\pm 1.0\%$ . Two possible sources of error were nevertheless introduced into the tests.

- (i) Workpiece induced
- (ii) Belt induced

The former source of error was minimised by using workpieces machined from the same billet. The latter source, however, presented more of a problem particularly in terms of the behaviour of the belts with respect to time. This investigation minimised this potential error by using a new belt for each grinding test. The abrasive belts were, therefore, grinding for less than one minute before being replaced by a new belt.

#### 7.4 Results

The results are presented in Tables 7.1a - 7.1d. These tables show a sudden significant vibration in the grinding coefficient as the metal removal rate is increased.

It is difficult, however, to form a correlation between metal removal rate and the onset of this grinding coefficient variation because each test was performed at a different belt speed and hence the conditions to achieve a particular metal removal rate differed. An alternative parameter, related to the metal removal rate, was therefore, required by which the test could be more thoroughly analysed. The mean volume of material removed per abrasive grit, a parameter which can represent all the metal removal rates independently of belt speed, was used.

The mean volumes of material removed by an abrasive grain per belt revolution (calculation shown in Appendix 4) are given in Table 7.2 and presented graphically in Figure 7.4. Optical examination of the workpiece after grinding showed that at belt speeds of 30, 40 and 50 m/sec thermal damage had occurred whereas the workpiece machined at a belt speed of 60 m/sec was not thermally damaged. Figures 7.5 and 7.6 show a thermally damaged workpiece (30 m/sec test) and an undamaged specimen (60 m/sec test) respectively. These photographs are typical of the specimens taken which exhibited or failed to exhibit burn.

The test using a belt speed of 60 m/sec was the only one which failed to burn the workpiece before belt breakage occurred and hence it was decided that this test should be repeated. The repeated test also failed to burn the workpiece and hence the original result was confirmed.

## 7.5 Discussion

Workpiece burn was observed in all cases where the gradient of the normal and tangential force graphs increased and the grinding coefficient decreased (Figure 7.4).

No workpiece burn was observed in any of the workpiece samples taken prior to the transition point or in the case of the 60 m/sec belt speed test where belt breakage occurred prior to the transition point being experienced. These observations confirm the findings of other researchers [39;1977: 42;1971]. Malkin and Cook [42;1971] observed forces to rise rapidly at the onset of workpiece burn whereas Cebalo [39;1977] concluded that a grinding coefficient value below 0.4 results in the production of workpiece burn.

The grinding force chip volume graphs (Figure 7.4) illustrate that as the belt speed is increased a larger force is needed to remove the same volume/grit/belt revolution. The forces approximately doubled when increasing the belt speed from 30 to 60 m/sec. The grinding force/metal removal rate relationship is, therefore, a linear one for this particular workpiece material because the metal removal rate will also double with the belt speed as each grit can remove twice as many chips in unit time. This was in agreement with the work of Werner [52;1978] who reported that the benefits from a reduction in grinding forces for high speed grinding do not apply in the case of materials which tend to load the surface of the grinding wheel (e.g. low carbon steels). It was reported that in the case of these materials the grinding force for a particular metal removal rate is independent of wheelspeed.

Higher belt speeds (50 and 60 m/sec) also produced another phenomenon: a third linear region on the force-chip volume graphs (see Figure 7.4). The tests were designed by using metal removal rate as a variable. Higher belt speeds remove smaller volume chips to achieve the same metal removal rate. The smaller initial chip volume on the higher belt speed tests (50 and 60 m/sec) produced a linear relationship between grinding forces and chip volume not experienced on the other tests.

This linear region is similar to the one reported by Hahn [23;1963] and hence it is proposed that the lower chip volumes of the 50 and 60 m/sec tests produced ploughing rather than cutting. It is expected that the other belt speeds would experience this phenomenon if the initial metal removal rate was lower. This phenomenon has, however, little relevance to the existing research.

The transition from an unburnt to a burnt specimen is influenced by the volume of material removed by an abrasive grain on each belt revolution. A 7% variation from the mean chip volume ( $1.43 \pm 0.1 \times 10^3 \text{ mm}^3$ ) includes all the transition points. The significance of this volume can be seen when considering the average void volume between abrasive grains,  $7 \times 10^3 \text{ mm}^3$  (see Appendix 4). The value of  $7 \times 10^3$  is an upper bound mean because it assumes no neighbouring grits impinge on this volume. If an assumption is made that the void is packed with spheres, the occupation would be approximately 50% of the available volume. A void filled with grinding debris would occupy an even smaller percentage of the volume. It is not unreasonable to assume, therefore, that the volume of the grinding debris is approaching the available void volume, and that instead of heat being carried away from the workpiece in the grinding chips, it is conducting back into the workpiece from chip-workpiece contact thus causing the workpiece to burn.

A severely loaded belt would be expected as the available voids fill with grinding debris. The grinding coefficient transition point, however, was not accompanied by a severely loaded belt in any of the three tests exhibiting this phenomenon. This suggests that this wheel loading is a transient problem as the debris can dislodge from the voids once the void is clear of the workpiece.

Further increases in metal removal rate, however, did lead to permanent belt loading. It is possible that a combination of excessive redundant work and high temperatures will cause the grinding chips to weld and hence mechanical interlocking will prevent them from being dislodged from the void.

The transient wheel loading theory can explain the increase in gradients for both the normal force and tangential force vs chip volume graphs. An increase in the tangential force component will occur because of the increased contact area between the grinding chips and the workpiece. The normal force component will also increase as a result of the interaction between the grinding chips and the void base because more redundant work will be necessary to remove material. This increase in redundant work will also arise from individual grinding chip interactions and the tendency for the grinding chips to be forced out of the contact zone, a phenomenon first reported by Werner [52;1978].

#### 7.5.1 Adaptive Control Application

The prototype cylindrical plunge grinding machine used to develop algorithms for grinding process adaptive control monitors the normal and tangential grinding forces. This in-process monitoring can provide the current status of the grinding coefficient and hence predict and prevent thermally damaged workpieces. The grinding coefficient, however, varies from one grinding wheel/workpiece combination to another because of the varying influence of the frictional component of the grinding force [40;1980].

The frictional component when grinding high speed steel, for example, was found to be higher than the chip formation force and hence an high grinding coefficient would be expected when grinding high speed steel. The variation in the grinding coefficient will necessitate the development of a large grinding database to include acceptable and unacceptable grinding coefficient values for all workpiece material/grinding parameter combinations. Such a development is impractical and hence an alternative is required. In-process modelling offers that alternative.

The adaptive control strategy developed on the prototype cylindrical plunge grinding machine employs an identification stage where the feedrate is increased from an initially programmed value (Chapter 4). This initial value will be conservative feedrate and hence will provide gentle grinding conditions (Section 2.5). The normal and tangential force values can be recorded at each of the programmed feedrates. This will provide an initial table of force magnitudes similar to Table 7.1. If the grinding coefficient at each feedrate is of the same order of magnitude, which is the most probable outcome since gentle grinding conditions will still prevail, this value can be recorded as one which will not cause workpiece burn.

This strategy, in its present format, may not detect workpiece burn. Its aim is to identify the grinding coefficient prior to workpiece burn so that a significant reduction in this value will signify the onset of burning. The identification stage of the strategy, however, must be carried out for either gentle or conventional grinding conditions rather than abusive ones.

If the initial feedrate is sufficiently high to produce abusive grinding, a grinding coefficient will be recorded which may already be thermally damaging the workpiece. Monitoring this coefficient during a subsequent grinding cycle for a reduction in the magnitude will result in workpiece burn being undetected and hence safeguards are required to ensure that the identification stage does not produce abusive grinding conditions.

An acceptable range of grinding coefficient values must satisfy two criteria:

- (i) All values must be of the same order of magnitude to ensure that all the results occur from the same linear region of the force-metal removal rate relationship.
- (ii) The values must be in excess of some limiting value to ensure that they are from the pre-burn region of the relationship.

If either of these criteria are not satisfied abusive conditions will occur in the identification stage. This could be overcome by reducing the initial feedrate by 50% and repeating the identification stage.

When a pre-burn value of the grinding coefficient has been computed and the grinding machine is operating under constant-force adaptive-control machining, a workpiece burn prediction algorithm can be initiated to operate concurrently with the existing adaptive control strategies. This algorithm would monitor the grinding force components, calculate the grinding coefficient and compare the current magnitude with the computer pre-burn value.

If a significant reduction occurs (e.g. 15-20%) between the current and expected values, workpiece burn can be diagnosed and the adaptive controller could either abort the grinding cycle and inform the operator on a VDU; or automatically reduce the permitted normal force value in the constant normal force machining cycle to produce less abusive grinding conditions.

BELT SPEED = 30 M/SEC

METAL REMOVAL RATE mm <sup>3</sup> /mm/sec	NORMAL FORCE NEWTONS	TANGENTIAL FORCE NEWTONS	GRINDING COEFFICIENT μ	VISUAL BURN DEPTH mms	WORKSURFACE TEMPERATURE AFTER GRINDING °C	COMMENTS
5	560	310	0.55	-	41	
10	950	600	0.65	-	54	
15	1250	720	0.58	-	66	
20	1550	900	0.58	-	76	Straw discolouration of worksurface
25	1990	1080	0.57	-	84	
30	2250	1250	0.56	0.75	93	Blue discolouration
35	2700	1550	0.57	1.25	100	Severely loaded belt
40	3100	1800	0.58	1.5	114	
45	3800	2000	0.53	1.5	127	Silver discolouration
50	4100	2200	0.53	1.5	134	Dark blue discolouration
55	4900	2150	0.43	2.0	-	Belt breakage

- 234(1) -

NOTE: Designation here for severely loaded belt=loaded particles greater than 2.5mms in diameter

TABLE 7.1a ABRASIVE BELT GRINDING DATA

BELT SPEED = 40 M/SEC

METAL REMOVAL RATE mm <sup>3</sup> /mm/sec	NORMAL FORCE NEWTONS	TANGENTIAL FORCE NEWTONS	GRINDING COEFFICIENT μ	VISUAL BURN DEPTH mms	WORKSURFACE TEMPERATURE AFTER GRINDING °C	COMMENTS
5	240	170	0.71	-	33	
10	500	300	0.6	-	43	
15	720	440	0.61	-	65	
20	940	580	0.62	-	77	Straw discolouration
25	1060	620	0.58	-	80	
30	1250	740	0.59	0.5	90	
35	1700	940	0.55	0.75	100	Blue discolouration
40	2400	1220	0.51	1.25	98	Belt severely loaded
45	2500	1300	0.52	1.0	-	Belt breakage

TABLE 7.1b ABRASIVE BELT GRINDING DATA

BELT SPEED = 50 M/SEC

METAL REMOVAL RATE mm <sup>3</sup> /mm/sec	NORMAL FORCE NEWTONS	TANGENTIAL FORCE NEWTONS	GRINDING COEFFICIENT μ	VISUAL BURN DEPTH mms	WORKSURFACE TEMPERATURE AFTER GRINDING °C	COMMENTS
5	340	180	0.53	-	31	
10	580	300	0.52	-	44	
15	680	400	0.59	-	58	
20	960	510	0.53	-	73	
25	1200	680	0.57	-	78	Straw discolouration
30	1300	740	0.57	-	87	
35	1550	820	0.53	0.5	93	
40	1750	900	0.51	0.75	91	Blue discolouration
45	1950	1000	0.51	0.75	112	Belt severely loaded
50	2250	1050	0.47	1.0	100	Silver discolouration
55	3400	850	0.25	1.0	-	Belt breakage

TABLE 7.1c ABRASIVE BELT GRINDING DATA

BELT SPEED = 60 M/SEC

METAL REMOVAL RATE mm <sup>3</sup> /mm/sec	NORMAL FORCE NEWTONS	TANGENTIAL FORCE NEWTONS	GRINDING COEFFICIENT μ	VISUAL BURN DEPTH mms	WORKSURFACE TEMPERATURE AFTER GRINDING °C	COMMENTS
5	280	170	0.61	-	40	
10	420	250	0.59	-	47	
15	540	340	0.63	-	58	
20	720	400	0.56	-	72	Straw discolouration
25	900	480	0.53	-	81	
30	1080	560	0.52	-	87	
35	1300	620	0.48	0.5	94	
40	1450	700	0.48	0.75	90	Blue discolouration
45	1550	780	0.5	0.75	102	
50	2000	840	0.42	1.0	116	Silver discolouration
55	2300	940	0.41	1.0	-	Belt breakage

NOTE: No appreciable belt loading occurred

TABLE 7.1d ABRASIVE BELT GRINDING DATA

METAL REMOVAL RATE mm <sup>3</sup> /mm/sec	BELT SPEED M/SEC			
	30	40	50	60
5	0.72	0.55	0.44	0.36
10	1.03	0.77	0.62	0.52
15	1.26	0.95	0.76	0.63
20	1.46	1.09	0.88	0.73
25	1.63	1.22	0.98	0.82
30	1.77	1.34	1.07	0.89
35	1.93	1.45	1.16	0.96
40	2.06	1.55	1.24	1.03
45	2.19	1.64	1.31	1.09
50	2.31	-	1.38	1.15
55	2.42	-	1.45	1.21

All values  $1 \times 10^{-3} \text{ mm}^3$

TABLE 7.2 AVERAGE VOLUME REMOVED/GRAIN/BELT  
REVOLUTION

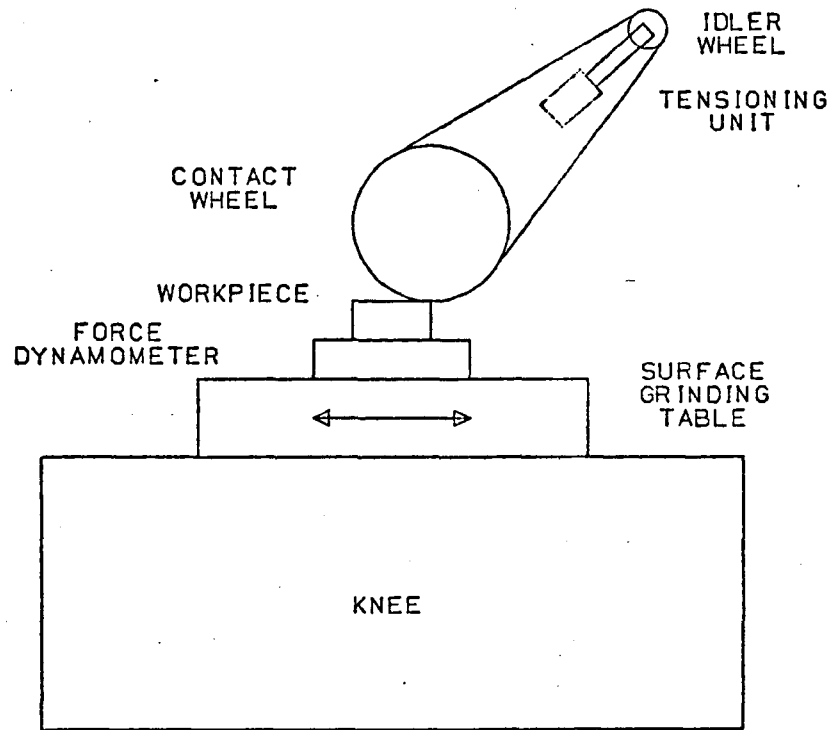


FIGURE 7.1 ABRASIVE BELT RESEARCH MACHINE SCHEMATIC

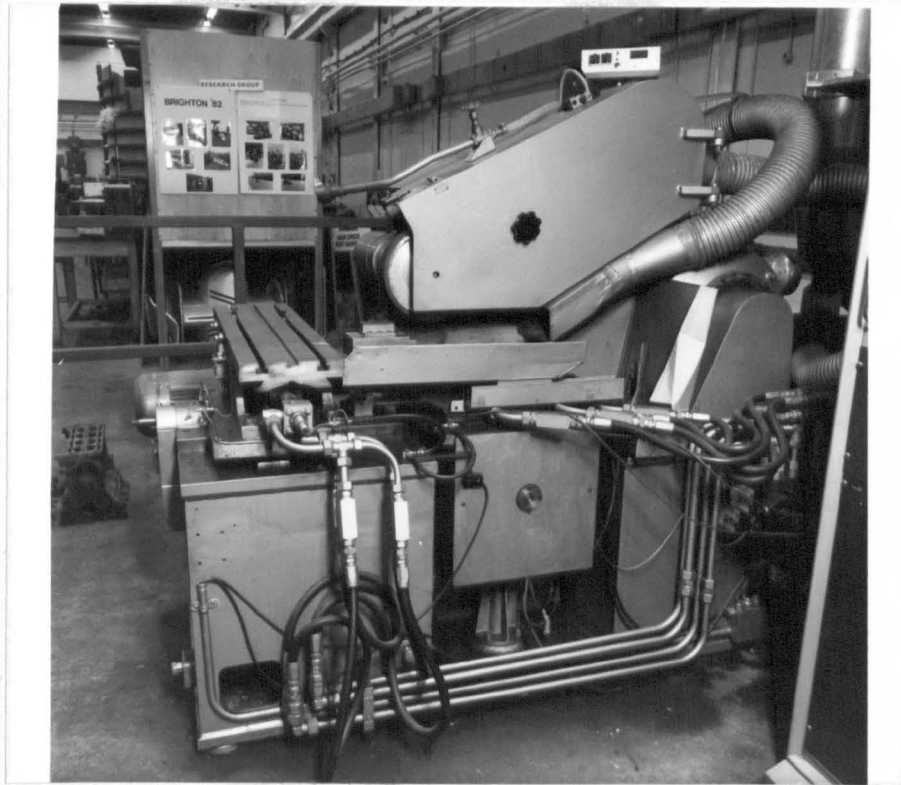


FIGURE 7.2 ABRASIVE BELT RESEARCH MACHINE



FIGURE 7.3 BELT TENSIONING MECHANISM

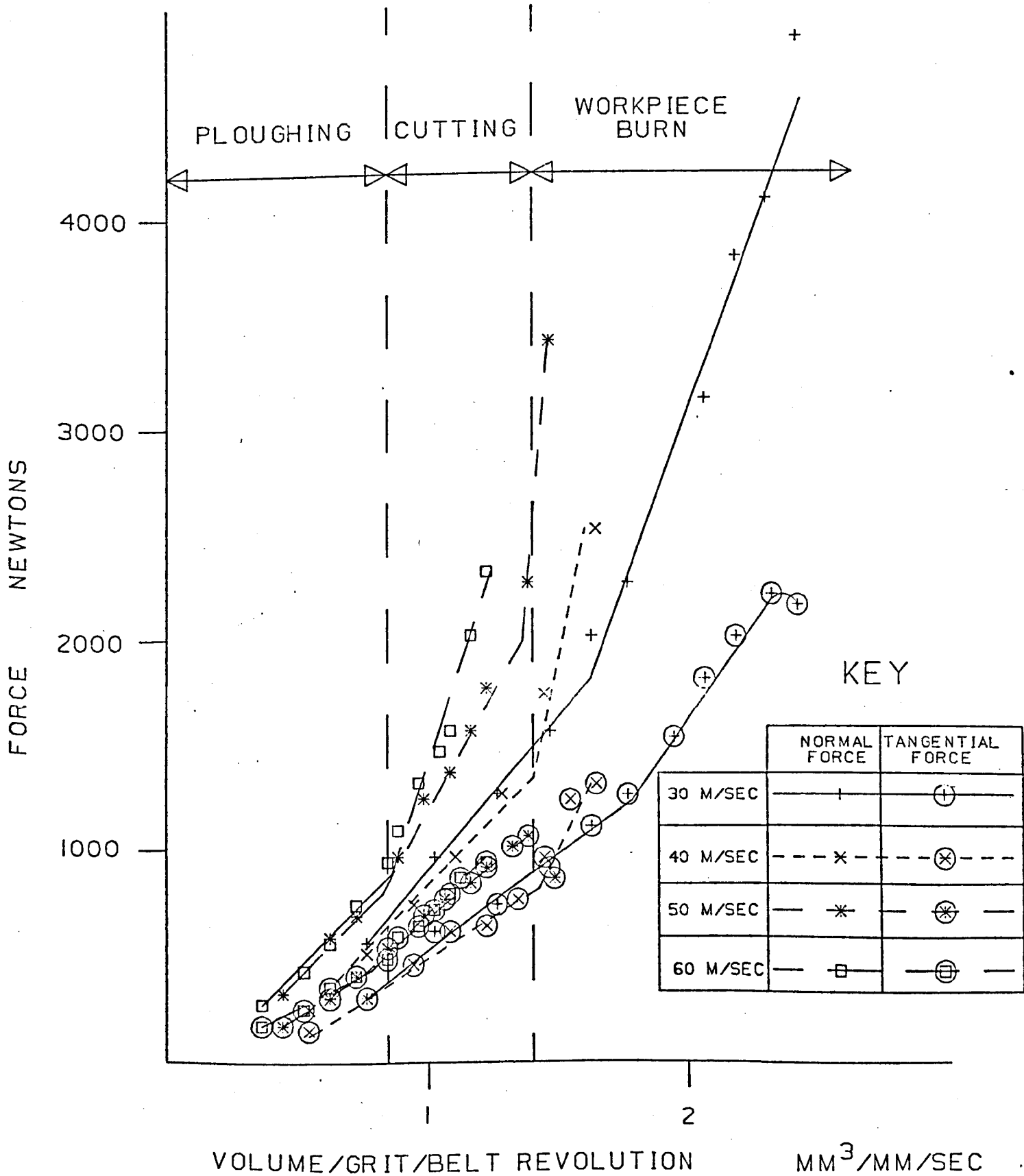
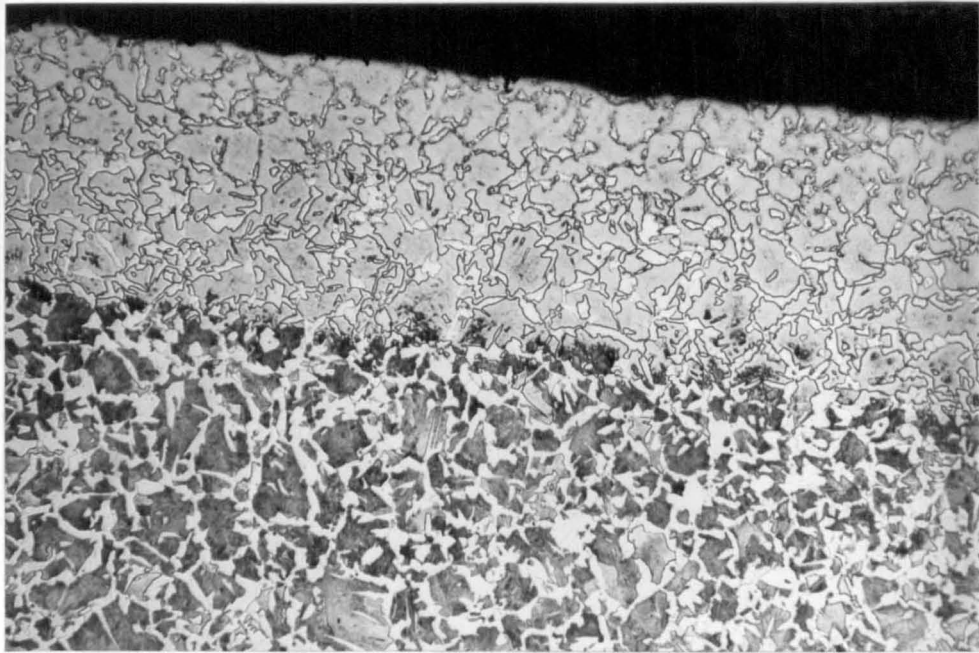
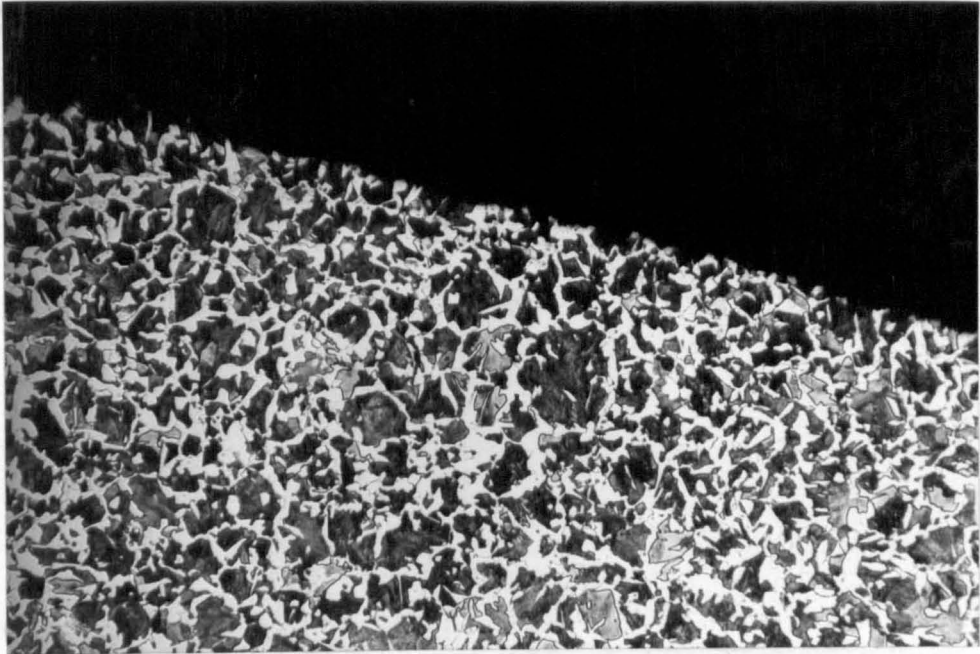


FIGURE 7.4 GRAPHS OF NORMAL AND TANGENTIAL FORCES VERSUS VOLUME REMOVED PER GRIT PER BELT REVOLUTION



MAGNIFICATION = 83

FIGURE 7.5 SURFACE LAYER ALTERATION CAUSED BY  
WORKPIECE BURN



MAGNIFICATION = 83

FIGURE 7.6 STRUCTURE OF THERMALLY UNAFFECTED COMPONENT

## CONCLUSIONS

The predominant grit wear mechanism has been found to have the greatest influence on grinding wheel regenerative chatter. Grinding using low metal removal rates produces attritious wear of the abrasive grains and promotes an increasing level of self-excited chatter vibration. The higher metal removal rates associated with rough grinding cause grits to wear by fracture and vibration levels to remain low.

Grinding chatter can be used to control the redress life of a wheel. Rough grinding will not require frequent redressing because the chatter magnitude will remain low. The amplitude of vibration, however, will increase during finish grinding and hence a preset maximum amplitude can be placed on chatter which when exceeded will initiate an automatic dressing cycle.

The use of rough and finish grinding cycles can minimise the wheel redressing frequency. Fracture wear, which will be experienced if the rough grinding feedrate is sufficiently high, has been shown to damp vibration levels. Increasing levels of self-excited chatter vibration experienced during finish grinding can thus be eliminated by the subsequent component roughing cycles. Dressing under such grinding conditions will only be necessary to maintain a wheel profile.

The frequency of self-excited chatter vibration is dependent on the stiffness of the wheel/workpiece system. Three distinct patterns of chatter frequency vibration were observed during this research.

1. A decrease in chatter frequency which accompanies a decrease in vibration levels.
2. The results of the constant metal removal rate tests where the increasing amplitude occurs at a constant natural frequency.
3. The decrease in chatter frequency which accompanies an increase in vibration levels during the constant normal force tests.

All three chatter vibration patterns have been explained by considering three factors which influence the stiffness of the wheel/workpiece system.

1. Increasing vibration amplitude which reduces the stiffness.
2. Increasing grinding forces which increase the system stiffness.
3. Increasing wear flats on the wheel which also increase the stiffness.

A decrease in chatter frequency will result as the vibration level decreases since fracture wear will be the predominant wear mechanism and hence grinding forces and wear land will decrease.

The constant metal removal rate tests exhibiting increasing levels of vibration at a constant frequency produced increasing forces and wear flat areas. It is concluded that the reduction in stiffness resulting from the vibration increase, is approximately equal to the increase in stiffness produced by the increasing wear lands and grinding forces.

The decreasing chatter frequency observed during the constant normal force tests resulted because the vibration levels and wear lands increased during these tests but the grinding forces were constrained.

Models have been developed which relate component surface finish results with the magnitudes of self-excited chatter vibration. These models were developed by constraining all the other grinding parameters, and although many of the models have coefficients of determination in excess of 0.9, they were incapable of predicting surface finish results unless the grinding conditions were similar to those of the original model. The inclusion of an additional term in the model to represent either the metal removal rate or the normal force expanded the working range of the model. Although these relationships provided excellent correlations ( $R^2=0.9-0.97$ ) they were still restricted by other grinding process variables (e.g. dressing conditions, workpiece material, grinding wheel type etc.) The development of an off-line model to predict component surface finishes, therefore, is prohibited by the number of tests necessary to collect all the grinding data and ultimately by the database size to store this data. On line model identification (adaptive control) will eliminate these restrictions.

A method has been proposed to develop a model to predict component surface finish during the grinding process. This method requires the development of in-process surface finish monitoring which will then be utilised in a model identification stage. Surface finish control will then be possible for the range of grinding parameters used in the original model. New models can then be developed for alternative grinding parameters.

In-process surface finish monitoring has proved difficult to realise. An alternative method of model development has, therefore, been proposed which uses the manually measured component surface finish at the end of the grinding cycle. This method will offer a practical alternative to in-process monitoring if a sufficient number of components are ground between wheel dressing treatments.

The majority of ground components operate under severe mechanical conditions and hence the grinding process, in addition to producing the desired component surface finish, must avoid detrimental temperature-related surface alterations. The prevention of workpiece burn was, therefore, studied in this investigation. This investigation was a preliminary one and hence the number tests performed was limited. A grinding coefficient transition point was, however, observed at the onset of workpiece burn. The grinding coefficient can be computed by normal and tangential force monitoring and hence if this transition point is detected, thermally damaged components can be avoided by reducing the wheel infeed rate.

The transition from an unburnt to a burnt specimen was found to occur at a particular chip volume. This volume has been related to the available void volume between abrasive grains and hence it appears that workpiece burn can be predicted prior to grinding. More work is again needed to confirm the results of the preliminary investigation.

## RECOMMENDATIONS FOR FUTURE WORK

This investigation requires further work in the areas summarised below.

1. The feasibility of in-process surface finish monitoring should be examined. The following two current research projects should be considered.

(a) The use of a contact spring-mass element [115; 1980].

(b) The laser technique being developed for turned components [144;1982: 145;1983].

Consideration must also be given to the coolant and grinding debris problems which will affect both techniques.

2. The workpiece burn tests were only considered to be a preliminary study. More work, investigating different belt and material combinations, is necessary to confirm the findings of this research. It is recommended that abrasive belts rather than grinding wheels, should be used for this work because of safety considerations. If the findings are verified using belts, grinding wheels could be tested without the need to use the same high metal removal rates which were originally necessary to study the phenomenon.
3. The surface integrity investigations only used work materials which are considered to be easy-to-grind (EN3 and EN8). It is recommended that similar investigations are carried out using materials which are classified [52] as difficult-to-grind (e.g. stainless steel or nickel based alloys).

4. Dressing has been shown to influence grinding forces and component surface finishes. These influences should be quantified to enable automatic dressing cycles to select optimum diamond depths of cut and traverse rates to satisfy the particular grinding conditions and component surface integrity requirements.
  
5. It will be necessary to implement the present and future findings in a grinding process adaptive control philosophy. This will involve selecting the appropriate hardware, formulating control strategies and writing control software. Implementing the adaptive control philosophy may involve distributed processing, a research area which is becoming increasingly important with the development of integrated manufacturing systems.

## REFERENCES

1. B.S. 1134 Part 2, 1972
2. LORD, R., 'Plunge Form Abrasive Machining', Manufacturing Engineering, Vol 86, No. 6, 1981, p 76-78
3. SMITH, R., 'Energy Adaptive Grinding', Amer. Mach., Vol 121, July 1977, p 115-119
4. WADA, R., and KODAMA. H., 'Adaptive Control in Grinding', Bull of Japan Soc of Prec. Eng., Vol 11 No 1, Mar 1977, p 1-10
5. HAHN, R.S., and LINDSAY, R.P., 'The Influence of Process Variables on Material Removal, Surface Integrity and Vibration in Grinding', Proc MTDR Conf., 1969, p 95-117
6. ALDEN, G.I., 'Operation of Grinding Wheel in Machine Grinding', Trans ASME, Vol 36, 1914
7. GUEST, J.J., 'The Theory on Grinding', Proc I Mech.E., Oct, 1915
8. ERNST, H., 'Metal Cutting - Art to Science', Machining Theory and Practice, American Society of Metals, Cleveland, Ohio, 1950, p 1-4
9. BACKER, W.R., MARSHALL, E.R., and SHAW, M.C., 'The Size Effect in Metal Cutting', Trans ASME, Vol 74, 1952, p 61
10. BACKER, W.R., and MERCHANT, M.E., 'On the Basic Mechanics of the Grinding Process', Trans ASME, Jan 1958, p 141-148
11. REICHENBACH, G.S., MAYER, J.E., KALPAKCIOGLU, S., AND SHAW, M.C., 'The Role of Chip Thickness in Grinding', Trans ASME, Vol. 78, 1956, p 847-859
12. SHAW, M.C., 'The Grinding of Metals', Conf on Technology and Engineering Manufacturing, I.Mech. E., 1958
13. MARSHALL, E.R., and SHAW, M.C., 'Forces in Dry Surface Grinding', Trans ASME, Vol 74, 1952, p 51

14. HERRING, C., and GALT, J.K., 'Elastic and Plastic Properties of Very Small Metal Specimens', Phys Rev., 1952, Vol 85, No 6, p 1060
15. HOLLIS, W.S., 'Crystal Filaments', The Production Engineer, Vol 40 No 9, p 611.
16. HATHERLY, M., and MALIN, A.S., 'Deformation of Copper and Low Stacking Fault Energy', Metals Technology, Vol 6, 1979, p 308
17. MALKIN, S., and JOSEPH, N., 'Minimum Energy in Abrasive Processes', Wear, Vol 32, No 1, 1975, p 15-23.
18. SARAGARDA, A.A., and KHIMACH, O.V., 'Zonal Cutting Forces and Temperature in Diamond Grinding', Russian Engineering Journal, Vol 53, No 6, 1973, p 73-76.
19. SATO, K., 'On the Surface Roughness in Grinding', Tech. Reports, Tohoku University, Vol 20, No 1, 1955
20. RED'KO, S.D., 'The Active Grits on Grinding Wheels', Machines and Tooling, Vol 31, 1960
21. TAKENAKA, N., 'A Study of the Grinding Wheel Action by a Single Grit', CIRP Annals, Vol 13, 1966, p 183
22. KUMAGAYA, N., 'Spontaneity of Cutting Edges of Abrasive Grains in a Grinding Wheel', Bull. of Japan Soc of Grinding Engineers, No 1, 1966, p 1.
23. HAHN, R.S., 'On the Nature of the Grinding Process' 3rd MTDR Conf, University of Birmingham, 1963.
24. NAKAYAMA, K., and SHAW, M.C., 'Study of the Finish Produced in Surface Grinding: Part 2 - Analytical', Proc I. Mech E., Vol 182, 1967-68, p 179-194
25. BRECKNER, J.N., and SHAW, M.C., 'Specific Energy in Single Point Grinding', CIRP Annals, Vol 23, No 1, 1974

26. KANNAPPAN, S., and MALKIN, S., 'Effect of Grain Size and Operating Parameters on the Mechanics of Grinding', Journal of Eng for Ind., Trans ASME, Series B, Vol 94, 1972, p 838
27. DOYLE, E.D., and DEAN, 'An Insight into Grinding from a Materials Viewpoint', CIRP Annals, 1980, p 571-575
28. SHAW. M.C., 'Interpretation of Grinding Data', Carnegie Mellon University, Pittsburg, Jan, 1971
29. SNOEYS, R., 'The Mean Undeformed Chip Thickness as a Basic Parameter in Grinding', CIRP Annals, 1971, p 183
30. LINDSAY, R.P., 'On the Surface Finish Metal Removal Rate Relationship in Precision Grinding' Journal of Eng for Ind., Trans ASME, Series B, Aug, 1973
31. SNOEYS, R., PETERS, J., and DECNEUT, A., 'The Significance of Chip Thickness in Grinding', CIRP Annals, Vol 23, No 2, 1974, p 227-237
32. PETERS, J., SNOEYS, R., and DECNEUT, A., 'The Proper Selection of Grinding Conditions in Cylindrical Plunge Grinding', MTDR, Conf, 1975
33. HAHN, R.S., FLEISCHER, P., and GRIFFITH, R.C., 'On the Selection and Design of Grinding Cycles', MTDR Conf, 1966, p 599-613
34. KOBAYASHI, A., 'On the Grinding Force', Bull of Japan Soc of Grinding Engs, No 1, 1961, p 19
35. HAHN, R.S., 'Relations Between Grinding Conditions and Thermal Damage in the Workpiece', Journal of Eng for Ind, Trans ASME, Series B, Vol 78, 1956, p 807
36. GRISBROOK, H., 'Precision Grinding Research', The Production Engineer, May, 1960
37. ARMAREGO, E.T.A., and BROWN, R.H., 'On the Size Effect in Metal Cutting', Int Journal of Prod Research, Vol 1, No 3, 1962, p 75.

38. GRISBROOK, H., HOLLIER, R.H., and VARLEY, P.G., 'Related Patterns of Grinding Forces, Wheel Wear and Surface Finish', *Int Journal of Prod Res*, Vol 1, No 3, 1962, p 57-74
39. CEBALO, R., 'Possibility of Comparison and Application of Conventional and Creep Feed Grinding', *Production and Industrial Systems, Selected Papers*, 1977, p 861-870
40. LICHUN Li and JIZAI Fu., 'A Study of Grinding Force Mathematical Model', *CIRP Annals*, Vol 29, No 1, 1980, p 245-249
41. BHATTACHARYYA, S.K., 'Characteristics of Wheel Wear in Precision Surface Grinding', PhD Thesis, University of Birmingham, 1970
42. MALKIN, S., and COOK, N.H. 'The Wear of Grinding Wheels - Part 1 - Attritious Wear', *Trans ASME, Series B*, Nov, 1971, p 1120-1128
43. PACITTI, V and RUBENSTEIN, C., 'The Influence of Dressing Depth of Cut on the Performance of a Single Point Diamond Dressed Alumina Grinding Wheel', *Int Journal of Mach Tool Des Res*, Vol 12, 1972 p 267-279
44. MAKINO, H., 'Chattering Phenomenon as the Criterion of Redress Life of the Grinding Wheel: A Study on the Establishment of Optimum Conditions in Precision Grinding of Hardened Steel', 15th MTDR, 1974
45. FLETCHER, N.P., 'Single Point Dressing of Aluminium Oxide Grinding Wheels and its Influence on Cylindrical Traverse Grinding', *Int. Journal of Mach Des Res*, Vol 20, 1978, p 55-65
46. YOSSFON, S., and RUBENSTEIN, C., 'The Grinding of Materials Exhibiting High Adersion. Part 2 Forces', *Journal of Eng for Ind*, *Trans ASME, Series B*, Vol 103, May 1981, p 156-164

47. HAHN, R.S., 'The Effect of Wheel Work Conformity in Precision Grinding', Journal of Eng for Ind, Trans ASME, Series B, Vol 77, 1955, p 1325-29
48. NAKAYAMA, K., BRECKNER, J., and SHAW, M.C., 'Grinding Wheel Elasticity' Journal of Eng for Ind, Trans ASME, Series B, May, 1971, p 609-614
49. SARINI, D.P., 'Elastic Deflections in Grinding', CIRP Annals, Vol 29, No 1, 1980, p 189-194
50. KUMAR, K.V., and SHAW, M.C., 'The Role of Wheel Work Deflections in Grinding Operations', Journal of Eng for Ind, Trans ASME, Series B, Vol 103, Feb, 1981, p 243-248
51. HAHN, R.S., 'The Influence of Threshold Forces on Size, Roundness and Contour Errors in Precision Grinding', CIRP Annals, Vol 30 No 1, 1981, p 251-254
52. WERNER, G., 'Influence of Work Material on Grinding Forces', CIRP Annals, Vol 27, No 1, 1978, p 243-248
53. NAGPAL, B.K., 'Studies in Adaptive Control of Cylindrical Grinding' PhD Thesis, University of Birmingham, 1972
54. MORAN, H., 'Thermal Aspects of Grinding', MSc Thesis, University of Birmingham, 1967
55. ARORA, G.K., 'Identification of High Speed Grinding', PhD Thesis, University of Birmingham, 1972
56. YOSSFON, S., and RUBENSTEIN, C., 'The Grinding of Materials Exhibiting High Adhesion. Part 1 Mechanisms', Journal of Eng for Ind., Trans ASME, Series B, Vol 103, May, 1981, p 144-155
57. KIRK, J.A., 'An Evaluation of Grinding Performance for Single and Polycrystal Grit Aluminium Oxide Grinding Wheels', Journal of Eng for Ind., Trans ASME, Series B, Vol 96, No 4, Nov, 1974, p 1177-83

58. LUR'E, G.B., 'Nomogram for Determining Burn Free Cylindrical Plunge Grinding Rates', *Machines and Tooling*, Vol 46, No 1, 1975
59. MALKIN, S., and ANDERSON, R.B., 'Thermal Aspects of Grinding. Part 1 Energy Partition', *Journal of Eng for Ind., Trans ASME, Series B*, Vol 96, No 4, Nov, 1974, p 1177-1183.
60. MALKIN, S., 'Burning Limit for Surface and Cylindrical Grinding of Steel', *CIRP Annals*, Vol 27, No 1, 1978, p 233-236
61. TORRACE, A.A., 'Metallurgical Effects Associated with Grinding', 19th MTDR Conf, 1978, p 637-644
62. MALKIN, S., 'Selection of Operating Parameters in Surface Grinding of Steels', *Journal of Eng for Ind., Trans ASME, Series B*, Feb 1976, p 56-62.
63. MALKIN, S., 'Thermal Aspects of Grinding. Part 2 Surface Temperature and Workpiece Burn', *Journal of Eng for Ind., Trans ASME, Series B*, Vol 96, No 4, Nov 1974, p 1184-91
64. POWELL, J.W., and HOWES, T.D., 'A Study of the Heat Flux at Which Burn Occurs in Creep Feed Grinding', 19th MTDR Conf., 1978
65. KONIG, W., and MESSER, J., 'Influence of the Composition and Structure of Steels on the Grinding Process', *CIRP Annals*, Vol 30, No 2, 1981, p 547-552.
66. WERNER, P.G., and SCHLINGENSIEPEN, R., 'Creep Feed - An Effective Method to Reduce Surface Temperatures in High Efficiency Grinding Processes', *Proc 8th North American Manufacturing Research Conf.*, 1980 p 312-319
67. SNOEYS, R., MARIS, M., and PETERS, J., 'Thermally Induced Damage in Grinding', *CIRP Annals*, Vol 27 No 2, 1978, p 571-581

68. OUTWATER, J.O., and SHAW, M.C., 'Surface Temperatures in Grinding' Trans ASME, Series B, Vol 74, 1952
69. LITTMAN, W.E., and WULFT, J., 'The Influence of the Grinding Process on the Structure of Hardened Steel', Trans ASME, Vol 76, 1954
70. SAUER, W.J., 'Thermal Aspects of Grinding', Proc Int Grinding Conf., Pittsburg, 1972, p 391-411
71. SATO, K., 'Grinding Temperatures', Bull of Japan Soc of Grinding Engs, Vol 1, 1961, p 31
72. DES RUISSEAUX, N., and ZERKLE, R.D., 'Thermal Analysis of the Grinding Process', Journal of Eng for Ind, Trans ASME, Series B Vol 92, 1972
73. JAEGER, J.C., 'Moving Sources of Heat and Temperatues at Sliding Contacts', Proc Royal Soc, New South Wales, Vol, 76, 1942.
74. MAYER, J.E. and SHAW, M.C., 'Grinding Temperatures', Journal of Eng for Ind, Trans ASME, Series B Vol 79, 1957
75. FURUICHI, R., and NAKAYAMA, M., 'Influence of Grinding Fluids on Wear of Abrasive Grains', Journal of Japan Soc of Mech Eng, Vol 31, No 231.
76. FISHER, R.C., 'How Wet is Your Grinding?' American Machinist, Vol 107, No 7., 1963
77. KONIG, W., SCHREITMULLER, H., SPERLING, F., WERNER, G., and YOUNIS, M., 'A Survey of the Present State of High Speed Grinding', CIRP Annals Vol 19, 1971, p 275
78. HAHN, R.S., 'Grinding Chatter in Precision Grinding Operations - Causes and Cures', North American Metalworking Res Conf., Michigan, 1979
79. RANATAUNGA, R.J.K.S.K., 'Identification of Grindability', PhD Thesis, University of Birmingham 1974.

80. KALISZER, H., and LIMB, M., 'Application of Ultrasonic Techniques to the Grinding Process', 7th MTDR Conf, 1966.
81. SNOEYS, R., and BROWN, D., 'Dominating Parameters in Grinding Wheel and Workpiece Regenerative Chatter', 10th MTDR Conf, 1969
82. BANEK, I., 'Self Excited Vibrations in Grinding', Machines and Tooling, Vol 46, No 6, 1975
83. INASAKI, I., TANOU, K., and YONETSU, S., 'Regenerative Chatter in Cylindrical Plunge Grinding', Bull of Japan Soc of Mech Eng, Vol 20, Dec 1977.
84. HAHN, R.S., 'On the Theory of Regenerative Chatter in Precision Grinding Operations', Trans ASME, 1954.
85. SHIOZAKI, S., FURUKAWA, Y., and OGAWA T., 'Stability Analysis of Cylindrical Grinding Under the Effect of Workpiece Shape', Bull of Japan Soc of Mech Eng, Vol 20, No 148 Oct 1977.
86. PEKLENIK, J., 'Contribution to the Theory of Grinding', Mechanical Journal, 1959
87. FUKUDA, R., 'Frequency Components and Amplitude Modulation of Chatter Vibration During Cylindrical Grinding', Bull of Japan Soc of Prec Eng, Vol 10, No 2, June 1976, p 51-56
88. INAZAKI, I., and YONETSU, S., 'Surface Waves Generated on the Grinding Wheel', Bull of Japan Soc of Mech Eng, Vol 11, No 47, 1968, p 922-929
89. KALISZER, H., and TRMAL, G., 'Forced Vibration During Cylindrical Plunge Grinding and its Effects on Surface Topography', Proc Int Conf on Grinding, New Developments in Grinding, 1972, p 708-733
90. KALISZER, H., 'Analysis of Chatter Vibrations', 11th MTDR Conf, 1970, p 615-631

91. MAKINO, H., 'Chattering Phenomenon as a Criterion for Redress Life of a Grinding Wheel : A Study on the Establishment of Optimum Operational Conditions in the Precision Grinding of Hardened Steel', MTDR Conf 1974, p 325-332
92. SZEKERES, F., 'Objective Method for Determining Grinding Wheel Life', MTDR Conf, 1971
93. HAHN, R.S., 'Vibration Problems and Solutions in Grinding', ASME Paper MR69-246, 1969
94. BARTALUCCI, and LISINI, G.C., 'Grinding Process Instability', Trans ASME, Vol 91, 1969, P 597-606
95. SHIOZAKI, S., MIYASHITA, M., and FURUKAWA, Y., 'Generation and Growing Up Process of Self Excited Chatter Vibration in Grinding', Bull of Japan Soc of Mech Eng, Vol 13, No 63, 1970, p 1139-1150
96. PETERS, J., and AERENS, R., 'Evaluation of Some Factors Influencing Tool Life in Grinding', CIRP Annals, Vol 26, No 1, 1977, p 161-163.
97. TAKAYANAGI, K., INASAKI, I., and YONETSU, S., 'Regenerative Chatter Behaviour During One Cycle of Cylindrical Plunge Grinding', Bull of Japan Soc of Prec Eng, Vol 12, No 3, 1978, p 121-126
98. SRINIVASAN, K., 'Application of the Regenerative Specturm Method to Wheel Regenerative Chatter in Grinding', Journal of Eng for Ind, Trans ASME, Series B, Vol 104, Feb 1982, p 46-54
99. BARTALUCCI, B., LISINI, G.G., and PINOTTI, P.C., 'Grinding at Variable Speed', MTDR Conf, 1973, p 653-658
100. CEGRELL, G., 'Variable Wheel Speed - A Way to Increase the Metal Removal Rate', MTDR Conf, 1973, p 653-658

101. HAHN, R.S., 'Metal Cutting Chatter and its Elimination', Journal of Eng for Ind, Trans ASME, Series B, 1953, p 1073
102. DOI, S., 'An Experimental Study of the Chatter Vibrations in Grinding Operations', Trans ASME, Vol 80, 1958, p 133
103. SWEENEY, G., 'Dynamics of Grinding', PhD Thesis, University of Birmingham
104. INOUE, H., 'Chattering Phenomenon in the Grinding Process', Bull of Japan Soc of Prec Eng, Vol 3, No 3, 1969, p 67-68
105. LURIE, G.B., 'Vibrations in Grinding', Machines and Tooling, Vol 30, No 6, 1959, p 17-19
106. FIELD, M., and KOSTER, W.P., 'Surface Integrity in Grinding', Int Grinding Conf, Pittsburg, 1972.
107. NEE, A.Y.C., and TAY, A.O., 'On the Measurement of Surface Grinding Temperature', Int Journal of Mach Des Res, Vol 21, No 3, 1981, p 279-291
108. HAHN, R.S., and LINDSAY, R.P., 'The Production of Fine Surface Finishes While Maintaining Good Surface Integrity at High Production Rates by Grinding', MTDR Conf, 1973, p 645-652
109. FIELD, M., and KOSTER, W., 'Optimising Grinding Parameters to Combine High Productivity with High Surface Integrity', CIRP Annals, Vol 27, No 1, 1978, p 523-526
110. TRMAL, G., MANNING, B., KALISZER, H., and HEFFORD, E., 'Measurement of Visible Defects on a Ground Surface', 19th MTDR Conf, 1978, p 623-628
111. TURLEY, D.M., and DOYLE, E.D., 'Effect of Material Aspects on the Production of Machined and Ground Surfaces', Wear, Vol 57, p 237-246
112. HAHN, R.S., and LINDSAY, R.P., 'Some Factors Effecting Surface Finish in Grinding', CIRP Annals, Vol 14, No 1, 1966, p 47-52

113. TAKEYAMA, H., SEKIGUCHI, H., MURATA, R., and MATSUZAKI, H.,  
'In Process Detection of Surface Roughness in Machining', CIRP  
Annals, Vol 25, No 1, 1976, p 467-471
114. VERKERK, J., and PEKELHARING, A.J., 'Predictive Measurement  
of the Spark Out Roughness During Plunge Grinding  
Operations', CIRP Annals, Vol 27, No 1 1978, p 227-231
115. SALJE, E., SCHARF, E., and MUSHARDT, H., 'Surface Finish  
Feedback Control in Grinding', SME Technical Paper, MR80-333,  
1980
116. BHATEJA, C.P. CHISHOLM, A.W.J., and PATTISON, E.J., 'A Computer-  
Aided Study of the Texture of the Working Surfaces of Grinding  
Wheels, 10th MTDR Conf, 1971, p 535-541
117. PANDE, S.J., and LAL, G.K., 'Related Patterns of Dressing Particles  
and Grinding Wheel Life', 8th North American Manufacturing Res  
Conf., 1980, p 320-323
118. BHATEJA, C.P., PATTINSON, E.J., and CHISHOLM, A.W.J., 'The  
Influence of Dressing on the Performance of Grinding Wheels',  
CIRP Annals, Vol 21, No 1, 1972, p 81-82
119. PETERS, J., 'Economic Selection of Grinding Wheels. Introduction of a  
Wheel Efficiency Parameter', Proc Int Grinding Conf, Pittsburg,  
1972
120. PANDE, S.J., and LAL, G.K., 'Effect of Dressing on Grinding Wheel  
Performance', Inst Journal of Mach Des Res, Vol 19, 1979,  
p 171-179
121. ERNST, W., 'Erhohte Schnittgeschwindigkeit beim Aussenrund-  
Einstechschleifen und ihr Einfluss auf das Schleifergebnis und  
die Wirtschaftlichkeit', Diss, T.H., Aachen, 1964
122. GUHRING, K., 'Hochleistungsschleifen-Eine Methode zur  
Leistungssteigerung der Schleifverfahren durch hohe  
Schnittgeschwindigkeiten, Diss, T.H. Aachen, 1967

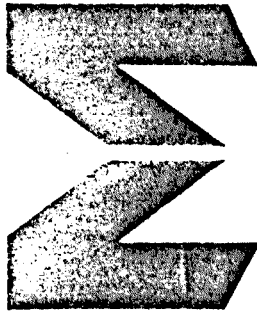
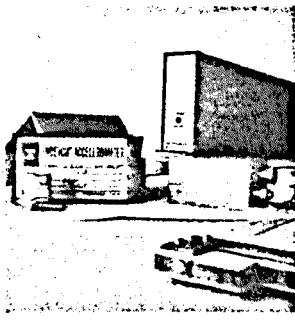
123. OPITZ AND GUHRING 'High Speed Grinding', CIRP Annals, Vol 16, 1968, p 61-73
124. BROWN, E.L., SCHIERLOH, F.L., and MCMILLAN, A.R., 'High Speed O.D. Plunge Grinding', SME Tech Paper, MR79-952
125. THOMPSON, R.A., 'On the Doubly Regenerative Stability of a Grinder the Combined Effect of Wheel and Workspeed', Journal of Eng for Ind, Trans ASME, Series B, Feb 1977, p 237-241
126. INOUE, H., NOGUCHI, H., TAKAHASHI, U., and SUZUKI, S., 'Research on High Efficiency Grinding', Proc Int Grinding Conf, Pittsburg, 1972, p 600-621
127. MILNER, D.A., 'An Introduction to Adaptive Control', Prod Eng, Mar 1975
128. HAHN, R.S., 'Controlled Force Grinding - A New Technique for Precision Internal Grinding', Journal of Eng for Ind, Trans ASME, Series B, Aug 1964
129. WADA, R., 'Application of Adaptive Control to a Cylindrical Grinding Machine', Toyoda Machine Works Ltd., Kariya, Japan. An Article from Japanese NC Machine Tools
130. MULLER, P.A., 'Trainable Adaptive Control for Automated Machining', Soc of Manuf Eng, Tech Paper, MS72-132, 1972
131. INOUE, H., TAMAKOHRI, K., SUTOH, T., NOGUCHI, H., WAIDA, T., and SATA, T., 'An Adaptive Control System of the Grinding Process', Int Conf on Prod Eng, Tokyo, Japan, 1974
132. AMITAY, G., MALKIN, S., and YOREN, Y., 'Adaptive Control Optimisation of Grinding', Journal of Eng for Ind, Trans ASME, Series B, Vol 103, Feb 1981, p 103-108
133. GALL, D.A., 'Adaptive Control of the Abrasive Cut-Off Operation' CIRP Annals, Vol 17, 1969, p 395-399

134. TIPTON, H., 'Adaptive Control of Metal Cutting Machine Tools', Int Journal of Mach Tool Des Res, Vol 18, No 2, April 1979, p 27-33
135. PLESHAKOV, F.K., 'Adaptive Control of Surface Grinding', Machines and Tooling, Vol 45, No 8, 1974, p 50-51
136. RATMIROV, V.A., ET AL, 'Adaptive Control of an NC Cylindrical Grinding Machine', Machines and Tooling, Vol 48, No 8, 1977 p 4-6
137. KALISZER, H., MISHINA, O., and WEBSTER, J., 'Adaptively Controlled Surface Roughness and Roundness During Grinding', MTDR Conf, 1979, p 471-478
138. WALLIS, C., 'Computer Controlled Grinding Machine', MSc Thesis, University of Birmingham
139. EDWARDS, D.M., 'Some Aspects of Adaptive Control', MSc Thesis, University of Birmingham, 1978
140. BENNETT, J., 'Software for Adaptive Control of a Computer Controlled Grinding Machine', MSc Thesis, University of Birmingham, 1982
141. PEKELHARING, A.J., 'Wear of Finish Turning Tools', Proc of OECD Seminar on Metal Cutting, Paris, 1966, p 269-292
142. WALLBANK, J., 'Stress Distribution in Metal Cutting', to be published
143. HARRISON, K., 'Coated Abrasive Machining', PhD Thesis, Univeristy of Birmingham, 1978.
144. THWAITE, E.G., 'The Extension of Optical Angular Scattering Techniques to the Measurement of Intermediate Scale Roughness', CIRP Annals, Vol 31, No 1, 1982 p463-465
145. HINGLE, H.T., and RAKELS, J.H., 'The Practical Application of Defraction Techniques to Assess Surface Finish of Diamond Turned Parts', CIRP Annals, Vol 32, No. 1, 1983, p499-501

146. The Mechanical and Physical Properties of the British Standard EN  
Steels (Editors Woodman and Mottram), Pergamon Press
147. Private communication with Dr Harrison Senior Research Fellow,  
University of Warwick

APPENDIX I. VIBRATION TRANSDUCER TECHNICAL DATA SHEET

ENDEVCO PRODUCT DATA

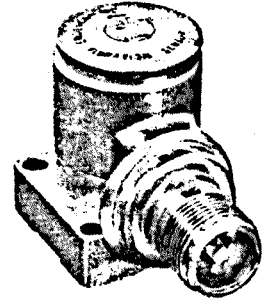


MODEL 5241

INDUSTRIAL  
VIBRATION SENSOR

The Endevco® 5241 Vibration Sensor includes the Endevco® exclusive ISOSHEAR® piezoelectric transduction element and an impedance conversion circuit. The case and internal construction is ruggedized and hermetically sealed to permit operation without degradation in humid and contaminated environments.

The power requirement is low-current dc voltage. Electrical connection is through a rugged, 3-pin connector of MIL-C-5015 configuration. The circuit is protected from damage if any or all of the cable leads are shorted together or to ground.

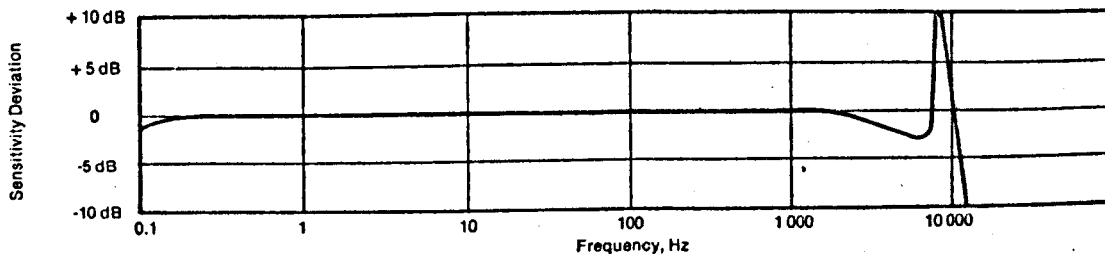


PRELIMINARY SPECIFICATIONS FOR MODEL 5241 VIBRATION SENSOR

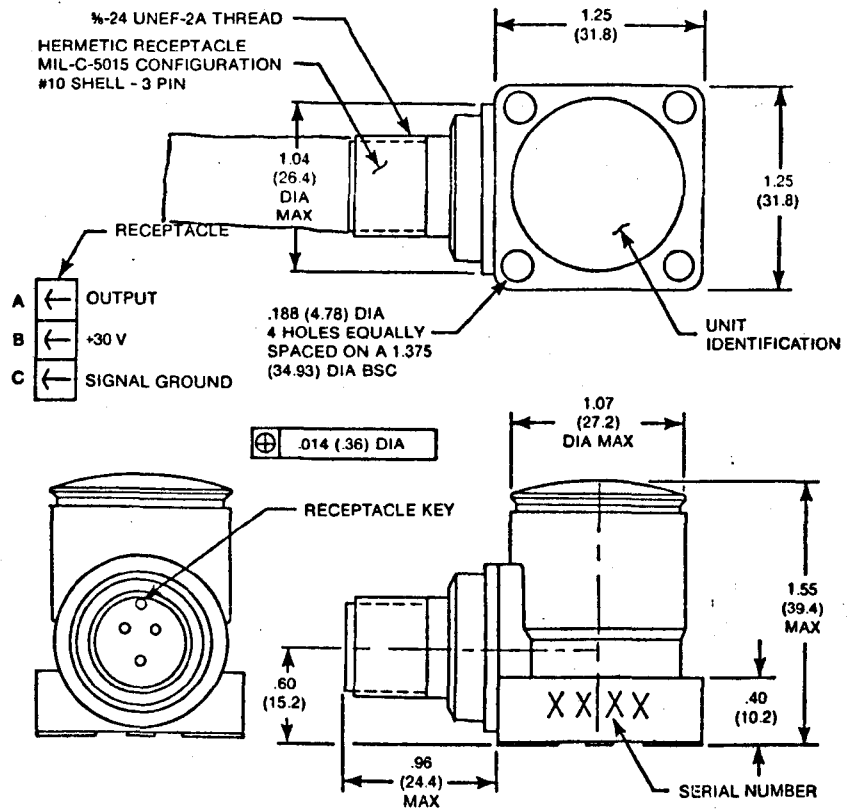
DYNAMIC

RANGE	10 g rms at 30 Vdc
SENSITIVITY (at 100 Hz)	790 mV/g ±5%, with 30 Vdc excitation
FREQUENCY RESPONSE	±10%, 0.2 Hz to 2 000 Hz (sinusoidal)
RESIDUAL NOISE (case grounded) BROAD BAND ACCELERATION	0.0002 g rms, typical
TEMPERATURE RESPONSE, TYPICAL	±5% from 0°F to +150°F (-20°C to +65°C) ±15% from -60°F to +250°F (-50°C to +125°C)
OUTPUT LOAD REQUIREMENT	1 MΩ minimum shunted by cable capacitance up to 0.25 μF (5 000 ft typical) with sensitivity attenuation of 0.5% per 0.025 μF (500 ft)
VOLTAGE REQUIREMENT	30 Vdc
CURRENT DRAIN	1.5 mA steady state. Additional 8 mA required per 0.025 μF cable capacitance (500 ft typical) up to 0.25 μF maximum. Current proportionately reduced as power supply reduced
POWER SUPPLY RIPPLE REJECTION	30 dB attenuation at 120 Hz, typical
INSULATION	10 MΩ minimum at 100 Vdc from case to each pin
MAGNETIC SENSITIVITY	0.0001 equivalent g output per gauss, typical in 60 Hz magnetic field measured at 100 gauss

TYPICAL FREQUENCY RESPONSE



**SPECIFICATIONS FOR MODEL 5241 VIBRATION SENSOR**



**STANDARD TOLERANCE**

INCHES	(MILLIMETRES)
.XX = ±.03	(.X = ±.8)
.XXX = ±.010	(.XX = ±.25)

**PHYSICAL**

CASE	304L Stainless Steel
WEIGHT	6 oz (170 g)
MOUNTING	Four through-holes for #8 bolts on 1.375 in. diameter BSC
CONNECTOR	Stainless steel #10 shell 3-pin, MIL-C-5015 configuration, mates with MS3106-10SL-3S
ACCESSORIES (optional)	Connector MS3106A-10SL-3S (EP 162) Cable Clamp MS3057A-4 (EHF68)

**ENVIRONMENTAL**

TEMPERATURE	-60°F to +250°F (-50°C to +125°C)
HUMIDITY	Hermetically sealed by welding and glass to metal seal
SHOCK	1 000 g pk

Continued product improvement necessitates that Endevco reserve the right to modify these specifications without notice.

**RELIABILITY:** Endevco maintains a program of constant surveillance over all products to ensure a high level of reliability. This program includes attention to reliability factors during product design, the support of stringent Quality Control requirements, and compulsory corrective action procedures. These measures, together with conservative specifications, have made the name Endevco synonymous with reliability.



RANCHO VIEJO ROAD · SAN JUAN CAPISTRANO, CA 92675 · TELEPHONE (714) 493-8181

APPENDIX 2 EN3 and EN8 MATERIAL SPECIFICATIONS [146]

## "20" CARBON STEEL

### SPECIFICATION

#### CHEMICAL COMPOSITION (%)

	C	Si	Mn	S	P
En 3	0.25 max	0.05-0.35	1.00 max	0.060 max	0.060 max
En 3A	0.15-0.25	0.05-0.35	0.40-0.90	0.060 max	0.060 max
En 3B (1)	0.25 max (2)	0.35 max	1.00 max	0.060 max	0.060 max
En 3C	0.17-0.23	0.05-0.35	0.60-1.00	0.050 max	0.050 max
En 3D (1)	0.15-0.25	0.05-0.35	0.60-1.00	0.060 max	0.060 max

(1) Bars to En 3B and En 3D are to be supplied in the cold drawn condition

(2) When stated in the order, the carbon content for bars up to and including 2 1/2" dia or width across flats shall not exceed 0.20 per cent

#### MECHANICAL PROPERTIES

	Limiting Ruling Section (in.)	Tensile Strength (R <sub>m</sub> ) Tons/sq.in.	Elongation (%) (A)
En 3	6	25-35	25 min
En 3A, 3C	6	28 min	25 min
En 3B	—	28 min	17 min
En 3D	1 1/2 or less	35 min	15 min
"	over 1 1/2 to 2 1/2	30 min	15 min
"	over 2 1/2	28 min	15 min

## APPLICATIONS

A general purpose mild steel for welded or riveted structures, forgings, machined parts, hot pressings, etc. This steel will only withstand a moderate amount of cold deformation, and for cold forming generally, steels in the En 2 series should be specified.

En 3C is intended for special applications, e.g. where transverse properties are of importance in design.

Cold drawn bars En3B and En3D have the advantages of scale free finish, to close tolerances, improved tensile strength, with enhanced machinability and reasonable toughness at the expense of some directionality in properties but giving a low yield in compression unless low temperature heat treated.

Typical uses are: Shafts, staybolts, brake pedal levers, gear selectors, clutch and brake housings, motor car wheel hubs, various motorcycle and scooter lug stampings, valve gate and body forgings, wagon buffers, commutator screws, mine haulage and cage suspensions, general haulage gear.

## WELDING

(See Introduction for key to symbols used in this table).

En No.	Welding Process						Remarks
	M.A.	G.	I.G.	S.	F.	B.	
3	a	a	a	c	a	h	M. A. Precautions are necessary when the carbon and manganese contents are near the maximum, particularly with large sections. The mechanical properties of cold drawn bars are adversely affected by all welding processes
3A	"	"	"	"	"	"	
3B	"	"	"	"	"	"	
3C	"	"	"	"	"	"	
3D	"	"	"	"	"	"	

Reproduced by kind permission of H.M.S.O.

This series of steels is suitable for general welding, but should not be employed for spot projection or seam welding unless the welding machines have been adapted for post heating.

## MACHINABILITY

This steel has good machinability similar to that of En 2. It has also been taken as having a machinability index of 100 as a standard for comparison with the other En Steels.

## HOT WORKING AND HEAT TREATMENT TEMPERATURES

Forging, rolling and stamping	1200°C max, finish above 880 °C
Annealing	880—910°C Furnace cool
Normalizing	880—910°C Air cool
Sub-critical annealing	630—700°C
Hardening	•880—910°C Oil or Water Quench
Tempering	550—660°C Air cool

# "40" CARBON STEEL

## SPECIFICATION

### CHEMICAL COMPOSITION (%)

	C	Si	Mn	S	P
En 8	0.35-0.45	0.05-0.35	0.60-1.00	0.060 max	0.060 max
En 8A*	0.33-0.38	0.05-0.35	0.70-0.90	0.060 max	0.060 max
En 8B*	0.35-0.40	0.05-0.35	0.70-0.90	0.060 max	0.060 max
En 8C*	0.38-0.43	0.05-0.35	0.70-0.90	0.060 max	0.060 max
En 8D*	0.40-0.45	0.05-0.35	0.70-0.90	0.060 max	0.060 max
En 8E*	0.35-0.40	0.05-0.35	0.90-1.10	0.060 max	0.060 max
En 8K	0.35-0.45	0.05-0.35	0.60-1.00	0.050 max	0.050 max
En 8M	0.35-0.45	0.25 max	0.90-1.30	0.12-0.20	0.060 max
En 8AM*	0.33-0.38	0.25 max	0.90-1.30	0.12-0.20	0.060 max
En 8BM*	0.35-0.40	0.25 max	0.90-1.30	0.12-0.20	0.060 max
En 8CM*	0.38-0.43	0.25 max	0.90-1.30	0.12-0.20	0.060 max
En 8DM*	0.40-0.45	0.25 max	0.90-1.30	0.12-0.20	0.060 max

\* Mechanical properties are not specified for these steels.

### MECHANICAL PROPERTIES

#### En 8

Property	Condition							
	Normalized	Hardened & Tempered			Cold Drawn			
		Q	R		Size (dia. or width across flats) in.			
Limiting ruling section in.	6	2 $\frac{1}{2}$	$\frac{1}{2}$	$\frac{3}{4}$	$\frac{1}{2}$	1 $\frac{1}{2}$ or less	Over 1 $\frac{1}{2}$ to 2 $\frac{1}{2}$	Over 2 $\frac{1}{2}$
Tensile strength, Tons/sq.in. min (R <sub>m</sub> )	35	40	45	45	45	42	39	37
Yield stress, Tons/sq.in. <sup>1</sup> (R <sub>s</sub> )	18	28	32	32	32			
Elongation, per cent, min (A)	20	22	20	20	20	10	10	10
Izod impact value, ft.lb, min	—	25	40	20	15			
Brinell Hardness number <sup>2</sup> (HB)	152/207	179/229	201/255	201/255	201/255	241 max	229 max	229 max

## MECHANICAL PROPERTIES

(continued)

## En 8K

Property	Condition		
	Normalized		Hardened and Tempered Q
Limiting ruling section, in	6	4	2 $\frac{1}{2}$
Tensile strength, Tons/sq.in., min ( $R_m$ )	35	35	40
Yield stress, <sup>1</sup> Tons/sq.in., min ( $R_s$ )	18	18	28
Proof stress (0.2 per cent) Tons/sq.in. min <sup>2</sup> (0.2 $R_p$ )	17	17	25
Elongation, per cent, min (A)	20	20	22
Izod impact value, ft.lb., min	10	15	25
Brinell hardness numbers <sup>3</sup>	152/207	152/207	179/229

## En 8M

Property	Conditions			
	Normalized	Hardened & Tempered		Cold Drawn Maximum Size (diameter or width across flats) in.
		Q	R	
Limiting ruling section, in.	6	2	$\frac{1}{2}$	1 $\frac{1}{2}$
Tensile strength Tons/sq.in. min ( $R_m$ )	35	40	45	38
Yield stress, Tons/sq.in. min <sup>1</sup> ( $R_s$ )	18	28	32	
Proof stress (0.2 per cent) Tons/sq.in. min <sup>2</sup> (0.2 $R_p$ )	—	25	30	
Elongation, per cent, min (A)	20	22	20	12
Izod impact value, ft.-lb., min	—	25	40	
Brinell hardness number <sup>3</sup> (HB)	152/207	179/229	201/255	229 max

- Notes. 1. Not to be used as acceptance values except by special arrangement between purchaser and manufacturer.  
 2. When specifically requested in the enquiry or order.  
 3. For information purposes only. Not contractual part of the specification.

## RELATED SPECIFICATIONS

En. No.	UNITED KINGDOM		AMERICA		FRANCE	GERMANY			SWEDEN	U.S.S.R.	
	B.S.	B.S. Air	S.A.E.	A.I.S.I.	A.F.N.O.R.	Werkstoff No.	Name	D.I.N.	S.I.S.	G.O.S.T.	Mark.
8	640 cl.1. 46/1	S93 S113 S116	1038 1039	C1038 C1039		1.0721	C45	17200 17240	14.1650	1050-60	40G
8A		S93	1035 1037	C1035 C1037	XC 35f	1.0651	C35	17200	14.1550		
8B		S93 S105			XC 38f					1050-60	35G
8C		S93	1039 1040	C1039 C1040						1050-60	40G
8D		S93 S105	1042 1043	C1042 C1043	XC 42f	1.0721	C45	17200 17240	14.1650		
8E		S93 S105							14.1650	1050-60	
8K	640 cl.1.	S93 S113 S116	1038 1039	C1038 C1039		1.0721	C45	17200 17240	14.1650	1050-60	40G
8M			1139	C1139							
8AM					35 MF 4				14.1957		
8BM									14.1957		

## APPLICATIONS

Widely used for applications where better properties than mild steel are required but the expense of an alloy steel is not justified.

Used for forgings and general engineering parts e.g. Dynamo and motor shafts, heat-treated bolts, crankshafts, connecting rods, driving rings and flanges, railway couplings, axles, brackets, housings, miscellaneous gun carriage and small arms parts not subjected to high stresses or severe wear. Owing to its low hardenability its use in the hardened and tempered condition is not recommended for large masses as the improvement in mechanical properties over the normalized condition is insufficient in such cases to justify the additional processes required.

These steels can be surface hardened by flame or induction methods giving a case hardness of 365-510 HV suitable for general gearing and parts not subject to high stresses.

**WELDING**

(See Introduction for key to symbols used in this table)

En. No.	Welding Process						Remarks
	MA.	G	I.G.	S	F	B	
8	c	bx	cx	f	b	j	The mechanical properties of cold drawn bars are adversely affected by all welding processes. M.A.: — Basic coated electrodes are required and post welding tempering is desirable
8K	c	bx	cx	f	b	j	
8M	c	f	f	f	f	j	

Reproduced by kind permission of H.M.S.O.

**MACHINABILITY**

The machinability of En 8 in the normalized condition is 72 per cent of that for mild steel En 3. In the hardened and tempered condition the machinability is 68 per cent of that for mild steel.

The free machining grade En 8M has similar machinability to En 3 in the normalized condition but in the hardened and tempered condition is 95 per cent of that for mild steel.

**HOT WORKING AND HEAT TREATMENT TEMPERATURES**

Forging Rolling and Stamping	1200 finish above 850°C
Annealing	830–860°C Furnace cool.
Normalizing	830–860°C Air cool.
Subcritical Annealing	630–700°C Air cool.
Hardening	830–860°C Oil, or Water quench.
Tempering	550–660°C Air cool.

**PHYSICAL PROPERTIES**

**SPECIFIC GRAVITY (d)**

Process of Manufacture	Chemical Composition (%)								Heat Treatment °C	Specific Gravity at 20°C	Ref.
	C	Si	Mn	S	P	Ni	Cr	Mo			
	0.39	0.23	0.65	0.017	0.020	0.12	—	—	Normalized Spheroidized	7.828	1
	"	"	"	"	"	"	—	—		7.838	1
	0.41	0.26	0.85	0.04	0.035	0.25	0.13	—	N.870	7.82	2
	0.41	0.14	0.50	—	—	0.12	—	—		7.81	3
B.O.H.	0.42	0.11	0.64	—	—	—	—	—	—	7.84	4
A.O.H.	0.44	0.20	0.69	0.038	0.037	0.04	0.03	0.01	A.860	7.844	4

**SPECIFIC HEAT (c)**

Process of Manufacture	Chemical Composition (%)								Heat Treatment °C	Mean Specific Heat, Cal/deg. C										Ref.
	C	Si	Mn	S	P	Ni	Cr	Mo		20 to 100°C	20 to 200°C	20 to 300°C	20 to 400°C	20 to 500°C	20 to 600°C	20 to 700°C	20 to 800°C	20 to 900°C	20 to 1020°C	
B.O.H.	0.42	0.11	0.64	0.029	0.031	0.06	Tr	—	A.860	0.115	0.119	0.122	0.127	0.132	0.133	0.144	0.159	0.155	0.155	4
A.O.H.	0.44	0.20	0.69	0.038	0.037	0.04	0.03	0.01	A.860	0.114	0.120	0.123	0.128	0.132	0.133	0.146	0.169	0.166	0.164	4

APPENDIX 3 METAL REMOVAL RATE CALCULATION

## METAL REMOVAL RATE CALCULATION

The metal removal rate can be defined in terms of the amount of material removed by a grinding wheel per second. This definition will be dependent on the grinding depth and width of cut, and the workspeed. The metal removal rate of different widths of workpiece or grinding wheel cannot be compared by this method because the width of cut will vary and hence an alternative method is used in this investigation. Metal removal rate is defined in terms of the amount of material removed from the workpiece per millimeter of workpiece width per second. The following formula was used to calculate metal removal rate:

$$\text{MRR, mm}^3/\text{mm}/\text{sec} = a \cdot V_w$$

where  $a$  = depth of cut/workpiece revolution, mms

$$V_w = \text{workspeed, mms}/\text{sec}$$

If the Q-Ratio, defined as the ratio of wheel-to-workspeed, is introduced into this equation.

$$\text{MRR} = \frac{a \cdot V_s}{Q}$$

where  $V_s$  = grinding wheel speed, mms/sec

APPENDIX 4 AVERAGE AMOUNT OF MATERIAL REMOVED PER  
ABRASIVE GRIT

## AVERAGE AMOUNT OF MATERIAL REMOVED PER ABRASIVE GRIT

The cross sectional geometry of the abraive grit protruding above the belt resin will determine the individual grit metal removal rate for a given depth of cut and belt speed combination. Electron microscope photography of the belt surface (Figure A4.1) revealed that this cross sectional geometry can be approximated by a rectangle.

A 60-grit (particle size  $0.25 \pm 0.02$  mms) abrasive belt was used in the investigation. Grits are embedded in the resin so that only 30-40% of their volume is available for cutting [147] and hence the maximum effective abrasive grain depth of cut is approximately 0.08 mms. The average volume removed by each grit per revolution of the belt is given by:

$$\text{Average volume removed per grit, } \bar{v} = 0.25 \bar{d} l \dots\dots A.41$$

where  $\bar{d}$  = mean grit depth of cut (which must not exceed 0.08 mms)  
 $l$  = belt/workpiece contact length

The calculation of the average volume removed per grit requires both the computation of the belt/workpeice contact length and the mean grit depth of cut. These parameters can be derived from the schematic representation of the abrasive belt and the workpiece shown in Figure A4.2. The belt/workpiece contact length, CD, can be obtained from the following analysis:

$$AB = AC - BC$$

$$\theta = \cos^{-1} \frac{AB}{AC}$$

$$CD = 2 \frac{AC \cdot \theta}{360}$$

This analysis assumes

- (i) the belt deflects on to the contact wheel.
- (ii) the deflection of the contact wheel is insignificantly small when compared to the wheel radius.

Using this computation the belt-workpiece contact lengths for each of the metal removal rates used in the investigation are shown in Table A4.1

The mean depth of cut by an abrasive grain can be calculated from

$$d = \frac{cc'}{V_s} \cdot V_w \dots\dots\dots A4.2$$

By substituting this equation in equation A4.1, the mean volume removed by an abrasive grit per belt revolution can be calculated by:

$$V = 0.25 \frac{cc'}{V_s} \cdot V_w \cdot l \dots\dots\dots A4.3$$

An optical microscope examination of the abrasive belt surface revealed that the average grit spacing,  $cc'$ , was 0.35 mms and hence equation A4.3 becomes

$$V = 0.0875 \frac{V_w \cdot l}{V_s} \dots\dots\dots A4.4$$

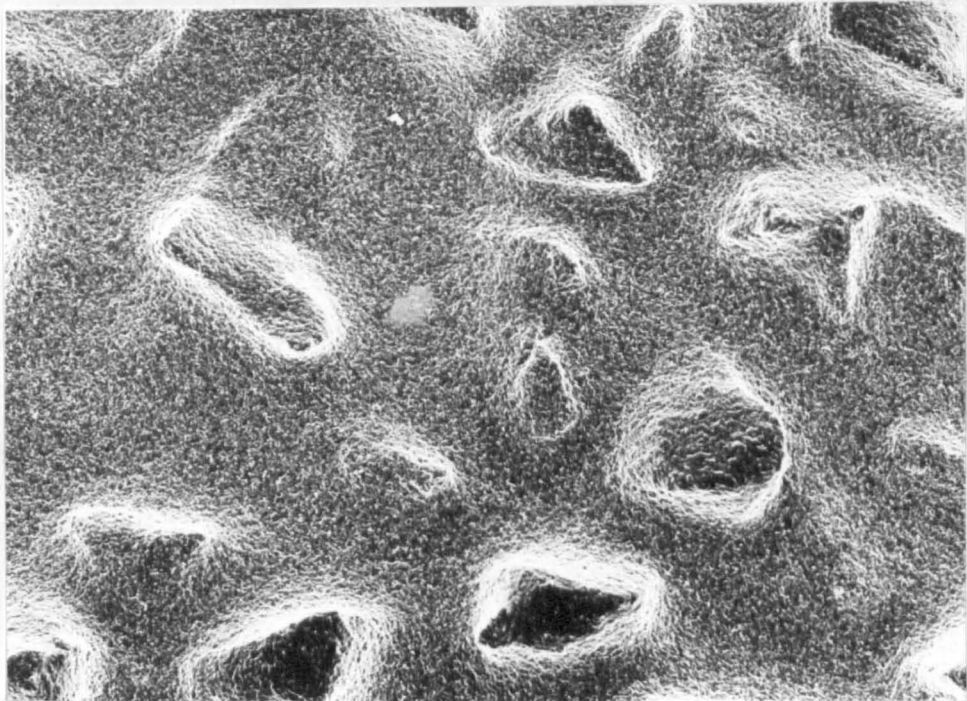
A4.1 Mean Void Volume

The mean void volume, which allows grinding chips to be formed, can be calculated from the expression.

$$\begin{aligned} \mathcal{V} &= \text{Grit Particle Size} \times \text{Grit Height} \times \text{Mean Grit Spacing} \\ &= 0.25 \times 0.08 \times 0.35 \\ &= 0.007 \text{ mms}^3 \end{aligned}$$

Metal Removal Rate mm <sup>3</sup> /mm/sec	Belt- Workpiece Contact Length mms
5	5.0
10	7.07
15	8.66
20	10.0
25	11.18
30	12.25
35	13.23
40	14.15
45	15.01
50	15.82
55	16.6

TABLE A4.1 BELT CONTACT LENGTHS



MAGNIFICATION = 56

FIGURE A4.1 ABRASIVE BELT SURFACE

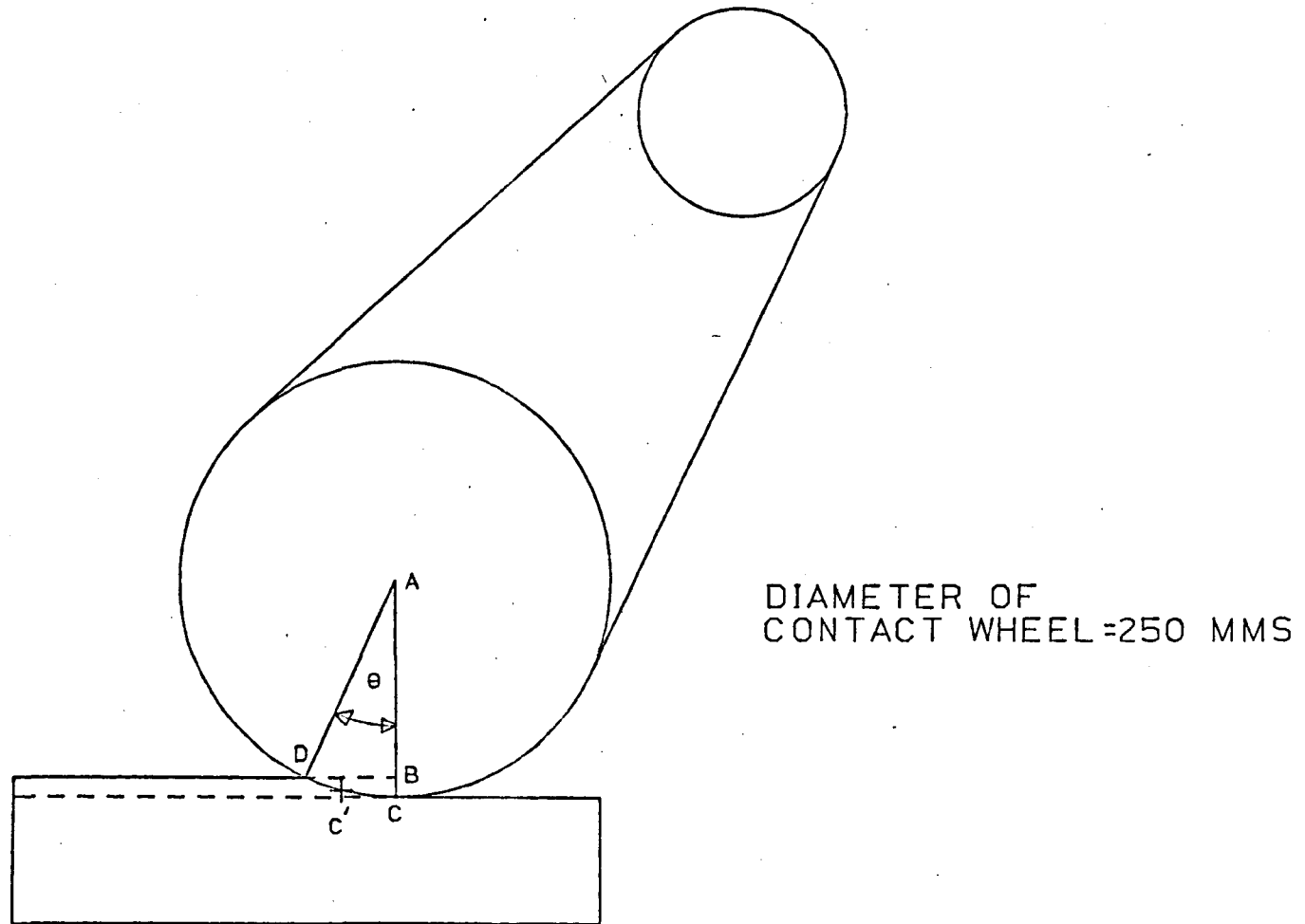


FIGURE A4.2 BELT WORKPIECE CONTACT LENGTH

APPENDIX 5 SIGNIFICANCE TESTS

APPENDIX 5.1

Dependant variable:- Tangential force after 2 minutes

Independent variables:- Metal removal rate and dressing

Data

		<u>DRESSING</u>			
		Fine	Medium	Coarse	Total
M	0.75	80	70	70	220
R	1.50	120	110	100	330
R	2.50	140	155	105	400
<b>TOTAL</b>		340	335	275	950

SOURCE	DEGREES OF FREEDOM	SUM OF SQUARES	MEAN SQUARE
MRR	2	5489.0	2744.5
Dressing	2	872.2	436.1
MRR/Dressing Interaction	4	710.8	177.7
<b>Total</b>	<b>8</b>	<b>7072</b>	

$$F_{\text{calc}} (\text{MRR}) = \frac{2744.5}{177.7} = 15.44 = \text{significant at } \alpha = 0.025$$

$$F_{\text{calc}} (\text{Dressing}) = \frac{436.1}{177.7} = 2.454 = \text{not significant at } \alpha = 0.05$$

APPENDIX 5.2

Dependant variable:- Tangential force after 6 minutes

Independent variables:- Metal removal rate and dressing

Data

		<u>DRESSING</u>			
		Fine	Medium	Coarse	Total
M	0.75	90	75	75	240
R	1.50	130	115	110	355
R	2.50	160	155	125	440
<b>TOTAL</b>		<b>380</b>	<b>345</b>	<b>310</b>	<b>1035</b>

SOURCE	DEGREES OF FREEDOM	SUM OF SQUARES	MEAN SQUARE
MRR	2	6717.0	3358.5
Dressing	2	816.7	408.35
MRR/Dressing Interaction	4	266.3	66.575
Total	8	7800	

$$F_{\text{calc}} (\text{MRR}) = \frac{3358.5}{66.575} = 50.45 = \text{significant at } \alpha = 0.005$$

$$F_{\text{calc}} (\text{Dressing}) = \frac{408.35}{66.575} = 6.134 = \text{not significant at } \alpha = 0.05$$

APPENDIX 5.3

Dependant variable:- Tangential force after 10 minutes

Independent variables:- Metal removal rate and dressing

Data

		<u>DRESSING</u>			
		Fine	Medium	Coarse	Total
M	0.75	95	80	80	255
R	1.50	135	115	115	365
R	2.50	165	170	130	465
TOTAL		395	365	325	1085

SOURCE	DEGREES OF FREEDOM	SUM OF SQUARES	MEAN SQUARE
MRR	2	7356.0	3678.0
Dressing	2	822.2	411.1
MRR/Dressing Interaction	4	543.8	135.95
Total	8	8722.0	

$$F_{\text{calc}} (\text{MRR}) = \frac{3678}{135.95} = 27.05 = \text{significant at } \alpha = 0.005$$

$$F_{\text{calc}} (\text{Dressing}) = \frac{411.1}{135.95} = 3.024 = \text{not significant at } \alpha = 0.05$$

APPENDIX 5.4

Dependant variable: - Tangential force results from the  
2.5mm<sup>3</sup>/mm/sec metal removal rate test

Independent variables: - Grinding time and dressing

Data

		Fine	Coarse	Total
	2	140	105	245
	6	160	125	285
	10	165	130	295
T	14	170	135	305
I	18	160	140	300
M	22	170	150	320
E	26	170	180	350
	30	160	190	350
TOTAL		1295	1155	2450

SOURCE	DEGREES OF FREEDOM	SUM OF SQUARES	MEAN SQUARE
Time	7	4194	599.1
Dressing	1	1225	1225
Time/ Dressing Interaction	7	2125	303.6
Total	15	7544	

$$F_{\text{calc}} (\text{Time}) = \frac{599.1}{303.6} = 1.97 = \text{not significant at } \alpha = 0.05$$

$$F_{\text{calc}} (\text{Dressing}) = \frac{1225}{303.6} = 4.03 = \text{not significant at } \alpha = 0.05$$

APPENDIX 5.5

Dependant variable: - Tangential force results from the  
1.5mm<sup>3</sup>/mm/sec metal removal rate test

Independent variables: - Grinding time and dressing

Data

		Fine	Coarse	Total
	2	120	100	220
	6	130	110	240
	10	135	115	250
T	14	130	120	250
I	18	135	120	255
M	22	135	135	270
E	26	140	130	270
	30	140	130	270
TOTAL		1065	960	2025

SOURCE	DEGREES OF FREEDOM	SUM OF SQUARES	MEAN SQUARE
Time	7	1073	153.3
Dressing	1	689.1	689.1
Time/ Dressing Interaction	7	173.9	24.84
Total	15	1936	

$$F_{\text{calc}} (\text{Time}) = \frac{153.3}{24.84} = 6.17 = \text{significant at } \alpha = 0.025$$

$$F_{\text{calc}} (\text{Dressing}) = \frac{689.1}{24.84} = 27.74 = \text{significant at } \alpha = 0.005$$

APPENDIX 5.6

Dependant variable: - Tangential force results from the  
0.75mm<sup>3</sup>/mm/sec metal removal rate test

Independent variables: - Grinding time and dressing

Data

		Fine	Coarse	Total
	2	80	70	150
	6	90	75	165
	10	95	80	175
T	14	95	85	180
I	18	95	85	180
M	22	95	85	180
E	26	95	85	180
	30	95	95	190
TOTAL		740	660	1400

SOURCE	DEGREES OF FREEDOM	SUM OF SQUARES	MEAN SQUARE
Time	7	525	75
Dressing	1	400	400
Time/ Dressing Interaction	7	75	10.71
Total	15	1000	

$$F_{\text{calc}} (\text{Time}) = \frac{75}{10.71} = 7.0 = \text{significant at } \alpha = 0.01$$

$$F_{\text{calc}} (\text{Dressing}) = \frac{400}{10.71} = 37.35 = \text{significant at } \alpha = 0.005$$

APPENDIX 5.7

Dependant variable:- Time

Independent variables:- Metal removal rate and dressing

Data

		<u>DRESSING</u>			
		Fine	Medium	Coarse	Total
M	0.75	20	60	28	108
R	1.50	10	10	22	42
R	2.50	2	2	10	14
TOTAL		32	72	60	164

SOURCE	DEGREES OF FREEDOM	SUM OF SQUARES	MEAN SQUARE
MRR	2	1553	776.5
Dressing	2	280.9	140.45
MRR/Dressing Interaction	4	754.1	188.525
Total	8	2588	

$$F_{\text{calc}} (\text{MRR}) = \frac{776.5}{188.525} = 5.529 = \text{not significant at } \alpha = 0.05$$

$$F_{\text{calc}} (\text{Dressing}) = \frac{140.45}{188.525} = 0.745 = \text{not significant at } \alpha = 0.05$$

APPENDIX 5.8

Dependant variable:- Surface finish after 2 minutes

Independent variables:- Metal removal rate and dressing

Data

		<u>DRESSING</u>			
		Fine	Medium	Coarse	Total
M	0.75	0.5	0.53	0.82	1.85
R	1.50	0.67	0.62	0.96	2.25
R	2.50	0.75	0.76	1.23	2.74
TOTAL		1.92	1.91	3.01	6.84

SOURCE	DEGREES OF FREEDOM	SUM OF SQUARES	MEAN SQUARE
MRR	2	0.1325	0.06625
Dressing	2	0.2665	0.13325
MRR/Dressing Interaction	4	0.0138	0.00345
Total	8	0.4128	

$$F_{\text{calc}} (\text{MRR}) = \frac{0.06625}{0.00345} = 19.20 = \text{significant at } \alpha = 0.01$$

$$F_{\text{calc}} (\text{Dressing}) = \frac{0.13325}{0.00345} = 38.62 = \text{significant at } \alpha = 0.005$$

APPENDIX 5.9

Dependant variable:- Surface finish after 4 minutes

Independent variables:- Metal removal rate and dressing

Data

		<u>DRESSING</u>			
		Fine	Medium	Coarse	Total
M	0.75	0.52	0.55	0.82	1.89
R	1.50	0.67	0.69	1.01	2.37
R	2.50	0.9	0.89	1.33	3.12
<b>TOTAL</b>		<b>2.09</b>	<b>2.13</b>	<b>3.16</b>	<b>7.38</b>

SOURCE	DEGREES OF FREEDOM	SUM OF SQUARES	MEAN SQUARE
MRR	2	0.2562	0.1281
Dressing	2	0.2453	0.12265
MRR/Dressing Interaction	4	0.0083	0.002075
Total	8	0.5098	

$$F_{\text{calc}} (\text{MRR}) = \frac{0.1281}{0.002075} = 61.73 = \text{significant at } \alpha = 0.005$$

$$F_{\text{calc}} (\text{Dressing}) = \frac{0.12265}{0.002075} = 59.12 = \text{significant at } \alpha = 0.005$$

APPENDIX 5.10

Dependant variable:- Surface finish after 6 minutes

Independent variables:- Metal removal rate and dressing

Data

		<u>DRESSING</u>			
		Fine	Medium	Coarse	Total
M	0.75	0.53	0.56	0.69	1.78
R	1.50	0.78	0.71	1.02	2.51
R	2.50	1.06	0.99	1.28	3.33
TOTAL		2.37	2.26	2.99	7.62

SOURCE	DEGREES OF FREEDOM	SUM OF SQUARES	MEAN SQUARE
MRR	2	0.4009	0.20045
Dressing	2	0.1033	0.05165
MRR/Dressing Interaction	4	0.0098	0.00245
Total	8	0.5140	

$$F_{\text{calc}} (\text{MRR}) = \frac{0.20045}{0.00245} = 81.82 = \text{significant at } \alpha = 0.005$$

$$F_{\text{calc}} (\text{Dressing}) = \frac{0.05165}{0.00245} = 21.08 = \text{significant at } \alpha = 0.01$$

APPENDIX 5.11

Dependant variable:- Surface finish after 8 minutes

Independent variables:- Metal removal rate and dressing

Data

		<u>DRESSING</u>			
		Fine	Medium	Coarse	Total
M	0.75	0.58	0.57	0.77	1.92
R	1.50	0.81	0.77	1.03	2.61
R	2.50	1.06	1.08	1.29	3.43
TOTAL		2.45	2.42	3.09	7.96

SOURCE	DEGREES OF FREEDOM	SUM OF SQUARES	MEAN SQUARE
MRR	2	0.3810	0.1905
Dressing	2	0.09549	0.047745
MRR/Dressing Interaction	4	0.00151	0.0003775
Total	8	0.4780	

$$F_{\text{calc}} (\text{MRR}) = \frac{0.1905}{0.0003775} = 504.63 = \text{significant at } \alpha = 0.005$$

$$F_{\text{calc}} (\text{Dressing}) = \frac{0.047745}{0.0003775} = 12.65 = \text{significant at } \alpha = 0.025$$

APPENDIX 5.12

Dependant variable:- Surface finish after 10 minutes

Independent variables:- Metal removal rate and dressing

Data

		<u>DRESSING</u>			
		Fine	Medium	Coarse	Total
M	0.75	0.58	0.61	0.74	1.93
R	1.50	0.82	0.84	1.10	2.76
R	2.50	1.07	1.13	1.37	3.57
TOTAL		2.47	2.58	3.21	8.26

SOURCE	DEGREES OF FREEDOM	SUM OF SQUARES	MEAN SQUARE
MRR	2	0.4483	0.22415
Dressing	2	0.1063	0.05315
MRR/Dressing Interaction	4	0.0074	0.00185
Total	8	0.5620	

$$F_{\text{calc}} (\text{MRR}) = \frac{0.22415}{0.00185} = 121.2 = \text{significant at } \alpha = 0.005$$

$$F_{\text{calc}} (\text{Dressing}) = \frac{0.05315}{0.00185} = 28.73 = \text{significant at } \alpha = 0.005$$

APPENDIX 5.13

Dependant variable:- Surface finish after 12 minutes

Independent variables:- Metal removal rate and dressing

Data

		<u>DRESSING</u>			
		Fine	Medium	Coarse	Total
M	0.75	0.57	0.60	0.70	1.87
R	1.50	0.87	0.84	1.10	2.81
R	2.50	1.09	1.20	1.38	3.67
<b>TOTAL</b>		<b>2.53</b>	<b>2.64</b>	<b>3.18</b>	<b>8.35</b>

SOURCE	DEGREES OF FREEDOM	SUM OF SQUARES	MEAN SQUARE
MRR	2	0.5401	0.27005
Dressing	2	0.08069	0.040345
MRR/Dressing Interaction	4	0.01221	0.0030525
Total	8	0.6330	

$$F_{\text{calc}} (\text{MRR}) = \frac{0.27005}{0.0030525} = 88.47 = \text{significant at } \alpha = 0.005$$

$$F_{\text{calc}} (\text{Dressing}) = \frac{0.040345}{0.0030525} = 13.22 = \text{significant at } \alpha = 0.025$$

APPENDIX 5.14

Dependant variable:- Surface finish after 14 minutes

Independent variables:- Metal removal rate and dressing

Data

		<u>DRESSING</u>			
		Fine	Medium	Coarse	Total
M	0.75	0.61	0.62	0.76	1.99
R	1.50	0.89	0.79	1.10	2.78
R	2.50	1.18	1.15	1.37	3.7
TOTAL		2.68	2.56	3.23	8.47

SOURCE	DEGREES OF FREEDOM	SUM OF SQUARES	MEAN SQUARE
MRR	2	0.4883	0.24415
Dressing	2	0.08509	0.042545
MRR/Dressing Interaction	4	0.00751	0.0018775
Total	8	0.5809	

$$F_{\text{calc}} (\text{MRR}) = \frac{0.24415}{0.0018775} = 130 = \text{significant at } \alpha = 0.005$$

$$F_{\text{calc}} (\text{Dressing}) = \frac{0.042545}{0.0018775} = 22.66 = \text{significant at } \alpha = 0.01$$

APPENDIX 5.15

Dependant variable:- Surface finish after 16 minutes

Independent variables:- Metal removal rate and dressing

Data

		<u>DRESSING</u>			
		Fine	Medium	Coarse	Total
M	0.75	0.61	0.58	0.82	2.01
R	1.50	0.88	0.79	1.11	2.78
R	2.50	1.16	1.23	1.36	3.75
TOTAL		2.65	2.60	3.29	8.54

SOURCE	DEGREES OF FREEDOM	SUM OF SQUARES	MEAN SQUARE
MRR	2	0.5068	0.2534
Dressing	2	0.09869	0.049345
MRR/Dressing Interaction	4	0.01061	0.0026525
Total	8	0.6161	

$$F_{\text{calc}} (\text{MRR}) = \frac{0.2534}{0.0026525} = 95.53 = \text{significant at } \alpha = 0.005$$

$$F_{\text{calc}} (\text{Dressing}) = \frac{0.049345}{0.0026525} = 18.6 = \text{significant at } \alpha = 0.01$$

APPENDIX 5.16

Dependant variable:- Surface finish after 18 minutes

Independent variables:- Metal removal rate and dressing

Data

		<u>DRESSING</u>			
		Fine	Medium	Coarse	Total
M	0.75	0.65	0.65	0.75	2.05
R	1.50	0.90	0.79	1.11	2.8
R	2.50	1.17	1.18	1.36	3.71
TOTAL		2.72	2.62	3.22	8.56

SOURCE	DEGREES OF FREEDOM	SUM OF SQUARES	MEAN SQUARE
MRR	2	0.4607	0.23035
Dressing	2	0.06889	0.034445
MRR/Dressing Interaction	4	0.01351	0.0033775
Total	8	0.5431	

$$F_{\text{calc}} (\text{MRR}) = \frac{0.23035}{0.0033775} = 68.2 = \text{significant at } \alpha = 0.005$$

$$F_{\text{calc}} (\text{Dressing}) = \frac{0.034445}{0.0033775} = 10.2 = \text{significant at } \alpha = 0.05$$

APPENDIX 5.17

Dependant variable:- Surface finish after 20 minutes

Independent variables:- Metal removal rate and dressing

Data

		<u>DRESSING</u>			
		Fine	Medium	Coarse	Total
M	0.75	0.66	0.62	0.7	1.98
R	1.50	0.88	0.82	1.12	2.82
R	2.50	1.29	1.16	1.32	3.77
TOTAL		2.83	2.6	3.14	8.57

SOURCE	DEGREES OF FREEDOM	SUM OF SQUARES	MEAN SQUARE
MRR	2	0.5345	0.26725
Dressing	2	0.04896	0.02448
MRR/Dressing Interaction	4	0.01934	0.004835
Total	8	0.6028	

$$F_{\text{calc}} (\text{MRR}) = \frac{0.26725}{0.004835} = 55.27 = \text{significant at } \alpha = 0.005$$

$$F_{\text{calc}} (\text{Dressing}) = \frac{0.02448}{0.004835} = 5.06 = \text{not significant at } \alpha = 0.05$$

APPENDIX 6 REGRESSION ANALYSIS RESULTS

## REGRESSION ANALYSIS RESULTS

### A6.1 LR-NF Test Results

Dependent variable:- surface finish. 0.44, 0.65, 0.63, 0.67, 0.72, 1.07,  
1.19, 1.27, 3.2, 2.2, 1.91.

Independent variable:- final metal removal rate. 0.36, 0.56, 0.37, 0.62,  
0.52, 1.09, 1.58, 1.66, 3.03, 2.53, 2.48

Number of results = 11

5% significance level coefficient of determination = 0.364

Coefficient of determination from results,  $R^2 = 0.9$

Equation:- Surface finish =  $0.26 + 0.81 \text{ MRR}$

### A6.2 LR-NF-100 and LR-NF-200 Test Results

Dependent variable:- surface finish. 0.44, 0.65, 0.63, 0.67, 0.72, 1.07,  
1.19, 1.27

Independent variables:- normal force. 100, 100, 100, 100, 100, 200,  
200, 200.

tangential force. 75, 80, 70, 80, 70, 120, 120, 130

wheelpower force. 4.4, 4.8, 3.4, 4.4, 3.8, 7.6,  
8.2, 8.0

final metal removal rate. 0.36, 0.56, 0.37, 0.62,  
0.52, 1.09, 1.58, 1.66

Number of results = 8

5% significance level coefficient of determination,  $R^2 = 0.500$

### Surface Finish vs Final Metal Removal Rate

Coefficient of determination,  $R^2 = 0.94$

Equation:- Surface finish =  $0.36 + 0.55 \text{ MRR}$

### Surface Finish vs Normal Force

Coefficient of determination,  $R^2 = 0.9$

Equation:- Surface finish =  $0.07 + 0.00555 F_N$

### Surface Finish vs Tangential Force

Coefficient of determination,  $R^2 = 0.89$

Equation:- Surface finish =  $-0.22 + 0.01 F_T$

### Surface Finish vs Wheelpower

Coefficient of determination,  $R^2 = 0.85$

Equation:- Surface finish =  $0.05 + 0.14 W_p$

### A6.3 Vibration Results from LR-NF-100 and LR-NF-200

Dependent variable:- surface finish. 0.44, 0.65, 0.63, 0.67, 0.72, 1.07,  
1.19, 1.27

Independent variables:- peak vibration level. 6.5, 6.4, 4.8, 5.7, 1.9,  
7.0, 8.3, 5.1

100Hz band pass average vibration level. 3.8, 3.5, 2.3, 1.9, 1.1, 2.3,  
3.7, 2.9

200Hz band pass average vibration level. 2.6, 2.5, 1.9, 1.2, 0.8, 1.6,  
2.6, 2.7

300Hz band pass average vibration level. 2.0, 2.0, 1.5, 0.9, 0.6, 1.3,  
2.0, 2.2

400Hz band pass average vibration level. 1.6, 1.6, 1.2, 0.6, 0.6, 1.1,  
1.6, 1.8

Number of results = 8

5% significance level coefficient of determination  $R^2 = 0.500$

Surface Finish vs Peak Vibration Level

Coefficient of determination,  $R^2 = 0.08$

Surface Finish vs 100Hz Band Pass Vibration

Coefficient of determination,  $R^2 = 0.01$

Surface Finish vs 200Hz Band Pass Vibration

Coefficient of determination,  $R^2 = 0.06$

Surface Finish vs 300Hz Band Pass Vibration

Coefficient of determination,  $R^2 = 0.08$

Surface Finish vs 400Hz Band Pass Vibration

Coefficient of determination,  $R^2 = 0.10$

NOTE 1 None of the equations are given because of the poor correlations.

2 No correlation improvement could be obtained by using logarithmic values for either surface finish or vibration. This can be attributed to the scatter of results.

#### A6.4 Surface Finsih Results from SR-MRR-1

Dependent variable:- surface finish. 1.09, 0.56, 0.98, 0.94, 0.92, 0.9, 0.8, 0.74, 0.82, 0.79, 0.84, 0.49, 0.58, 0.94, 0.9, 1.02

Independent variable:- peak vibration level. 0.3, 1.8, 1.4, 1.5, 2.5, 1.6, 1.7, 2.5, 4.1, 6.3, 10.0, 1.5, 3.3, 4.0, 6.3, 10.7  
100Hz average vibration. 0.2, 0.6, 0.8, 0.9, 1.3, 1.0, 0.8, 1.3, 1.5, 2.2, 2.3, 0.8, 1.6, 2.0, 2.7, 3.0  
200Hz average vibration. 0.1, 0.3, 0.5, 0.5, 0.8, 0.8, 0.6, 0.9, 0.9, 1.3, 1.3, 0.8, 1.3, 1.1, 1.5, 1.7  
300Hz average vibration. 0.1, 0.3, 0.3, 0.5, 0.6, 0.6, 0.5, 0.7, 0.7, 1.0, 1.0, 0.7, 1.1, 0.8, 1.1, 1.2  
400Hz average vibration. 0.1, 0.2, 0.2, 0.4, 0.6, 0.6, 0.4, 0.6., 0.6, 0.8, 0.8, 0.6, 0.9, 0.7, 0.8, 1.0  
Time to exceed vibration. 60, 0.5, 60, 38, 39.5, 60, 26, 27.5, 29, 31.5, 32.5, 0.5, 1.5, 16.5, 20.5, 32.5

Number of readings = 16

5% significance level coefficient of determination,  $R^2 = 0.247$

Surface Finish vs Peak Vibration Level

Coefficient of determination,  $R^2 = 0.03$

Surface Finish vs 100Hz Average Vibration

Coefficient of determination,  $R^2 = 0.03$

Surface Finish vs 200Hz Average Vibration

Coefficient of determination,  $R^2 = \text{zero}$

Surface Finish vs 300Hz Average Vibration

Coefficient of determination,  $R^2 = 0.02$

Surface Finish vs 400Hz Average Vibration

Coefficient of determination,  $R^2 = 0.01$

Surface Finish vs Time

Coefficient of determination,  $R^2 = 0.69$

A6.5 Surface Finish Results from SR-MRR-2

Dependent variable:- surface finish. 1.14, 1.13, 1.25, 1.33, 1.11, 1.18,  
1.34, 1.36, 1.41, 1.04, 1.36, 1.49, 1.61, 1.62

Independent variables:- peak vibration level. 1.5, 2.5, 4.5, 6.6, 1.5,  
2.5, 4.0, 6.3, 10.1, 1.5, 2.5, 4.4, 6.3, 10.3,  
100Hz average vibration. 1.0, 1.4, 1.9, 2.9, 1.0,  
1.4, 2.4, 3.5, 3.3, 1.5, 2.5, 4.4, 6.3, 10.3,  
200Hz average vibration. 0.6, 0.8, 1.3, 1.8, 0.7,  
1.0, 1.7, 2.5, 2.8, 0.5, 1.0, 1.1, 2.6, 2.8

300Hz average vibration. 0.4, 0.6, 0.9, 1.3, 0.5,  
0.7, 1.2, 1.9, 2.1, 0.5, 0.7, 1.2, 1.9, 2.2  
400Hz average vibration. 0.4, 0.4, 0.7, 1.0, 0.4,  
0.6, 1.0, 1.5, 1.7, 0.4, 0.6, 0.9, 1.6, 1.8  
Time to exceed vibration. 3.5, 6.5, 9.5, 12, 7, 9,  
18, 24.5, 29.5, 2.5, 18, 25, 40, 41

Number of readings = 14

5% significance level coefficient of determination,  $R^2 = 0.209$

#### Surface Finish vs Peak Vibration Level

Coefficient of determination,  $R^2 = 0.60$

#### Surface Finish vs 100Hz Average Vibration

Coefficient of determination,  $R^2 = 0.65$

#### Surface Finish vs 200Hz Average Vibration

Coefficient of determination,  $R^2 = 0.65$

#### Surface Finish vs 300Hz Average Vibration

Coefficient of determination,  $R^2 = 0.71$

$$\text{Equation, } R_a = 1.04 + 0.24 V_{300}$$

#### Surface Finish vs 400Hz Average Vibration

Coefficient of determination,  $R^2 = 0.73$

$$\text{Equation, } R_a = 1.04 + 0.297 V_{400}$$

### Surface Finish vs Time

Coefficient of determination,  $R^2 = 0.92$

Equation,  $R_a = 1.07 + 0.0136 \text{ time}$

### A6.6 Surface Finish Results for the SR-MRR-1-70 Test

Dependent variable: surface finish. 0.8, 0.74, 0.82, 0.79, 0.84

Independent variables: peak vibration . 1.7, 2.5, 4.1, 6.3, 10.0

100Hz average vibration. 0.8, 1.3, 1.5, 2.2, 2.3,

200Hz average vibration. 0.6, 0.9, 0.9, 1.3, 1.3

300Hz average vibration. 0.5, 0.7, 0.7, 1.0, 1.0

400Hz average vibration. 0.4, 0.6, 0.6, 0.8, 0.8

Number of readings = 5

5% significance level coefficient of determination,  $R^2 = 0.771$

### Surface Finish vs Peak Vibration Level

Coefficient of determination,  $R^2 = 0.40$

### Surface Finish vs 100Hz Average Vibration

Coefficient of determination,  $R^2 = 0.16$

### Surface Finish vs 200Hz Average Vibration

Coefficient of determination,  $R^2 = 0.08$

### Surface Finish vs 300Hz Average Vibration

Coefficient of determination,  $R^2 = 0.09$

### Surface Finish vs 400Hz Average Vibration

Coefficient of determination,  $R^2 = 0.06$

### A6.7 Surface Finsih Results for the SR-MRR-1-90 Test

Dependent variable: surface finish. 0.49, 0.58, 0.94, 0.9, 1.02

Independent variables: peak vibration level. 1.5, 3.3, 4.0, 6.3, 10.7

100Hz average vibration. 0.8, 1.6, 2.0, 2.7, 3.0

200Hz average vibration. 0.8, 1.3, 1.1, 1.5, 1.7

300Hz average vibration. 0.7, 1.1, 0.8, 1.1, 1.2

400Hz average vibration. 0.6, 0.9, 0.7, 0.8, 1.0

Number of readings = 5

5% significance level coefficient of determination,  $R^2 = 0.771$

### Surface Finish vs Peak Vibration Level

Coefficient of determination,  $R^2 = 0.66$

### Surface Finish vs 100Hz Average Vibration

Coefficient of determination,  $R^2 = 0.83$

Equation:  $R_a = 0.294 + 0.234 V_{100}$

### Surface Finish vs 200Hz Average Vibration

Coefficient of determination,  $R^2 = 0.5$

### Surface Finish vs 300Hz Average Vibration

Coefficient of determination,  $R^2 = 0.22$

### Surface Finish vs 400Hz Average Vibration

Coefficient of determination,  $R^2 = 0.22$

### Surface finish vs Logarithm of Peak Vibration

Coefficient of determination,  $R^2 = 0.78$

$$\text{Equation: } R_a = 0.378 + 0.653 \log_{10} V_{\text{PEAK}}$$

### Surface finish vs Logarithm of 100Hz Average Vibration

Coefficient of determination,  $R^2 = 0.81$

$$\text{Equation: } R_a = 0.541 + 0.929 \log_{10} V_{100}$$

### Surface finish vs Logarithm of 200Hz Average Vibration

Coefficient of determination,  $R^2 = 0.51$

### Surface finish vs Logarithm of 300Hz Average Vibration

Coefficient of determination,  $R^2 = 0.23$

### Surface finish vs Logarithm of 400Hz Average Vibration

Coefficient of determination,  $R^2 = 0.24$

### A6.8 Surface Finish Results from the SR-MRR-2-30 Test

Dependent variable:- surface finish. 1.14, 1.13, 1.25, 1.33

Independent variable:- peak vibration level. 1.5, 2.5, 4.5, 6.6

100Hz average vibration. 1.0, 1.4, 1.9, 2.9

200Hz average vibration. 0.6, 0.8, 1.3, 1.8

300Hz average vibration. 0.4, 0.6, 0.9, 1.3

400Hz average vibration. 0.4, 0.4, 0.7, 1.0

Number of readings = 4

5% significance level coefficient of determination,  $R^2 = 0.902$

Surface Finish vs Peak Vibration Level

Coefficient of determination,  $R^2 = 0.95$

$$\text{Equation: } R_a = 1.06 + 0.0411 V_{\text{PEAK}}$$

Surface Finish vs 100Hz Average Vibration

Coefficient of determination,  $R^2 = 0.91$

$$\text{Equation: } R_a = 1.01 + 0.111 V_{100}$$

Surface Finish vs 200Hz Average Vibration

Coefficient of determination,  $R^2 = 0.96$

$$\text{Equation: } R_a = 1.02 + 0.174 V_{200}$$

Surface Finish vs 300Hz Average Vibration

Coefficient of determination,  $R^2 = 0.93$

$$\text{Equation: } R_a = 1.02 + 0.235 V_{300}$$

Surface Finish vs 400Hz Average Vibration

Coefficient of determination,  $R^2 = 0.99$

$$\text{Equation: } R_a = 1.01 + 0.33 V_{400}$$

Surface finish vs Logarithm of Peak Vibration

Coefficient of determination,  $R^2 = 0.86$

Surface finish vs Logarithm of 100Hz Average Vibration

Coefficient of determination,  $R^2 = 0.88$

### A6.9 Surface Finish Results from the SR-MRR-2-40 Test

Dependent variable: surface finish. 1.11, 1.18, 1.34, 1.36, 1.41

Independent variables: peak vibration level. 1.5, 2.5, 4.0, 6.3, 10.1

100Hz average vibration. 1.0, 1.4, 2.4, 3.5, 3.3

200Hz average vibration. 0.7, 1.0, 1.7, 2.5, 2.8

300Hz average vibration. 0.5, 0.7, 1.2, 1.9, 2.1

400Hz average vibration. 0.4, 0.6, 1.0, 1.5, 1.7

Number of readings = 5

5% significance level coefficient of determination,  $R^2 = 0.771$

#### Surface Finish vs Peak Vibration Level

Coefficient of determination,  $R^2 = 0.78$

$$\text{Equation: } R_a = 1.12 + 0.033 V_{\text{PEAK}}$$

#### Surface Finish vs 100Hz Average Vibration

Coefficient of determination,  $R^2 = 0.91$

$$\text{Equation: } R_a = 1.03 + 0.11 V_{100}$$

#### Surface Finish vs 200Hz Average Vibration

Coefficient of determination,  $R^2 = 0.91$

$$\text{Equation: } R_a = 1.05 + 0.134 V_{200}$$

#### Surface Finish vs 300Hz Average Vibration

Coefficient of determination,  $R^2 = 0.89$

$$\text{Equation: } R_a = 1.06 + 0.17 V_{300}$$

#### Surface Finish vs 400Hz Average Vibration

Coefficient of determination,  $R^2 = 0.9$

$$\text{Equation: } R_a = 1.05 + 0.218 V_{400}$$

#### Surface finish vs Logarithm of Peak Vibration

Coefficient of determination,  $R^2 = 0.93$

$$\text{Equation: } R_a = 1.05 + 0.38 \log_{10} V_{\text{PEAK}}$$

#### Surface finish vs Logarithm of 100Hz Average Vibration

Coefficient of determination,  $R^2 = 0.96$

$$\text{Equation: } R_a = 1.11 + 0.527 \log_{10} V_{100}$$

#### Surface finish vs Logarithm of 200Hz Average Vibration

Coefficient of determination,  $R^2 = 0.97$

$$\text{Equation: } R_a = 1.19 + 0.489 \log_{10} V_{200}$$

#### Surface finish vs Logarithm of 300Hz Average Vibration

Coefficient of determination,  $R^2 = 0.96$

$$\text{Equation: } R_a = 1.26 + 0.464 \log_{10} V_{300}$$

#### Surface finish vs Logarithm of 400Hz Average Vibration

Coefficient of determination,  $R^2 = 0.96$

$$\text{Equation: } R_a = 1.3 + 0.474 \log_{10} V_{400}$$

#### A6.10 Surface Finish Results for the SR-MRR-2-50 Test

Dependent variable:- surface finish. 1.04, 1.36, 1.49, 1.61, 1.62

Independent variable:- peak vibration. 1.5, 2.5, 4.4, 6.3, 10.3,

100Hz average vibration. 0.6, 1.1, 2.0, 3.2, 3.8

200Hz average vibration. 0.5, 1.0, 1.1, 2.6, 2.8

300Hz average vibration. 0.5, 0.7, 1.2, 1.9, 2.2

400Hz average vibration. 0.4, 0.6, 0.9, 1.6, 1.8

Number of readings = 5

5% significance level coefficient of determination,  $R^2 = 0.771$

### Surface Finish vs Peak Vibration Level

Coefficient of determination,  $R^2 = 0.68$

### Surface Finish vs 100Hz Average Vibration

Coefficient of determination,  $R^2 = 0.82$

$$\text{Equation: } R_a = 1.08 + 0.159 V_{100}$$

### Surface Finish vs 200Hz Average Vibration

Coefficient of determination,  $R^2 = 0.74$

### Surface Finish vs 300Hz Average Vibration

Coefficient of determination,  $R^2 = 0.79$

$$\text{Equation: } R_a = 1.05 + 0.288 V_{300}$$

### Surface Finish vs 400Hz Average Vibration

Coefficient of determination,  $R^2 = 0.77$

### Surface finish vs Logarithm of Peak Vibration

Coefficient of determination,  $R^2 = 0.89$

$$\text{Equation: } R_a = 1.01 + 0.686 \log_{10} V_{\text{PEAK}}$$

### Surface finish vs Logarithm of 100Hz Average Vibration

Coefficient of determination,  $R^2 = 0.96$

$$\text{Equation: } R_a = 1.26 + 0.746 \log_{10} V_{100}$$

### Surface finish vs Logarithm of 200Hz Average Vibration

Coefficient of determination,  $R^2 = 0.89$

$$\text{Equation: } R_a = 1.34 + 0.723 \log_{10} V_{200}$$

Surface finish vs Logarithm of 300Hz Average Vibration

Coefficient of determination,  $R^2 = 0.9$

$$\text{Equation: } R_a = 1.38 + 0.822 \log_{10} V_{300}$$

Surface finish vs Logarithm of 400Hz Average Vibration

Coefficient of determination,  $R^2 = 0.9$

$$\text{Equation: } R_a = 1.46 + 0.818 \log_{10} V_{400}$$

A6.11 Surface Finish Results from the LR-NF Tests

Dependent variable:- surface finish. 0.44, 0.65, 0.63, 0.67, 0.72, 1.07,  
1.19, 1.27

Independent variables: normal force. 100, 100, 100, 100, 100, 200, 200,  
200

metal removal rate. 0.36, 0.56, 0.37, 0.62, 0.52,  
1.09, 1.58, 1.66

peak vibration level. 6.5, 6.4, 4.8, 5.7, 1.9, 7.0,  
8.3, 5.1

100Hz average vibration. 3.8, 3.5, 2.3, 1.9, 1.1,  
2.3, 3.7, 2.9

200Hz average vibration. 2.6, 2.5, 1.9, 1.2, 0.8,  
1.6, 2.6, 2.7

300Hz average vibration. 2.0, 2.0, 1.5, 0.9, 0.6,  
1.3, 2.0, 2.2

400Hz average vibration. 1.6, 1.6, 1.2, 0.6, 0.6,  
1.1, 1.6, 1.8

Number of results = 8

5% significance level coefficient of determination,  $R^2 = 0.500$

### Surface finish vs MRR and Peak Vibration

Coefficient of determination,  $R^2 = 0.97$

$$\text{Equation: } R_a = 0.466 + 0.604\text{MRR} - 0.0249 V_{\text{PEAK}}$$

### Surface finish vs Normal Force and Peak Vibration

Coefficient of determination,  $R^2 = 0.93$

$$\text{Equation: } R_a = 0.164 + 0.00628\text{NF} - 0.0336 V_{\text{PEAK}}$$

### Surface finish vs MRR and 100Hz Vibration

Coefficient of determination,  $R^2 = 0.97$

$$\text{Equation: } R_a = 0.496 + 0.583 \text{ MRR} - 0.059 V_{100}$$

### Surface finish vs Normal Force and 100Hz Vibration

Coefficient of determination,  $R^2 = 0.92$

$$\text{Equation: } R_a = 0.171 + 0.00577\text{NF} - 0.05 V_{100}$$

### Surface finish vs MRR and 200Hz Vibration

Coefficient of determination,  $R^2 = 0.97$

$$\text{Equation: } R_a = 0.471 + 0.596 \text{ MRR} - 0.0702 V_{200}$$

### Surface finish vs Normal Force and 200Hz Vibration

Coefficient of determination,  $R^2 = 0.91$

$$\text{Equation: } R_a = 0.122 + 0.00576\text{NF} - 0.042 V_{200}$$

### Surface finish vs MRR and 300Hz Vibration

Coefficient of determination,  $R^2 = 0.96$

$$\text{Equation: } R_a = 0.459 + 0.595 \text{ MRR} - 0.0844 V_{300}$$

Surface finish vs Normal Force and 300Hz Vibration

Coefficient of determination,  $R^2 = 0.9$

$$\text{Equation: } R_a = 0.114 + 0.00576NF - 0.0487 V_{300}$$

Surface finish vs MRR and 400Hz Vibration

Coefficient of determination,  $R^2 = 0.96$

$$\text{Equation: } R_a = 0.448 + 0.592 \text{ MRR} - 0.0937 V_{400}$$

Surface finish vs Normal Force and 400Hz Vibration

Coefficient of determination,  $R^2 = 0.9$

$$\text{Equation: } R_a = 0.112 + 0.00578NF - 0.609 V_{400}$$

Surface finish vs MRR and the Logarithm of the Peak Vibration Level

Coefficient of determination,  $R^2 = 0.95$

$$\text{Equation: } R_a = 0.485 + 0.59\text{MRR} - 0.209 \log_{10} V_{\text{PEAK}}$$

Surface finish vs Normal Force and the Logarithm of the Peak Vibration Level

Coefficient of determination,  $R^2 = 0.92$

$$\text{Equation: } R_a = 0.204 + 0.00609NF - 0.286 \log_{10} V_{\text{PEAK}}$$

Surface finish vs MRR and the Logarithm of the 100Hz Vibration

Coefficient of determination,  $R^2 = 0.97$

$$\text{Equation: } R_a = 0.452 + 0.584\text{MRR} - 0.289 \log_{10} V_{100}$$

Surface finish vs Normal Force and the Logarithm of 100Hz Vibration

Coefficient of determination,  $R^2 = 0.92$

$$\text{Equation: } R_a = 0.138 + 0.00583NF - 0.273 \log_{10} V_{100}$$

Surface finish vs MRR and the Logarithm of the 200Hz Vibration

Coefficient of determination,  $R^2 = 0.96$

$$\text{Equation: } R_a = 0.34 + 0.589\text{MRR} - 0.246 \log_{10} V_{200}$$

Surface finish vs Normal Force and the Logarithm of 200Hz Vibration

Coefficient of determination,  $R^2 = 0.91$

$$\text{Equation: } R_a = 0.0828 + 0.00581\text{NF} - 0.194 \log_{10} V_{200}$$

Surface finish vs MRR and the Logarithm of the 300Hz Vibration

Coefficient of determination,  $R^2 = 0.96$

$$\text{Equation: } R_a = 0.368 + 0.588\text{MRR} - 0.22 \log_{10} V_{300}$$

Surface finish vs Normal Force and the Logarithm of 300Hz Vibration

Coefficient of determination,  $R^2 = 0.91$

$$\text{Equation: } R_a = 0.0583 + 0.00583\text{NF} - 0.187 \log_{10} V_{300}$$

Surface finish vs MRR and the Logarithm of the 400Hz Vibration

Coefficient of determination,  $R^2 = 0.95$

$$\text{Equation: } R_a = 0.35 + 0.583\text{MRR} - 0.188 \log_{10} V_{400}$$

Surface finish vs Normal Force and the Logarithm of 400Hz Vibration

Coefficient of determination,  $R^2 = 0.91$

$$\text{Equation: } R_a = 0.0385 + 0.00585\text{NF} - 0.193 \log_{10} V_{400}$$

## A6.12 Regression Analysis to Decide on Variable Dressing Significance

### Test

Variables: normal force after 2 minutes. 150, 125, 125, 200, 210, 190,  
250, 320, 200

tangential force after 2 minutes. 80, 70, 70, 120, 110, 100,  
140, 155, 105

wheelpower after 2 minutes. 4.8, 4.8, 3.6, 7.2, 6.8, 6.0,  
10.4, 10.4, 7.4

Number of variables = 9

5% significance level coefficient of determination,  $R^2 = 0.444$

### Normal Force vs Tangential Force

Coefficient of determination,  $R^2 = 0.95$

Equation:  $NF = -17.8 + 2.03 TF$

### Normal Force vs Wheelpower

Coefficient of determination,  $R^2 = 0.81$

Equation:  $NF = -42.9 + 33.1 WP$

### Tangential Force vs Wheelpower

Coefficient of determination,  $R^2 = 0.93$

Equation:  $TF = 23.1 + 12.1 WP$

A6.13 Regression Analysis on the Surface Finish Data of the  
SR-FD-1.5-50 Test

Dependent variable:- surface finish. 0.82, 0.89, 0.9

Independent variable:- 100Hz average vibration. 1.67, 1.91, 2.24

Number of variables = 3

5% significance level coefficient of determination,  $R^2 = 0.994$

Coefficient of determination from the test,  $R^2 = 0.77$

A6.14 Regression Analysis on the Surface Finish Data of the  
SR-MD-1.5-50 Test

Dependent variable:- surface finish. 0.84, 0.79, 0.79

Independent variable: 100Hz average vibration. 1.58, 1.71, 1.85

Number of results = 3

5% significance level coefficient of determination,  $R^2 = 0.994$

Coefficient of determination from the test,  $R^2 = 0.73$

A6.15 Regression Analysis on the Surface Finish Data of the  
SR-FD-2.5-50 Test

Dependent variable:- surface finish. 0.75, 1.06, 1.07, 1.18, 1.17 (The initial reading was omitted for the  $R_a$  vs 200Hz test since there was no appreciable vibration level in this band pass after 2 minutes (see Table 6.10a)).

Independent variables: 100Hz average vibration. 1.66, 2.27, 2.40, 2.56,  
2.56  
200Hz average vibration. 1.88, 2.09, 2.16, 2.25

Number of readings = 5 for 100Hz and 4 for 200Hz

5% significance level of coefficient of determination,  $R^2 = 0.771$  for 5 readings and  $R^2 = 0.902$  for 4 readings

#### Surface finish vs 100Hz Average Vibration

Coefficient of determination,  $R^2 = 0.99$

$$\text{Equation:- } R_a = -0.02 + 0.466 V_{100}$$

#### Surface finish vs 200Hz Average Vibration

Coefficient of determination,  $R^2 = 0.68$

#### A6.16 Regression Analysis on the Surface Finish Data of the SR-MD-2.5-50 Test

Dependent variable:- surface finish. 0.76, 0.99, 1.13, 1.15, 1.18 (The first two readings were omitted for the  $R_a$  vs 200Hz and the  $R_a$  vs 300Hz tests since there was no appreciable vibration level in either band pass until 10 minutes of testing (See Table 6.10a))

Independent variables: 100Hz average vibration. 1.67, 2.07, 2.62, 2.48, 2.71  
200Hz average vibration. 2.1, 2.16, 2.29  
300Hz average vibration. 1.88, 1.96, 2.01

Number of readings = 5 for 100Hz and 3 for 200Hz and 300Hz

5% significance level of coefficient of determination,  $R^2 = 0.771$  for 5 results and  $R^2 = 0.994$  for 3 results

Surface finish vs 100Hz Average Vibration

Coefficient of determination,  $R^2 = 0.95$

$$\text{Equation:- } R_a = 0.14 + 0.391 V_{100}$$

Surface finish vs 200Hz Average Vibration

Coefficient of determination,  $R^2 = 0.99$

Surface finish vs 300Hz Average Vibration

Coefficient of determination,  $R^2 = 0.94$

A6.17 Regression Analysis on the Surface Finish Data of the

SR-CD-2.5-50 Test

Dependent variable:- surface finish. 1.37, 1.37, 1.36

Independent variable: 100Hz average vibration. 1.87, 2.32, 2.56

Number of readings = 3

5% significance level of coefficient of determination,  $R^2 = 0.994$

Coefficient of determination for the test,  $R^2 = 0.59$